ERDC/CHL TR-08-5

Coastal and Hydraulics Laboratory

US Army Corps of Engineers®
Engineer Research and Development Center

Impact of Savannah Harbor Deep Draft Navigation Project on Tybee Island Shelf and Shoreline

Jane McKee Smith, Donald K. Stauble, Brian P. Williams, and Michael J. Wutkowski

April 2008

ERDC/CHL TR-08-5
April 2008

Impact of Savannah Harbor Deep Draft Navigation Project on Tybee Island Shelf and Shoreline

Jane McKee Smith and Donald K. Stauble

Coastal and Hydraulics Laboratory
U.S. Army Engineer Research and Development Center
3909 Halls Ferry Road
Vicksburg, MS 39180-6199

Brian P. Williams

U.S. Army Engineer District, Wilmington
Regional Engineering Center
69A Hagood Avenue
Charleston, SC 29403-5107

Michael J. Wutkowski

U.S. Army Engineer District, Wilmington
69 Darlington Avenue
Wilmington, NC 28402-1890

Final report

Prepared for U.S. Army Engineer District, Savannah
P.O. Box 889
Savannah, GA 31402-0889

and Headquarters, U.S. Army Corps of Engineers
Washington, DC 20314-1000

Abstract: The purpose of this study is to determine if the Savannah Harbor Deep Draft Navigation Project is adversely impacting the shores of Tybee Island (including sand lost from the beach and the Tybee shelf). The study methodology includes numerical modeling of waves, currents, water levels, and sediment transport rates and sediment budgets analysis for pre-project and post-project conditions. Sediment budgets were developed for the period 1854 to 1897 (pre-project) and 1897 to 2005/06/07 (post-project). The post-project bathymetry change shows a pattern of ebb shoal deflation on the Tybee shelf, which is a typical consequence of jetty construction and channel deepening. The ebb shoal deflation resulted from sediment pathways across the channel being disrupted. The major impact of the project is the loss of sand from the Tybee shelf. The ebb shoal deflation also resulted in shoreline change on Tybee Island, including erosion on the northern end of the island and accretion on the southern end of the island.

The impact of the project is evaluated as the difference in volume loss rates (post-project minus pre-project) for the Tybee Island shelf cell of the sediment budget plus the estimated shoreline change rate (converted to a volume). The estimated combined shelf and shoreline impact at Tybee Island is 73.6 percent (including beach fill placement) or 78.5 percent (excluding beach fill placement) (±20 percent). This means that an estimated 73.6 percent (or 78.6 percent) of the reduction in sand volume on the Tybee shelf and shoreline is due to the project, with the remainder of the erosion attributed to the natural processes.

Contents

Figures and Tables

Figures

Tables

Preface

This report describes procedures and results of a study to evaluate the impact of the Savannah Harbor Deep Draft Navigation Project on the Tybee Island shelf and shoreline. The study was conducted jointly by the U.S. Army Engineer Research and Development Center (ERDC), Coastal and Hydraulics Laboratory (CHL), and the U.S. Army Engineer District (USAED), Wilmington, for the USAED, Savannah. The study was conducted during the period March 2007 to December 2007.

The Project Delivery Team included Hampton Spradley (Project Manager), USAED, Savannah; Monica Simon-Dodd (lead Technical Planner), USAED, Mobile; Lyle Maciejewski (Operations), USAED, Savannah; Wilbur Wiggins (Coastal Engineering), USAED, Wilmington; Steve Calver (Environmental), USAED, Mobile; and Ned Durden (Survey), USAED, Savannah. Oversight was provided by Roger Burke, Chief (retired), Plan Formulation Branch, USAED, Mobile, and Dan Parrott, Chief, Civil Programs and Project Management Branch, USAED, Savannah. The local sponsor was the city of Tybee Island, GA. Report technical review was provided by Julie Dean Rosati, CHL; Lynn M. Bocamazo, USAED, New York; and Dr. Kevin Bodge, Olsen Associates, Inc.

The study was a collaborative effort by Dr. Jane McKee Smith, Coastal Processes Branch, CHL; Dr. Donald K. Stauble, Coastal Engineering Branch, CHL; and Brian P. Williams and Michael J. Wutkowski, Coastal, Hydrology, and Hydraulics Section, USAED, Wilmington. This study was performed under the general supervision of Ty V. Wamsley, Chief, Coastal Processes Branch, CHL; Bruce A. Ebersole, Chief, Flood and Storm Protection Division, CHL; Dr. William D. Martin, Deputy Director, CHL; and Thomas W. Richardson, Director, CHL.

COL Richard B. Jenkins was Commander and Executive Director of ERDC. Dr. James R. Houston was Director.

1 Introduction

Congress authorized construction of the Federal navigation project at Savannah Harbor, which began in 1874 with channel dredging. The Savannah River empties into the Atlantic Ocean on the border between Georgia and South Carolina. The shoreline is composed of several short barrier islands known as the Sea Islands along the Georgia Bight, an embayment in the north-south orientation of the coast (Figure 1-1). The main barrier islands to the north of the Savannah River entrance are Hilton Head, Daufuskie, and Turtle. Calibogue Sound is a north-south oriented inlet separating Hilton Head Island from the embayed Daufuskie Island. The New River entrance bisects Daufuskie and Turtle Islands. The Wright River entrance separates Turtle Island from Oyster Bed Island. The main navigation channel of the Savannah River is south of Oyster Bed Island.

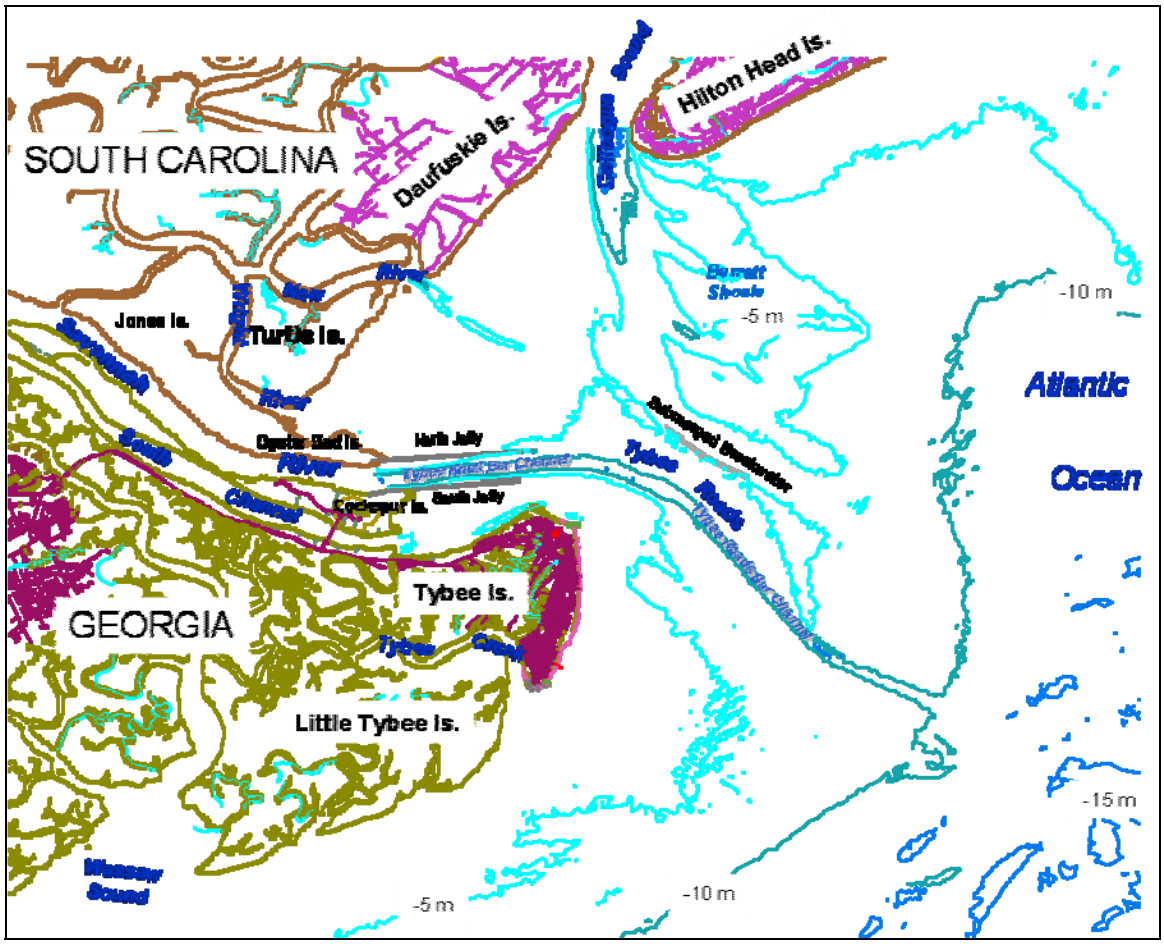

Figure 1-1. Location map of the Savannah River entrance.

Cockspur Island separates the main navigation channel from the South Channel of the Savannah River. Tybee Island is located to the south of the Savannah River entrance. Tybee Creek separates Tybee from Little Tybee Island to the south. The large Wassaw Sound is located to the south of Little Tybee Island.

As part of the Federal Project, two 3,660-m- (12,000-ft-) long jetties were constructed at the mouth of the Savannah River entrance to stabilize the two river channels (Savannah River and South Channels, Figure 1) and their associated sand bars. The North Jetty was completed in 1890 (Oyster Bed Jetty) and the South Jetty was completed in 1896 (Cockspur Jetty) (Sargent 1988). In 1897, a submerged offshore breakwater was completed at the south end of Barrett Shoals to provide a shelter for vessels entering Tybee Roads. The earliest record of dredging was in 1910 (Figure 1-2).

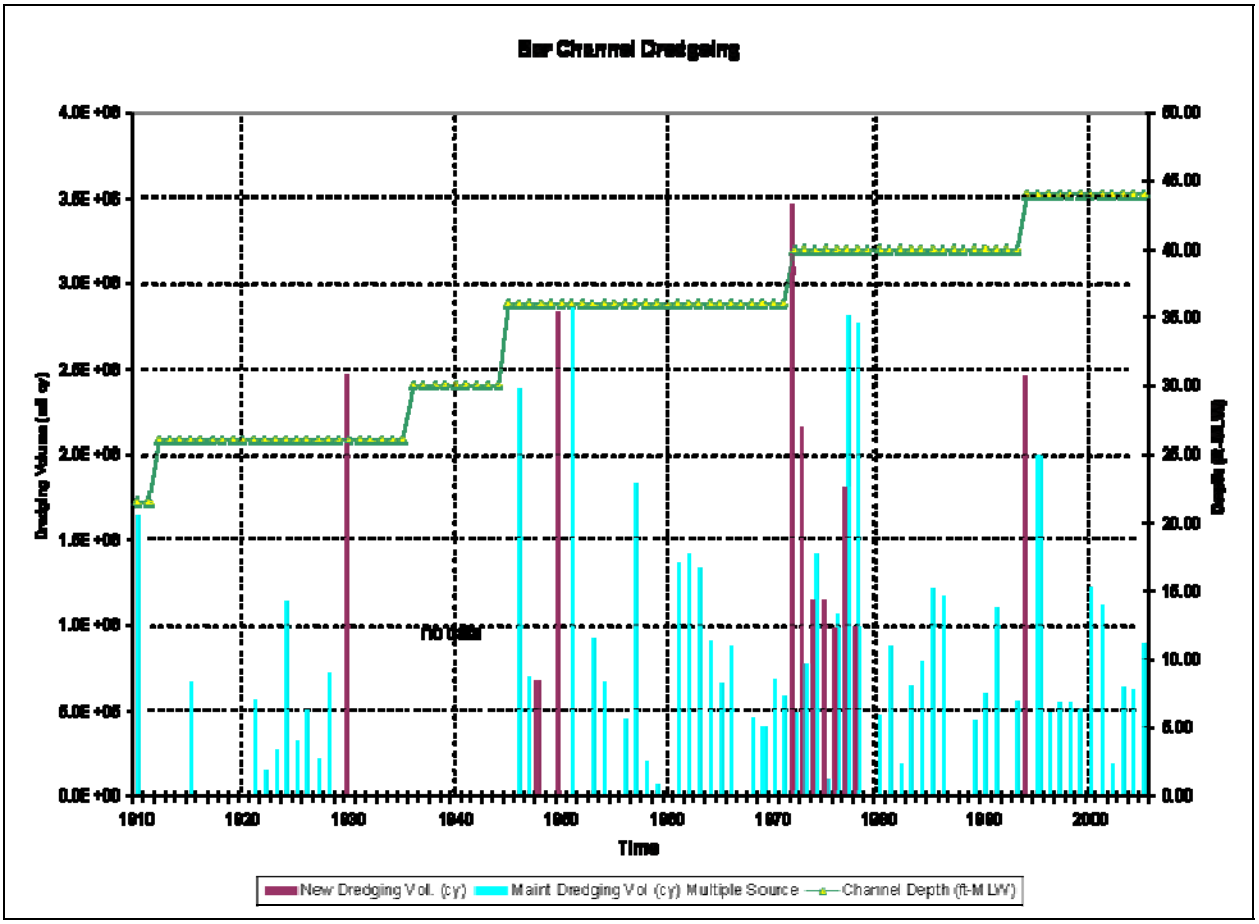

Figure 1-2. Plot of navigation channel depth and dredging volumes with time for the Savannah River Bar Channel.

The navigation channel of the Savannah River was deepened from 21.5 ft mean low water (MLW) to a depth of 26 ft MLW in 1912 to accommodate larger ships. Navigable depth was increased in 1936 to 30 ft MLW and in 1945 to 36 ft MLW. The channel was widened and deepened in 1972 to a depth of 40 ft MLW. In 1994, the authorized depth of the channel was increased to 44 ft MLW. At present, the navigation channel extends approximately 31 miles from Savannah Harbor adjacent to the City of Savannah down river to the entrance just east of Fort Pulaski on Cockspur Island and across Tybee Roads into the Atlantic Ocean. Most dredged material was placed in an Offshore Dredge Material Disposal Site (ODMDS). Construction and maintenance of the Federal navigation channel at Savannah Harbor has resulted in disruption of sediment transport pathways across Tybee Roads. The magnitude and frequency of channel dredging indicates that the Savannah River entrance channel is an efficient trap for wave- and current-induced sediment transport. The mean tidal range in this region is equal to 6.91 ft (2.11 m) (Fort Pulaski tide gauge).

Tybee Island, located directly downdrift of the Savannah Harbor navigation channel has experienced shoreline recession, particularly along the north-south oriented oceanfront between 1st St. and 6th St. To mitigate for this erosion, several shore protection structures were built at various places along the beach since 1912 with various results as summarized in Ortel et al. (1985) (Figure 1-3). The latest shore protection efforts include a beach nourishment project that placed sand on the beach at four separate times from 1986 to 2000. An 800-ft-long north terminal groin was constructed in 1975 to trap sand that is being transported to the north. A 600-ft-long south terminal groin was constructed in 1986–87 to trap and hold fill sand on the southern end of Tybee Island. Erosion south of this groin required construction of two additional T-head groins and an L-head terminal groin further to the south in 1994 to retain sand at the very southern end of the island.

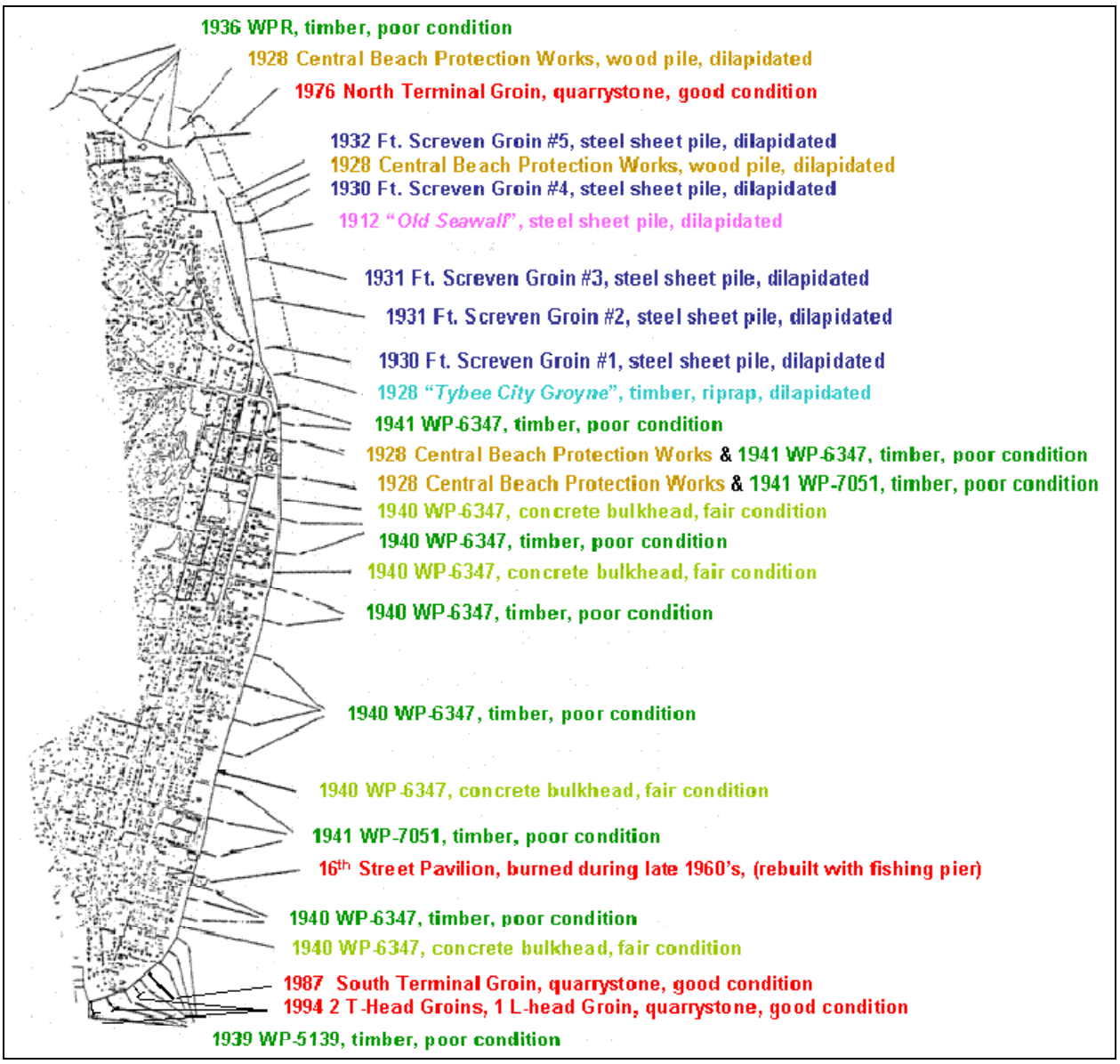

Figure 1-3. Historical shore protection structures used along Tybee Island, GA (after Oertel et al. 1985).

The purpose of this study is to determine if the Savannah Harbor Deep Draft Navigation Project is adversely impacting or has in the past adversely impacted the shores of Tybee Island (including sand lost from the beach and the Tybee shelf). Congress authorized construction of the Federal navigation project at Savannah Harbor, which began in 1874 with channel dredging. The construction of two jetties at the mouth of the Savannah River entrances was completed in 1896, and an offshore breakwater was completed in 1897 at the south end of Barrett Shoals. The navigation channel has been dredged annually and deepened several times to its present configuration.

The methodology used in this study included both numerical modeling and sediment budget components. The modeling included waves, currents, water levels, and sediment transport rates for pre-project bathymetry and post-project bathymetry. The model output is used to identify sediment pathways and changes to wave, current, and sediment transport patterns as a result of the project. Sediment budgets were developed for pre-project and post-project conditions. The sediment budget is an accounting of sediment transport pathways and magnitudes in the pre- and post-project time periods. The budgets are the key elements for assessing the impact of the project. The accuracy of the sediment budgets is dependent on the quality and quantity of the bathymetry and shoreline data available for the region. Sediment budgets were developed for the period 1854 to 1897 (pre-project) and 1897 to 2005/06/07 (post-project). These dates were chosen based on the best available survey data. Data from other time periods were used to augment these data where gaps existed. Bathymetry changes were calculated over both of these time periods. As documented in the channel-deepening report in 2006 (Smith et al. 2006), the post-project bathymetry change shows a pattern of ebb shoal deflation on the Tybee shelf, which is a typical consequence of jetty construction and channel deepening. The ebb shoal deflation resulted from sediment pathways across the channel being disrupted. The major impact of the project is the loss of sand from the Tybee shelf. The ebb shoal deflation also resulted in shoreline change on Tybee Island, including erosion on the northern end of the island and accretion on the southern end of the island. Beach nourishment has also added sand to the beach which has been reworked by coastal processes.

The impact of the project is evaluated as the difference in volume loss rates (post-project minus pre-project) for the Tybee Island shelf cell of the sediment budget plus the estimated shoreline change rate (converted to a volume). The Tybee shelf is part of a large ebb shoal complex associated with the Savannah River inlet. Ebb shoals form as a balance of sediment that is jetted out of an inlet by offshore (ebb) currents and sediment that is returned to the inlet by onshore (flood) currents and waves. Ebb shoals are the pathway for sediment to travel around an inlet to the downdrift beaches (and updrift beaches, during periods of reversal in sediment transport direction) (Tybee Island and Oyster Bed Island, respectively). Disruption of these pathways and deflation of the ebb shoal lead to erosion of the downdrift (and possibly updrift) beaches because natural sand bypassing around the inlet is interrupted. The estimated combined shelf and shoreline impact at Tybee Island is 73.6 percent (including the effect

of the beach fill placement) or 78.5 percent (excluding the effect of the beach fill placement) (±20 percent). This means that an estimated 73.6 percent (or 78.5 percent) of the reduction in sand volume on the Tybee shelf and shoreline is due to the project, with the remainder of the erosion attributed to the natural processes. The reduction in sand volume has occurred mainly on the Tybee shelf, with both losses and gains of sand on the Tybee beaches (north and south, respectively). This report documents the full analysis.

Chapter 2 of this report describes the bathymetry and shoreline data, volume change analysis, and the pre- and post-project sediment budgets. Chapters 3–5 describe the numerical modeling of circulation, waves, and sediment transport, respectively. Chapter 6 concludes with the summary of the project impact.

2 Shoreline and Volume Change Analysis

This chapter investigates the long-term trends at Savannah River entrance to place the Federal navigation project in perspective. The goals are to assess the impact of the Savannah Harbor navigation project on the regional morphology and to quantify the influence of the navigation project on losses along Tybee Island and the Tybee shelf. These impacts will be quantified through a combination of shoreline change analysis, bathymetric volume change calculations, and hydrodynamic and sediment transport modeling (Chapters 3–5).

Data available for the Savannah entrance prior to the navigation project include National Oceanic and Atmospheric Administration (NOAA) National Ocean Survey (NOS) topographic and hydrographic surveys (known as T-sheets and H-sheets, respectively). All survey data from the 1800s are likely to have a high degree of error. Therefore, regional volume and shoreline change trends were characterized over as long of a period as possible to minimize errors in the analyses. Additional charts were scanned to provide more pre-project information. Additional bathymetric and shoreline data were collected in 2005, 2006, and 2007 to update the present conditions, and allow comparisons with historic data. Although dredging was authorized in 1874, the locations and dredged volumes are not documented. It is assumed that these dredged volumes were small and located within the inner harbor (ATM 2001) and have a minimal impact on Tybee Island. Based on the completion of the structures (1896 and 1897), documented channel deepening in the early 1900s, and the desire to minimize measurement error by extending over long periods of time, the pre-project time period was defined at 1854–1897 (43 years) and the post-project period as 1897–2007 (110 years).

Shoreline change analysis

Data were acquired from various sources to evaluate the shoreline change history of both Tybee Island on the Georgia side of Savannah River entrance and the three islands on the South Carolina side of the entrance.

Table 2-1 summarizes the MHW shorelines that were used in this study and the sources of the data. All of the early data were digitized field surveys from NOAA/NOS T-sheets. The USACE Savannah District (SAS) supplied some of the data from their digital files that were derived from the NOAA/NOS T-sheets. Additional charts were obtained in digital scanned form from NOAA, National Ocean Service, Office of Coastal Survey image archives of historical maps and charts, and the shorelines were digitized using the Diger 2 software at the Coastal and Hydraulics Laboratory (CHL). Some of the shorelines were digitized by Coastal Carolina University from paper maps from a previous joint NOAA/CERC (Coastal Engineering Research Center) shoreline movement study covering Tybee Island Georgia to Cape Fear, North Carolina (Anders et al. 1990). These shorelines were compiled by NOAA from field survey T-sheets, and the 1982 shoreline was from aerial photography and is archived at the USACE CHL. The U.S. Geological Survey (USGS) completed a study on long-term shoreline change along the Southeast Atlantic coast using four shoreline periods to calculate change rates (Miller et al. 2005). This analysis used the NOAA/CERC shorelines from 1863, 1920 (South Carolina beaches only) and 1963 shorelines, and NOAA T-sheets from 1925 for Georgia beaches (Tybee Island). The 1999 Georgia and 2000 South Carolina shorelines were derived from LIDAR surveys conducted by the USGS. SAS supplied a set of beach profiles surveyed in February 2005. An additional set of profile surveys were collected for this study by SAS in March 2007 and sent to CHL for processing. The MHW shoreline was derived from the MHW elevation of 0.94 m (3.07 ft) above North American Vertical Datum 1988 (NAVD88) from each profile data set based on the NOAA Tide Station 8670870 at Fort Pulaski, located on Cockspur Island at the mouth of the Savannah River. The MHW shoreline was contoured using ArcView GIS software. A digital aerial photograph flown in October 2005, with a resolution of 1 ft, was supplied by Wilber Wiggins of SAS. A visual shoreline was digitized off the high-resolution air photo in the GIS using the local high water mark visible on the air photo.

Table 2-1. Historic shorelines used in report.

Date	Georgia	Source	South Carolina	Source
1854	x	SAS	x	SAS
1863	x	USGS NOAA/CERC	x	USGS NOAA/CERC
1867	x	NOAA Coast Chart 440	x	NOAA Coast Chart 440
1873	x	NOAA Coast Chart 55	x	NOAA Coast Chart 55
1899	x	NOAA Coast Chart 156	x	NOAA Coast Chart 156
1900	x	SAS		
1910		NOAA Coast Chart 155	x	NOAA Coast Chart 155
1920	x	SAS	x	SAS/USGS
1925	x	USGS		
1964	x	NOAA/CERC	x	USGS NOAA/CERC
1970			x	NOAA/CERC
1971	x	USGS		
1982/84			x	NOAA
1992		NOAA		
1993	x	SAS	x	SAS
1997	x	SAS	x	SAS
1999	x	USGS LIDAR		
2000			x	USGS LIDAR
2005	x	Profiles - Feb Air Photo Oct - SAS		
2007	x	Profiles - SAS		

The 1854 pre-jetty through 1925 post-jetty historical shoreline positions generated for this study for Tybee Island are shown in Figure 2-1. The shoreline position was relatively stable from 1854 to 1873. A distinct change in shoreline orientation can be seen between the 1873 shoreline and the 1899 shoreline. A bulge in the northern Tybee shoreline evident in the 1854 to 1873 shoreline was removed by landward retreat of the north end of the island by 1920. The loss of this large volume of sand is likely due to changes in the transport patterns due to the project. The circulation and sediment transport modeling (Chapters 3 and 5, respectively) show a pre-project gyre in this area that pushes sediment from the shallow South Channel back toward the beach. The gyre is pushed north post-project and cannot effectively circulate sediment out of the deepened channel.

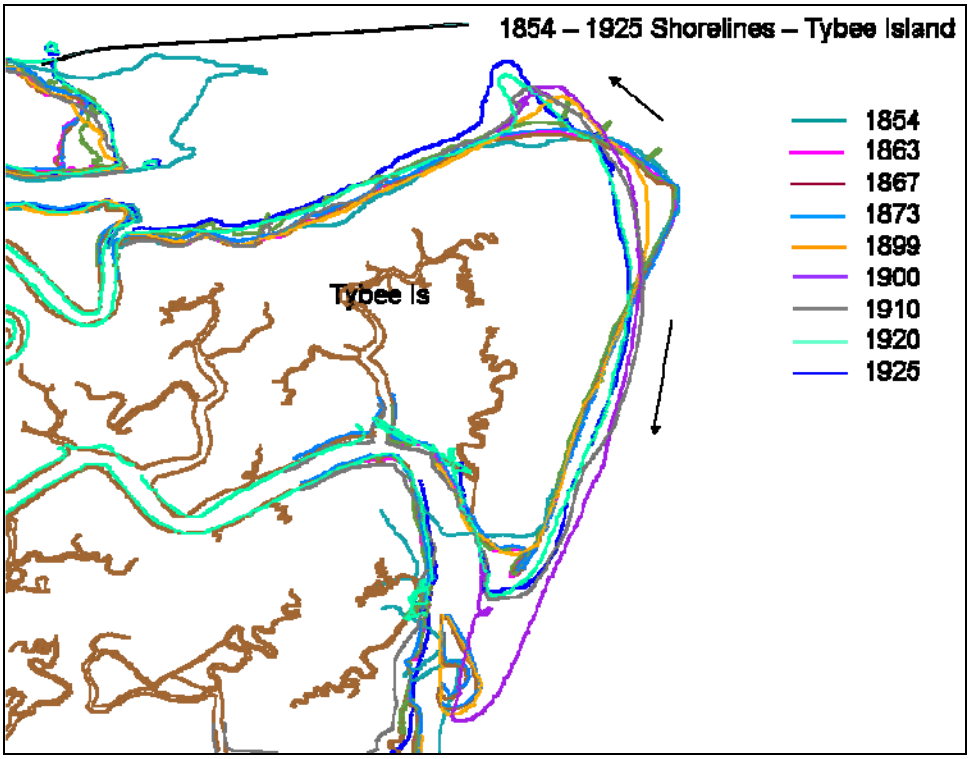

Figure 2-1. Pre-project historical shoreline positions along Tybee Island showing erosion of bulge at north end.

Increased hurricane activity at that time may have also contributed to the erosion of the bulge. The island grew southward at its southern tip and accreted seaward south of the budge at the same time as the ocean shoreline was reorienting itself between 1899 and 1925. The northern end of the island also expanded to the north and west. A more detailed look at the shoreline change over time at the northern end of Tybee is illustrated in Figure 2-2. The general trend is for the north tip of Tybee Island to migrate northward into the southern channel of the Savannah River and also to progressively move westward over time.

The central portion of Tybee Island has shown erosion of the bulge between 1867 and 1899 thru 1900, 1910, and 1920 to 1925 with a movement of sand in this central portion of the island mostly to the south. A "hot spot" (region of increased erosion) is located between 1st St. and 6th St. where the shoreline has rotated around a nodal point in the vicinity of 2nd St. (Figure 2-3). South of the nodal point the shoreline has moved seaward over time. The southern part of the island has grown to the south and seaward over the historic period with the most change taking place between 1899 and 1925 (Figure 2-4). After 1925, the shoreline position was more stable, with the most marked changes due to the construction of structures and beach fill placement (Figure 2-5).

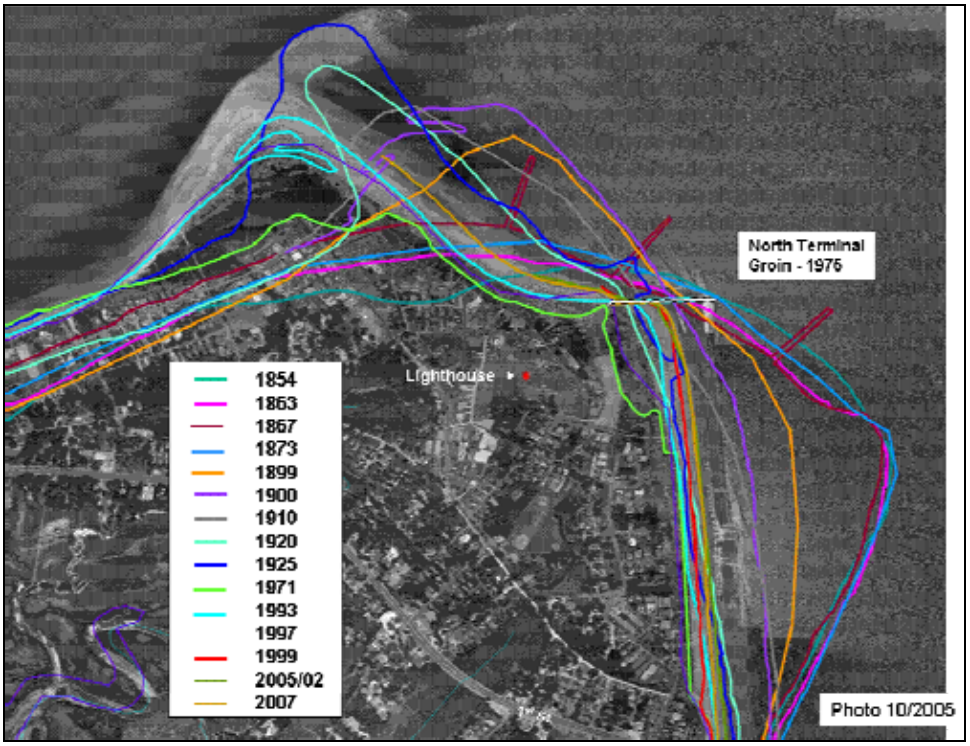

Figure 2-2. Historical shoreline positions along the northern portion of Tybee Island.

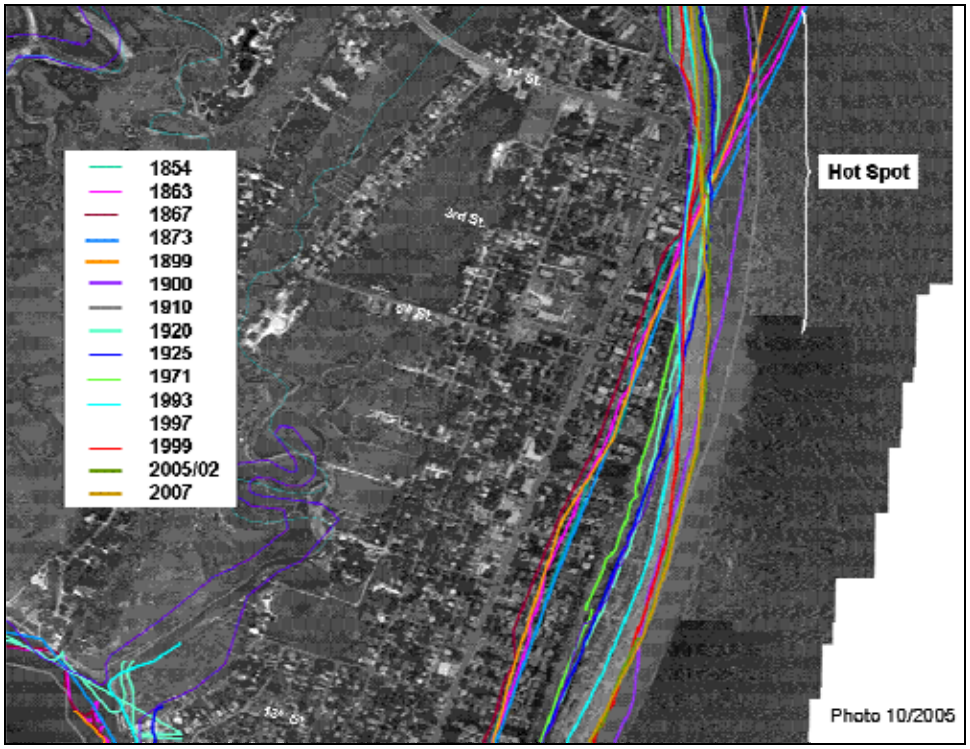

Figure 2-3. Historical shoreline positions along central Tybee Island in the vicinity of the hot spot.

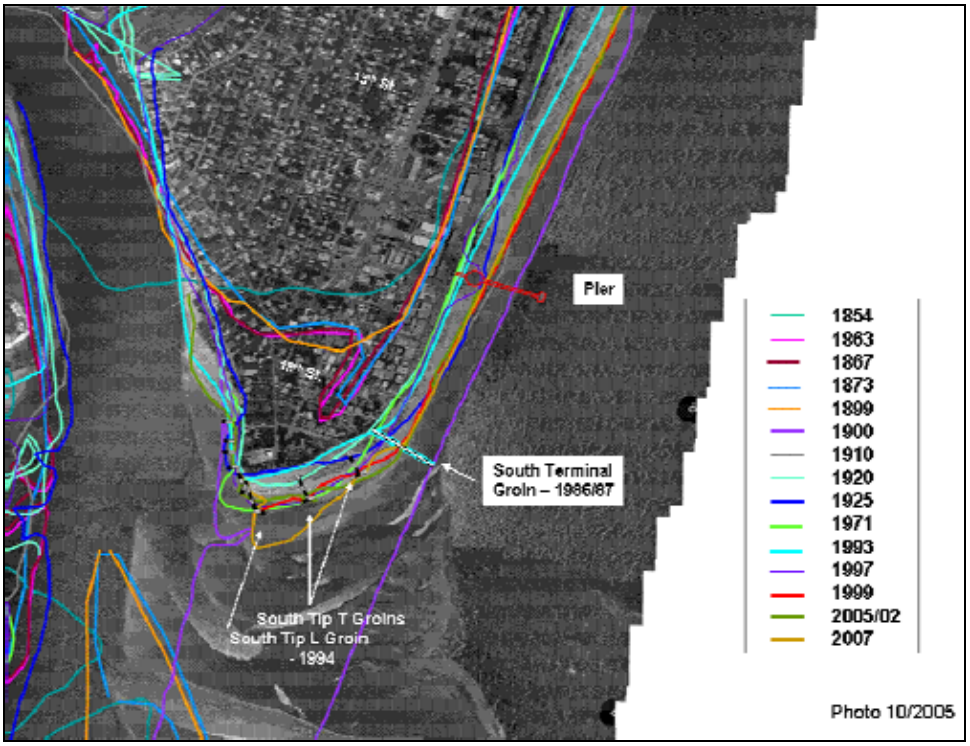

Figure 2-4. Historical shoreline positions of the south end of Tybee Island.

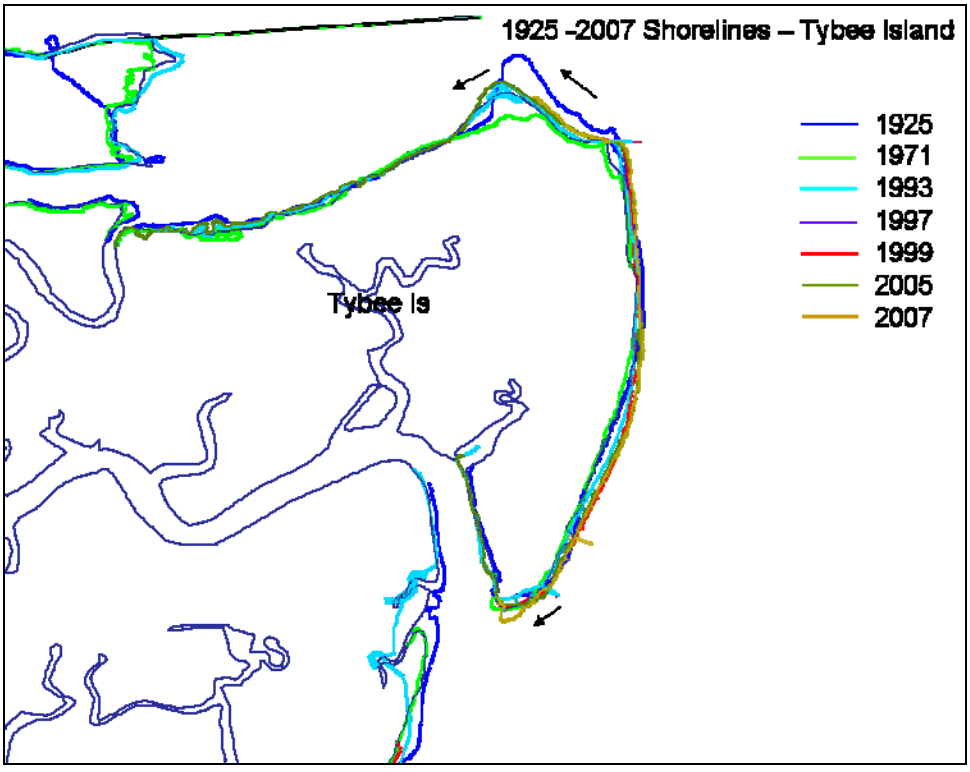

Figure 2-5. Shoreline change relative to recent beach fills and shore protection structure construction.

Shore protection and navigation channel projects are summarized in Table 2-2. Numerous seawall and groin structures were constructed from 1912 to 1941 to protect the upland from erosion as shown in Figure 1-3. In 1976 the north terminal groin was constructed and a 2.2 mil cu yd beach fill was placed on the beachfront from the groin south to 18th St. (Figure 2-6). The south terminal groin was constructed in 1986–87 and the north terminal groin was rehabilitated. A second 1.2 mil cu yd fill was placed on the beach between the two terminal groins at that time as well as placement of 0.157 mil cu yd of fill to the south of the south terminal groin. Fill material was placed between the north terminal groin and 3rd St. in 1993 to mitigate for the hot spot erosion. Erosion persisted at the south end of the island so two T-head groins and a L-head groin were constructed in 1994 south of the south terminal groin to help retain sand. In 1995, 0.285 mil cu yd of fill was placed on the southern end of the island between 13th St. and the south terminal groin and 50,000 cu yd of fill was placed between that groin and the L-head groin. Another 1.5 mil cu yd of fill was placed between the two terminal groins in 2000, with an additional 0.2 mil cu yd of fill placed between the south terminal groin and the L-head groin on the south end.

Table 2-2. Navigation and shoreline erosion control projects, Tybee Island vicinity.

Date	Construction
1874	Initial dredging of navigation channel to 15.5 ft MLW
1886–1896	Construction of North and South Jetties at entrance to Savannah R.
1896	Channel dredged to 19 ft MLW
1897	Construction of submerged offshore breakwater at Tybee Roads
1910	Dredging of navigation channel to 21.5 ft MLW
1912	Construction of steel pile old seawall 1st St. vicinity
1915	Navigation channel deepened to 26 ft MLW
1928	Construction of wood groins along beach
1930	Construction of 2 groins along Fort Screven beachfront
1931	Construction of 3 additional groins along Fort Screven beachfront
1936	Construction of wood groins by Works Progress Administration along beachfront
	Navigation channel deepened to 30 ft MLW
1937	Construction of wood groins by WPA along beachfront
1938	Construction of wood groins by WPA along beachfront
1939	Construction of wood groins by WPA along beachfront
1940	Construction of wood groins by WPA along beachfront
	Construction of concrete bulkhead (seawall) along ocean front
1941	Construction of wood groins by WPA along beachfront

Date	Construction
1945	Navigation channel deepened to 36 ft MLW
1964	Placed riprap in front of seawall
1972	Navigation channel deepened to 40 ft MLW
1975–1976	Construction of 800 ft long north terminal groin
	2.2 mil cu yd beach fill placed between north terminal groin and 18th St.
1986–1987	600 ft south terminal groin constructed
	North terminal groin rehabilitated
	1.2 mil cu yd fill placed between groins
	0.157 mil cu yd fill placed south of south terminal groin
1993–1994	1.5 mil cu yd Fill placed North Terminal Groin to 3rd St.
	Navigation channel deepened to 44 ft MLW
	South Beach 2 T-head groins and 1 L-head groin constructed
1995	0.282 mil cu yd fill placed between 13th St. and south terminal groin
	0.05 mil cu yd fill placed between south terminal groin and L-head groin
2000	1.5 mil cu yd fill placed between terminal groins
	0.2 mil cu yd fill placed between south terminal groin and L-head groin
Source: Oertel et al. 1985; Savannah District; ATM 2001.	

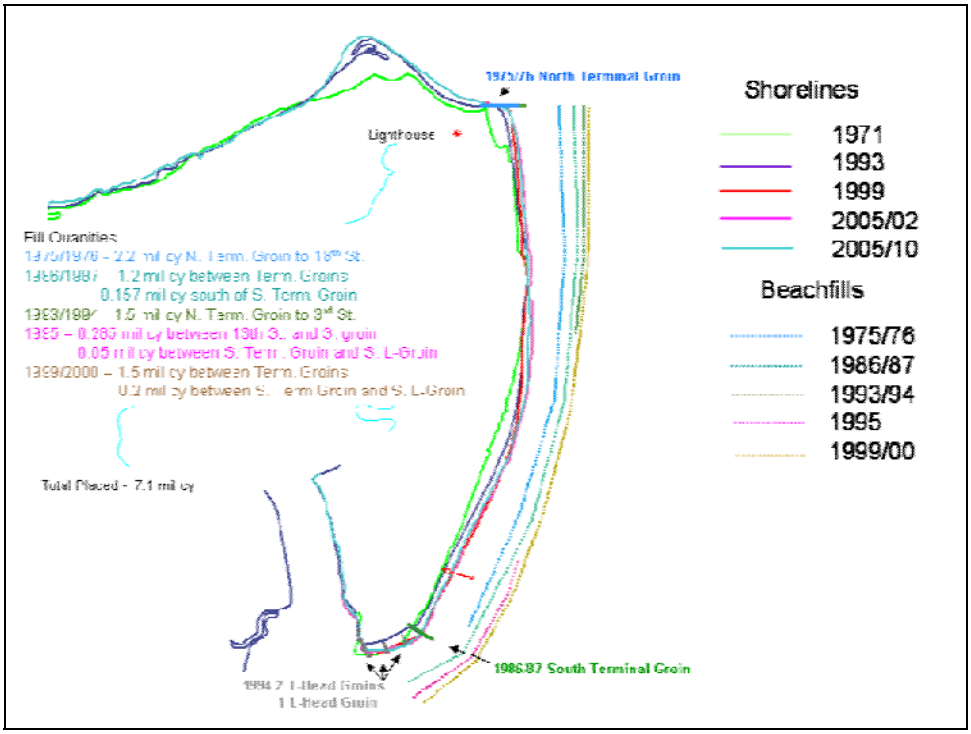

Figure 2-6. Shoreline change relative to recent beach fills and shore protection structure construction.

Bathymetry change analysis

Historic bathymetry was collected from several sources. ATM supplied bathymetry used in their report which contained a correction for sea level rise to the 1960–1978 tidal epic and a correction for each data set to the National Geodetic Vertical Datum 1929 (NGVD29) vertical datum for the dates 1854, 1897, and 1920. Additional historic bathymetric data sets were collected from NOAA's GEODAS database of NOS hydrographic surveys of coastal waters in the study area and were referenced either to MLW or mean lower low water (MLLW) depending on date of collection of either 1934, 1970–83 composite or 1994. The Savannah District supplied before and after dredging surveys, as well as surveys of the navigation channel and a February 2005 beach and nearshore survey. NOAA NOS provided some recent surveys of the channel area that they collected during 2006 for hazards to navigation requirements. A recent survey of the area off Tybee Island was lacking so in March 2007 the SAS Survey Section collected beach profiles and bathymetry lines of that area. The 2005 channel survey was combined with the 2006 NOAA spot surveys and the 2007 SAS surveys to produce a composite bathymetry of the recent sea bed and beach off Tybee.

Table 2-3 summarizes the historic bathymetric data sets used in this study. In order for all data to be converted to a common datum of NAVD88 meters vertical datum using the latest NOAA tidal epoch of 1983–2001 and latitude/longitude NAD83 horizontal datum, several conversions were required. This effort was needed to allow comparisons and change analysis. The early historical data collected before the NGVD29 vertical datum was established by NOAA required several steps to convert the depth readings data to the common datum. A technique was used based on suggestions from NOAA NOS (James Hubbard, NOAA-NOS, personal communication, 15 April 2005). The best way to compute the 1854, 1867, 1873, 1897, 1899, 1910, and 1920 bathymetry sets in the vicinity of Tybee Island was to apply a reverse sea level trend using the NOAA NOS Fort Pulaski Tide Gauge Station 8670870 located at the mouth of the Savannah River (Figure 2-7). The sea level trend for that station was downloaded from NOAA sea level online and is shown in Figure 2-8 where the tidal level recorded starts in 1935 and extends to 1999. The sea level rise trend computed from NOAA at this station is 3.05 mm/yr (0.01 ft/yr) for the 64 years of record. The sea level correction was applied to each data set (1854, 1867, 1873, 1897, 1910 and 1920) that was older than the NGVD29 datum as listed in Table 2-3. The data supplied by ATM were

Table 2-3. Historic bathymetry data sets.

Date	Source	Original Data	Vertical Conversion	Horizontal Conversion	Remarks
Hydrographic Survey					
1854	ATM	H439	Back convert NGVD29 to NAVD88	GA State Plane East to Lat/Long NAD83	-1.59 m SL corr
1867	NOAA Archives	H-440	Convert from chart MLW to NAVD88	Lat/Long NAD27 to NAD83	-1.55 m SL corr.
1873	NOAA Archives	CP975 (H-55)	Convert from chart MLW to NAVD88	Lat/Long NAD27 to NAD83	-1.53 m SL corr
1897	ATM	H-2296	Back convert NGVD29 to NAVD88	GA State Plane East to Lat/Long NAD83	-1.46 m SL corr
1899	NOAA Archives	CP2534 (H-156)	Convert from chart MLW to NAVD88	Lat/Long NAD27 toNAD83	-1.45 m SL corr
1910	NOAA Archives	CP2990 (H-155)	Convert from chart MLW to NAVD88	Lat/Long NAD27 to NAD83	-1.42 m SL corr
1920	ATM	H-4154	Back convert NGVD29 to NAVD88	GA State Plane East to Lat/Long NAD83	-1.39 m SL corr
1931–34	NOAA-GEODAS	H05592 - 03F11085 1934	Convert from MLW to NAVD88	Lat/Long NAD27 to NAD83	Covers Savannah River Entrance area only - not used
		H05571 - 03F11218 1934	Convert from MLW to NAVD88	Lat/Long NAD27 to NAD83	
1973–80	NOAA-GEODAS	H09197 - 03F12061 1971-73	Convert from MLW to NAVD88	Data supplied in Lat/Long NAD83	
		H09314 - 03081138 1973	Convert from MLW to NAVD88		
		H09144 - 03081139 1973	Convert from MLW to NAVD88		
		H09459 - 03F12085 1974	Convert from MLW to NAVD88		
		H09865 - 03141047 1980	Convert from MLLW to NAVD88		
1994–95	NOAA-GEODAS	H10577 – 03081184 1994	Convert from MLLW to NAVD88	Data supplied in Lat/Long NAD83	Coverage only of southern half of study area – not used
		H10582 – 03081186 1994	Convert from MLLW to NAVD88		
		H10591 – 03081187 1994	Convert from MLLW to NAVD88		
		H10629 – 03081195 1995-95	Convert from MLLW to NAVD88		
		H10631 – 03081197 1994	Convert from MLLW to NAVD88		

Date	Source	Original Data	Vertical Conversion	Horizontal Conversion	Remarks
Hydrographic Survey (cont.)					
2006	NOAA NOS	H11466	Convert from MLLW to NAVD88	GA State Plane East to Lat/Long NAD83	
		F00501a	Convert from MLLW to NAVD88	GA State Plane East to Lat/Long NAD83	
		F00501c	Convert from MLLW to NAVD88	GA State Plane East to Lat/Long NAD83	
		Fortune Epoch Grounding	Convert from MLLW to NAVD88	GA State Plane East to Lat/Long NAD83	
Channel Surveys Only					
17–18 Dec 1998	SAS	bd_99.xyz (not used)	Convert from MLW to NAVD88	GA State Plane East to Lat/Long NAD83	Before Dredge
Jan, Feb, Apr 1999		ad-99.xyz (not used)	Convert from MLW to NAVD88	GA State Plane East to Lat/Long NAD83	After Dredge
Jan, Feb 2000		bd_00.xyz (not used)	Convert from MLW to NAVD88	GA State Plane East to Lat/Long NAD83	Before Dredge
Sep-2005		exam-savhbar-sept2005.xyz	Convert from MLLW to NAVD88	GA State Plane East to Lat/Long NAD83	Exam Survey
Profile Surveys					
Feb-2005	SAS	tybee-feb2005land.xyz profiles	Convert from MLLW to NAVD88	GA State Plane East to Lat/Long NAD83	Land Survey
		tybee-feb2005-1.xyz profiles	Convert from MLLW to NAVD88	GA State Plane East to Lat/Long NAD83	Boat Survey
Mar-2007	SAS		Convert from MLLW to NAVD88	GA State Plane East to Lat/Long NAD83	Land & Boat Survey

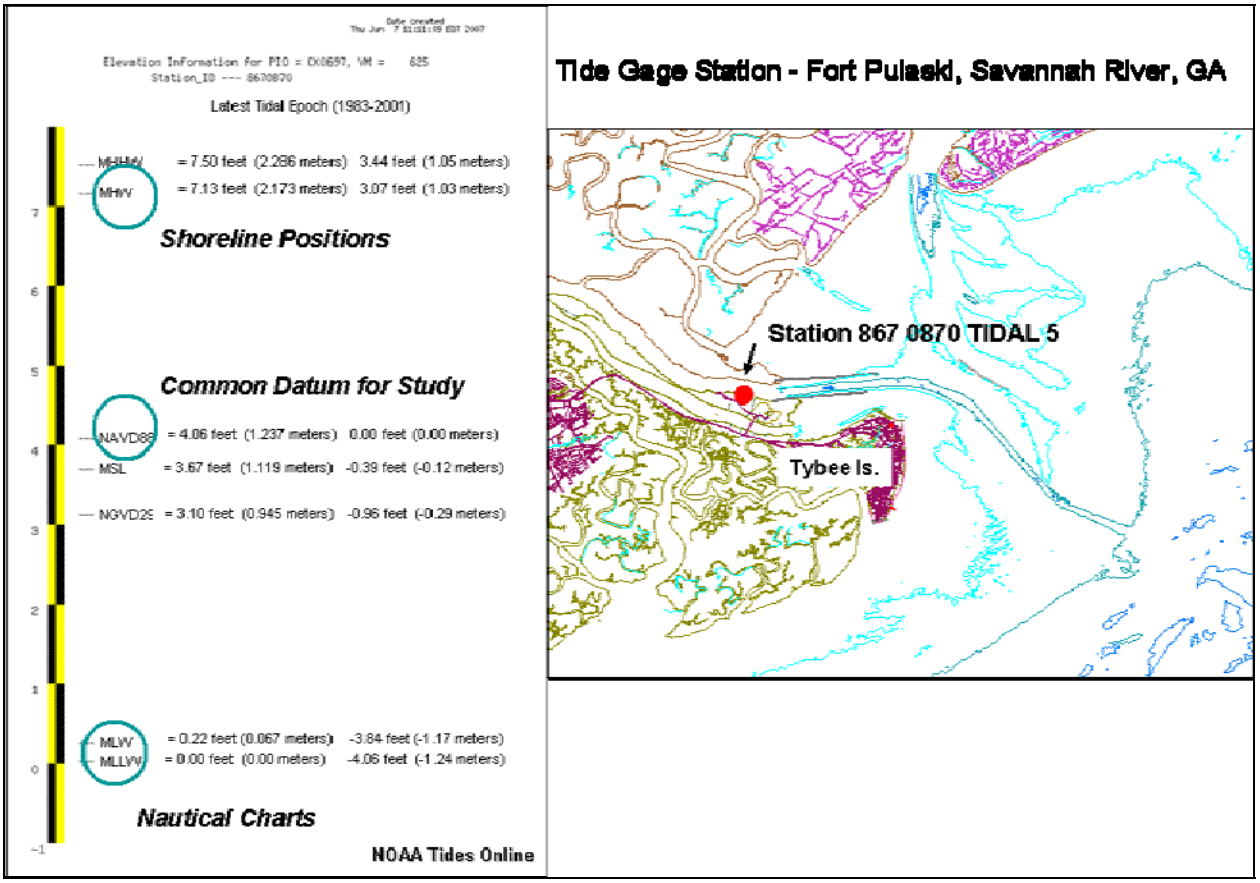

Figure 2-7. Location of tide gauge at Fort Pulaski and diagram of tidal range.

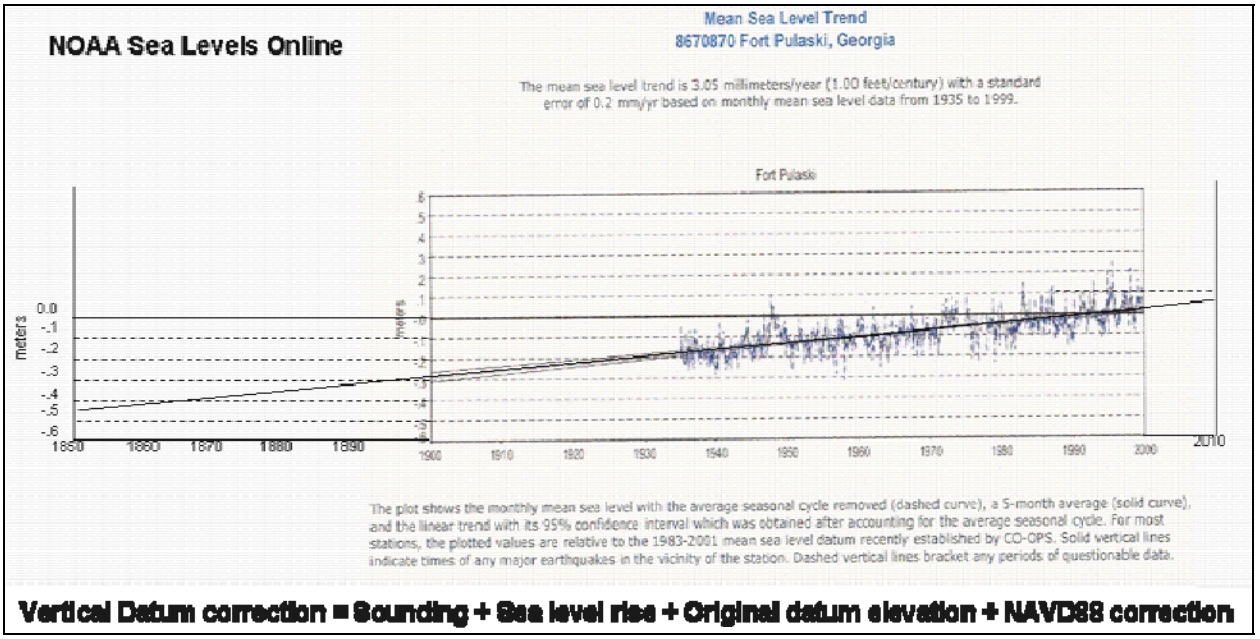

Figure 2-8. Plot of sea level rise at tide gauge station at Fort Pulaski.

back-converted from their original conversion to NGVD29 based on the old tidal epoch of 1960–1976 and shorter sea level rise record of 1935–1994 used in their report to NAVD88 using the new tidal epoch of 1983–2001 and sea level corrections were applied based on the latest 1935 to 1999 sea level rise record. Figure 2-9 shows the technique for digitizing the NOAA/NOS H-sheets and entering the data into the GIS. The data were then converted into a common horizontal and vertical coordinate system for cross comparison and change evaluation. Triangulated Irregular Networks (TINs or three-dimensional surfaces) were constructed for each date.

The first bathymetric data set available was collected in 1854. Figure 2-10 shows the pre-project nearshore bathymetry and natural channel orientations of the Calibogue Sound, New River, Wright River and Savannah River entrances (see Figure 1-1 for river/sound locations). The Calibogue Sound bisects into two channels with a small marginal flood channel next to Hilton Head Island. The New River channel is oriented to the south.

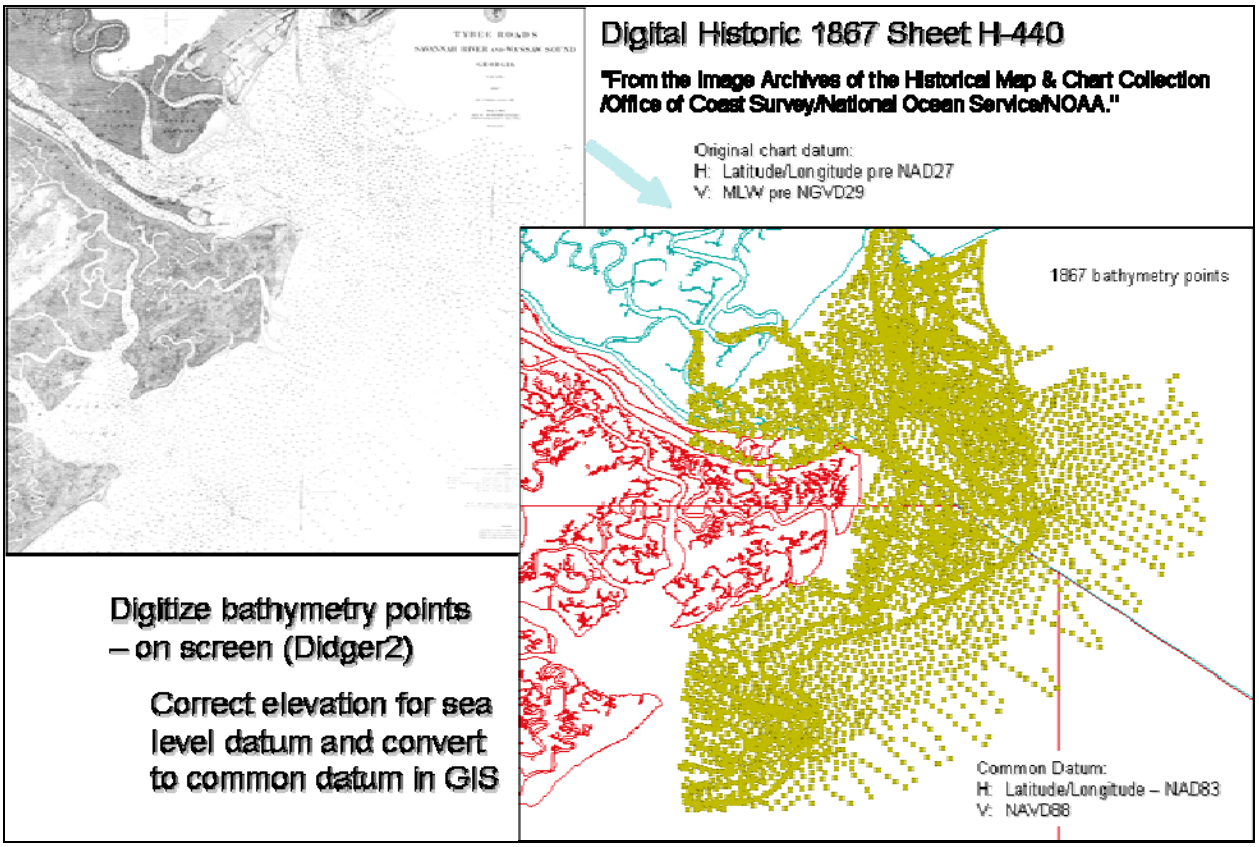

Figure 2-9. Process used to obtain early bathymetry data from digital NOAA H-sheets.

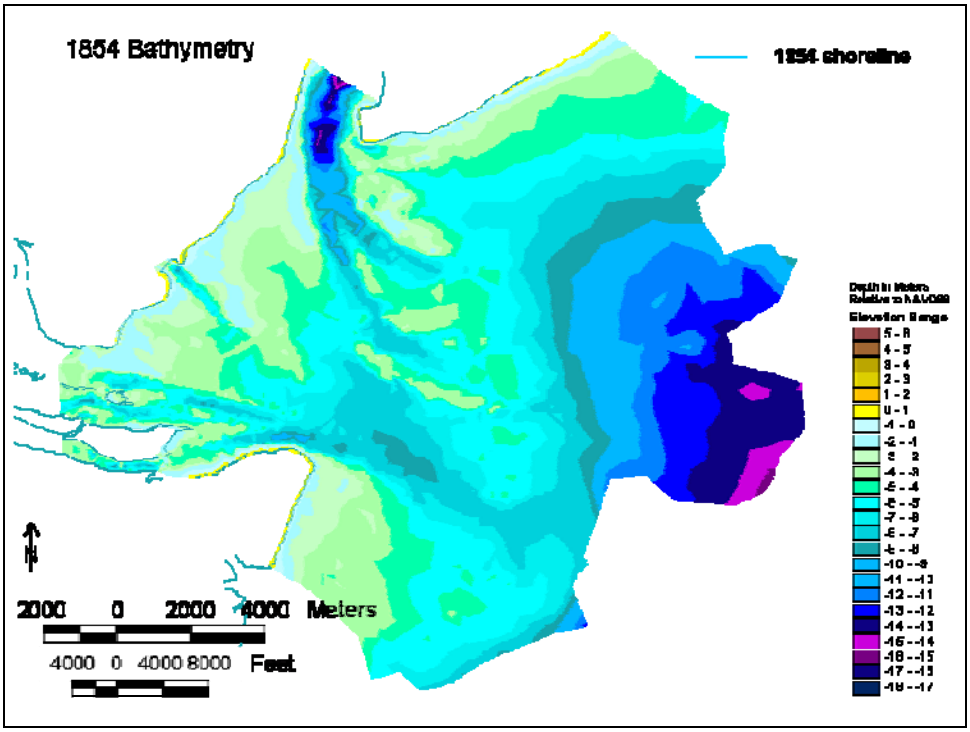

Figure 2-10. 1854 bathymetry representing the earliest pre-project conditions.

The Wright River and the Savannah River and South Channel all converge on one main channel in the vicinity of Tybee Roads. Figure 2-11 shows the 1867 bathymetry with a wide natural entrance channel opening into Tybee Roads (depths of 6 to 9 m (20 to 30 ft)) and wide shelf in front of Tybee Island (depths less than 5 to 6 m (16 to 20 ft)). Figure 2-12 depicts the bathymetry from the 1873 NOAA/NOS H-sheet, which also has a wide natural channel into the Savannah River. Both the main channel to the north and the southern channel are active with the channel cutting across Tybee Roads and Calibogue Sound/Savannah River entrance ebb delta complex. The shelf in front of Tybee Island is beginning to reorient to the south.

Figure 2-13 shows the 1897 bathymetry just after completion of jetty construction in 1896 at the entrance to the Savannah River and the 1897 submerged breakwater. The breakwater was constructed at the landward edge of the southern limit of Barrett Shoals (Figure 1-1). At this point in time, the structures have not yet begun to modify the bathymetry. The survey is limited in area but shows the South Channel and hints at the fact that the bulge still exists on the north end of Tybee Island and that the three channels of the Wright and Savannah Rivers still converge in Tybee Roads.

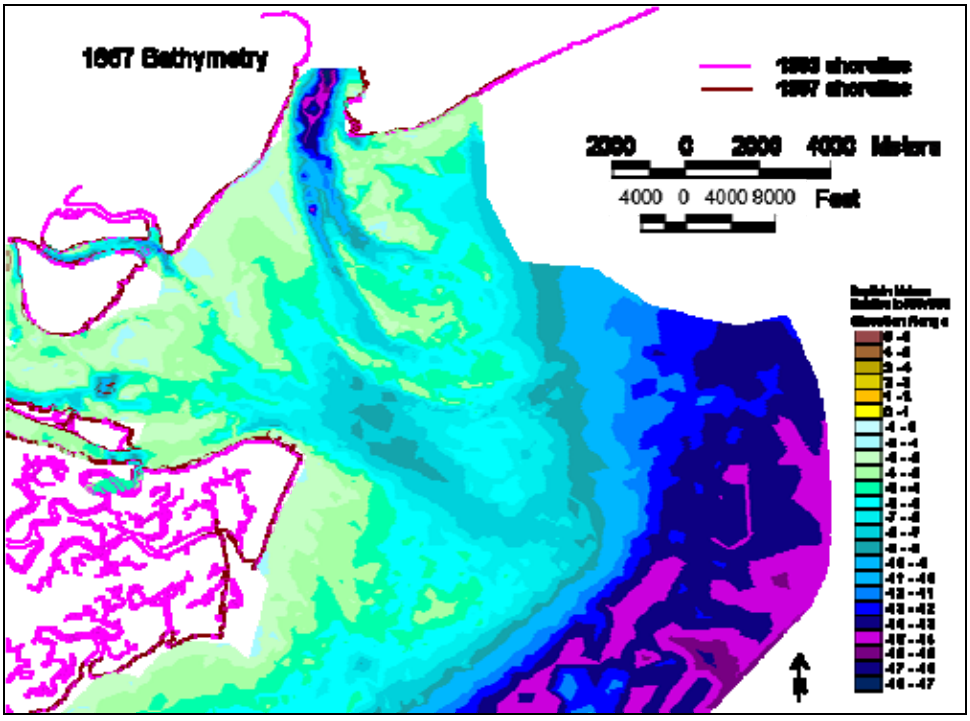

Figure 2-11. 1867 bathymetry representing pre-project conditions.

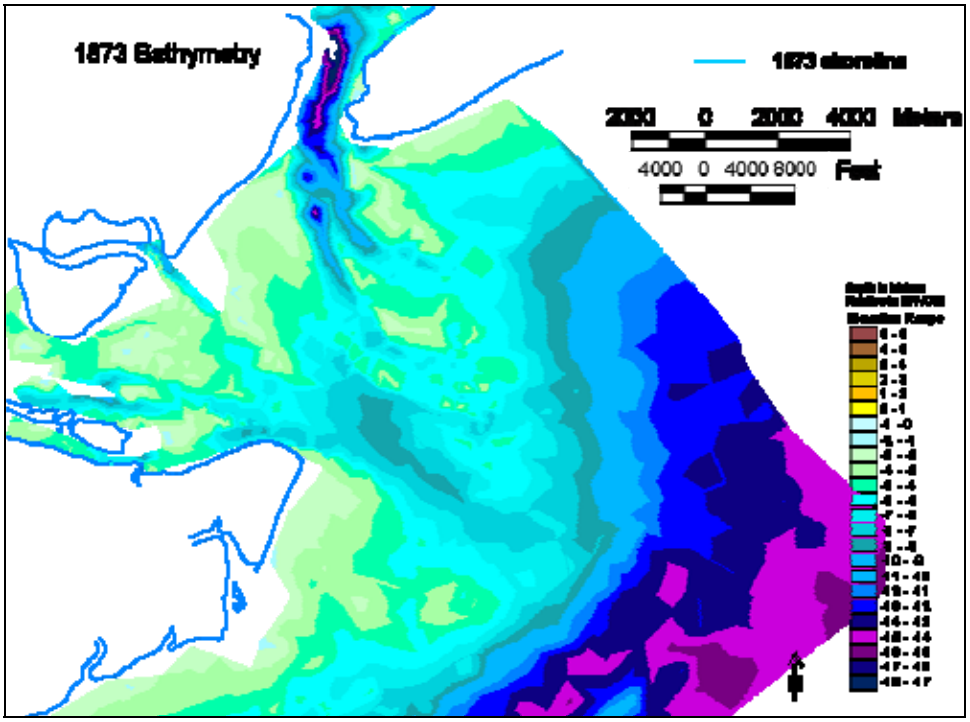

Figure 2-12. 1873 bathymetry representing pre-project conditions.

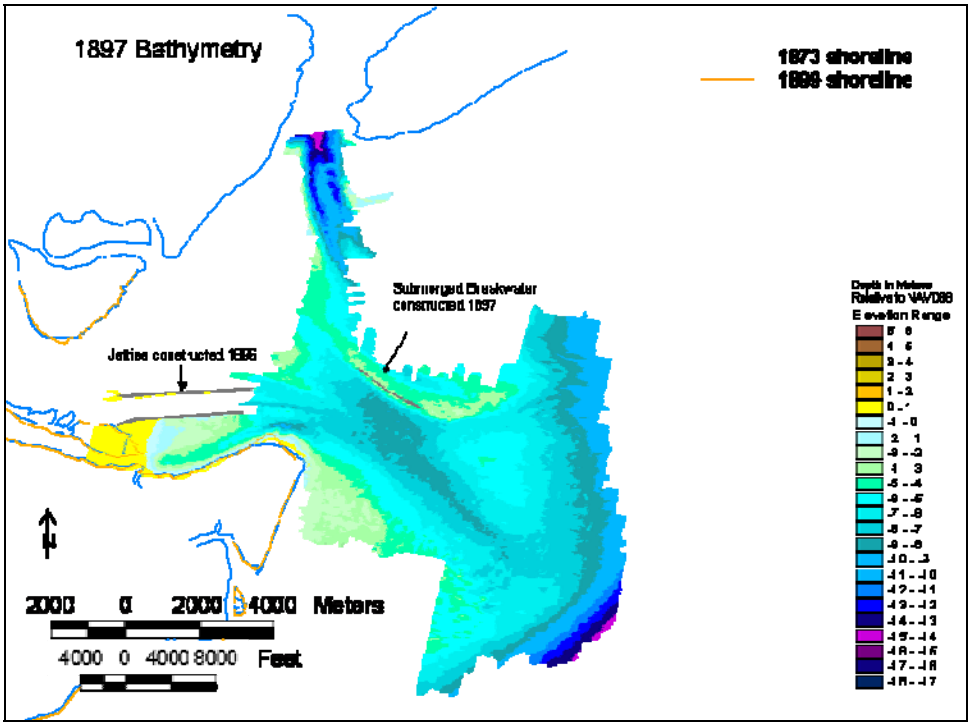

Figure 2-13. 1897 bathymetry representing the immediate post-jetty and submerged breakwater construction conditions.

A chart from 1899 (Figure 2-14) shows the southern half of the study area and the beginning of change in the orientation of the channel and Tybee Roads two years after jetty and submerged breakwater construction. The bulge on the north end of Tybee Island has now begun to erode (see Figure 2-1). By 1910 (Figure 2-15) the channel has orientated itself more to the southeast along the north end of the shelf in front of Tybee Island. The shoreline continues to erode along the north end of the island and the shelf has more of a triangular shape. The 1920 bathymetry is shown in Figure 2-16 and is limited in offshore coverage. This was the last survey that was corrected for sea level changes prior to the establishment of the National Geodetic Vertical Datum in 1929. Calibogue Sound channel has migrated to the south and has its distal limits controlled by the submerged breakwater which deflects the channel to the east. The jetties at the Savannah River entrance have caused this navigation channel to become the main channel with the South Channel shoaling as the north end of Tybee Island eroded. The 1920 shoreline shows a spit growing into the area formally occupied by the South Channel. The 1920 bathymetry shows deflation of the north Tybee shelf region along the south edge of the channel and accumulation in the north Tybee shoal. Results of the sediment modeling in Chapter 5 are consistent with these trends.

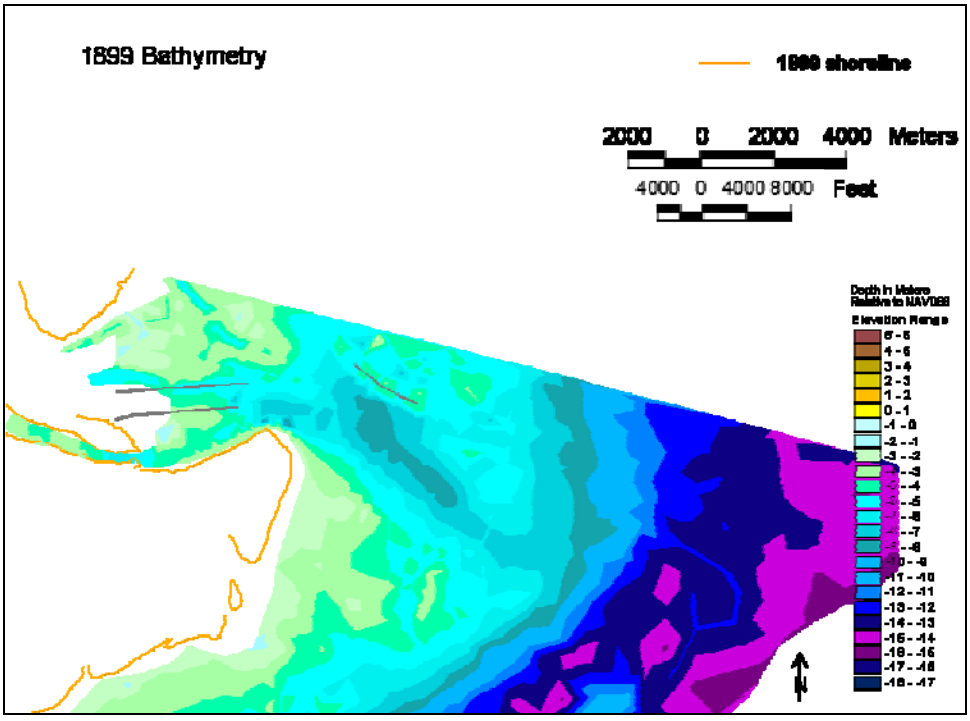

Figure 2-14. 1899 bathymetry representing conditions two years after jetty and submerged breakwater construction.

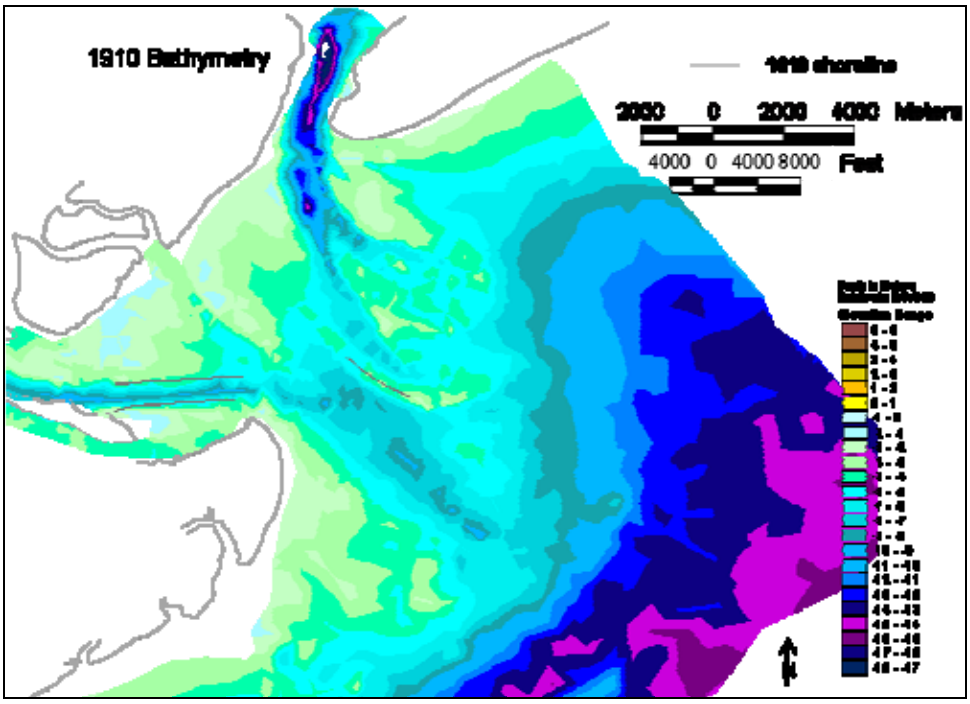

Figure 2-15. 1910 post-project bathymetry.

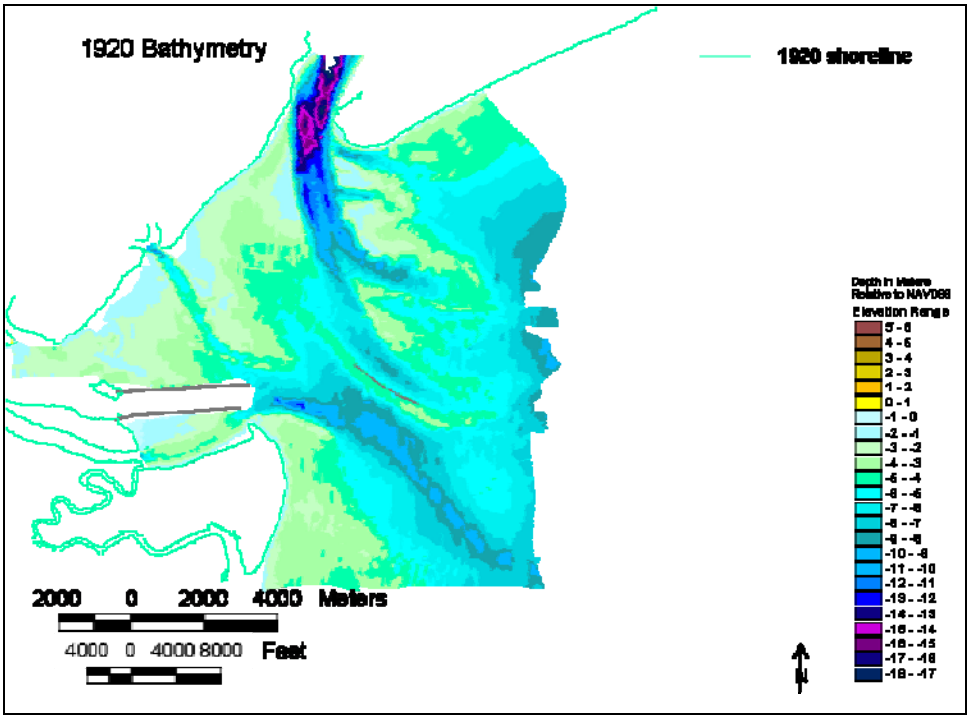

Figure 2-16. 1920 post-project bathymetry.

The 1934 data set was obtained from the NOAA NOS GEODAS online database, but the coverage was limited to the mouth of the Savannah River and was not used in analysis due to its limited area of coverage (Figure 2-17). The survey shows the establishment of a 7.9 m (26 ft) MLW depth dredged channel between the jetties on the North Channel of the Savannah River and the filling in of the South Channel at that time.

The next available data set in the area was a composite of four 1973 to 1974 bathymetric surveys as shown in Figure 2-18 from NOAA NOS down-loaded from their GEODAS database. A 1980/83 survey was also used to increase the coverage area to the south. The navigation channel is well established at this time and extends from the jetty out to the nearshore shelf. The channel is maintained to 12 m (40 ft) MLW at this time. The New River entrance channel has migrated northward and the Calibogue Sound Channel has migrated back to the north, leaving behind a cutoff channel just north of the submerged breakwater. The north Tybee shoal continues to grow, with accumulation north of the South Channel. Figure 2-19 shows more recent bathymetric surveys from the 1994/95 time frame, but it is limited in coverage to the southern portion of the study area. The channel is maintained at 13 m (44 ft) MLW at this time.

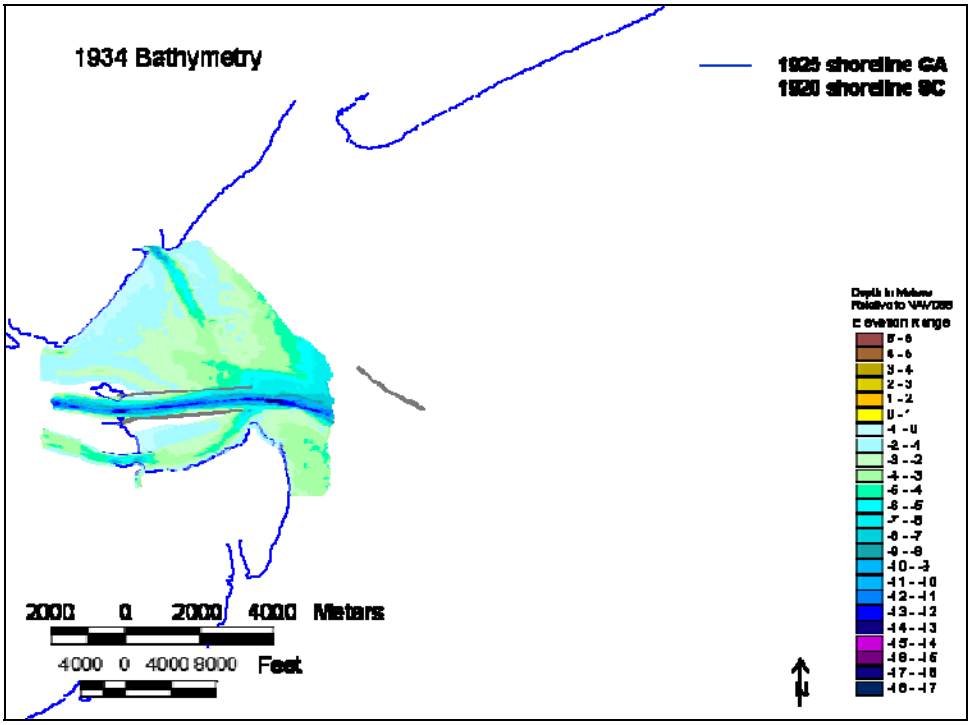

Figure 2-17. 1934 post-project bathymetry.

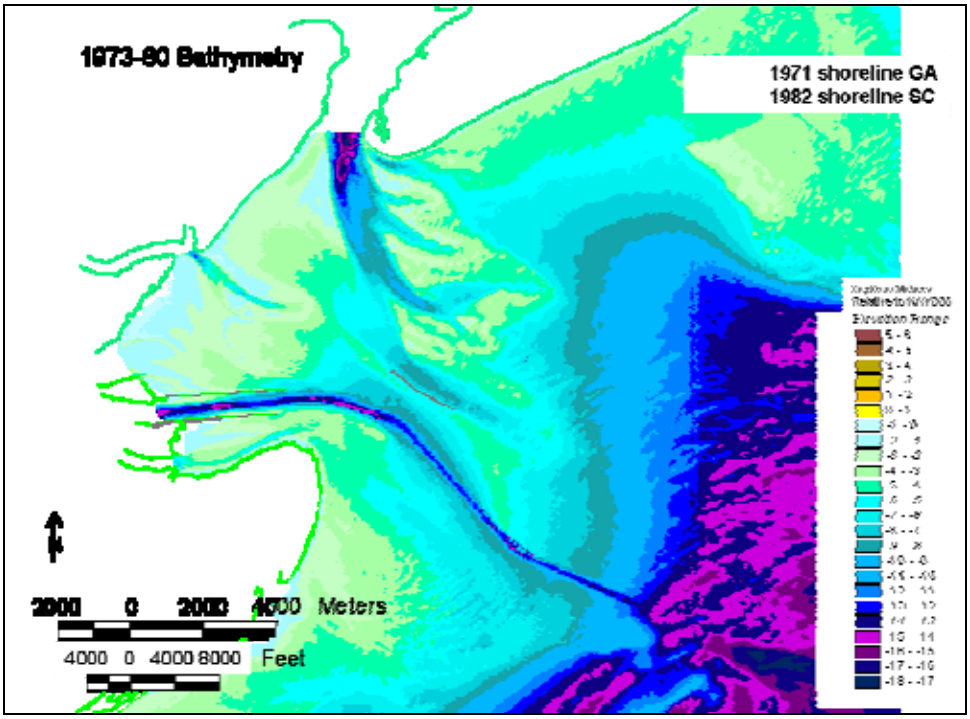

Figure 2-18. 1970/83 post-project bathymetry.

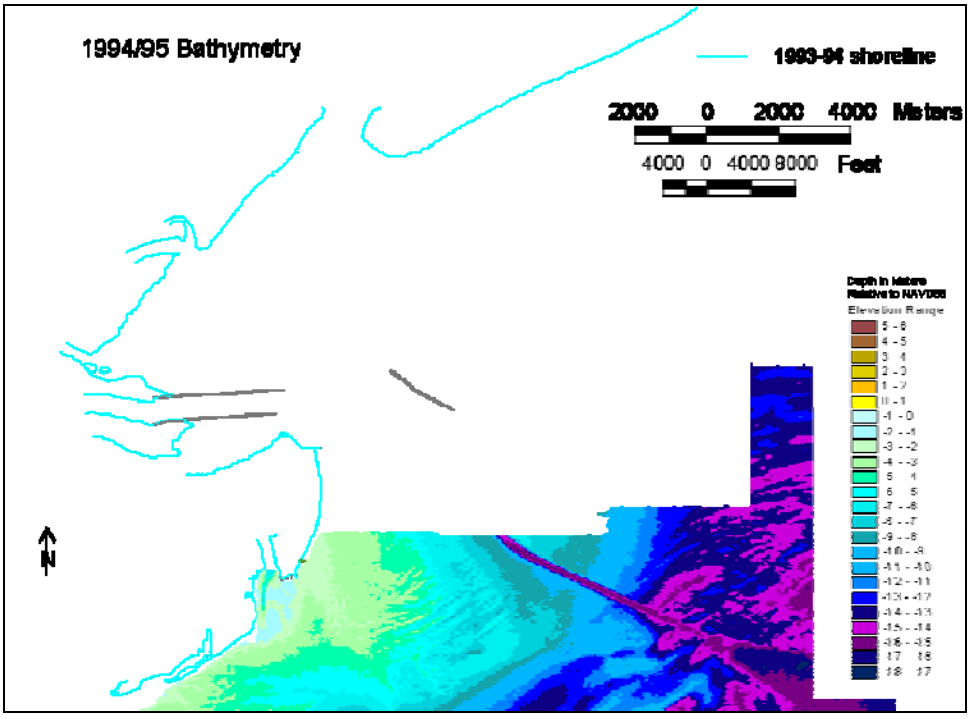

Figure 2-19. 1993/94 bathymetry.

The only recent surveys of the Tybee Island nearshore available for this study consisted of before and after dredge and examination surveys of the navigation channel itself. Figure 2-20 shows a composite of a series of surveys conducted from 2005 to 2007. A series of other before and after dredge surveys from 1989 to 2000 indicated that the dredging requires removal of a small area on the south side of the channel just off Tybee Island and to the east side of the channel on the southern end of the channel as it passes the lower end of Barrett Shoals. A survey consisting of beach and nearshore boat surveys along designated profiles was conducted in February 2005 along Tybee Island. That survey is limited to the nearshore area but shows the condition of the beach and nearshore 5 years after the most recent beach nourishment. An exam survey was conducted in September 2005 of the navigation channel again showing the tip of the north Tybee shoal encroaching on the channel just off the jetties and the encroachment of the southern tip of Barrett Shoals on the southern area of the channel. These appear to be the dominant areas where sediment enters the channel. To augment these data, additional surveys were obtained from NOAA NOS for selected areas in the vicinity of the dredged channel. These surveys were collected in small areas on several occasions in 2006 to check for hazards to navigation. Surveys were collected by the SAS in March 2007 of the beach and shelf off Tybee Island for this study to provide a present condition. This survey best represents the present condition of the area bathymetry.

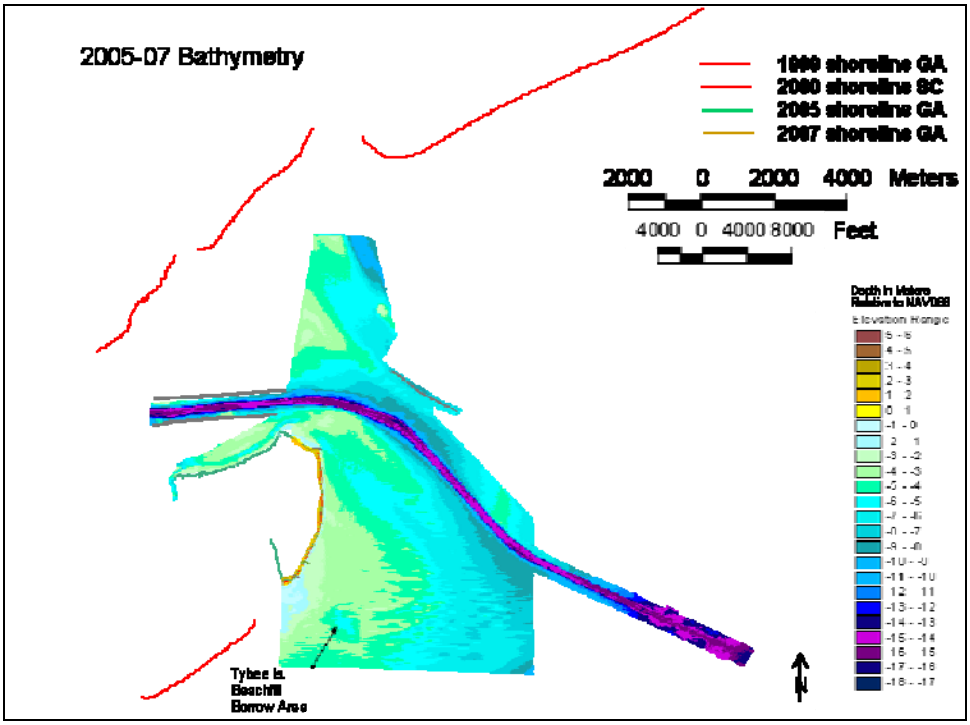

Figure 2-20. Combined 2005 channel, 2006 NOAA surveys, and March 2007 Tybee Island survey representing present conditions.

Bathymetric volume changes

Pre-project changes

This analysis covered pre-project bathymetry surveyed in 1854, 1867, 1873, and 1897, the latter which was immediately after construction of the two jetties at the mouth of the Savannah River and a submerged breakwater in the vicinity of Tybee Roads. Post-project bathymetric coverage began with the 1899 survey and included 1910; 1920; a composite of 1971 to 1974 and 1980 to 1983 bathymetry; and a new composite of a channel condition survey in 2005 by SAS, several spot surveys by NOS of navigation hazards in 2006, and a survey of the beach and nearshore of Tybee Island in 2005 and 2007 by SAS. The early data were collected by NOAA NOS's predecessor, the U.S. Coast and Geodetic Service (USC&GS) using lead line survey methods. The accuracy of the surveys is the best of that day, approximately +/-1 m. No standard datums were available at that time and the local datum of MLW was used on each chart. The data were transformed by CHL to the present standard vertical datum of NAVD88 and a horizontal datum of Latitude and Longitude in NAD83. This transformation also included sea level corrections for data surveyed before the NGVD 1929 was established based on NOAA's sea level curves recorded at

the Fort Pulaski tide gauge which has been in operation since 1935 (Table 2-3 and Figure 2-8). The data were further transformed to the present NAVD 1988 datum based on the NOS latest tidal epoch of 1983–2001 by CHL using ArcView software. All the data up until the 1970s were collected at a datum of MLW. NOAA switched to a vertical datum of MLLW around 1980. Table 2-4 shows the correction factors used based on the NOAA tidal gauge elevation information. The conversion from MLLW to NAVD88 was 1.24 m (4.06 ft), MLW to NAVD88 was 1.17 m (3.84 ft), and NGVD29 to NAVD88 was 0.29 m (0.96 ft). Each of these conversions has the potential to add uncertainty to the analysis, but care was taken to bring all of the data into a common horizontal and vertical datum for analysis. Once the data were in a common datum for both the vertical and horizontal, cross comparisons of depth change could be made, channel position changes could be measured, and changes in morphologic features such as shoals could be evaluated.

Table 2-4. Elevation information for NOAA Tide Gauge Station 8670870 referenced to 1983–2001 tidal epoch.

Tidal Datum	MLLW	MLW	NGVD29	NAVD88
Mean Higher High Water (MHHW)	2.29 m (7.50 ft)	2.22 m (7.28 ft)	1.34 m (4.4 ft)	1.05 m (3.44 ft)
Mean High Water (MHW)	2.17 m (7.13 ft)	2.10 m (6.89 ft)	1.23 m (4.03 ft)	0.94 m (3.07 ft)
North American Vertical Datum (NAVD88)	1.24 m (4.06 ft)	1.17 m (3.84 ft)	0.29 m (0.96 ft)	0
Mean Tide Level (MTL)	1.12 m (3.67 ft)	1.05 m (3.44 ft)	0.17 m (0.57 ft)	-0.12 m (-0.39 ft)
National Geodetic Vertical Datum (NGVD29)	0.95 m (3.10 ft)	0.88 m (2.89 ft)	0	-0.29 m (-0.96 ft)
Mean Low Water (MLW)	0.07 m (0.22 ft)	0	-0.88 m (-2.89 ft)	-1.17 m (-3.84 ft)
Mean Lower Low Water (MLLW)	0	-0.07 m (-0.22 ft)	-0.95 m (-3.10 ft)	-1.24 m (-4.06 ft)

In order to understand the impact of the construction of structures and dredging of the Federal navigation channel has had on the Savannah River entrance area, a comparison was made between the conditions that existed before bar channel improvements to conditions that exist after dredging to deepen and widen the channel and construction of navigation improvement structures. The project was initiated with dredging of the channel in 1874 (ATM 2001), but no records are available until 1910 of dredging volumes and depths of the channel. The early dredging is assumed to be

small volumes and located in the inner harbor (ATM 2001). The dredging operations have deepened the channel five times from 3.8 m (21.5 ft) in the 1900's to the present 13.4 m (44 ft) MLW (Table 2-5). Each time the channel was deepened or widened new dredging was initiated and required removal of larger quantities of sediment from the channel (Figure 1-2). Almost annual maintenance has been required to keep the channel at the design depth. Most of the sediment was placed on the ODMDS, except for a beach fill in 1993/94 which placed the dredged sediment on the beach.

Table 2-5. Bar channel dredging.

Year	Channel Depth, ft-MLW	New Dredging Vol., cu yd	Maint. Dredging Vol,[1] cu yd
1910	21.5		1,640,000
1915	26.0		667,000
1921	26.0		565,000
1922	26.0		156,700
1923	26.0		270,200
1924	26.0		1,142,200
1925	26.0		322,800
1926	26.0		502,200
1927	26.0		217,000
1928	26.0		716,700
1930	26.0	2,470,500	
1931	26.0	NO DATA BETWEEN 1931–1945	NO DATA BETWEEN 1931–1945
1944	30.0		
1945	36.0		
1946	36.0		2,381,00
1947	36.0		695,700
1948	36.0	671,400	
1950	36.0	2,830,700	
1951	36.0		2,864,500
1953	36.0		916,500
1954	36.0		667,300
1956	36.0		450,600
1957	36.0		1,826,300
1958	36.0		202,200
1959	36.0		66,800
1961	36.0		1,368,200
1962	36.0		1,414,200
1963	36.0		1,339,300
1964	36.0		903,100
1965	36.0		655,500

Year	Channel Depth, ft-MLW	New Dredging Vol., cu yd	Maint. Dredging Vol,[1] cu yd
1966	36.0		879,500
1968	36.0		458,400
1969	36.0		401,800
1970	36.0		677,900
1971	36.0		582,400
1972	40.0	3,469,600	489,700
1973	40.0	2,151,700	771,900
1974	40.0	1,146,300	1,415,700
1975	40.0	1,146,300	96,500
1976	40.0	979,200	1,066,000
1977	40.0	1,806,400	2,811,200
1978	40.0	988,500	2,763,700
1980	40.0		471,100
1981	40.0		865,700
1982	40.0		188,300
1983	40.0		644,900
1984	40.0		789,800
1985	40.0		1,212,478
1986	40.0		1,166,528
1989	40.0		442,414
1990	40.0		600,000
1991	40.0		1,104,991
1993	40.0		554,707
1994	44.0	2,454,441	
1995	44.0		1,993,061
1996	44.0		486,108
1997	44.0		544,508
1998	44.0		548,044
1999	44.0		508,885
2000	44.0		1,217,300
2001	44.0		1,117,856
2002	44.0		186,537
2003	44.0		635,163
2004	44.0		620,642
2005	44.0		888,101

[1] Maintenance dredging data sources are annual reports data in black; dredging records data in green, and recent SAS data in blue.

This study has been hampered by lack of good coverage both spatially and temporally of historic shoreline position, bathymetry, multiple dredging records, and storm climatology. There were three bathymetric surveys

before the project was initiated (1854, 1867, and 1873) and one at the end of construction of the jetties and breakwater (1897). This data set was surveyed before a standard national vertical datum was established. ATM (2001) did initial calculations to correct to the NGVD29 datum. This study has updated the correction using the latest tidal epoch and a technique recommended by NOS to correct for sea level rise before the datum was established using a longer record for sea level elevations between 1933 and 1999. The data in this present study have been adjusted to the new more accurate NAVD88 datum.

Difference maps were constructed using the ArcView GIS software to assess the changes in bathymetry between surveys. Figure 2-21 shows the change between 1854 and 1867. Both surveys were before construction of the two jetties and submerged breakwater. Areas of loss in bed elevation are shown in red and gain in elevations is shown in green. The channel centerlines show the change in orientation of four channels off Calibogue Sound and three channels that merge into one main channel off the mouth of the Savannah River. There was less than 1 m (3.28 ft) of change over most of the area (yellow = +0 to 1 m gain and grey = -0 to -1 m loss). More significant gain and loss of sediment was found in the vicinity of the Calibogue Sound channels that have migrated to the south, showing gain on the north side of the channel and loss on the south in the vicinity of Barrett Shoals. Gain in sediment was also found on the north end of Tybee Island.

From 1867 to 1873, little had changed in the bathymetry of the area. There was erosion on the east side of Calibogue Sound and accretion on the west side of the channel. Some erosion was seen off the north end of Tybee Island and in the mouth of the Savannah River (Figure 2-22). There was little change in orientation of the channel centerlines at that time.
Figure 2-23 shows the bathymetric change from 1873 to 1897. This period covers from before construction to the immediate post construction of the two navigation jetties in 1896 and the offshore submerged breakwater completed in 1897. The 1897 survey was limited in coverage so the difference map was limited to the common area between the two surveys.

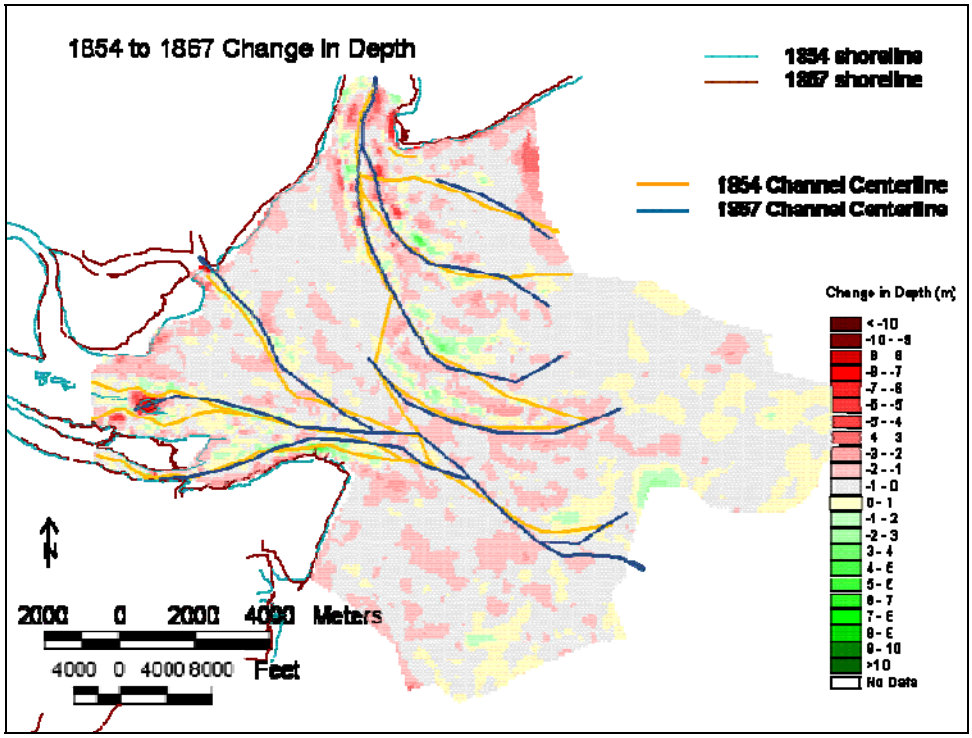

Figure 2-21. 1854 to 1867 change in bathymetry.

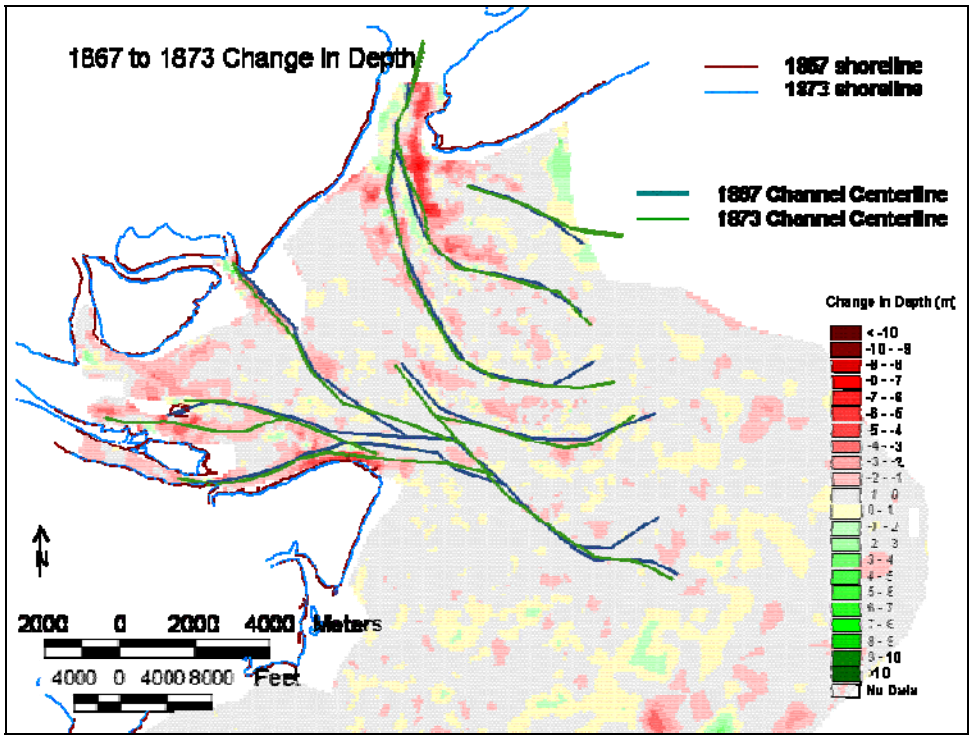

Figure 2-22. 1867 to 1873 change in bathymetry.

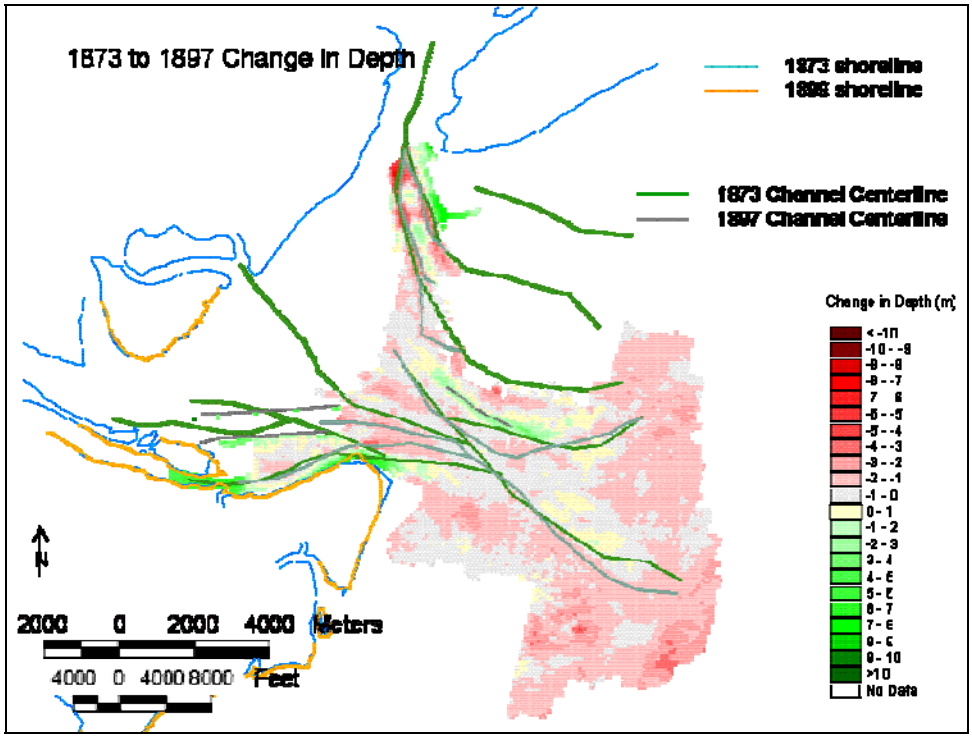

Figure 2-23. 1873 to 1897 change in bathymetry.

The main change was the reorientation of the channels at the entrance of Savannah River, Wright River, and New River from four channels that merged into two channels (green lines) in the nearshore to a main channel of the Savannah River now orientated between the jetties and a secondary channel coming from the South Channel of the Savannah River (gray lines). The channel from New River and Wright River entrances was not surveyed in 1897. The channel complex exiting Calibogue Sound has three distinct channel branches trending off the main channel to the east in 1873. The limited coverage of the 1897 data does not cover all of the channels, but the general trend is for movement to the south. Loss of sediment was measured in Calibogue Sound entrance channel and in most of the channels in the vicinity of Tybee Roads. Gain of sediment was measured at the submerged breakwater at the southern end of Barrett Shoals and on the north tip of Tybee Island. This was due to the collapse of the northern tip of the island, with some sand transport to the north and the deposition of sand in a newly formed northern spit and in the near-shore. This northern spit accumulation on Tybee Island forced the South Channel to move further northward. The first indications of deflation can be seen on the north portion of the Tybee Island shelf and accumulation on the North Tybee Shoal. Shorelines available from 1854, 1863, 1867, and 1873 show the bulge on the north end of Tybee Island was experiencing

small amounts of erosion to the north, with construction of three groins (seen in the 1867 shoreline) and accumulation on the north-facing shoreline of Tybee Island (Figure 2-2). No shorelines exist between a chart of 1873 and 1899 to pinpoint when the bulge began to erode away. The bathymetry presumably collected as an as-built record of the structures in 1897 and the shoreline measured in 1899 (two years after structure completion) show the beginnings of larger scale changes in shoreline. However, changes in bathymetry between 1897 and 1899 (Figure 2-24) do not indicate any significant deflation on the shelf in front of Tybee Island over this short two-year period between surveys. The area of survey was limited, but it can be seen that the channel centerline of the South Channel is moving to the north as the north spit is growing to the north. The two channels (northern channel from New River and the main Savannah River entrance) remain in place. From the available data, it appears that the shelf and shoreline of Tybee Island were experiencing some erosion before the structures were in place.

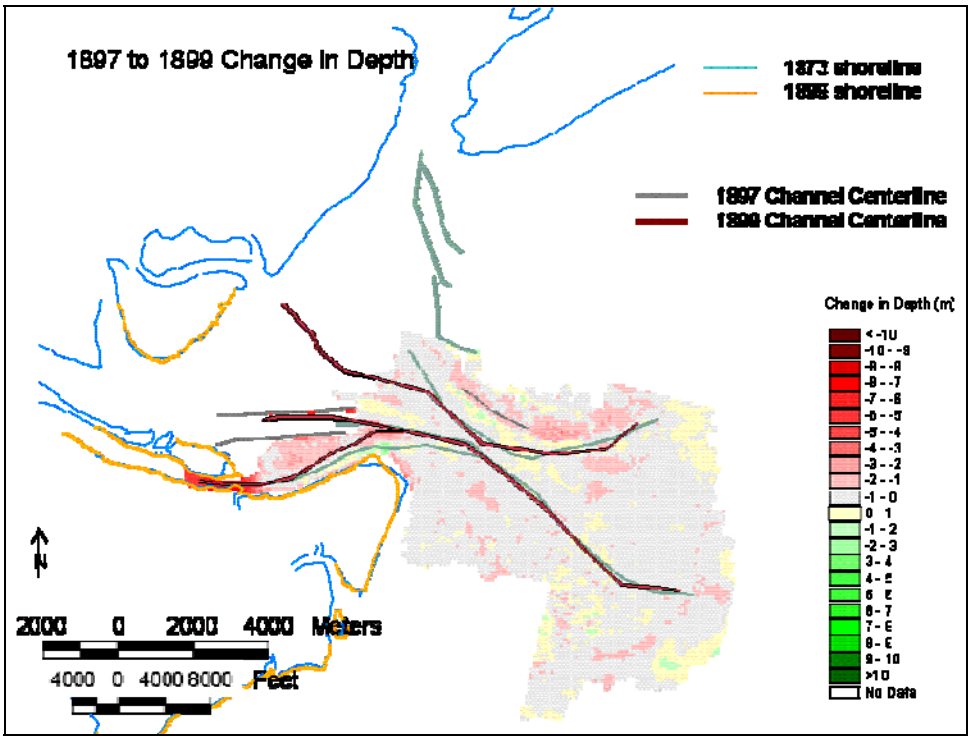

Figure 2-24. 1897 to 1899 change in bathymetry.

Post-project changes

Comparing the 1899 to 1910 bathymetric surveys shows scour in the channel between the jetties and accretion continuing on the shoal to the north of Tybee Island, further deflecting the South Channel to the north. (Figure 2-25). Shoreline change revealed the growth of the northern recurved spit into the South Channel. The survey comparison is limited to the southern half of the study area in this time period and does not show any significant scouring of the shelf off Tybee Island.

From 1910 to 1920 the four channels of the Calibogue Sound entrance remain but move further southward (Figure 2-26). Accretion of the bed is found in the lee of the submerged breakwater on the north end of Tybee Roads. The shoreline bulge of north Tybee Island has eroded and the shoreline spit continues to grow on the north end of the island. Accretion is also present in the north part of the north Tybee shoal area. The growth of the shoal and spit along the shoreline has deflected the South Channel to the north to merge with the main navigation channel of the Savannah River. The north portion of the Tybee Island shelf continues to deflate, and it appears the sediment is moving to the northwest, toward the north Tybee shoal (the sediment transport modeling presented in Chapter 5 supports this trend). The New River Channel also meets with the main channel seaward of the jetty tips. There is general loss of sediment in the rest of the shelf area. From available records, dredging of the channel was annual after 1910 with the first controlling depth of 6.6 m (21.5 ft), which was deepened to 7.9 m (26 ft) in 1915 (Table 2-5).

Due to limits in the coverage of the 1930 survey, it was not included in the comparison. Comparing the 1920 survey with the next available survey composite of 1970/83 showed there was a general southward shift in the individual east-west channels coming off the Calibogue Sound entrance (Figure 2-27). The 1920 channel locations have filled in and a new channel has eroded sediment south of each for the four channels. The southern-most channel has moved south and is now deflected to the east by the sub-merged breakwater. The southern tip of Barrett Shoals is now accreting (sediment transport modeling shows the same trend). The New River entrance channel has migrated to the north and is now detached from the main Savannah River navigation channel. There is a gain in sediment in the old 1920 New River channel and erosion of the bed in the new orientation, as well as a gain in sediment deposition at the mouth of that new channel.

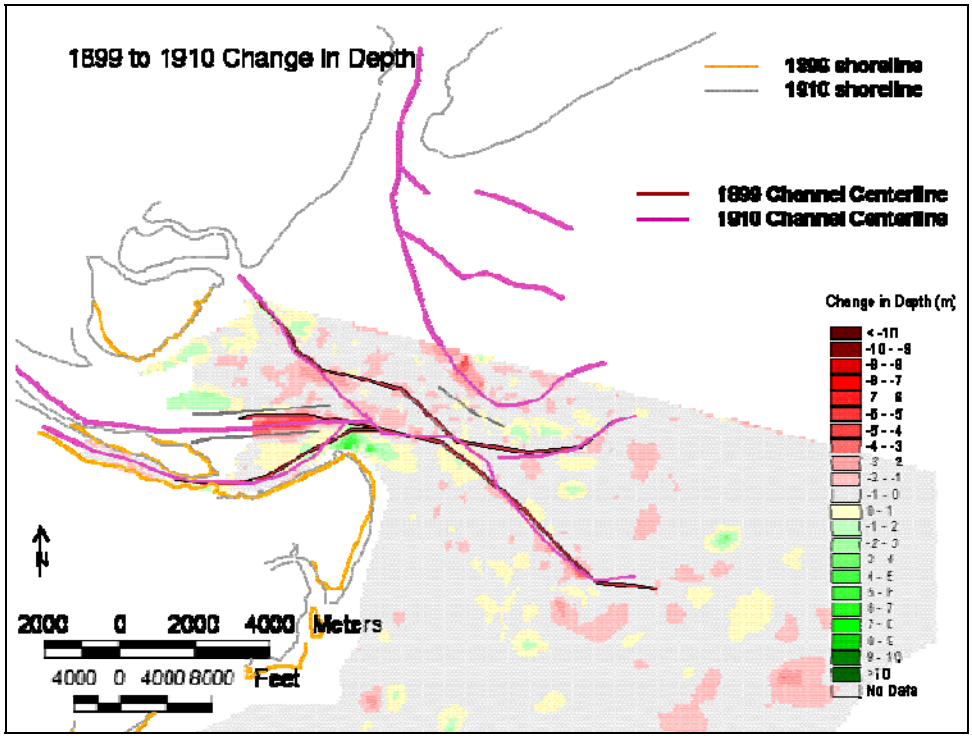

Figure 2-25. 1899 to 1910 change in bathymetry.

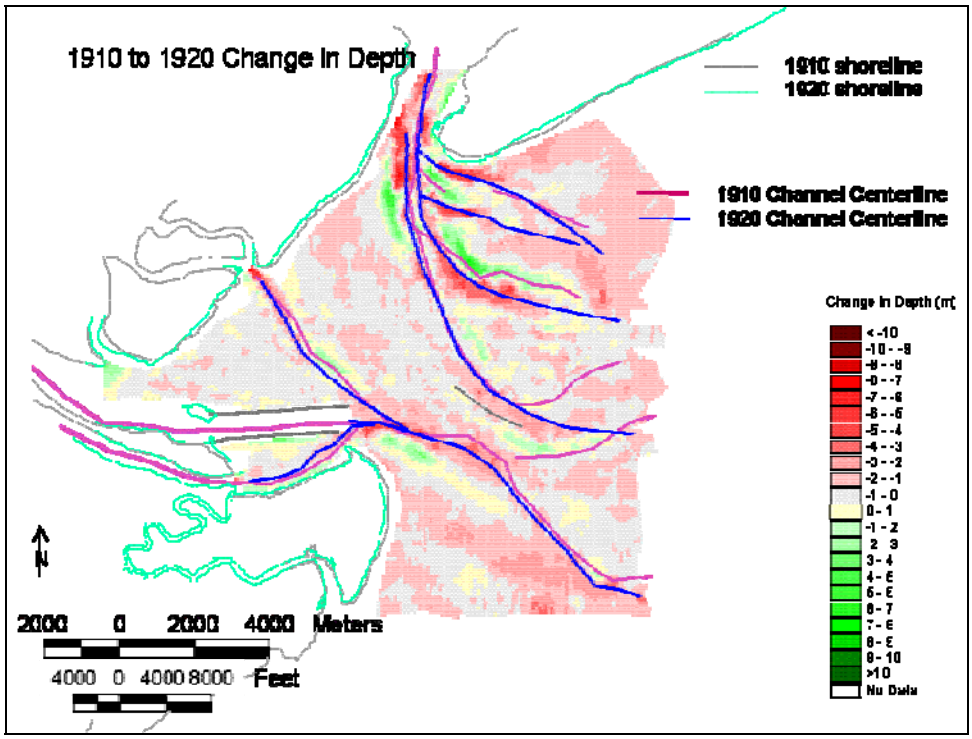

Figure 2-26. 1910 to 1920 change in bathymetry.

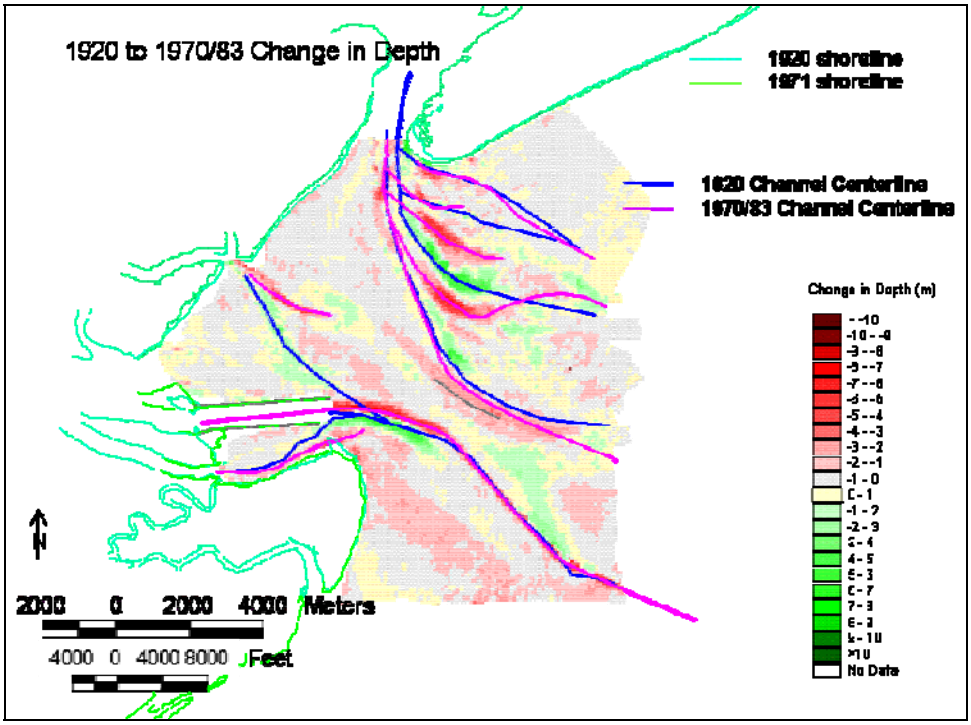

Figure 2-27. 1920 to 1970/83 change in bathymetry.

The spit on north Tybee Island has eroded and the South Channel is now reverted back to its pre-project position next to the island. The north spit had eroded back from a maximum reach in 1925 to 1971 allowing the South Channel to change orientation. The erosion was significant and the north terminal groin was constructed in 1975 along with the placement of the first beach nourishment from the groin south to 18th St. The main navigation channel has migrated northward out from between the jetties and the old channel has filled in due to the northwest movement of sediment and accumulation in the north Tybee shoal. The channel was deepened from 7.9 m (26 ft) to 11 m (36 ft) in 1945 and to 12 m (40 ft) in 1972. The comparison shows the establishment of a straight channel orientation of the Tybee Knoll Bar reach and the Tybee Roads Bar reach and the extension offshore. The pattern of deflation continues on the Tybee Island shelf and the southern portion of the north Tybee shoal. There is general loss of sediment on the Tybee Island shelf platform in front of the island as erosion was measured in the 1971 shoreline along almost the entire length of the island. The time period of 1920 to 1970/83 is longer than the time periods for the previous bathymetry changes discussed, and it includes several channel deepenings and an active tropical storm period (1950s–1960s).

Figure 2-19 shows 1994 NOAA bathymetry, but unfortunately the coverage is limited to the southern portion of the study area and was not used for bathymetry change calculations. The navigation channel was deepened to 13.4 m (44 ft) in 1994. The available newer bathymetry was limited to surveys of the navigation channel. A change analysis of channel surveys between 2000 and 2005 indicates that the channel has been dredged, except for the lower end of the Tybee Roads Bar Channel which has shown accretion (Figure 2-28). This accretion indicates that the southern tip of Barrett Shoals is a source of sediment to fill in the channel as sand moves southward and westward across the shoal. Accretion in the channel is also evident due to encroachment of the north Tybee shoal.

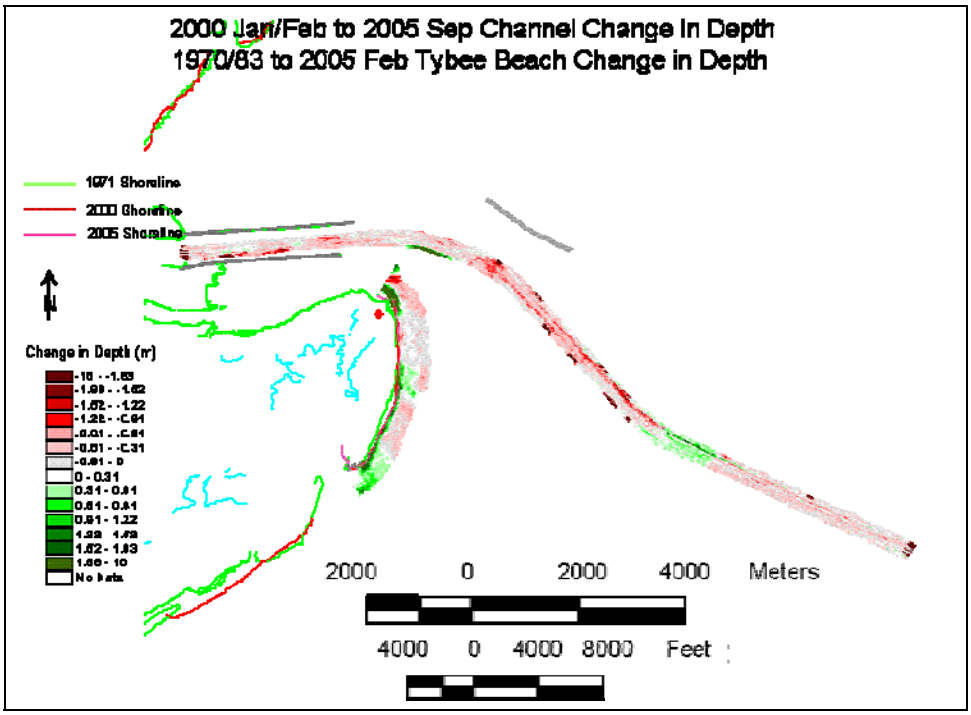

Figure 2-28. January/February 2000 to September 2005 change in channel bathymetry and 1970/83 to February 2005 change in nearshore bathymetry.

A comparison of the beach and nearshore survey in February 2005 with the 1970/83 survey along the Tybee Island beachfront shows accretion of the nearshore reflecting the four beach nourishment placements since 1975 (Figure 2-28). The nearshore on the north end of the island shows accretion indicating northward transport of fill from the hot spot around 2nd St. That area shows a net loss of sediment in the nearshore. A slight gain in sand is found on the shelf along the central part of the island where the shoreline orientation changes from north-south to more northeast-southwest. Accretion is also shown at the southern end of the island where

sediment is transported southward onto the ebb shoal of Tybee Creek Inlet.

A composite of 2005 channel, selected 2006 shelf surveys, and the 2007 beach and nearshore survey of Tybee Island specifically for this study was compared with the composite 1970/83 bathymetry. Due to the limited area of coverage of the recent survey the comparison was limited in area. The change in the bathymetry in Figure 2-29 shows the effects of almost annual dredging of the main navigation with loss within the channel. The four channels of the Calibogue Sound entrance were not within this survey area. The shoreline shows a return of the recurved northern spit at Tybee Island, which has again deflected the South Channel to the north. Small accretion along the shoreline and nearshore is due to beach fills and additional structures placed at the south end of the island between the survey dates. The Tybee Island shelf shows deflation in many areas.

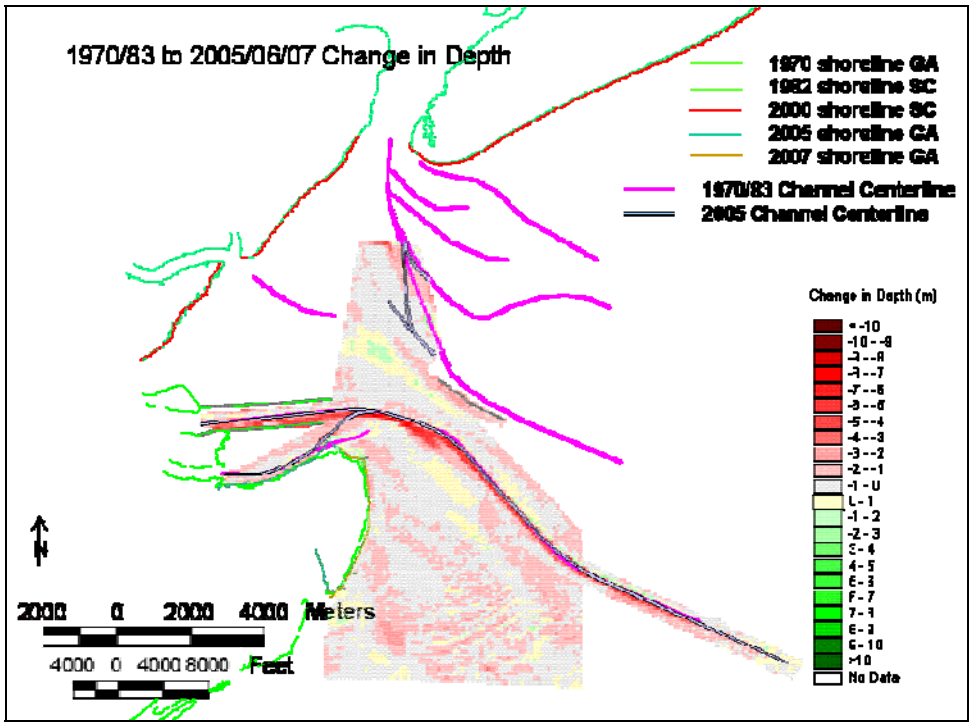

Figure 2-29. 1970/83 to 2005/06/07 change in bathymetry.

Morphodynamic evolution

Storm climate

Storms are an important force in transport of sediment and the formation/evolution of coastal morphology. Table 2-6 lists all tropical storms that have come within 200 miles of Tybee Island since 1851. These data were downloaded from the NOAA Coastal Services Center and contained a GIS database of all tropical storms from 1851 to 2002. Data for 2003 to 2006 were downloaded from the National Weather Service and transformed into GIS compatible data. Figure 2-30 shows the occurrence of these tropical storms by year. There were several active tropical storm seasons with more than three storms per season. This analysis does not include extratropical storms so there may be more storms than listed that could have affected the Tybee Island area. The period between 1872 and 1916 was active with several years having multiple occurrences of storms. There is some correlation between the change in the bulge in the north Tybee Island shoreline and the number of storms that occurred during this time period. Additional hurricane periods were 1952–1965, 1979–1989, and 1996–1999. The pre- and post-project periods selected (1854–1899 and 1899–2007) both include stormy periods.

Table 2-6. Tropical systems within 200 miles of Tybee Island.

Year	Dates	Name	Category	Pressure, mb	Winds, mph
1850					
1851	8/24	Not Named	H1	n/a	80
1852	8/27–8/28		TS		45
	10/10		TS		70
1853	10/21		H2		105
1854	9/8–9		H3	950	115
1855					
1856	8/31–9/1		TS		70
1857	9/12		H1		90
1858	9/15		TS		70
1959	10/28		H1		90
1860	8/13–8/14		TS		60
1861	11/1		TS		60
1862					
1863	9/17		TS		70
1864					

Year	Dates	Name	Category	Pressure, mb	Winds, mph
1865	8/20		TS		60
1866					
1867	6/21–6/23		H1		80
	10/6–10/8		TS		70
1868	10/5		TS		45
1869					
1870					
1871	8/18–8/23		H1		80
	8/27–8/28		TD		35
	9/6–9/7		TS		70
	10/5–10/6		TS		60
1872	10/23–10/24		H1		80
1873	6/2		TS		45
	9/19–9/20		TS		70
	9/23		TS		45
1874	9/28		H1	981	90
1875					
1876	9/21		H1		90
1877	9/20–9/21		TS		45
	9/28		TS		60
	10/3–10/4		TS		60
	10/27		TS		45
1878	9/11–9/12		H1	985	90
	10/11		TS		45
1879	8/18		H3		115
	10/28		TS		60
1880	9/8–9/9		TS		70
	10/9		TS		70
1881	8/27–8/28		H2	970	105
1882	9/11		TS		45
	9/22		TS		45
	10/11–10/12		TS		70
1883	9/10		H2		105
1884	9/10–9/13		TS		60
1885	8/24–8/25		H3		115
	8/31		TS		45
	9/21		TS		45
	9/30–10/1		TS		60

Year	Dates	Name	Category	Pressure, mb	Winds, mph
	10/12		TS		60
1886	6/21–6/22		H1		75
	7/1		TS		60
	7/19		TS		65
1887	8/19		H3		115
	8/23–8/24		H3		125
	10/20		TD		35
	10/30		TS		45
1888	9/9–9/10		TS		50
	10/11		H1		80
1889	6/17–6/18		TS		45
	9/24		TS		50
1890					
1891	10/8		TS		45
	10/10		TS		50
1892					
1893	6/16		TS		60
	8/28		H3	954	115
	10/3–10/4		TS		50
	10/13		H3		120
1894	9/26–9/27		H1		90
	10/9		H1		80
1895					
1896	7/8		TS		40
	9/29		H3	963	115
1897	9/21–9/22		TS		60
1898	8/30–9/1		H1		85
	10/2		H4	938	135
1899	8/14–8/15		H3		120
	10/5–10/6		TS		45
	10/31		H2		110
1900	10/12		E		40
1901	7/3		TS		40
	9/18		TS		40
1902	6/15		TS		40
1903	9/16		TD		35
1904	9/14		H1		80
	11/4		TD		35

Year	Dates	Name	Category	Pressure, mb	Winds, mph
1905					
1906	9/17–9/18		H1	977	80
	10/19–10/21		H1		90
	10/17		TS		40
1907	6/29		TS		65
	9/29		TS		40
1908	5/27–5/28		H1		75
	7/30		H1		80
	10/23		E		45
1909	7/2–7/3		TD		35
	8/31		TS		40
1910	10/19		TS		70
	8/27		E		40
	10/20–10/21		TS		70
1911	8/27–8/30		H1	983	75
1912	6/14		TS		40
	7/15		TS		50
1913	10/8–10/10		TS		50
1914	9/16–9/17		TS		45
1915	8/1–8/3		TS		50
1916	7/13–7/15		H2	983	100
	9/5		TS		40
	9/13		TD		35
	10/4		TS		45
1917					
1918					
1919					
1920	9/30		TS		40
1921	10/26		H1		90
1922					
1923					
1924	9/16		TS		50
	9/30		E		50
1925	12/1–12/2		H2		100
1926	7/28–7/29		TS	975	70
1927	10/3		TS		60
1928	9/9–9/11		TS		45
	9/17–9/18		H2	974	105

Year	Dates	Name	Category	Pressure, mb	Winds, mph
1929	10/1–10/2		TS		45
1930	9/10–9/11		TS		60
1931					
1932	9/15		TS		50
1933	9/5–9/7		TS		50
1934	5/28–5/31		TS		60
	7/21–7/22		TS		45
1935	9/5		TS		70
1936	8/21–8/22		TS		50
1937	7/30		TS		45
	8/30		TS		60
	9/21		TD		35
1938					
1939	10/24		TS		45
1940	8/2–8/3		TS		45
	8/11–8/12		H1	975	80
1941	10/8		TS		65
	10/20–10/21		TS		45
1942					
1943					
1944	8/1		H1	990	90
	10/19–10/20		TS	978	70
1945	6/24–6/25		H1		80
	9/16–9/17		H1	982	75
1946	5/6		TS		45
	10/8–10/9		TS		40
	11/2–11/3		TD		30
1947	9/24		TS	989	60
	10/7–10/8		TS		45
	10/14–10/16		H1	973	85
1948					
1949	8/27–8/28		TS	982	65
1950	9/7	EASY	TS		50
	10/19	KING	TS		40
	10/21	LOVE	TS		40
1951					
1952	8/30–8/31	ABLE	H2		105
1953	8/31–9/1		TS		60

Year	Dates	Name	Category	Pressure, mb	Winds, mph
	9/20		TS		45
	9/27	FLORENCE	E		60
1954	8/29–8/30	CAROL	H2		100
1955					
1956	9/25–9/26	FLOSSY	E		40
1957	6/9		TS		40
1958	9/27	HELENE	H3	934	125
1959	6/2	ARLENE	TD		30
	7/5–7/9	CINDY	H1		75
	9/29–9/30	GRACIE	H4	950	140
1960	7/29	BRENDA	TS		50
	9/11	DONNA	H2	966	105
1961	9/13–9/14		TD		35
1962	8/27	ALMA	TS		50
1963	10/24–10/25	GINNY	H2	976	105
1964	6/7–6/8		TD		35
	8/28–8/30	CLEO	TS	995	65
	9/9–9/13	DORA	H3	964	115
1965	6/15		TS		45
1966	6/10	ALMA	TS		65
1967					
1968	6/6–6/12	ABBY	TS		60
	6/19–6/20	BRENDA	TD	1012	30
	8/11	DOLLY	TD	1011	30
	10/19	GLADYS	H1	966	85
1969	9/8	GREDA	TS	1002	50
	10/3–10/4	JENNY	TD		35
1970	7/25–7/26	ALMA	TD	1005	30
	8/16–8/17		TD	1013	35
1971					
1972	5/27–5/28	ALPHA	SS	991	65
	6/20–6/21	AGNES	TD	992	35
	9/13–9/14	DAWN	TD		35
1973					
1974	6/25	Subtropical #1	SS	1000	65
	10/7	Subtropical #4	SS		45
1975	6/27–6/28	AMY	TD	1012	30
	10/25–10/26	HALLIE	SD	1005	35

Year	Dates	Name	Category	Pressure, mb	Winds, mph
1976	5/24	subtropical #1	SS	998	45
	8/20	DOTTIE	TS	999	45
	9/13–9/15	subtropical #3	SS	1011	45
1977	9/8	BABE	TD		30
	9/5	CLARA	TD	1014	25
1978	9/12	HOPE	TD	1010	30
1979	9/4–9/5	DAVID	H2	970	100
1980					
1981	8/19	DENNIS	TS	1002	45
1982	6/18	subtropical #1	SS	992	70
1983					
1984	9/9–9/13	DIANA	H3	960	115
	9/29	ISADORE	TS	1004	50
1985	7/24–7/25	BOB	H1	1002	75
	8/9	CLAUDETTE	SD	1013	30
	10/10–10/13	ISABEL	TD	1011	35
	11/22	KATE	H1	983	75
1986	6/6	ANDREW	TS	1004	50
	8/13–8/16	CHARLEY	TS	1002	45
1987					
1988	8/28	CHRIS	TS	1005	50
1989	9/22	HUGO	H4	935	140
1990					
1991					
1992	9/29–9/30	EARL	TS	1002	45
1993					
1994	11/21	GORDON	TD	1013	25
1995	6/5–6/6	ALLISON	TS	993	50
	8/25–8/27	JERRY	TD	1004	30
1996	6/18–6/19	ARTHUR	TS	1004	40
	7/12	BERTHA	H2	975	100
	9/5	FRAN	H3	952	115
	10/8	JOSEPHINE	E	990	50
1997					
1998	8/26	BONNIE	H3	965	115
	9/3–9/4	EARL	TS	990	50
1999	8/29–8/30	DENNIS	H2	964	105
	9/15–9/16	FLOYD	H3	943	115

Year	Dates	Name	Category	Pressure, mb	Winds, mph
	10/17	IRENE	H1	984	75
2000	9/18	GORDON	TD	1006	35
	9/23	HELENE	TD	1011	30
	10/4–10/5	LESLIE	SD	1010	35
2001	6/13	ALLISON	SD	1004	30
	9/15	GABRIELLE	TS	999	50
2002	9/2–9/5	EDOUARD	TS	1002	65
	10/10–10/11	KYLE	TS	1008	40
2003	9/6–9/7	HENRI	TD	1006	35
2004	8/14	CHARLIE	H1	994	75
	8/28–8/30	GASTON	TS	991	60
2005	9/13–9/14	OPHELIA	H1	980	75
	10/5–10/6	TAMMY	TS	1001	45
2006	6/14	ALBERTO	TS	1004	35
	8/31	ERNESTO	TS	994	50

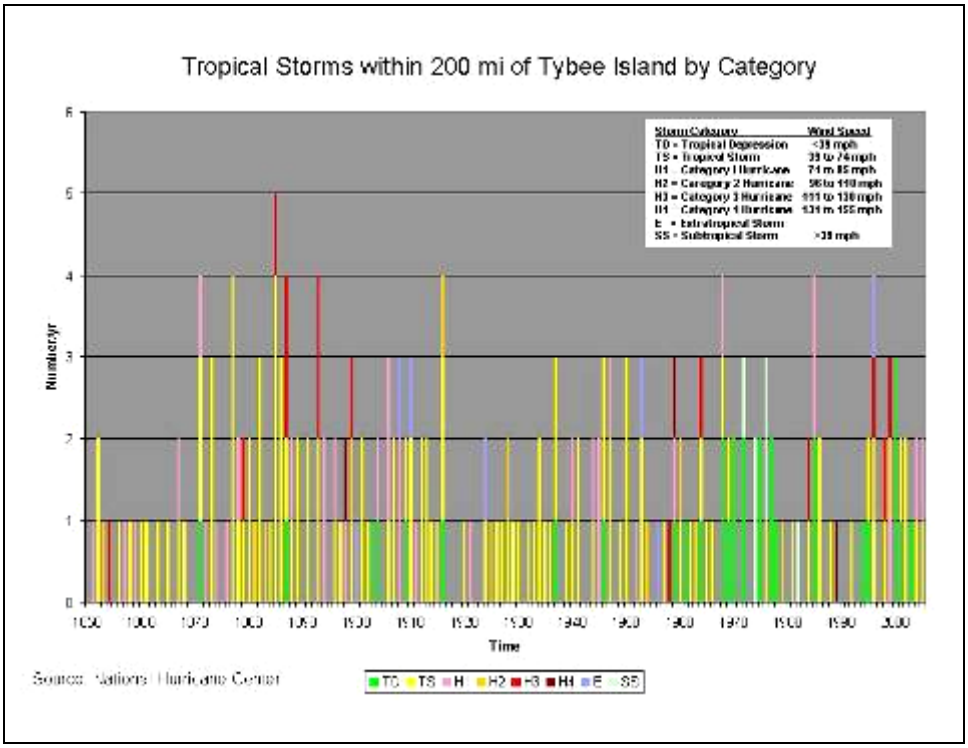

Figure 2-30. Tropical storm occurrence within 200 mi of Tybee Island 1850 to 2005.

Evaluation of bathymetric contour changes

The general trends in morphologic change in the nearshore can be illustrated with the change in the -5 m (-16.4 ft) and -10 m (-32.8 ft) depth contours. The change in contours for the pre-project conditions was analyzed from 1854 to 1897. The -5 m contour best represents the platform evolution of both Barrett Shoals to the north and Tybee Island shelf to the south. Figure 2-31 shows the pre-project change in the two contours. The 43 years prior to jetty construction shows a southerly shift in the -5 m contour on the south end of Barrett Shoals consistent with the general trend of southerly sediment transport along the South Atlantic coast. The channels trending eastward from the main Calibogue Sound channel have also migrated south. The -5 m contour outlines the channel edges out of the Savannah River on the shelf platform in front of Tybee Island and the outline of the shoal platform. Little change can be seen in the position of contours along the channel, but the offshore edge has migrated slightly offshore. Of interest is the fact that the -10 m (-32.8 ft) contour has remained relatively stable over this same time period.

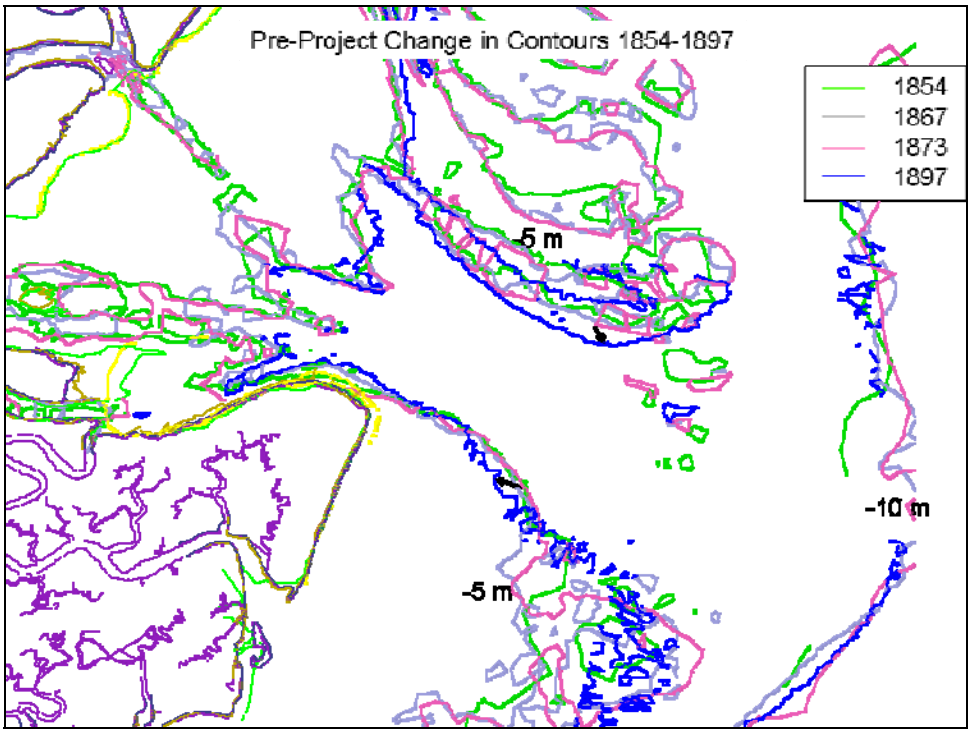

Figure 2-31. Pre-project changes in the -5 and -10 m contours.

After construction of the jetties and the submerged breakwater and commencement of nearly annual dredging of the navigation channel, a different trend is observed. Figure 2-32 shows the 100 years of post-project contour changes from 1897 to 2007. On the north side, the Barrett Shoals -5 m contour has migrated to the south. All of the contours by date are not completely shown due to limits of the surveys, but the arrows indicate the trend in migration. The -5 m contour on Tybee Island shelf shows the onshore retreat as the platform has become depleted. Along with this landward migration, the northern edge of the shoal has formed a wedge shape indicating landward retreat toward the shoreline of northern Tybee Island. A recurved spit of sediment has grown from the wedge into the north Tybee shoal area and is growing back to the southeast along the edge of the navigation channel. The spatial progression of this change in morphology has been consistent over time with retreat of the northern edge of the platform and evolution of the recurved spit back toward the platform. The circulation and sediment transport modeling shown in Chapters 3 and 5 are consistent with the morphological change. Again, the -10 m contour offshore has remained in a relatively constant position. The -10 m contour outlining the navigation channel has formed with the dredging of the channel to a depth past -10 m (-33 ft) after 1945.

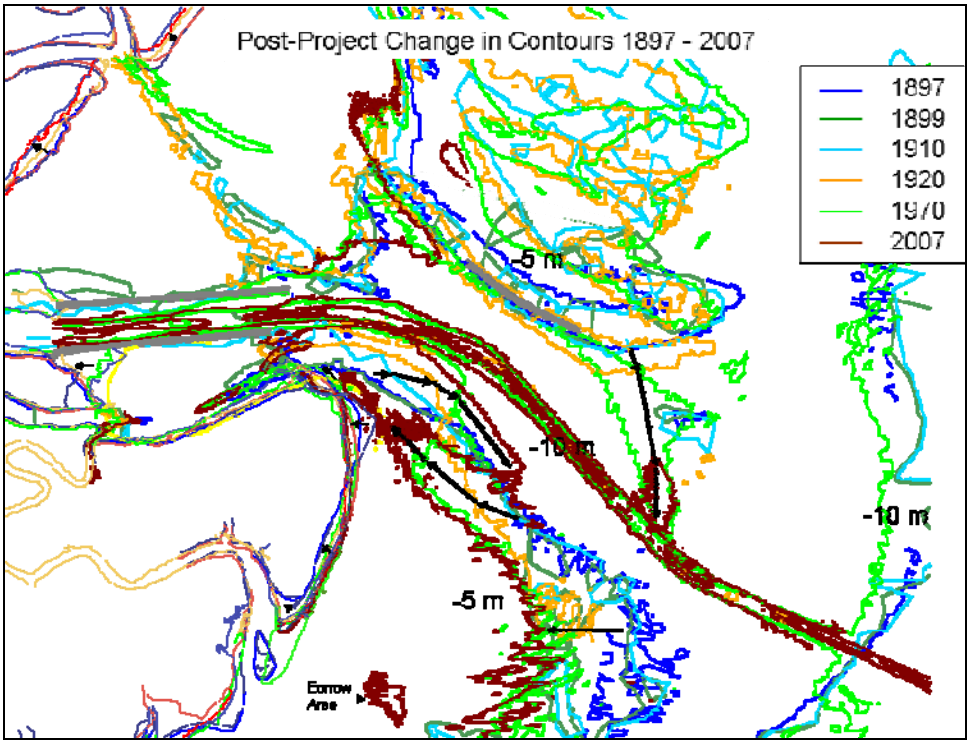

Figure 2-32. Post-project changes in the -5 and -10 m contours.

Channel evolution

A summary of the changes to the channels from the river entrances show that the channel centerlines have migrated south over the study period (except New River, which has migrated north). The left panel of Figure 2-33 shows the positions of the channel centerlines mapped from the pre-project (1854–1897) bathymetries. The location of the four channels associated with Calibogue Sound (channels 1 thru 4 on the figure) have remained relatively stable and only their seaward ends have migrated to the south in the pre-project time period. The main Savannah River entrance, South Channel, and the New River Channel all converge on a single fifth channel on the south. There is high variability in channel position through time, and there is some interaction between channels 4 and 5. Post-project (1899–2007), there are several changes that have evolved. The first channel off Calibogue Sound to the north has split into two channels (labeled 1a and 1b on the figure). All of the channels generally migrate to the south over time. Since the construction of the submerged breakwater, channels 3 and 4 have merged together and there is little interaction between channels 4 and 5. These channels migrate to the south consistent with net movement of sediment to the south along Barrett Shoals. By the 1970s the Savannah River entrance navigation channel had become fixed in its present location. The main navigation channel of the Savannah River entrance has moved north in the Tybee Knoll range as the jetties have controlled this part of the channel location. The South Channel has also migrated northward as sand that has accumulated in the North Tybee Shoal has migrated northward, consistent with northward movement of sand at north Tybee due to changing tidal flow patterns reshaping the nearshore in front of north Tybee Island.

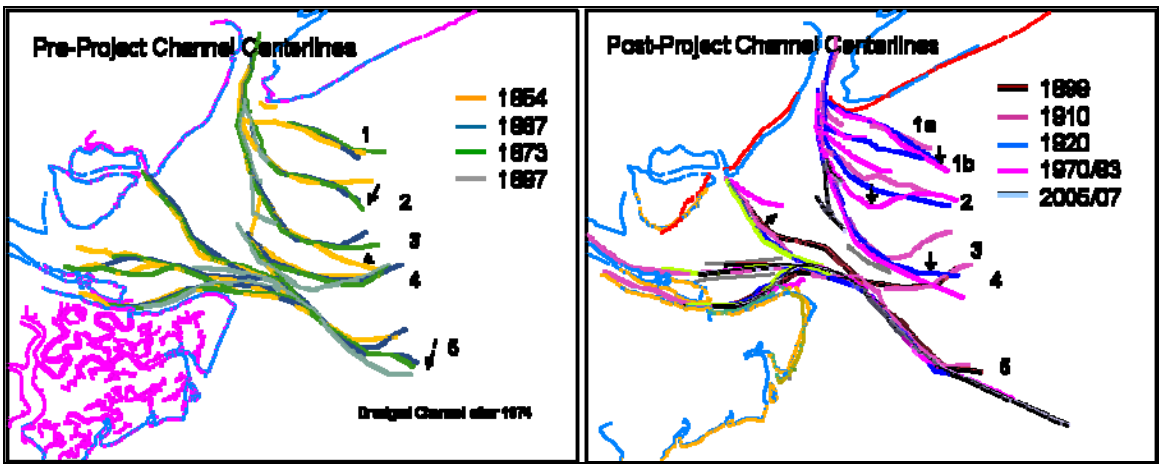

Figure 2-33. Change in channel centerline orientation.

Details of changes in the main Savannah River entrance channel in the vicinity of the jetties and the South Channel were examined to study the effects of the structural changes and dredging events on the evolution of the north end of Tybee Island. Figure 2-34 shows the pre- and post-jetty locations of the channel centerlines as measured off the respective bathymetries. Only the first and last channel centerline is plotted for clarity. The pre-project grouping showed that the Wright River Channel and the Savannah River Channel merge together then merge with the New River Channel. The South Channel is located along the edge of north Tybee Island and merges with the other channels farther seaward in Tybee Roads. This pattern is consistent over the pre-project 43-year time period. After jetty construction, breakwater placement and dredging, the main Savannah River Channel was funneled between the jetties, the Wright River Channel filled in, and the New River Channel moved to the north more into the influence of the Calibogue Sound channel complex. The erosion on north Tybee Island, the loss of the bulge and formation of the recurved spit on the north end of Tybee has forced the South Channel up into the main navigation channel just past the end of the South Jetty. The wedge of erosion can be seen in the 2007 bathymetry background close to the present shoreline with the recurved spit of sediment separating the two channels from the shelf.

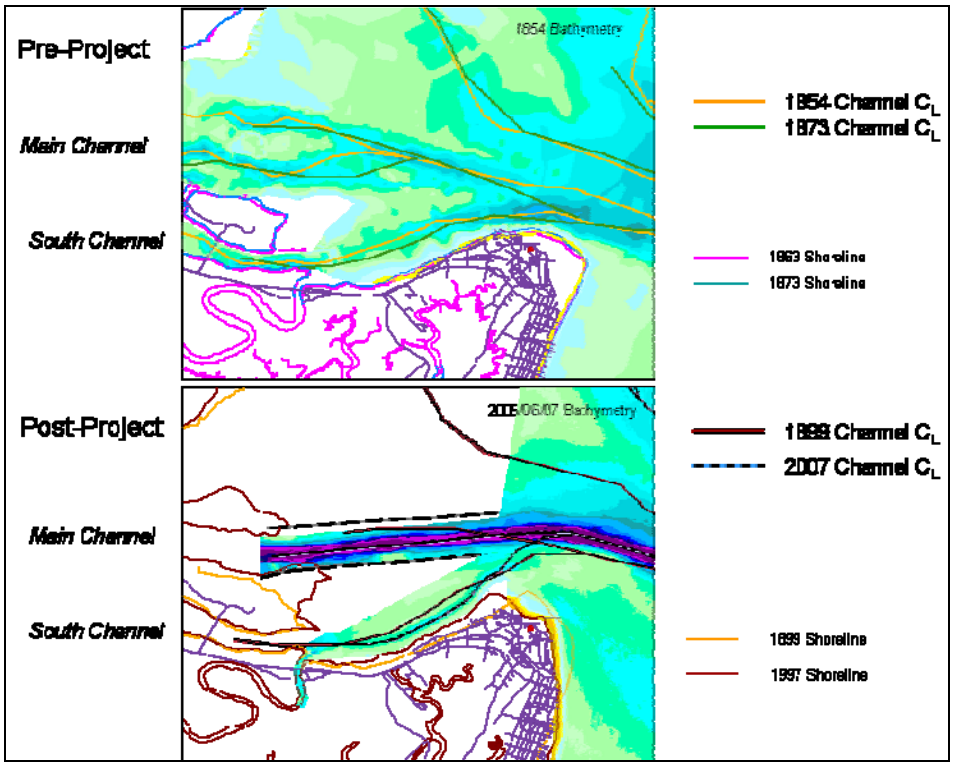

Figure 2-34. Change in channel centerlines at north Tybee Island

Sediment budget

Volume change cells

Based on bathymetric change patterns and distinct morphologic characteristics, eight morphologic areas were identified to calculate volume changes for the study area. Figure 2-35 shows the boundaries of each of these areas. The largest of these areas is Barrett Shoals, the ebb shoal which is bisected by several channels trending eastward with adjacent shoals that are related with the Calibogue Sound entrance channel. Calibogue Sound is composed of the main thalweg of the sound channel and is identified as a separate area. The shallow platform in front of Daufuskie and Turtle Islands is also identified as an area of shoals and the thalweg of the New River entrance channel. The shallow Wright River entrance channel is on the south end of this cell. The main navigation channel of the Savannah River is divided into the more east-west Tybee Knolls Bar Channel extending out from the two jetties and further offshore, and the more northwest-southeast trending Tybee Roads Bar Channel. The area on the north side of these bar channels has been called the Breakwater Lee Shoal area in the lee of the submerged breakwater area of Tybee Roads and is composed of shoals outside of the dredged channel.

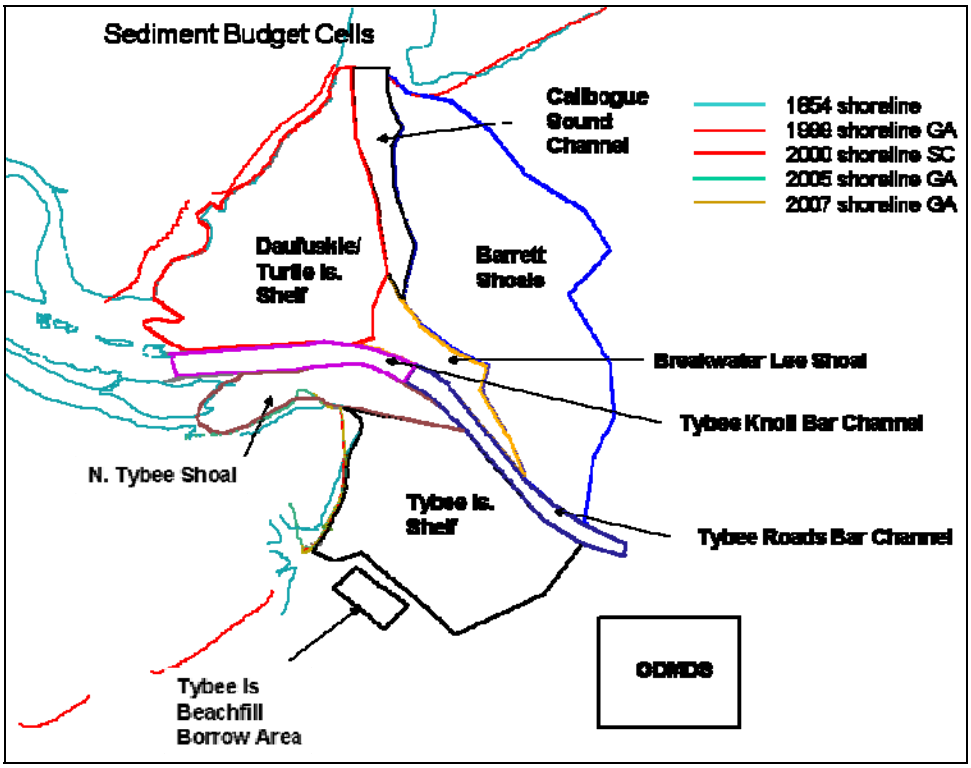

Figure 2-35. Volume change cells.

The shallow shelf platform in front of Tybee Island has been divided into two sections: the north Tybee shoal and the Tybee Island shelf based on the change in shoal configuration and depth contours over the study period. The channel reach west of the Tybee Knoll Channel (west of Station 0+000) is next explicitly included in the sediment budgets.

Pre-project volume and shoreline change—1854 to 1897

The pre-project study period has been defined as the period between 1854 and 1897. This period was defined based on available data and the fact that the Savannah River entrance jetties were completed in 1896 and the Tybee Roads submerged breakwater was completed in 1897. To study the "natural" changes that took place in the morphology of the Tybee Roads area before the project was implemented, a change analysis was done between the 1854 to 1897 bathymetries. The 1897 bathymetry was presumably the as-built survey and was not thought to have any major effects of the project realized in such a short time after construction. The 1854 survey coverage was sufficient to include the entire sediment budget cell area. The 1897 survey was limited to the Savannah River entrance area. To increase the area for comparison with the 1854 bathymetry, selected areas on the outer edges of the study area were supplemented with the next available pre-project survey of 1873. These areas included the Daufuskie/Turtle Island shelf, Barrett Shoals, and the southern portion of Tybee Island platform. This new composite bathymetry is shown in Figure 2-36.

The difference map of change between 1854–1897/1873 is shown in Figure 2-37. The main loss of material over this pre-project 43-year period is found where the channels have changed location. The three channels from Calibogue Sound have shifted to the south with erosion in the present location of the centerlines (red shades in figure show loss of sediment) and a filling in of the older channel locations (green shades in figure show gain of sediment). The New River entrance channel has scoured out a deeper channel in its original location. The south end of Barrett Shoals has lost sediment with the merged northern leg of the Wright River, main Savannah River, and South Channel trending east on its southern tip. A second channel (which will become the main dredged navigation channel) is located in the lower Tybee Roads Bar Channel cell area. A gain was found in the Tybee Knoll Bar Channel and the South Channel, just at their mouths.

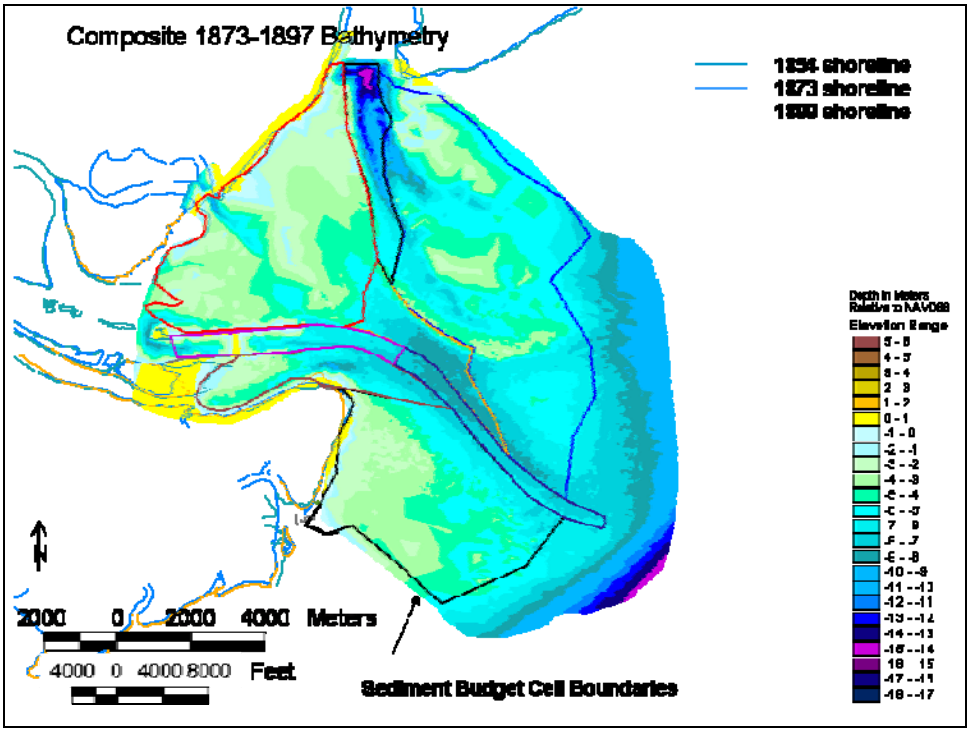

Figure 2-36. Composite 1897 bathymetry with portions of 1873 used in sediment budget calculations.

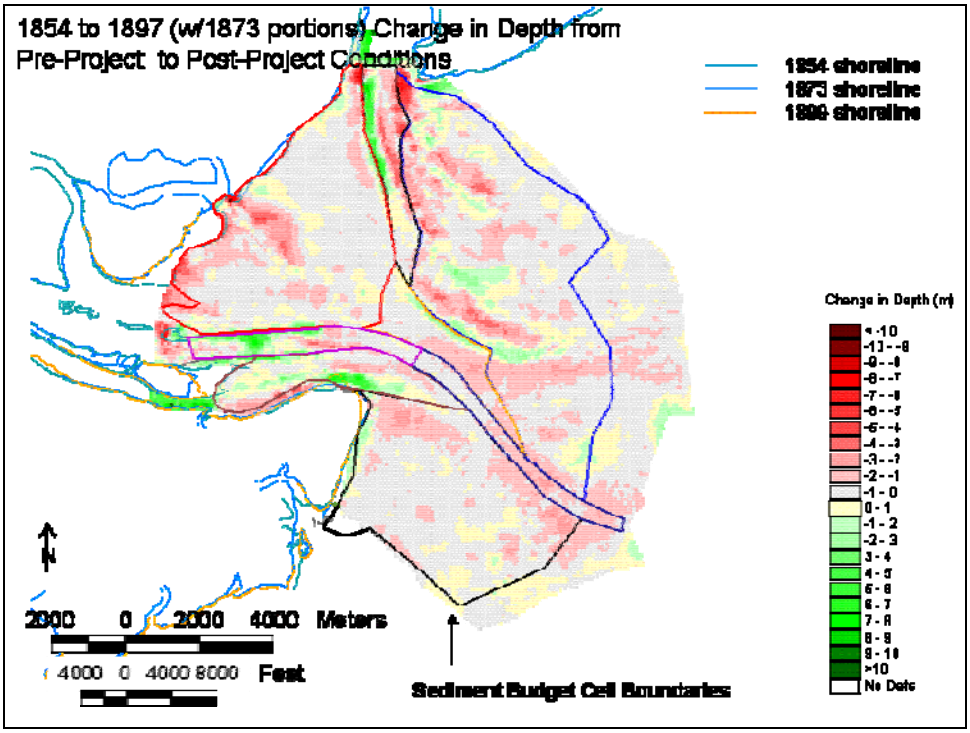

Figure 2-37. Change in bathymetry from pre-project (1854) to immediate post-project (1897 w/portions of 1873 data).

The change in the Tybee Island shoreline and the beginning of the removal of the bulge has resulted in gain of sediment on the north Tybee shoal and beach front. The Tybee Island shelf was losing sediment, particularly on its northern portion, even before dredging and structure construction.

The USGS has recently completed a study of the long-term change in shoreline position along the southeastern U.S. East Coast from North Carolina to Florida (Miller et al. 2005). Change rates of shoreline position, in units of m/yr, were calculated at 50-m transect spacing using linear regression applied to shoreline positions from their earliest (1863) to their most recent (1999/2000) data using the USGS developed Digital Shoreline Analysis System (DSAS) program in ArcView. Linear regression was selected because it has been shown to be the most statistically robust quantitative method when a limited number of shorelines are available and it is the most commonly applied statistical technique for expressing shoreline movement and estimating rates of change. Uncertainties for the long-term rates are reported in units of m/yr and represent a 90 percent confidence interval for the slope of the regression line. This means with 90 percent statistical confidence that the true rate of shoreline change falls within the range of ±2.7 m/yr along the Georgia coast (Miller et al. 2005). A modified DSAS analysis was done on the available shorelines from 1863 that the USGS used in their study with the 1899 shoreline available for the Tybee Island area. Using their 50-m alongshore spaced transects the difference was calculated between the two pre-project shorelines. The change in shorelines is shown in Figure 2-38. There was little change in shoreline position for the available 1863 and 1899 shorelines for South Carolina so the analysis focused on Tybee Island. The beginnings of the retreat of the bulge on the north end of the island can be seen with erosion between -0.5 to -6.2 m/yr over this 36 year period on the northern 1,300 m of shoreline. The central 2,500-m-long shoreline showed little shoreline change from -0.5 to 0.4 m/yr, averaging a slight -0.02 m/yr change. A spit located at the southern 100 m of Tybee Island in 1863 was eroded away by 1899 for a loss of between -0.9 and -3.3 m/yr.

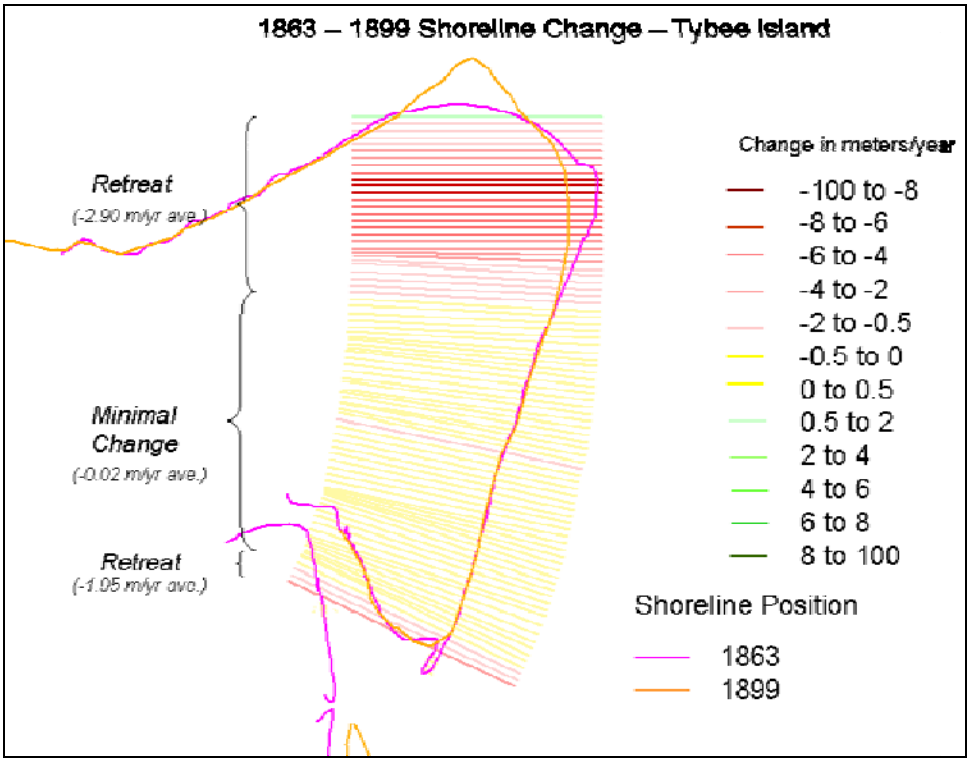

Figure 2-38. Change in Tybee Island shoreline between 1863 and 1899.

An analysis of the difference in depths between the 1854 bathymetry and the 1897/1873 bathymetry was conducted using ArcView Spatial Analysis. The differences at specific grid points spaced 7.6 m (25 ft) apart were summed for each sediment budget cell area shown in Figure 2-35 and divided by the number of years between the surveys (43) to produce an average rate of change for each morphologic area. Figure 2-39 shows the results of this analysis. The Barrett Shoals area lost a net 63,000 m^3/yr (82,400 cu yd/yr) as the southward shifting three channels filled in the old channel locations and formed new more southerly channels. A northern channel of the Savannah River complex (consisting of merged channels from the Wright River, the main Savannah River, and the South Channel) also exited to the east across the southern portion of Barrett Shoals. The Calibogue Sound channel had a net gain rate of 39,000 m^3/yr (51,100 cu yd/yr) as the channel has deepened on the east side and filled in on the west side, while elongating to the south. The Daufuskie/Turtle Islands shelf platform lost a net 49,500 m^3/yr (64,700 cu yd/yr) as sediment was eroded off the beaches of the two islands, eroded at the entrance to Wright River, and the New River entrance channel has scoured out its channel across the shelf.

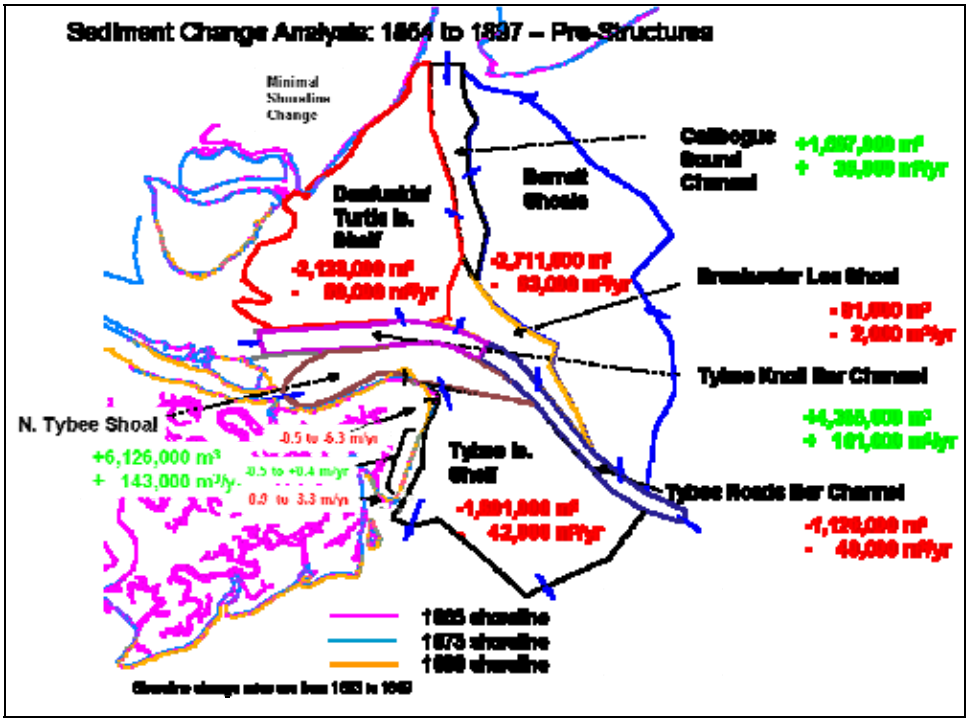

Figure 2-39. Change in volume between 1854 and 1897.

The Breakwater Lee Shoal area has lost 1,900 m³/yr (2,500 cu yd/yr) of sediment as sediment accumulated around the newly constructed submerged breakwater, but has scoured out from on the north side of Tybee Roads. The Tybee Knoll Bar Channel has gained 101,000 m³/yr (132,100 cu yd/yr) even though dredging started in 1874 somewhere along the channel, but no records were available of location or quantities (it is thought the dredging occurred in the river and not the bar channel). A small net loss of sediment was measured in the Tybee Roads Bar Channel of -40,000 m³/yr (-52,300 cu yd/yr), which was the natural southern branch of the merged Wright River, main Savannah River and South Channel. The north Tybee shoal area gained 142,500 m³/yr (186,400 cu yd/yr) of sediment with the beginnings of erosion of the bulge on Tybee Island and the deposition on the beach and shoal on the north end of Tybee Island. The shelf in front of Tybee Island has a net loss rate of 41,900 m³/yr (54,800 cu yd/yr). This net loss corresponds to the deflation of the northern portion of the shelf platform. The volume changes are bounded by the most seaward shoreline position over the study period (1854 to 2007) and thus do not include volume losses or gains resulting from shoreline change. Table 2-7 provides a summary of the volume changes.

Table 2-7. Volume change summary by area (see Figures 2-35 to 2-43).

Area	Volume Change Rate (1854–1897/1873) m^3/yr	Volume Change Rate (1897/1873–2005/06/07/1970/83) m^3/yr
Tybee Island Shelf 25 million m^2	-41,900 ± 30,000	-250,000 ± 33,000
North Tybee Shoal 7 million m^2	+143,000 ± 21,000	+30,000 ± 5,000
Daufuskie/Turtle Island Shelf 29 million m^2	-49,500 ± 19,500	+57,000 ± 5,000
Calibogue Sound Channel 5 million m^2	+39,000 ± 5,000	-50,000 ± 5,000
Barrett Shoals 40 million m^2	-63,000 ± 38,000	+56,000 ± 5,000
Breakwater Lee Shoal 5 million m^2	-1,900 ± 24,000	+13,000 ± 5,000
Tybee Knoll Bar Channel 4 million m^2	+101,000 ± 5,000	-232,000 ± 5,000
Tybee Roads Bar Channel 4 million m^2	-40,000 ± 31,000	-152,000 ± 5,000
Uncertainty estimated using 1.4 m depth error for 1854 to 1897/1873 and 1.0 m error for 1897/1873 to 2005/06/07/1970/86 (time = 43 and 110 yrs).		

The early surveys were taken with lead line (less accurate than present methods), but the surveys represent the best available data. Uncertainties were estimated to show the significance of the volume change rates. The uncertainties are very high due to inaccuracy of the early surveys, and they indicate that even moderate volume changes may not be meaningful. Uncertainties assigned to the survey depths were 1 m (3.3 ft) for 1854 and 1897 and 0.3 m (1 ft) for 1970/83 and 2005/06/07 data. These uncertainty estimates may be optimistic (Gibbs and Gelfenbaum 1999; Byrnes et al. 2002; Mills 2006[1]). Survey errors can be systematic or random (random error will tend to average out over volume calculations). Potential contributors to errors include use of lead line in early surveys (particularly in areas with a soft bottom), vertical reference, tide correction, horizontal reference, sea conditions, sampling, and interpolation. The uncertainty in depth change is estimated as root-mean-square of the errors in depth (depth change uncertainty = $((error_1)^2 + (error_2)^2)^{1/2}$), or approximately 1.4 m (4.6 ft) for 1854 to 1897/1873 and 1.0 m (3.3 ft) for 1897/1873 to 2005/06/07/1970/83. The uncertainty in volume change is estimated as the difference between the total volume change over a region and the

[1] Personal communication. 2006. J. Mills, NOAA Office of Coastal Survey.

volume change calculated exceeding the uncertainty in depth change (Byrnes et al. 2002). These volume change uncertainties have been converted to rates in Table 2-7. A minimum error of 5,000 m^3/yr was applied in Table 2.7.

Post-project volume and shoreline change—1897 to 2007

The post-project period from 1897 to 2007 required comparison of the bathymetry and shoreline change from those periods. Coverage of the most recent bathymetry was limited to the 2005 condition survey of the channel, 2006 survey of selected shelf areas of Tybee Roads (breakwater shelf area) and 2007 survey of the North Tybee Shoal and the Tybee Island shelf. To assess the changes in sediment elevation over this post-project period, a composite bathymetry was constructed by filling bathymetry gaps with survey data from the 1970/83 time frame. This included the northern area of the study of the Daufuskie/Turtle Island shelf, Calibogue Sound, and Barrett Shoals. The composite bathymetry plot (2005/06/07 supplemented with 1970/83 bathymetry) is shown in Figure 2-40. The four (1a, 1b, 2, and 3) channels from Calibogue Sound that bisect the Barrett Shoals can be seen on the north. The main dredged navigation channel orientation is now distinct and has been fixed in the location to the southeast through dredging. The deflation of the shelf in front of Tybee Island can be seen with a recurved spit of sediment forming within the north Tybee shoal.

The difference map that was generated in ArcView from the composite 1897/1873 and 2005/06/07 (with portions of 1970/83) is shown in Figure 2-41. The erosion patterns in the Calibogue Sound and Barrett Shoals area are a result of reorientation and shift to the south of the multi-channels coming off the main Calibogue Sound channel (red areas show scour of the present channels and green show deposition in the paleo-channel positions). The long dredging history of the main Savannah River navigation channel is reflected in the loss of sediment in the channel throat section. Deflation of the Tybee Island shelf has occurred on the seaward edge of the shelf and an erosional wedge is present on the northern edge of the Tybee Island shelf. The shoreline adjacent to the north end of the island in the vicinity of the wedge also shows erosion. Sediment gains are found in the recurved spit growing in the north Tybee shoal cell. Sediment deposition on the southern portion of the Daufuskie/Turtle Island shelf is due to a more northward reorientation of the channel out of the New River and accretion in the paleo-channel to the south.

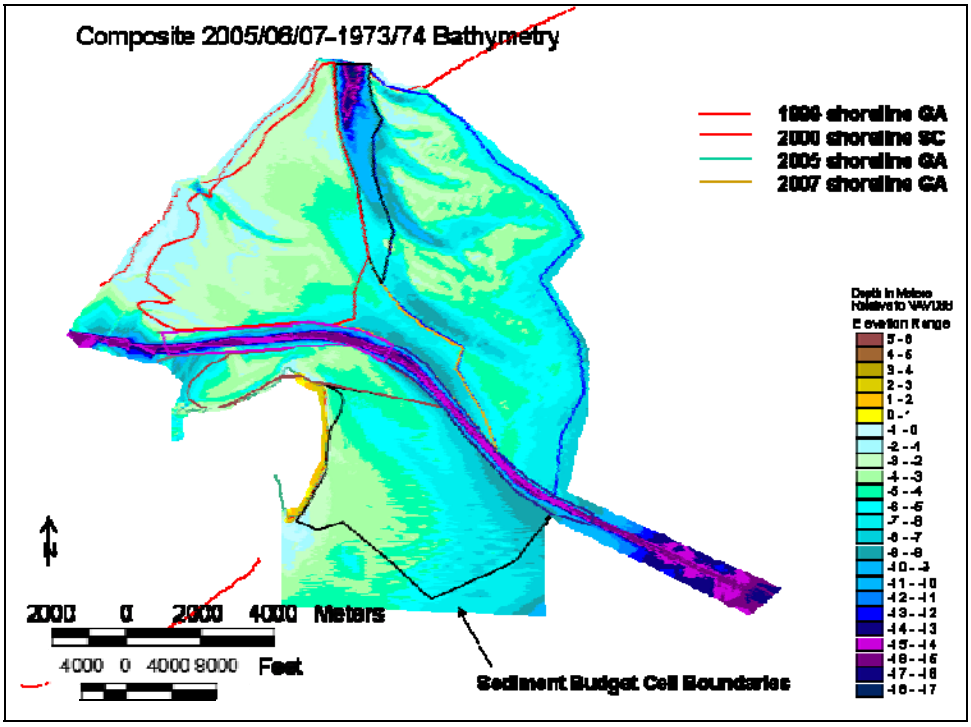

Figure 2-40. Composite 2005/06/07 bathymetry w/1973/80 bathymetry to characterize present conditions.

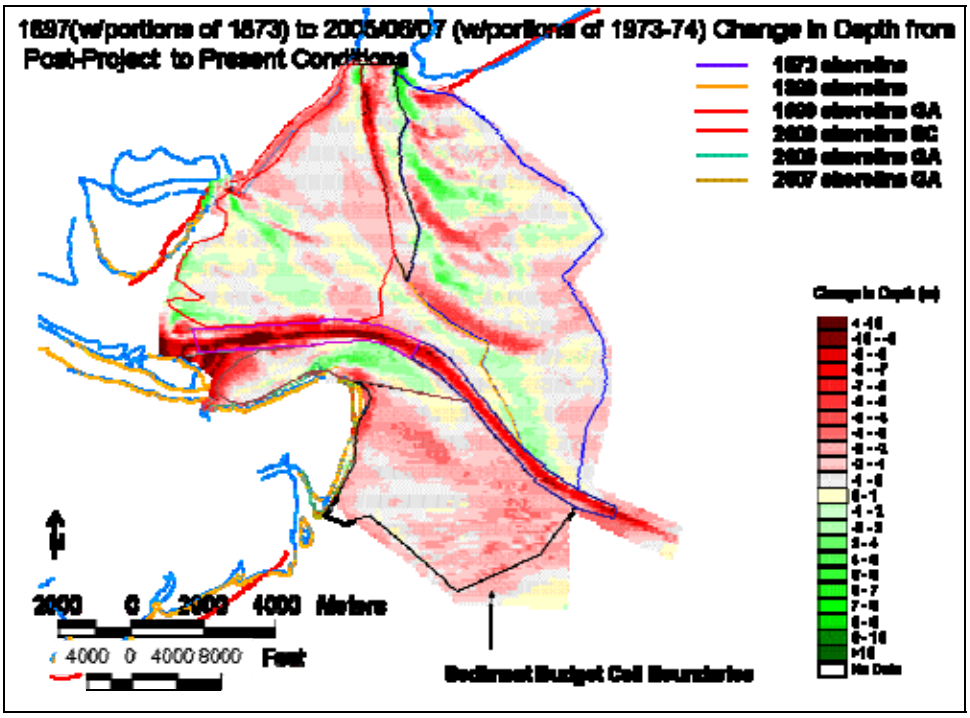

Figure 2-41. Change in volume between 1897 and 2007.

One of the USGS calculations was to measure the rate of change in shoreline movement from their first shoreline data set to their most recent LIDAR derived shoreline. In the case of the Tybee Island area, the shorelines were the 1863 to 1999. The shoreline change analysis done by the USGS (Miller et al. 2005) indicated that the 1863 shoreline was digitized from NOAA USC&GS T-sheets and the shoreline was based on plain table survey techniques to identify the MHW shoreline. The recent 1999 LIDAR surveys were identified by MHW tidal elevations based on the Fort Pulaski NOAA tidal gauge. The long-term shoreline change rate for Tybee Island reflects the erosion of the bulge on the north end with erosion of the shoreline from the north terminal groin southward in this area for the period between 1863 and 1999. The USGS analysis does not extend to the north of the north terminal groin due to the truncated position of the 1863 shoreline. The later shorelines visually show a gain as the spit and later shorelines extend to the north. The erosion rate in the area of the hot spot between 1st St. and 6th St. is up to -3.6 m /yr (11.8 ft/yr) (Miller et al. 2005). The nodal point around 2nd St. remains stable as the shoreline erodes to the north and accretes to the south of that area. The area south of the nodal point has measured accretion of up to +1.6 m/yr (5.2 ft/yr) from 1863 to 1999, which included all but the last beach fill period. The USGS data stop at the south terminal groin since the 1863 shoreline terminates at that point. The later shorelines have migrated to the south and the southern part of the island has grown to the south. The south terminal groin and the two T-head groins and terminal L-head groin as well as the beach fills have stabilized this southern portion of the island.

To update the shoreline change, a modified DSAS analysis was done using the 1899 shoreline representing an immediate post-project shoreline and comparing it with the latest 2007 shoreline calculated from the recent 2007 beach profiles and ground-truthed with a digitally rectified October 2005 aerial photograph. The north end of Tybee Island shows the erosion of the bulge and the movement of the spit to the north. The analysis starts where the USGS analysis did at the northward limit of the 1863 shoreline. Erosion ranging from -0.6 to -3.2 m/yr (-2.0 to -10.5 ft/yr) (average -1.64 m/yr (5.4 ft/yr)) was measured over the northern 1,400 m (4,600 ft) of shoreline starting at the north terminal groin (Figure 2-42). The nodal point of little change extends for 250 m (820 ft) alongshore with change ranging from -0.5 to +0.5 m/yr (-1.6 to +1.6 ft/yr) was measured with an average of -0.03 m/yr (0.1 ft/yr). The southern 2,200 m (7,200 ft) of shoreline showed a gain in sand and seaward movement of the shoreline

over the 108-year time period between +0.6 and 1.9 m/yr (2.0 to 6.2 ft/yr) with an average seaward movement of 1.81 m/yr (5.9 ft/yr). An additional 600 m (2,000 ft) of shoreline gain was seen south of the south terminal groin as sediment was trapped by the new T-head and L-head groins.

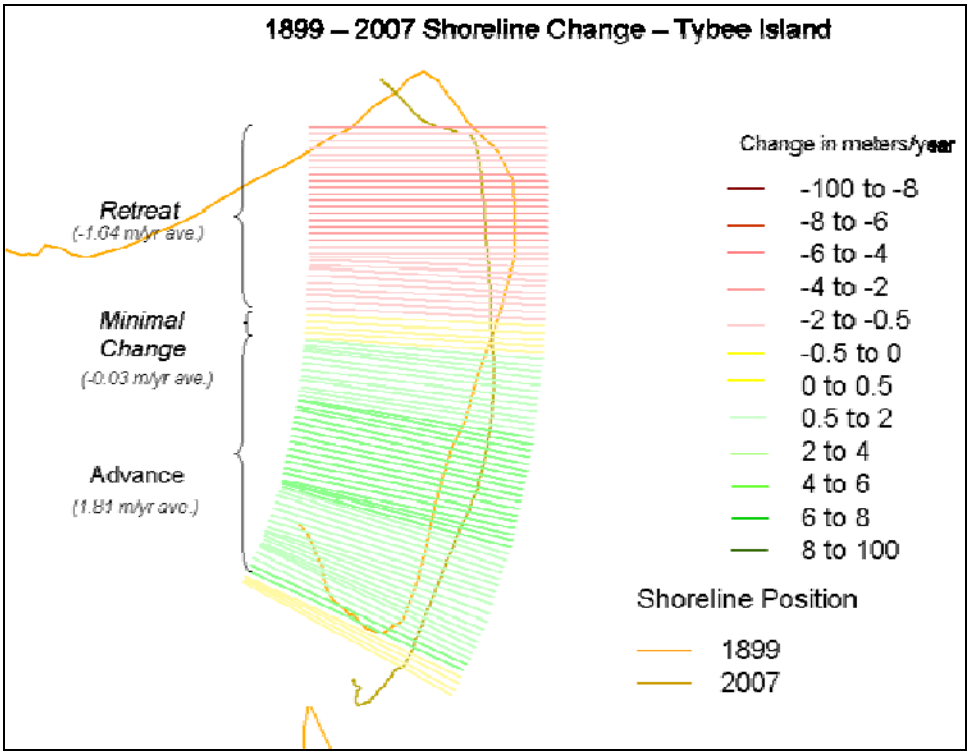

Figure 2-42. Change in Tybee Island shoreline from 1899 to 2007.

The USGS measured the long-term shoreline change from 1863 to 2000 in South Carolina which included the effects of the beach fills. Figure 2-43 shows the rate of change in m/yr for the South Carolina barrier islands in the study area over this 137-year period. The USGS rate of change data are representative of the study period and will be used even though the dates are different from the bathymetry change period of 1897 to 2007. Data for Hilton Head Island show that the south end of the island is growing around +0.5 to +4.2 m/yr (1.6 to 13.8 ft/yr) as the island shoreline progresses southward. In spite of the beach fill on Daufuskie Island in 1998, the long-term trend is for erosion along the entire length of the island with rates ranging from -0.5 to -2.1 m/yr (-1.6 to 6.9 ft/yr). Turtle Island is eroding up to -3 m/yr (9.8 ft/yr) except for the southern end that has migrated into the Wright River inlet at a rate of up to +3.8 m/yr (12.5 ft/yr).

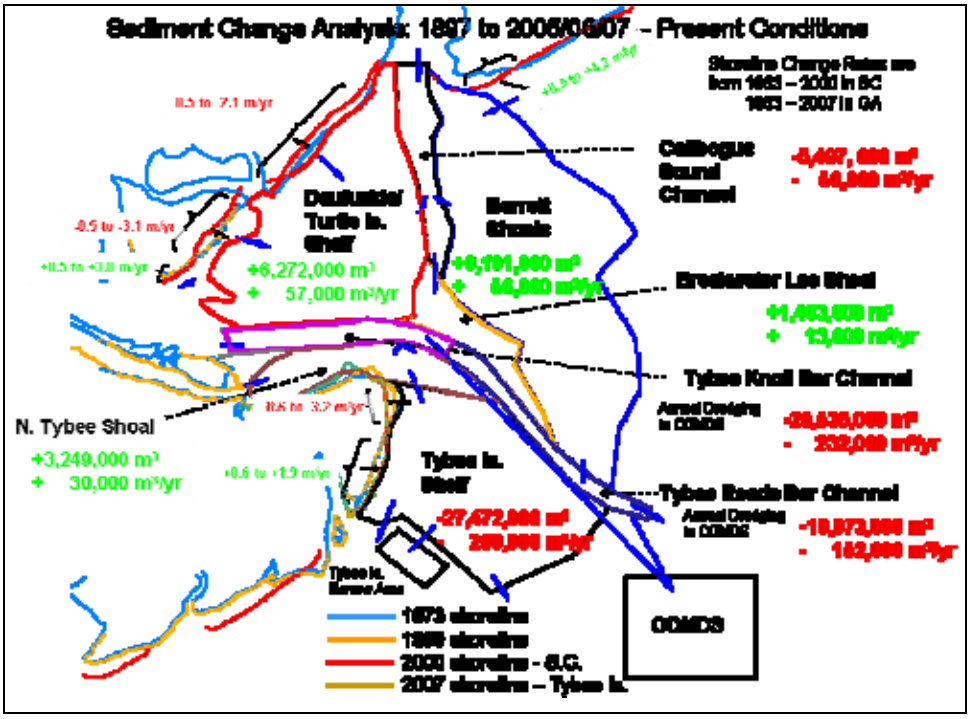

Figure 2-43. Change in volume between 1897 and 2007.

The post-project change analysis in the bathymetry within the volume change cells over the 110-year period is shown in Figure 2-43. The Barrett Shoals cell gained 56,000 m³/yr (73,000 cu yd/yr) with the reorientation of the four channels to the south exiting from Calibogue Sound resulting in infilling of the old channels and scour in the new orientation. The old channel at the southern end of the shoal originating from the Savannah River channel complex has been abandoned and has infilled to give a net gain in this cell. The Calibogue Sound channel has lost a net 50,000 m³/yr as the channel has deepened, while elongating to the south. The Daufuskie/Turtle Islands shelf platform has experienced a net gain of 57,000 m³/yr (75,000 cu yd/yr) as sediment is filled in the southern half of the shelf area due to the reorientation of New River channel to the north. Much of this sediment appears to have come off the beach. The Breakwater Lee Shoal area has now gained 13,000 m³/yr of sediment by what appears to be sediment accumulation in the lee of the submerged breakwater. The Tybee Knoll Bar Channel has lost 232,000 m³/yr (303,000 cu yd/yr) though the nearly annual dredging along the channel with deepening from -6.5 to -13.4 m (-21.5 to -44 ft). Continued net loss of sediment was measured in the Tybee Roads Bar Channel of -152,000 m³/yr (199,000 cu yd/yr), due to this annual dredging and the long-term deepening of the navigation channel. With the growth of the recurved spit in the north Tybee shoal area there has been a gain of

29,500 m^3/yr (38,600 cu yd/yr) of sediment. The shelf platform in front of Tybee Island has a net loss rate of -250,000 m^3/yr (-327,000 cu yd/yr). This net loss corresponds to the deflation of the northern portion of the shelf platform, loss of the nearshore beach profile, and general retreat of the outer edge of the shoal. The volume changes are bounded by the most seaward shoreline position over the study period (1854 to 2007) and thus do not include volume losses or gains resulting from shoreline change. Table 2-7 provides a summary of the volume changes.

Sediment budget calculations

A sediment budget was calculated using the pre-project and post-project shoreline and bathymetry changes. Lack of a full survey just prior to the project made it difficult to establish baseline pre-project conditions and resulted in uncertainty in rates of some key pathways. While sediment volume change within the budget cells was calculated using the data in the study, source and sink data at the boundaries of the budget were not available. A conceptual sediment budget was produced for both time periods with a general assumption of input and output to indicate the probable movement of sediment between the cells within the study area. These inputs and outputs were estimated based on volume changes and the numerical modeling of transport. The volume change cells end seaward of the shoreline, so an addition contribution from erosion/accretion of the shoreline was added. Recent profiles collected from Tybee Island are shown in Figure 2-44. These profiles indicate active profile change to -3 to -4 m (-10 to -13 ft) NAVD88, which is approximately the depth where the volume change calculation ends. An additional 1 m (3.3 ft) was added for the active berm height (~MHW). A value of 5 m (16.4 ft) was used to calculate volumes of sediment input to the budget from beach erosion or accretion from the northern third of Tybee Island and 4 m (13.1 ft) for the southern two-thirds of the island. For constructing the sediment budget, the Barrett Shoals, Calibogue Sound, and Breakwater Lee Shoal volume change cells were combined, as were the Tybee Knoll and Tybee Roads Bar Channel cells. By combining cells some uncertainty was reduced in the sediment sources and sinks. It was assumed that the input to the budget from the north (Hilton Head Island) and output to the south (from the Tybee Island shelf) were unchanged between pre- and post-project (based on modeling results, but neglecting possible changes in sediment supply). Sediment input from the Savannah River is assumed to be small in the post-project budget due to reduced sources and dredging in the river.

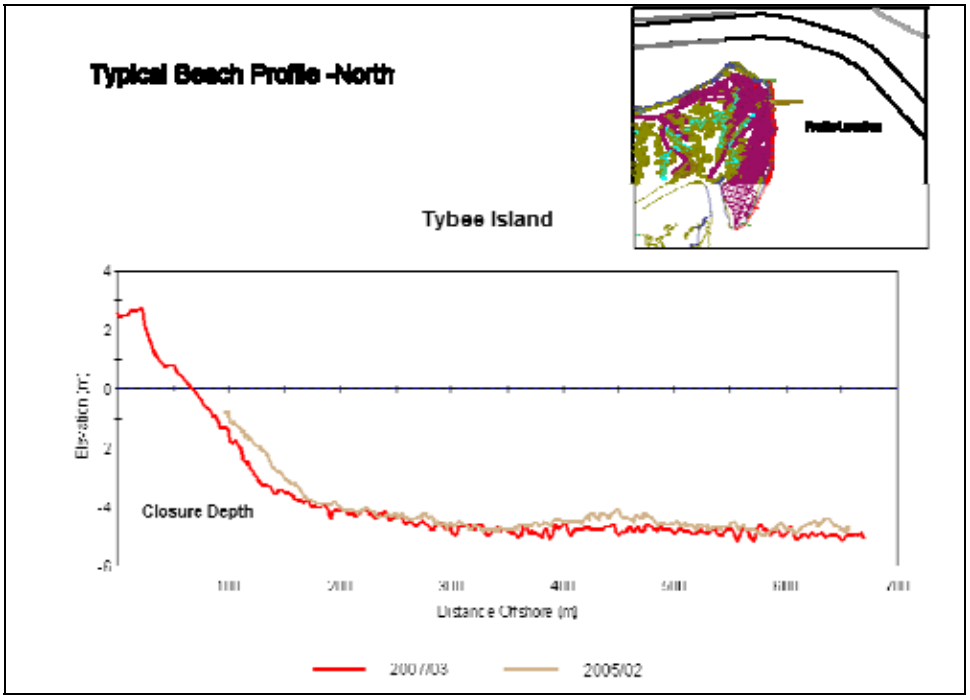

Figure 2-44. Closure depth used in sediment budget calculations based on recent profiles.

The sediment budgets are constructed around the volume change numbers, which provide the most reliable input available. The north and south sources and sinks to the budget are estimated from ranges provided by previous studies. The remaining numbers in the budget were calculated to balance the budget, and were estimated from relative patterns of volume change and the numerical modeling results. Only the net transport between budget cells are provided in the budget, although in many cases there is transport in both directions along the cell boundaries. The estimates of dredged volume rates places in the ODMDS include both dredging for maintenance and deepening. The sediment budget numbers are color coded to indicate their reliability (green for the most reliable and red for the least reliable). The pre-project sediment budget is shown in Figure 2-45 and the post-project sediment budget is shown in Figure 2-46.

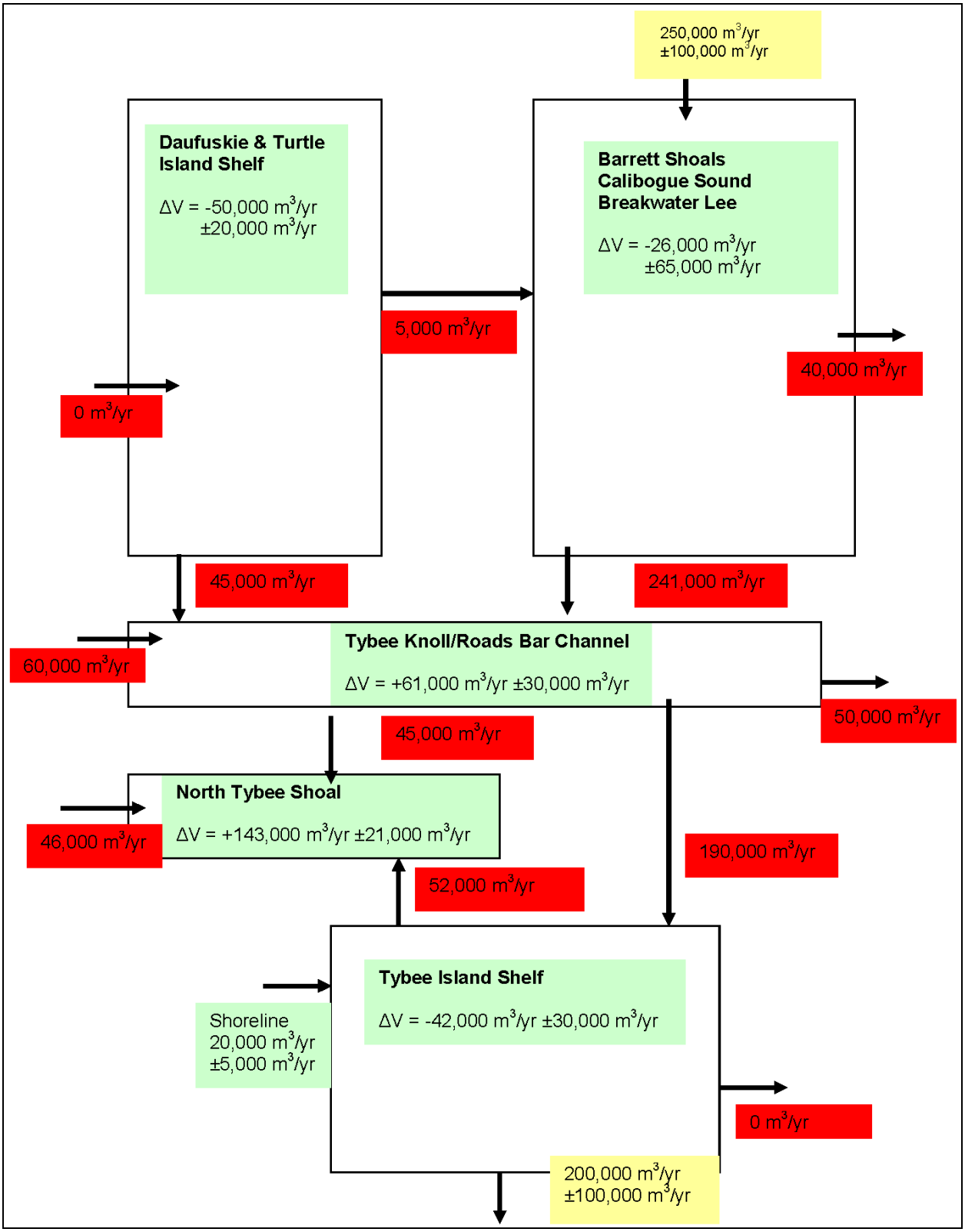

Figure 2-45. Sediment budget for pre-project conditions.

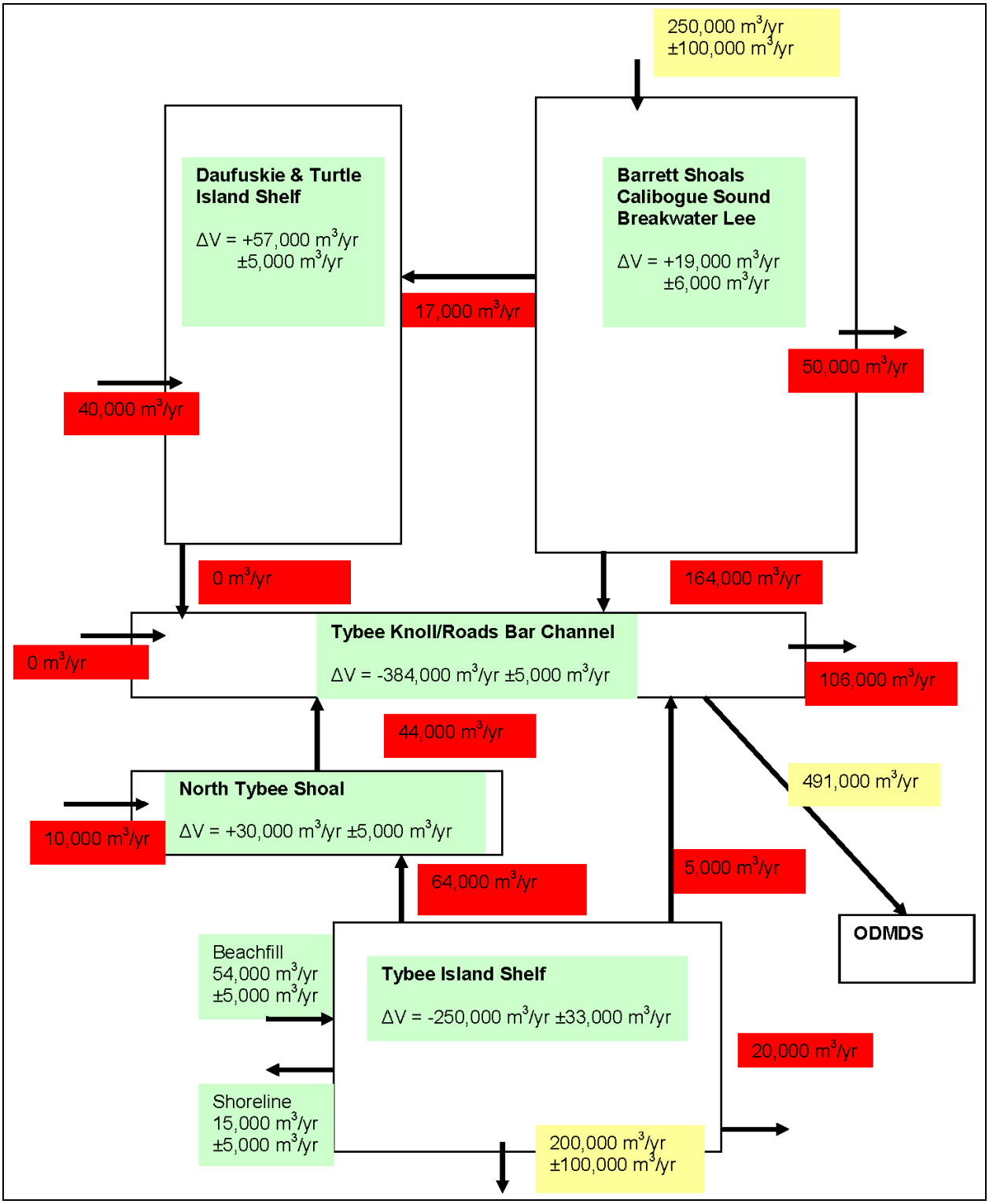

Figure 2-46. Sediment budget for post-project conditions.

Pre-project budget

The pre-project budget is constructed for 1854 to 1897. There dates were selected to include as long of a time period as possible (to improve the reliability of the difference calculations) prior to impact of the project (structures were completed in 1896 and 1897 and dredging of the bar channel began at approximately the same time (ATM 2001)). The USGS shoreline change analysis supports the bathymetric change patterns, although it extends over a slightly shorter time period (1863 to 1999/2000) than the entire study. The USGS data are shoreline position change rates in m/yr while the bathymetric analysis is measuring volume change in m^3/yr. Growth of the south end of Hilton Head Island indicates that net longshore drift along the shoreline is to the south in this area. Southerly growth in Hilton Head Island provides input of sediment into the Barrett Shoals area due to the northeast-southwest orientation of the island. In the pre-project budget there is a loss in volume within the Barrett Shoals area indicating that sediment output is higher than input. Sediment is lost to Calibogue Sound main channel, the Breakwater Shoal area, the shelf further offshore, and to the Tybee Roads Bar Channel from this shoal area based on bathymetric changes that occurred before the project was initiated. Calibogue Sound gained sediment in the pre-project budget period, most likely receiving sediment from the Barrett Shoals area. Some sediment may be input into the Calibogue Sound Channel from the sound itself. Additional material may be input from the Daufuskie/ Turtle Island Shoal area. Some material also must go out the south end into the Breakwater Shoal area. With little change in shoreline position between 1863 and 1899, little sediment was input into the Daufuskie/ Turtle Island Shoal area. Some material was likely input from the New River but there is a net loss of material from that cell. The loss was divided as input to Calibogue Sound, Breakwater Shoal, and the Tybee Knoll Bar cells. The southward orientation of the New River channel, the Wright River channel feeding into the main Savannah River Channel all support the loss of sediment in that cell. The Breakwater Shoal cell has a slight loss of sediment so all of the input (mostly from the north) is passed through this cell into the Savannah River complex channel to the south (through either Tybee Knoll or Tybee Roads). There is a gain in sediment in the Tybee Knoll Bar Channel cell indicating that there is deposition of material in this area before project initiation. Input into this cell is probably through input from the Savannah River and from the Wright River through the Daufuskie/Turtle Island Shoal cell. Before dredging there is some pass through to the Tybee Roads Bar Channel cell. Since there is a

complex river channel system in place, some of the sediment from this cell also flows into the North Tybee Shoal cell (which included the dominant channel at the time). The Tybee Roads Bar cell has input from Tybee Knoll Bar, Breakwater Shoal, and the north Tybee shoal cells. A net loss of sediment from the Tybee Roads Bar Cell probably goes seaward onto the shelf and to the south into the Tybee Island Shoal cell. The Tybee Island shoal cell is losing sediment before the project was built indicating that material must be transported southward out of the cell. Based on the beginnings of the bulge erosion on north Tybee Island and the growth of the north spit some material must also be transported north into the north Tybee shoal cell which is graining sediment. The Tybee Island shoreline is a source for the Tybee Island shelf cell for this time period, as sediment is eroded off the beach (Figure 2-38).

Post-project budget

The post-project budget was constructed for 1897 to 2007. The post-project budget shows significant changes from the pre-project budget. These changes occurred over a long period of time as the navigation channel was successively deepened. This budget includes the integrated effects of the project on the regional morphology over the past 110 years. Sediment is still input from the north along Hilton Head Island with the growth of the shoreline to the southwest (assumed unchanged from the pre-project condition). The net change in the Barrett Shoals cell is a gain in overall sediment volume. Sediment is input from the Calibogue Sound cell, which is now losing sediment. Most of the gain is in infilling of old channels, particularly in the southern part of the cell. Sediment may also be input from the south end of the Breakwater Shoal cell. Sediment may be accumulating at the south end of Barrett Shoals due to lack of episodic bypassing through channel migration. The Calibogue Sound cell now is losing material as more sediment is passed out of the cell than is added into it from the alongshore transport and input from the sound. Sediment is now leaving the cell to the Daufuskie/Turtle Island, the Breakwater Shoal, and Barrett Shoals cells. The long-term retreat of the MHW shoreline along Daufuskie and Turtle Islands and the gain in sediment in the Daufuskie/Turtle Island shelf platform indicates that the sediment (mostly fine sands and silts) are being eroded off the shoreline and deposited on the shelf in that area. Daufuskie/Turtle Island Shoal is now gaining slightly with shoreline erosion of both islands and input from the New River. The gains are in the southern section of the cell, where the New River channel has reoriented to the north and the old channel has filled in.

Some sediment is most likely leaving to go into the Breakwater Shoal and the Tybee Knoll Bar cells. The Breakwater Shoal cell is also gaining material in this budget, with input from the north greater than output to the channel and Barrett Shoals. The Bar Channel cell is losing sediment due to the annual dredging and channel deepening over time. The rate of average dredging has changed over time with channel deepening. Figure 2-47 shows that the average maintenance dredging rates have increased from 163,600 cu m/yr (214,000 cu yd/yr) with the channel depth of 8 m (26 ft) from 1910 to 1930 to around 576,000 cu m/yr (753,000 cu yd/yr) from 1945 to 1978 with a channel depth of between 9 and 11 m (30 and 36 ft), and finally to an average rate of 676,000 cu m/yr (860,000 cu yd/yr) with a depth of between 12 and 13 m (40 and 44 ft) from 1978 to the present. The slope of the curve represents the average rate of dredging and reflects the increased shoaling in the bar channels. Material dredged from the navigation channel has for the most part been disposed of in the ODMDS. The ODMDS was outside the limits of the 1854 bathymetry so no measurement of change could be made from the difference analysis. Dredging records indicate almost 54 million m^3 (71 million yd^3) has been removed from both bar channels between 1910 and 2006 (note that dredging records in Table 2-5 are in cubic yards). The difference between the net volume changes in the channels and the higher dredging volume is due to additional sediment input from the north Tybee shoal and Barrett Shoals, and possibly Tybee Island shoal.

The north-south shoreline orientation of Tybee Island and the shoreline change patterns indicate that sediment is being transported to the north and south of the nodal point in the very nearshore zone. The change in nearshore bathymetry from 1970/83 and 2005 indicate that this is the case. The north Tybee shoal area is gaining sediment from the shoreline and from the Tybee Island shelf platform. Some of this material is likely to be transported into the Tybee Knoll Bar Channel. The Tybee Island shelf is losing sediment on all pathways, with the exception of beach fills. The Tybee Island shoreline change rates indicate that the nearshore net sediment transport is to the north from the nodal point north, which adds material into the north Tybee shoal area. South of the nodal point sediment is transported south along the beach and ends up on the beach south of the south terminal groin and on the ebb shoal of Tybee Creek Inlet.

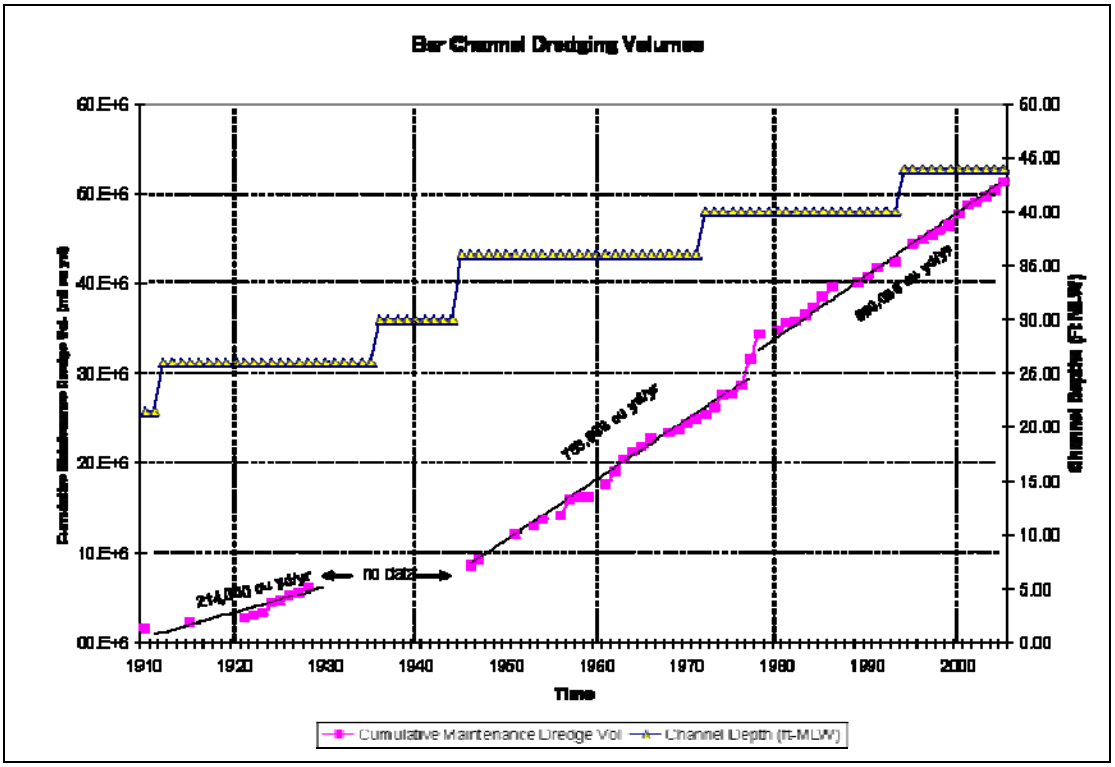

Figure 2-47. Cumulative maintenance dredging volumes along the Tybee Knoll and Tybee Roads Bar Channels.

The Tybee Island shoreline is a sink from the Tybee Island shelf cell for this time period, as the volume of sediment accreted on the southern shoreline is greater than the volume eroded from the northern shoreline (Figure 2-42). Data provided by SAS on changes in the Tybee Island borrow area off the south end of this present study indicate that the borrow area is infilling from the north, from sediment transported to the south across the Tybee Island cell.

Acknowledgments

Matt Goodrich of Applied Technology and Management Inc., Charleston, SC, supplied some of the historic bathymetry. Wilber Wiggins, USACE Savannah District, supplied several data sets and air photographs and information on dredging records, surveys, and erosion control efforts on Tybee Island. Mary Claire Allison, CHL, provided assistance with GIS analysis.

3 Circulation Modeling

A major task completed during the Savannah Harbor Entrance Channel: Nearshore Placement of Dredged Material Study (Gailani et al. 2003b) was the development, calibration, and application of a fine-grid hydrodynamic model of the Savannah River entrance channel and the surrounding ebb shoal and ocean-exposed coast. The ADvanced CIRCulation (ADCIRC) model (Luettich and Westerink 2004) was applied for generation of tidal currents, wind-driven currents, and storm surges needed for the sediment transport and wave models. ADCIRC is a two-dimensional, depth-integrated, finite-element, ocean circulation model that has been proven to accurately simulate tidal and storm conditions in nearshore regions. ADCIRC-calculated velocities and water levels were used to develop storm and non-storm hydrodynamic conditions in the river and on the ebb shoal. The accuracy of the model was evaluated using available tidal data at Fort Pulaski, in Tybee Creek, and offshore. In addition, Acoustic Doppler Current Profiler (ADCP) current data provided by Applied Technology and Management, Inc. (2001) were used to evaluate the model. During that study, the ADCIRC hydrodynamic model was applied for the following simulations: (1) July 1999 was simulated to represent a low wind condition summer month, in which forcing with tidal constituents were included; (2) November 1979, which included a number of storms, was simulated to represent an active month; and (3) Hurricane Hugo retracked to hit Savannah (September 1989). Hugo was selected as the extreme event for this study because it was a recent severe storm and good meteorological information was available to drive the hydrodynamic models. Hurricane Hugo made landfall northeast of Charleston, SC, as a Category 4 storm. Hugo was retracked in this study to hit Savannah (see also Gailani et al. 2003a). Figure 3-1 shows the location of the wind input point for the representative wind input velocities, for each simulation period, displayed in Figures 3-2 to 3-4.

The purpose of the present circulation modeling effort is to evaluate the changes in the water surface elevation and depth-averaged velocity patterns in the vicinity of Tybee Island between the existing and pre-project bathymetric conditions. The results of the Savannah Harbor Entrance Channel: Nearshore Placement of Dredged Material Study were utilized in the present effort to represent the exiting conditions.

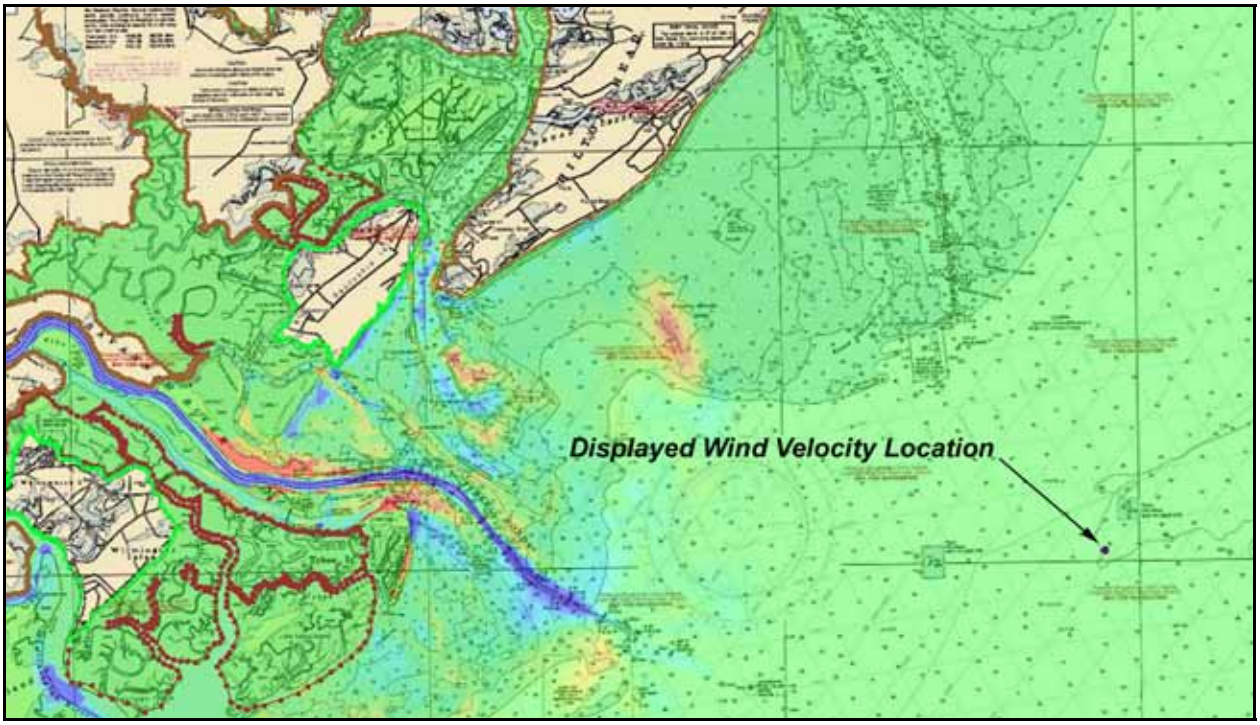

Figure 3-1. Representative input wind velocity location.

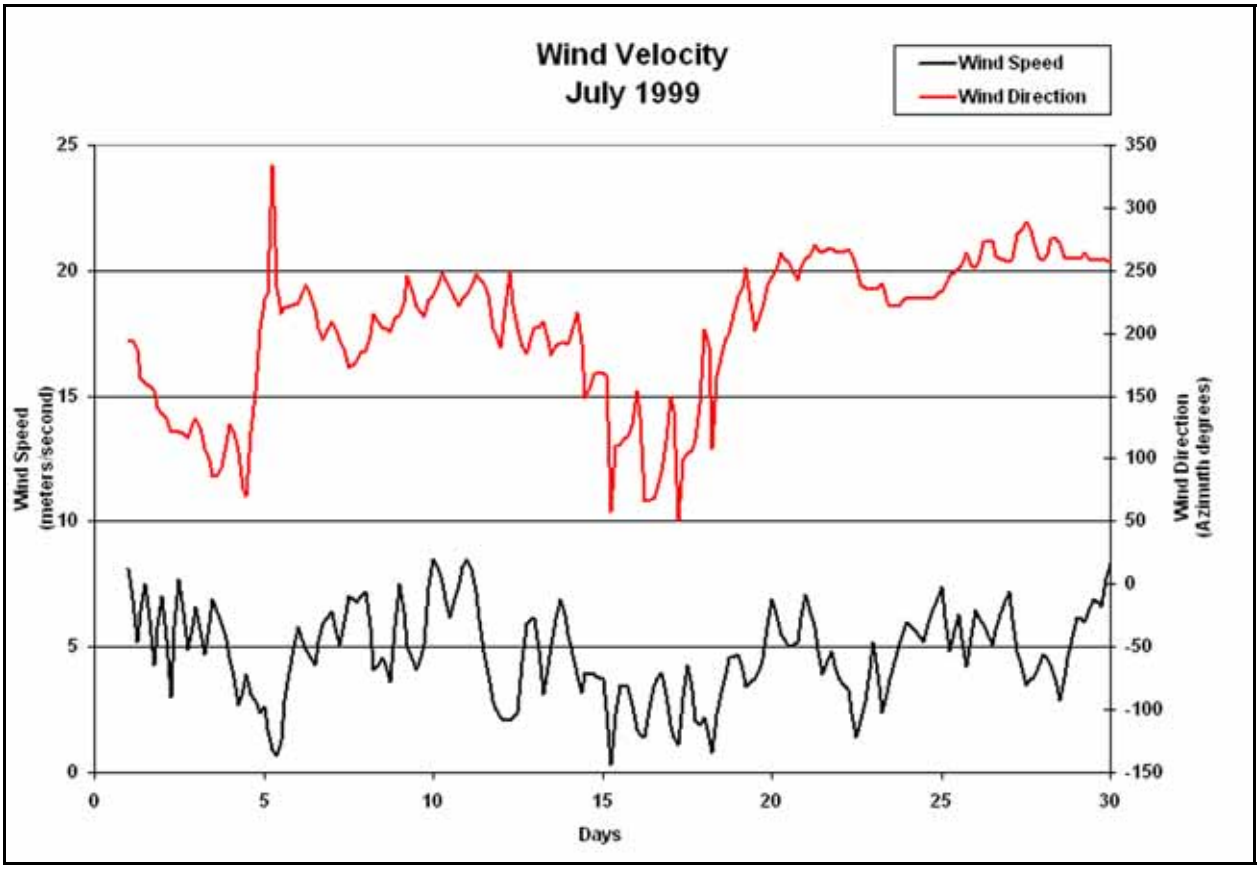

Figure 3-2. Representative input wind velocities July 1999.

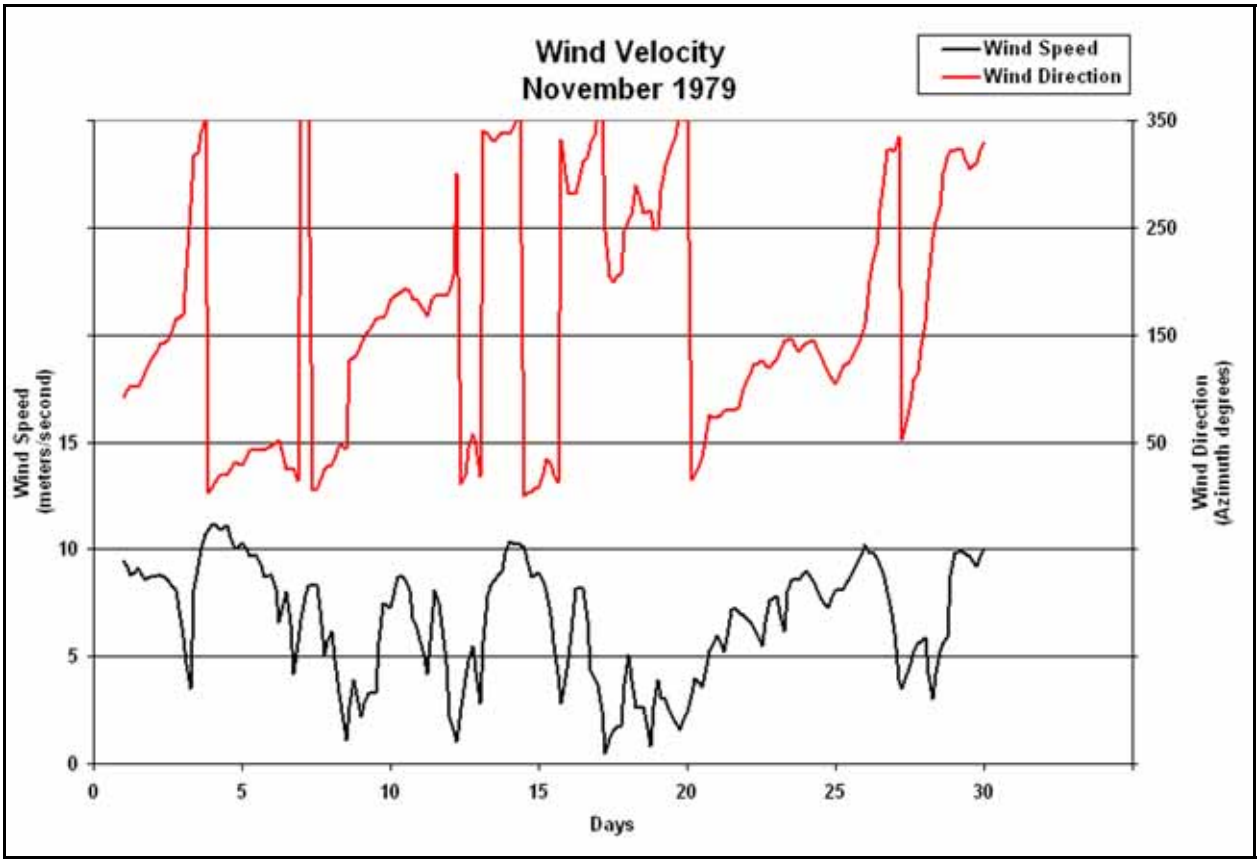

Figure 3-3. Representative input wind velocities November 1979.

The development of the ADCIRC model grid, boundary forcing functions, and the model verifications are presented in detail within the Savannah Harbor Entrance Channel: Nearshore Placement of Dredged Material Study Report.

The tasks employed to examine and compare existing and pre-project hydrodynamics include (1) reconstituting the ADCIRC model grid, input, and output files; (2) comparing model simulation water surface elevations to water surface elevation field measurements at Fort Pulaski to demonstrate that the original calibrated model has been reconstituted; (3) modifying the ADCIRC grid to represent existing and pre-project bathymetric conditions; and (4) the comparison of the existing and pre-project hydrodynamic model results for the three simulation periods described above. Table 3-1 summarizes the ADCIRC simulation parameters (Luettich and Westerink 2005). The final ADCIRC model simulations included the application of wave radiation stress gradients provided by the STWAVE model (Chapter 4).

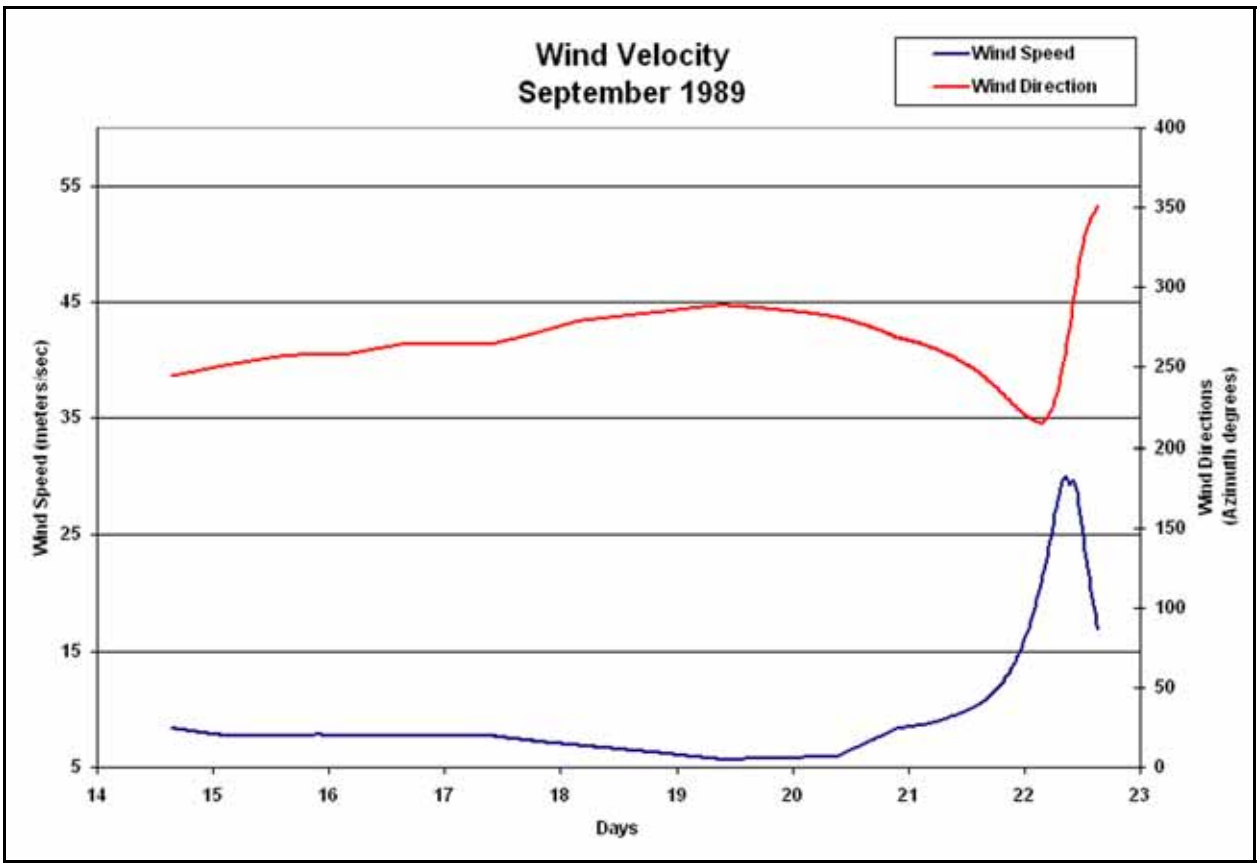

Figure 3-4. Representative input wind velocities September 1989.

Table 3-1. ADCIRC simulation parameters.

Coordinate System	Spherical
Model run type	Two dimensional, depth integrated
Nonlinear terms	Nonlinear quadratic bottom friction, finite amplitude terms included, advective terms included (including time derivative portion)
Forcing	Tidal potential, wind, pressure (for retracked Hugo), river inflow, and wave stresses
Ramp	One day, hyperbolic tangent ramp
τ_0 (generalized wave continuity equation weight)	0.01
Time step	1 sec for all runs except July 1999, which is 0.5 sec
Flood and dry parameters	Nominal water depth for dry node = 0.1 m, minimum number of time steps cell must remain dry before rewetting = 150, minimum number of time steps nodes must remain wet before drying = 0, minimum velocity for wetting 0.05 m/sec
Bottom friction coefficient	0.0025
Lateral eddy viscosity	3.0 m^2/sec
Tidal constituents	K1, O1, Q1, M2, S2, N2, K2

Grid generation

The ADCIRC grid geometry developed in the Savannah Harbor Entrance Channel: Nearshore Placement of Dredged Material Study was used in this study with modifications to the bathymetry. Two sets of ADCIRC grid bathymetry were generated, one to represent the bathymetry at the time of this study (existing condition, 2007) and the other to represent the topography and bathymetry in place prior to improvements of the Federal navigation channel and construction of the jetties and offshore submerged breakwater (pre-project condition, 1854). The existing condition ADCIRC grid bathymetry was created by merging several data sets. A 2007 survey by the Savannah District provided data from the Tybee beaches and seaward to capture the navigation channel including the Tybee Roads portion. A 2006 NOAA survey supplied areas of the South Channel near the northern portion of Tybee, the submerged breakwater, and the area surrounding Bloody Point Range (Figure 3-5). These two surveys took precedence over the remaining NOS products from 1995, 1994, 1983, 1980, 1974, and 1973. The NOS surveys were used to define the majority of the remaining model domain and were assigned precedence in order of their age. The navigation channel was defined by the present-day authorized depth instead of available survey data. Survey data in the channel capture the immediate condition of the channel and could have been taken immediately after maintenance dredging or immediately prior to maintenance dredging and would potentially result in circulation modeling results that are inconsistent with the full potential of the navigation channel. The STWAVE mesh development took the same approach in dealing with depths within the navigation channel.

There were limited topographic and bathymetric data available for the time period prior to construction of the jetties. Digitized bathymetric data from an 1854 map were used as the primary data source and similar data from an 1867 map were used to supplement the gaps and offshore areas not included in the 1854 data set. Digitized shorelines from the 1854 map were used to better define the various islands and smaller inlets and channels within the model domain. Figure 3-5 contains a color contour plot of the bathymetry differences between the existing and pre-project depths.

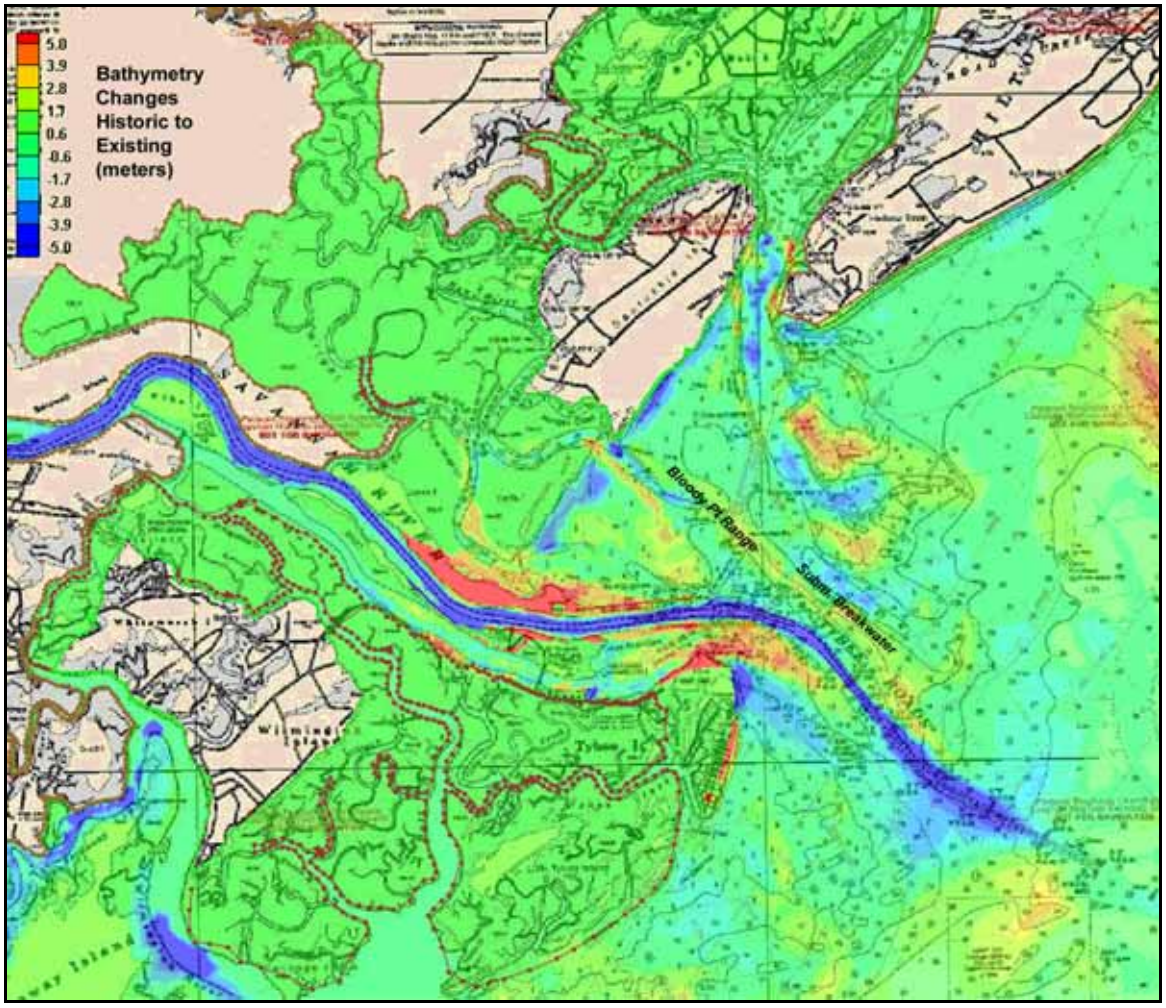

Figure 3-5. Pre-project and existing bathymetry differences (meters).

Validation

The same ADCIRC simulation parameters and mesh geometry used in the 2003 Nearshore Placement of Dredged Material Study were applied in this study. To verify that the calibrated grid and input files were successfully reconstituted, comparisons of the water surface elevation field measurements at Fort Pulaski were compared to model results for the three simulation time periods. Figures 3-6 to 3-8 contain the water surface elevation comparison plots for July 1999, November 1979, and 14–23 September 1989 relative to Mean Tide Level (MTL).

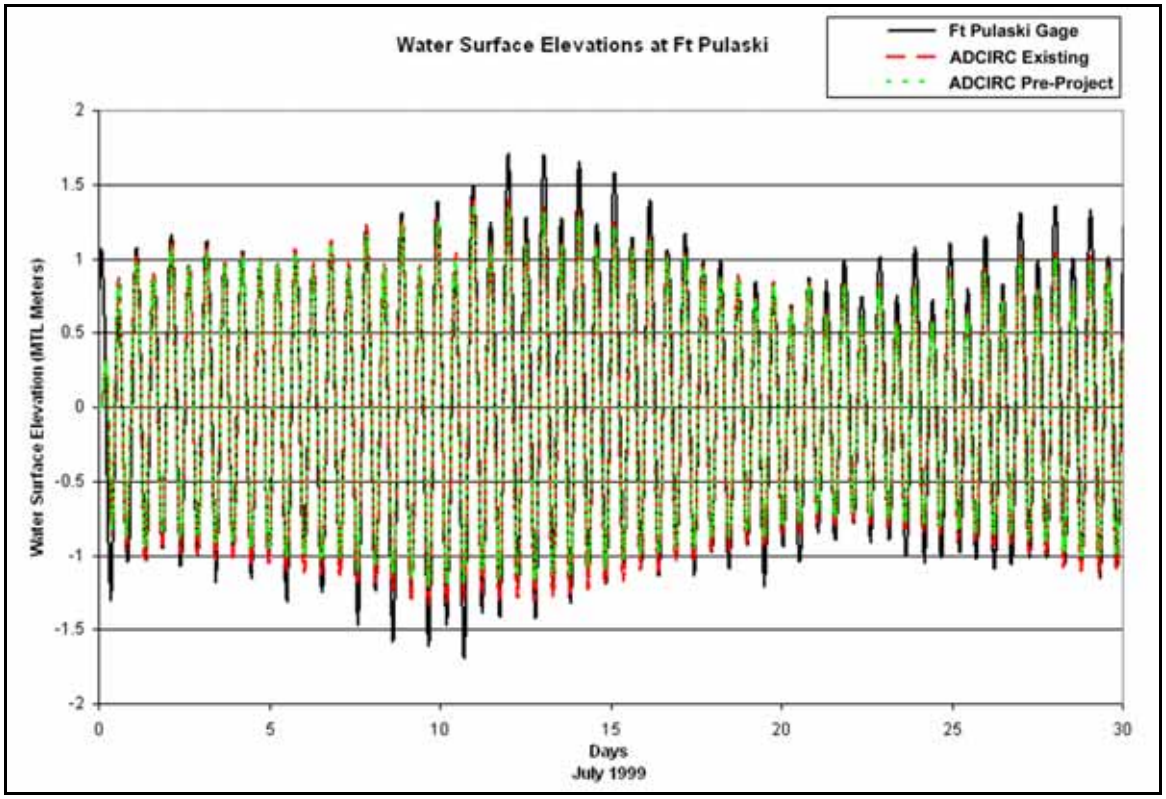

Figure 3-6. July 1999 water surface comparisons.

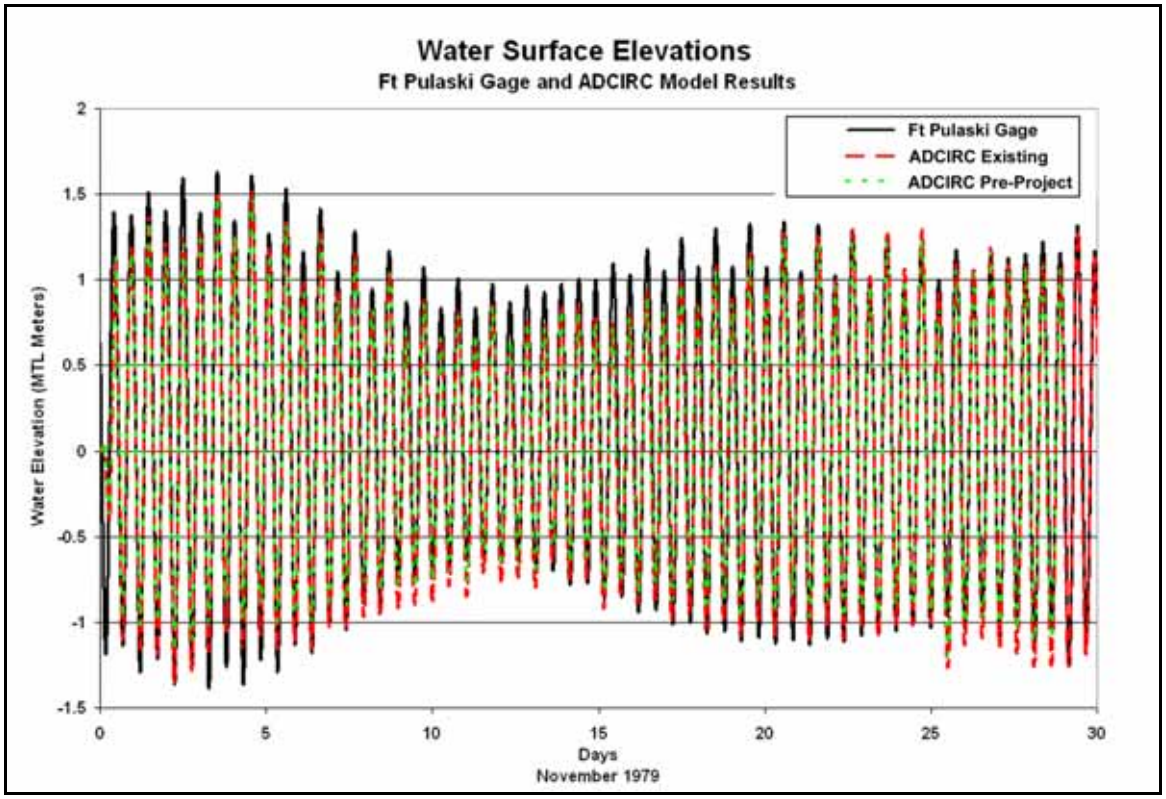

Figure 3-7. November 1979 water surface elevation comparisons.

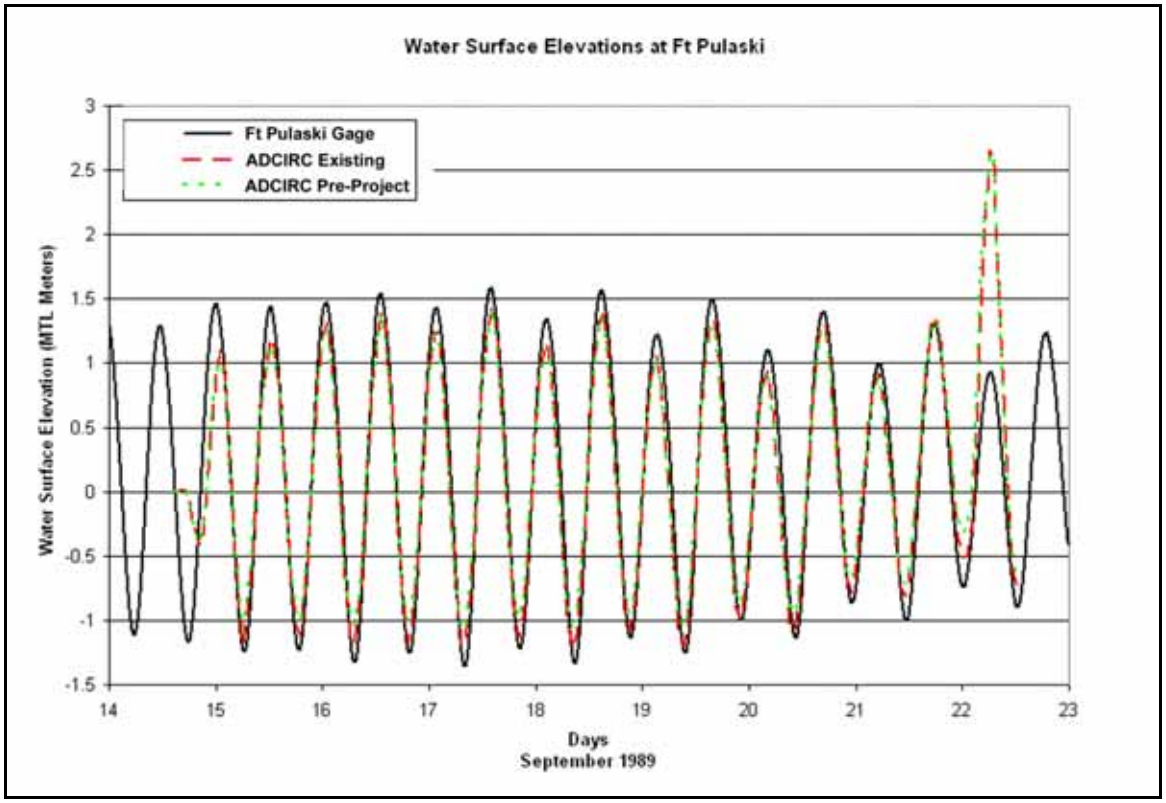

Figure 3-8. 14–23 September 1989 water surface elevation comparisons. The spike on the figure is the hypothetical retracked Hurricane Hugo, so it is not reflected in the measured data.

The graphs show that the calculated water surface elevations at Fort Pulaski compare favorably with the measured elevations. The root mean square of the differences between the calculated and measured water surface elevation at Fort Pulaski are 0.0040 m (0.013 ft) for November 1979, 0.0034 m (0.011 ft) for July 1999, and 0.0082 m (0.027 ft) for 15–21 September 1989. The deviation between the measured and calculated water surface elevation on 22 September 1989 is due to the retracked path of Hurricane Hugo.

Comparison of the present model results with Figure 8 of the Savannah Harbor Entrance Channel: Nearshore Placement of Dredged Material Study report demonstrates that the reconstitution of the original calibrated ADCIRC grid and input files was successful.

Circulation model results

The ADCIRC output includes water surface elevations and depth-averaged velocities. Differences in the water surface elevations and the residual currents for the existing and the pre-project (historic) bathymetries are

presented in this section. Output from the ADCIRC model is used as input to the wave (STWAVE) and sediment transport (GTRAN) models.

July 1999 simulations

Water surface elevation for the existing and pre-project simulations are virtually the same, as shown in Figures 3-9 and 3-10, for a point located off of central Tybee Island.

While the water surface elevations near Tybee did not change due to changes in the existing and pre-project bathymetry, the residual velocity patterns near the north and northeast portions of Tybee Island show significant changes (Figures 3-11 and 3-12). Residual velocity is the average flow speed and direction over the given time period (14–19 July 1999 for these figures).

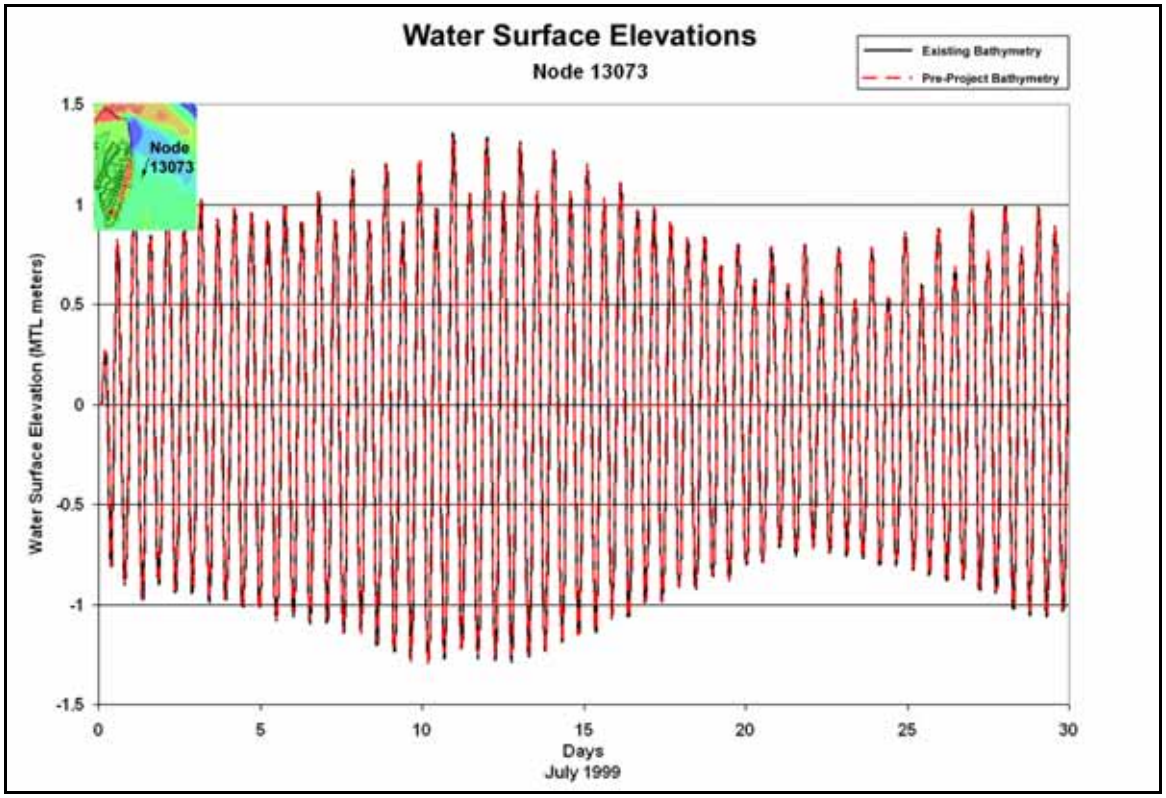

Figure 3-9. Existing and pre-project predicted water surface elevations 1–30 July 1999.

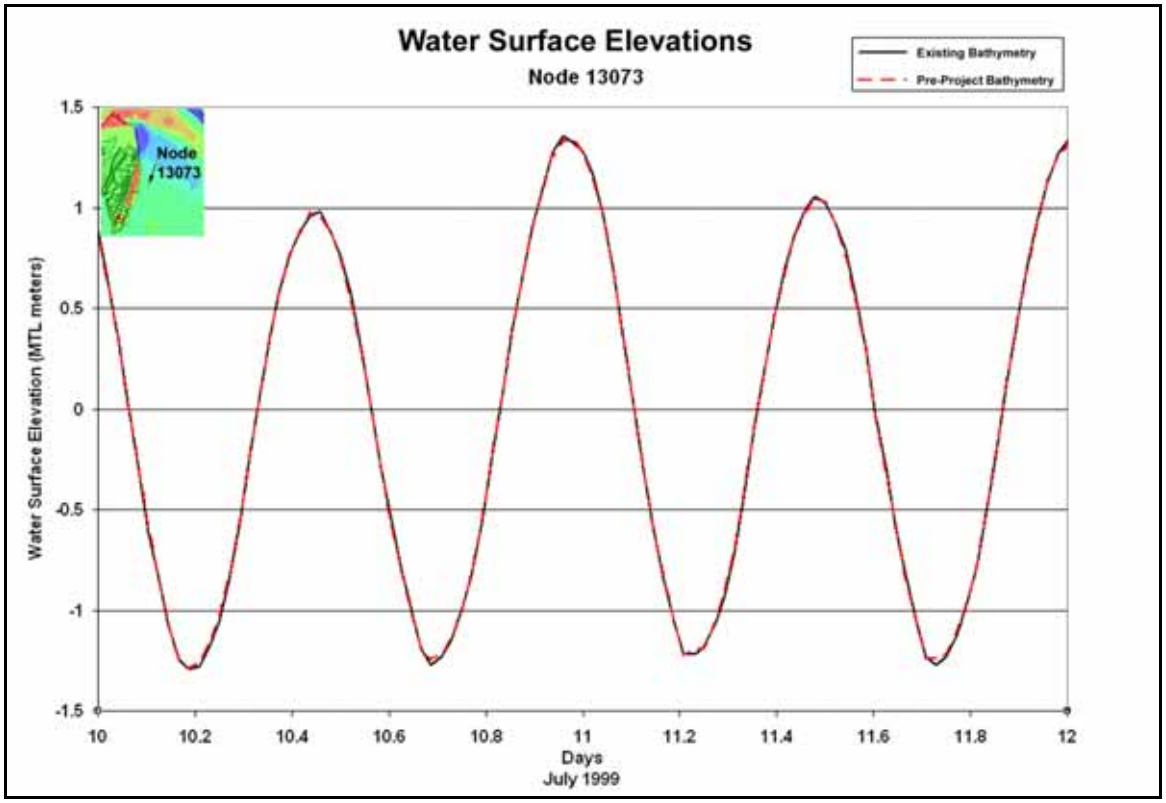

Figure 3-10. Existing and pre-project predicted water surface elevations 10–12 July 1999.

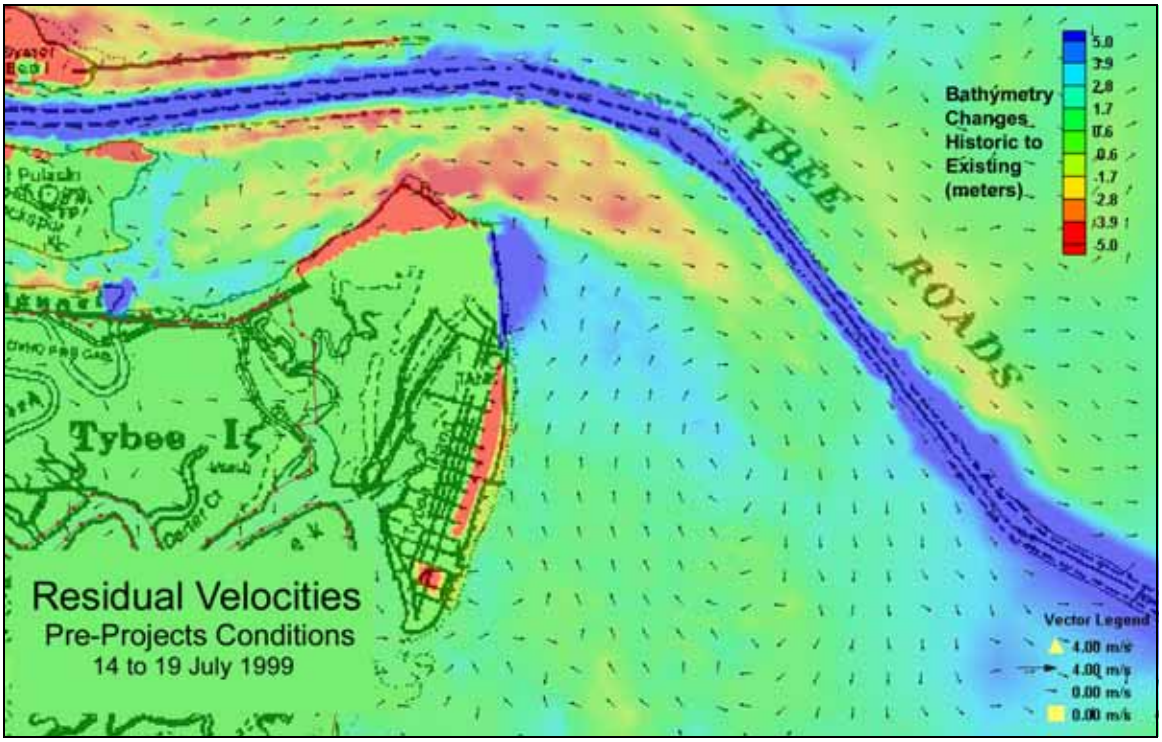

Figure 3-11. Residual velocities 14–19 July 1999, pre-project conditions.

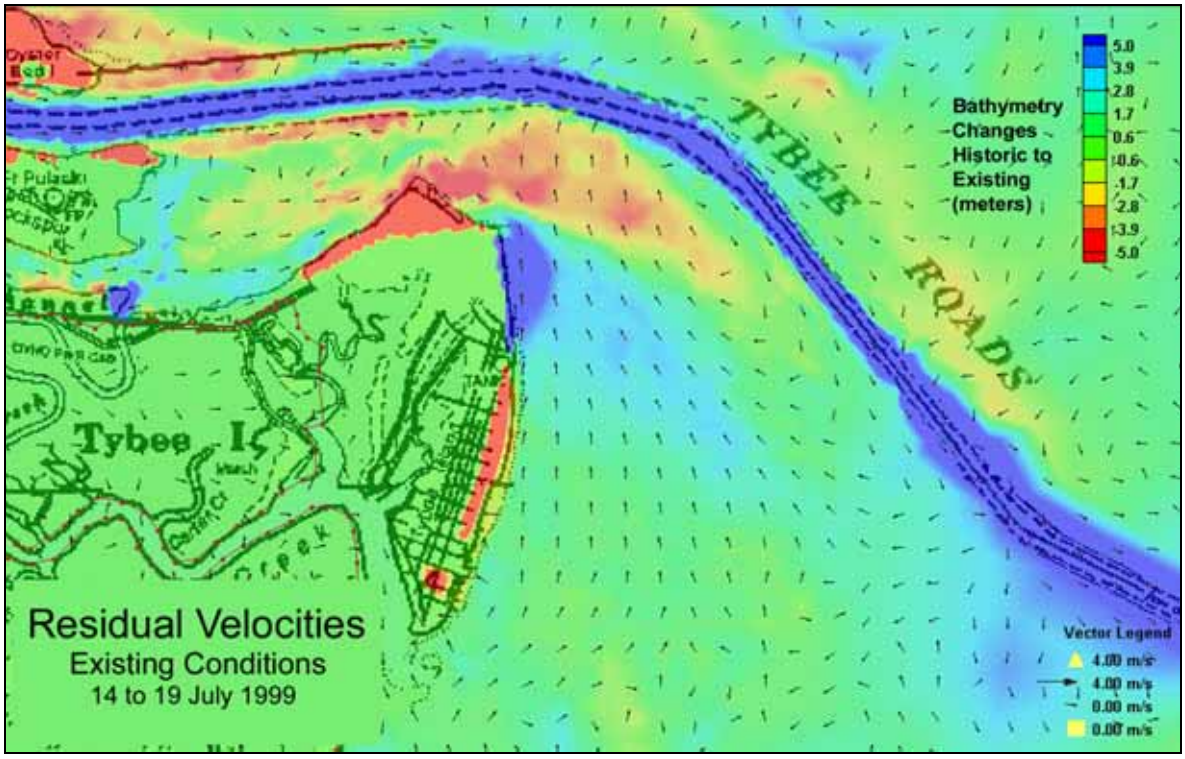

Figure 3-12. Residual velocities 14–19 July 1999, existing conditions.

For the pre-project conditions, residual currents north of Tybee Island flowed to the east and merged with a clockwise eddy which was centered off of the northern portion of Tybee Island. For existing conditions, the center of the residual velocity eddy shifted to the north and the residual velocities north of Tybee Island which had flowed eastward are now directed to the north. The northward shift of the residual velocity eddy is due to the 0.5 m/sec (1.6 ft/sec) increase of the velocity magnitudes in the deepened navigation channel for the existing bathymetric conditions (Figure 3-13). Figures 3-14 through 3-20 contain existing and pre-project velocity magnitude graphs for seven points along Tybee Island. The differences in velocity magnitude between the results for simulations with existing conditions and pre-project conditions vary between plus and minus 0.3 m/sec (1 ft/sec). The degree and timing of the velocity magnitude variation between the simulations depends on the location of the observation node and the wind conditions during the simulation. The most consistent change is north of Tybee Island where the velocity magnitudes for the existing conditions are consistently 0.1 to 0.2 m/sec (0.3 to 0.7 ft/sec) greater than for the pre-project conditions.

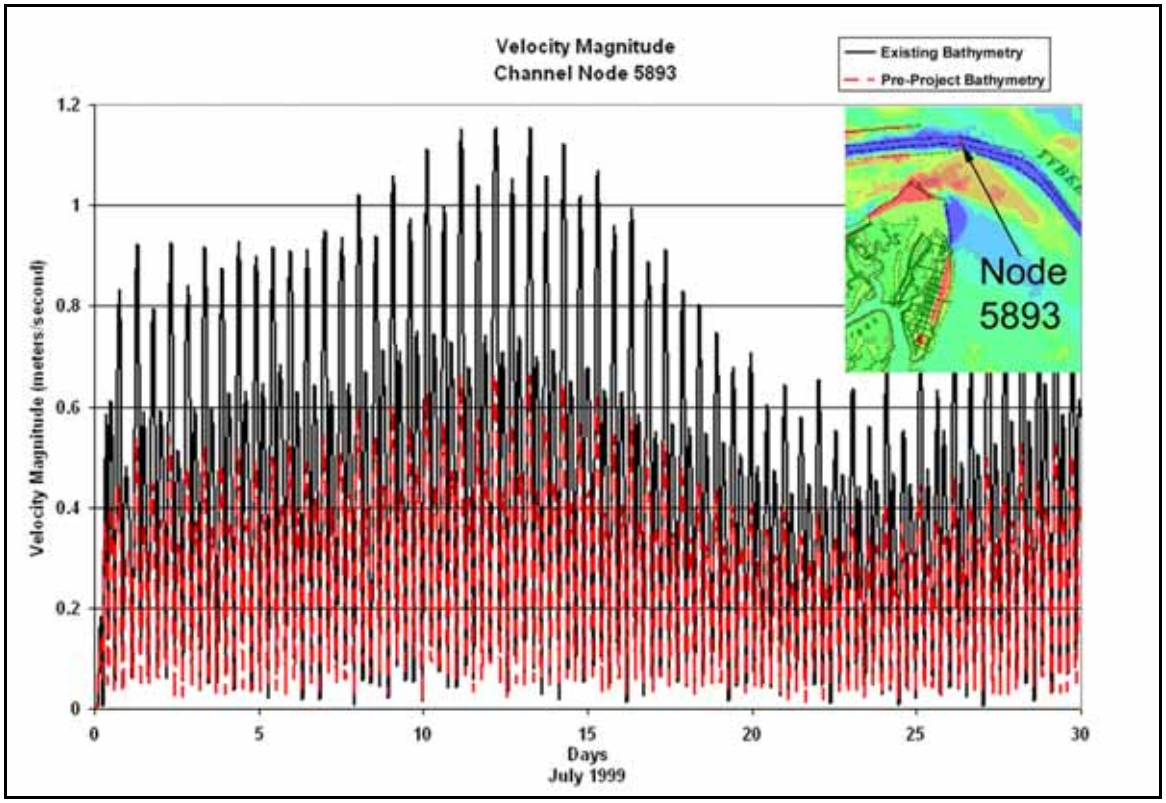

Figure 3-13. Velocity magnitudes for existing and pre-project conditions July 1999, Navigation Channel Node 5893.

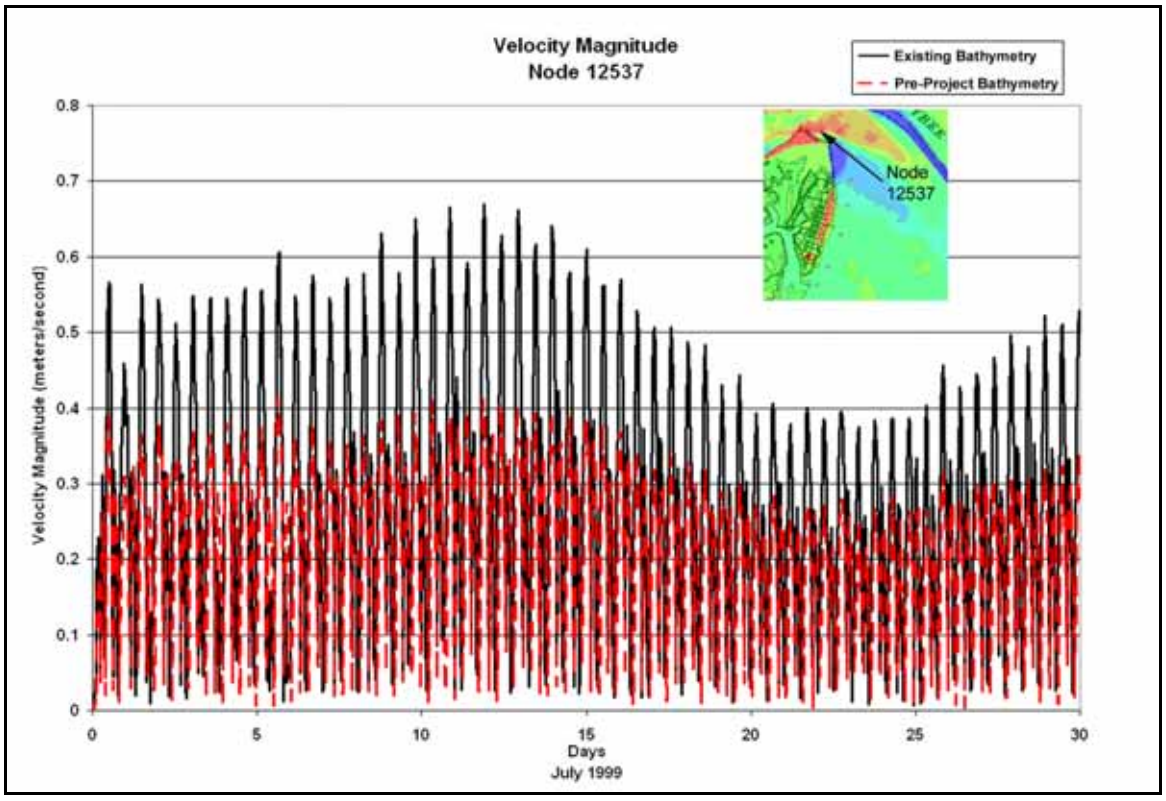

Figure 3-14. Velocity magnitudes for existing and pre-project conditions July 1999, Node 12537.

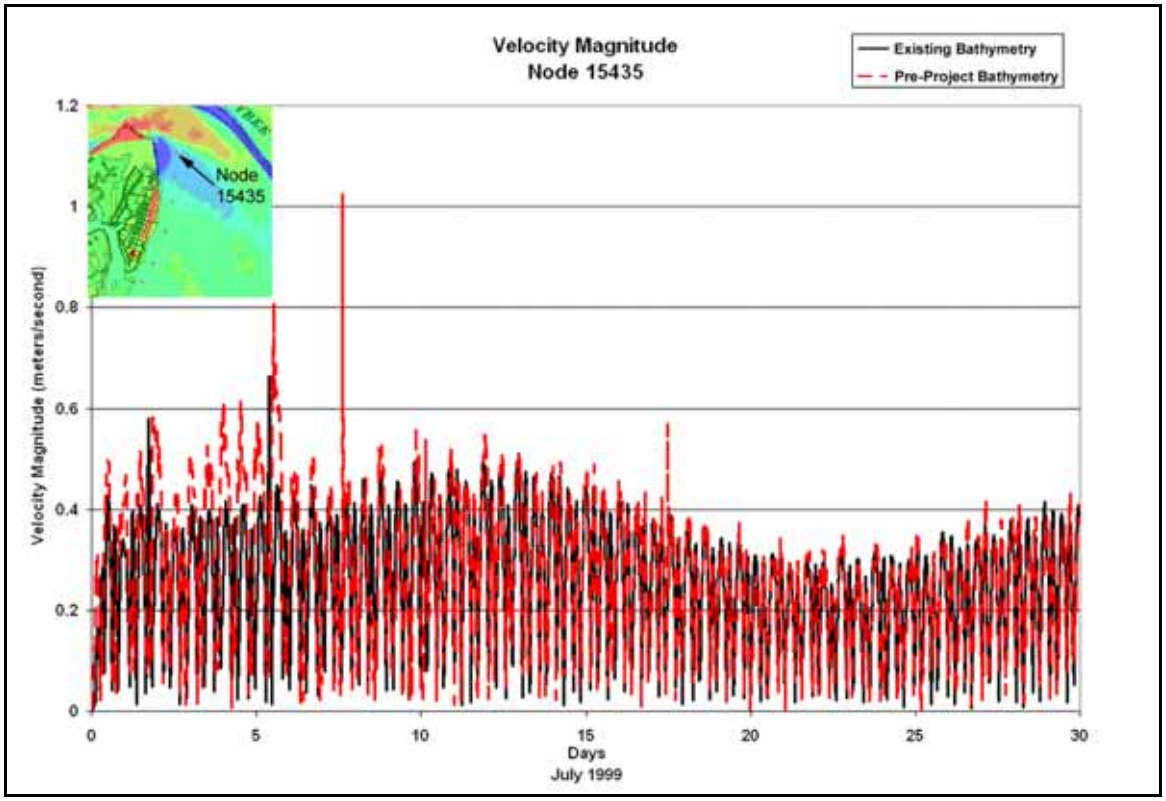

Figure 3-15. Velocity magnitudes for existing and pre-project conditions July 1999, Node 15435.

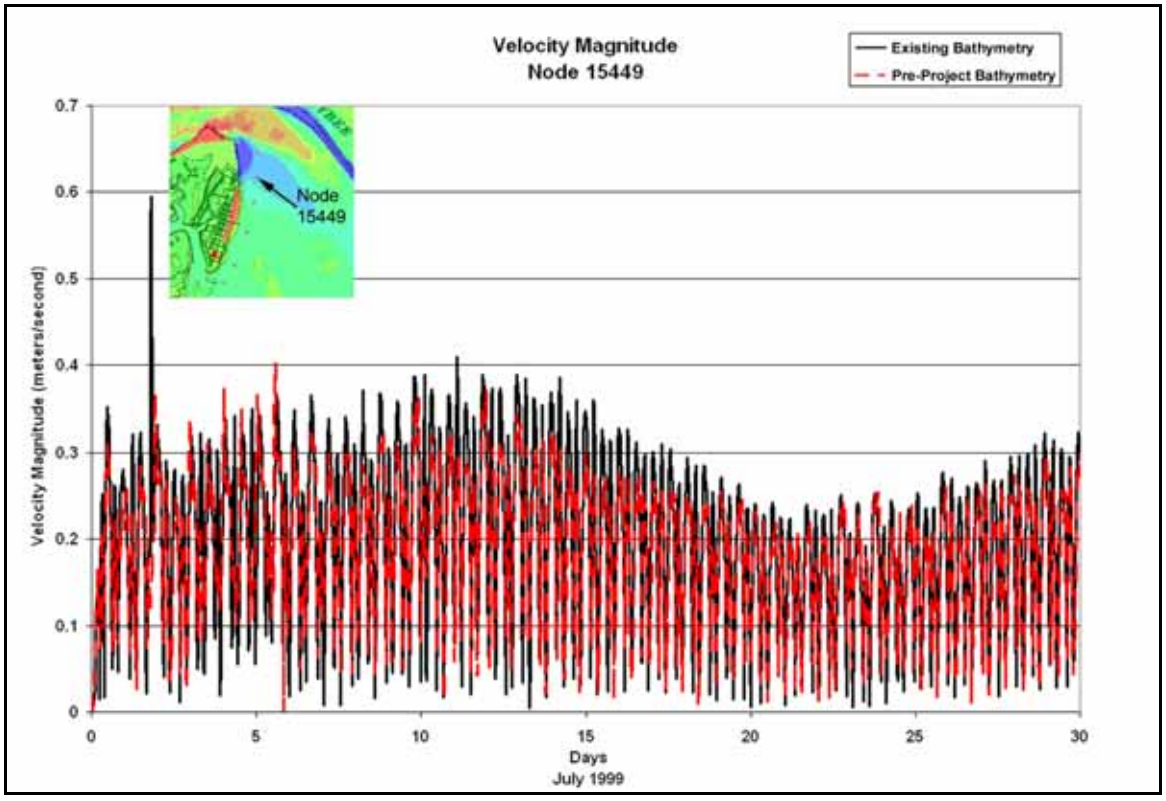

Figure 3-16. Velocity magnitudes for existing and pre-project conditions July 1999, Node 15449.

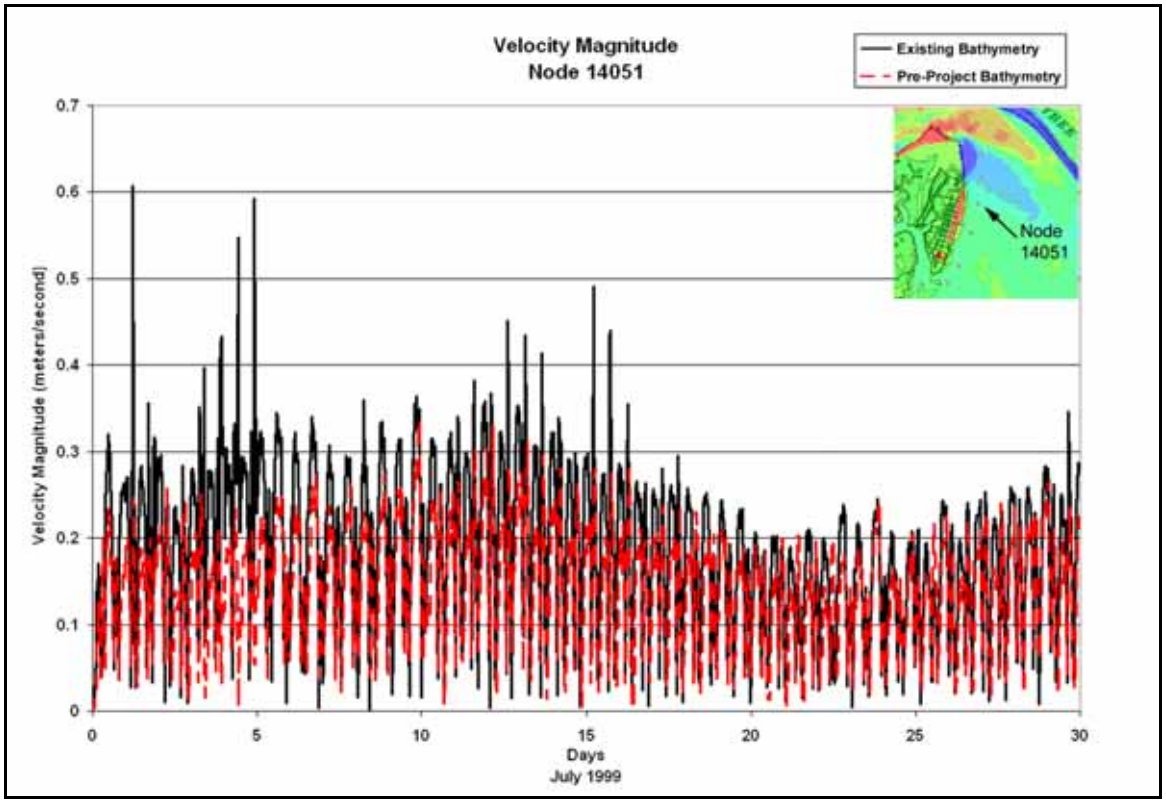

Figure 3-17. Velocity magnitudes for existing and pre-project conditions July 1999, Node 14051.

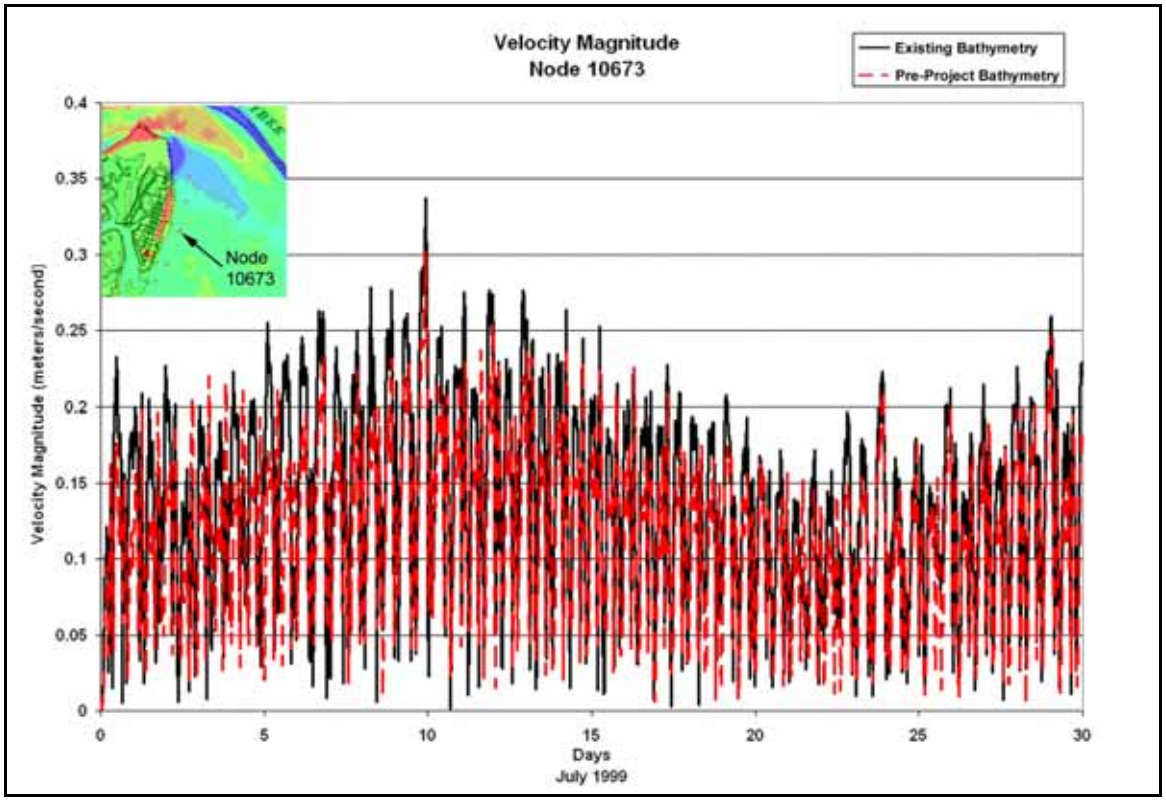

Figure 3-18. Velocity magnitudes for existing and pre-project conditions July 1999, Node 10673.

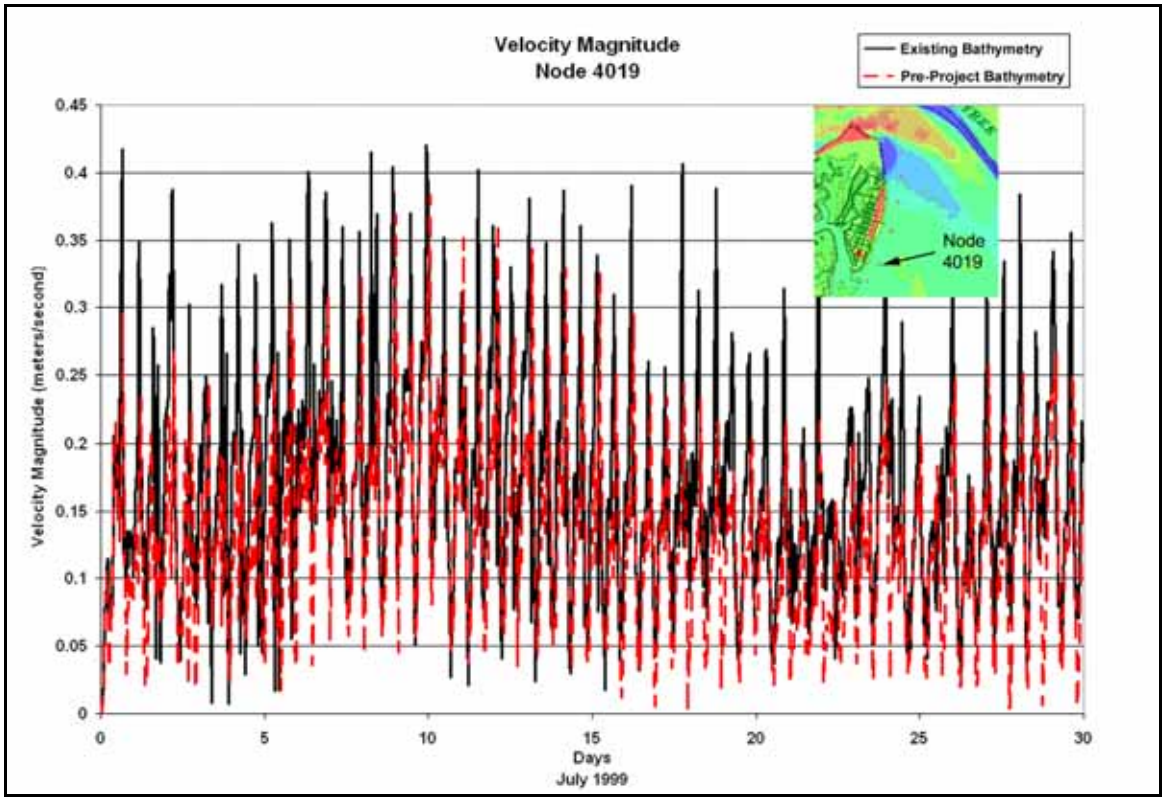

Figure 3-19. Velocity magnitudes for existing and pre-project conditions July 1999, Node 4019.

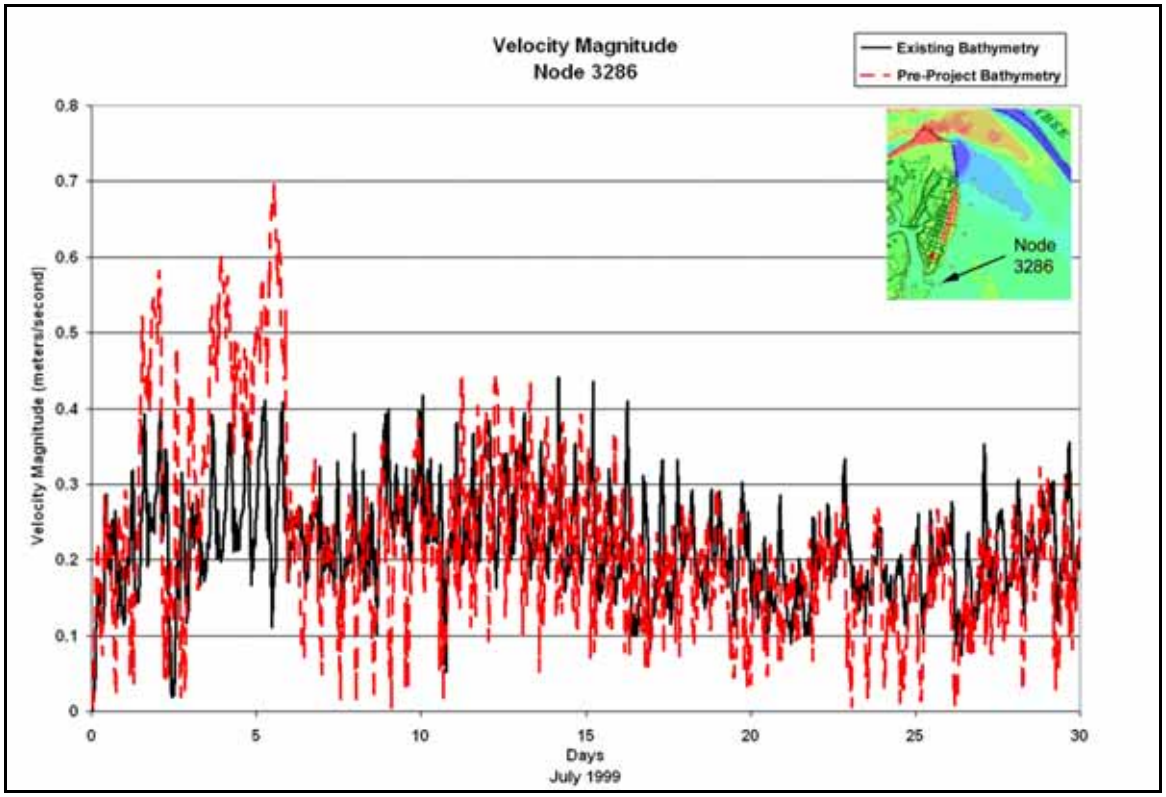

Figure 3-20. Velocity magnitudes for existing and pre-project conditions July 1999, Node 3286.

The peak velocities north of Tybee Island have increased in magnitude and reversed direction for the existing conditions due to the deeper main channel (the same forces that shifted the residual velocity eddy to the north) and the streamlining of the northeast corner of the island due to erosion (Figure 3-14).

Figures 3-21 and 3-22 are the maximum velocity at each grid node for the period 14–July 1999 for the pre-project and existing simulations, respectively. Examination of these pre-project and existing maximum velocity fields reveals that, in the area that has eroded offshore of the north end of Tybee Island (area shown in light blue in the figures), the direction of the maximum velocities has shifted from a southerly to a northerly direction. For the existing condition, currents flow onshore and to the northwest through this developing depression in the shelf. This trend is amplified in the plots of the maximum velocity fields for the period 20–25 July 1999 (Figures 3-23 and 3-24). The line between the ebb dominant (south and east flowing) and flood dominant (north and west flowing) residual currents is shifted further north along the entire Tybee shelf for the existing condition.

November 1979 simulations

As with the July 1999 simulation, the water surface elevations off Tybee Island are essentially the same for existing and pre-project conditions (Figure 3-25).

The northward shift of the residual velocity eddy located offshore of the northern end of Tybee Island that was observed in the July 1999 simulations is again apparent in the residual velocity plots for 14–19 November 1979 pre-project and existing simulations (Figures 3-26 and 3-27). This shift is correlated to the accretion on the north Tybee shoal (red/yellow area in the plot) and deepening of the navigation channel to the north. The eddy represents the shift from ebb dominant in the channel to flood dominant flow on the shelf.

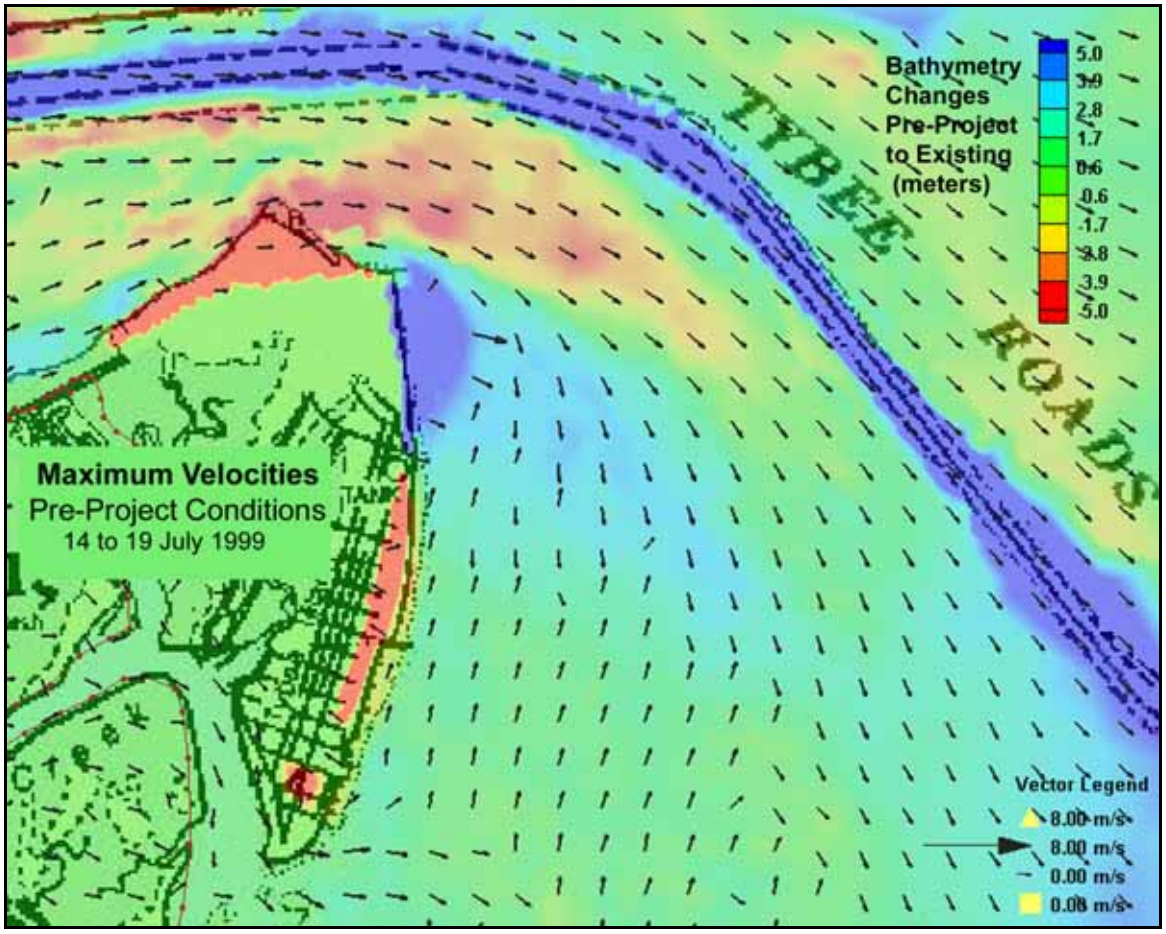

Figure 3-21. Maximum velocities 14–19 July 1999, pre-project conditions.

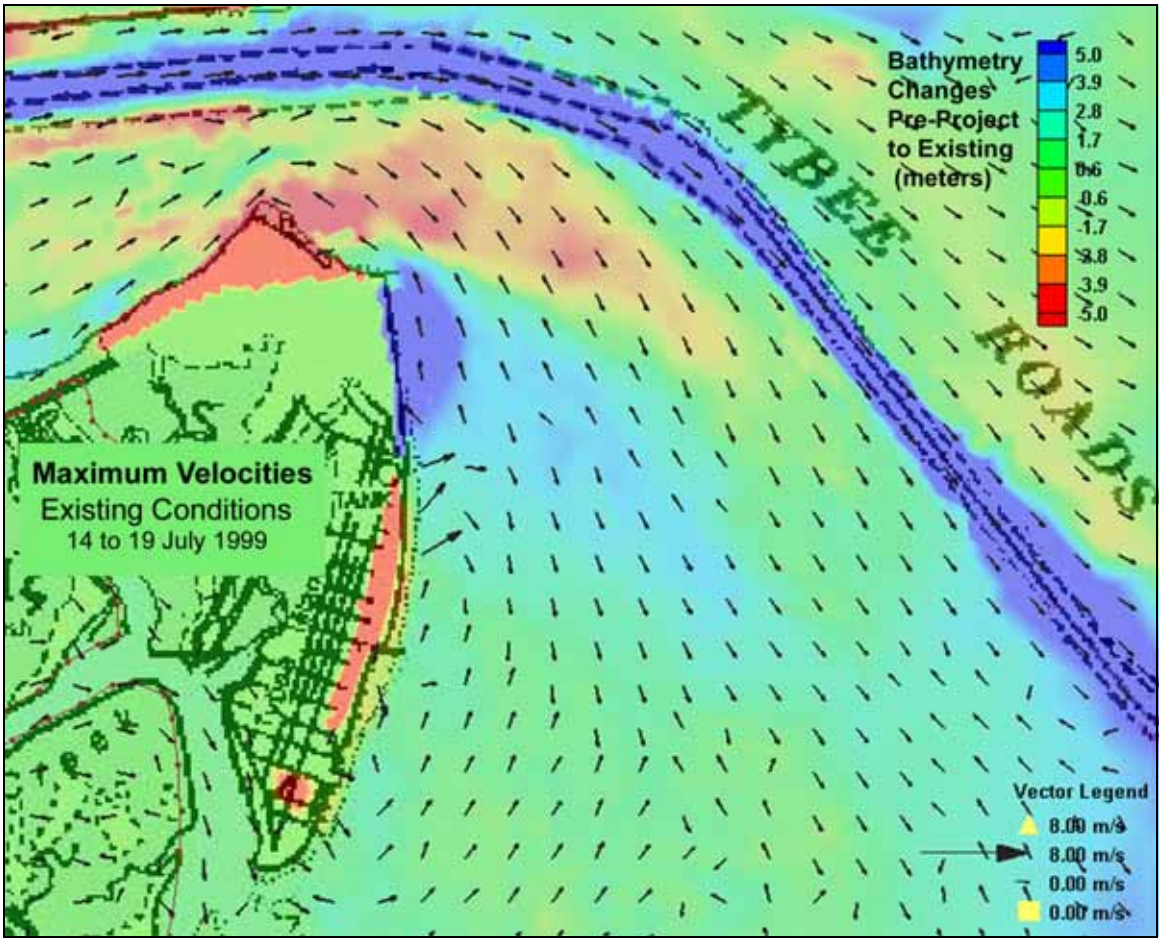

Figure 3-22. Maximum velocities 14–19 July 1999, existing conditions.

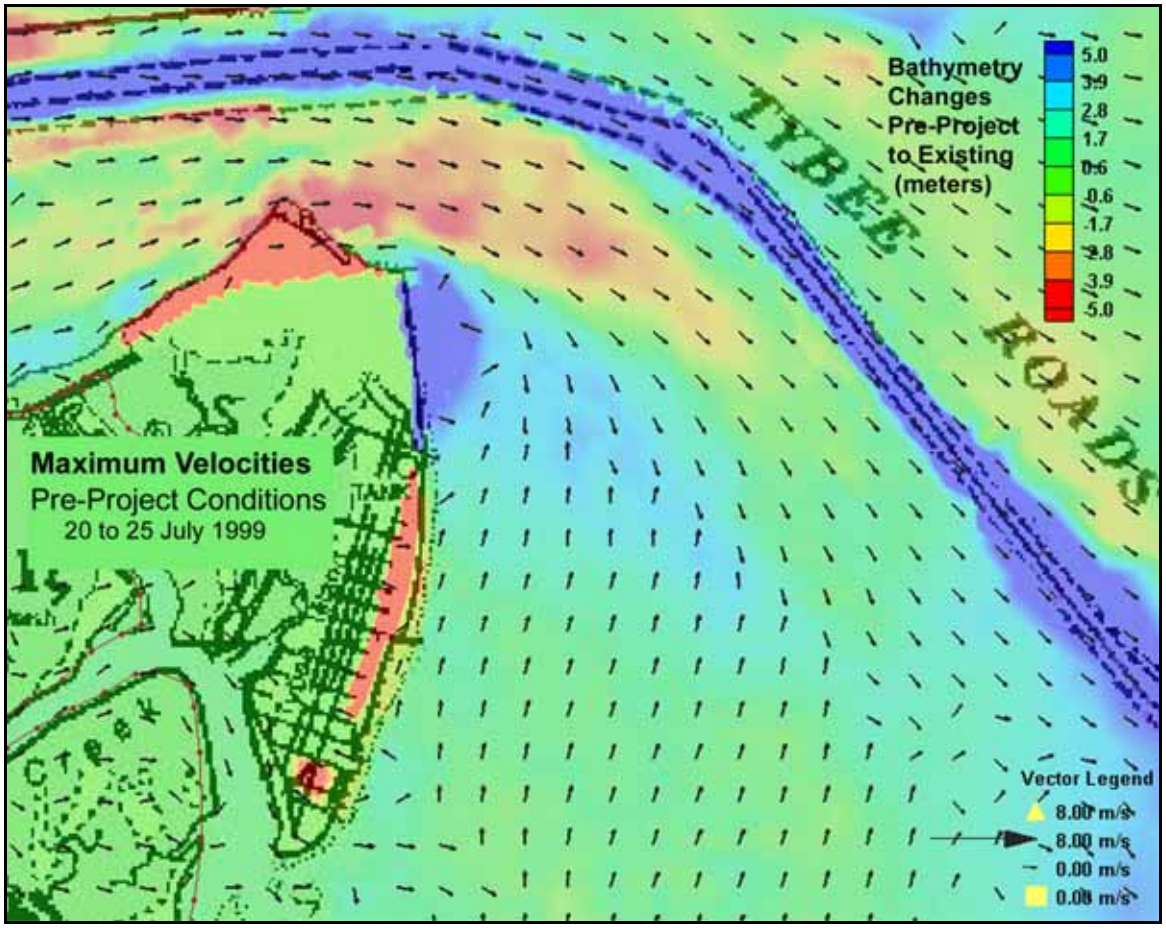

Figure 3-23. Maximum velocities 20–25 July 1999, pre-project conditions.

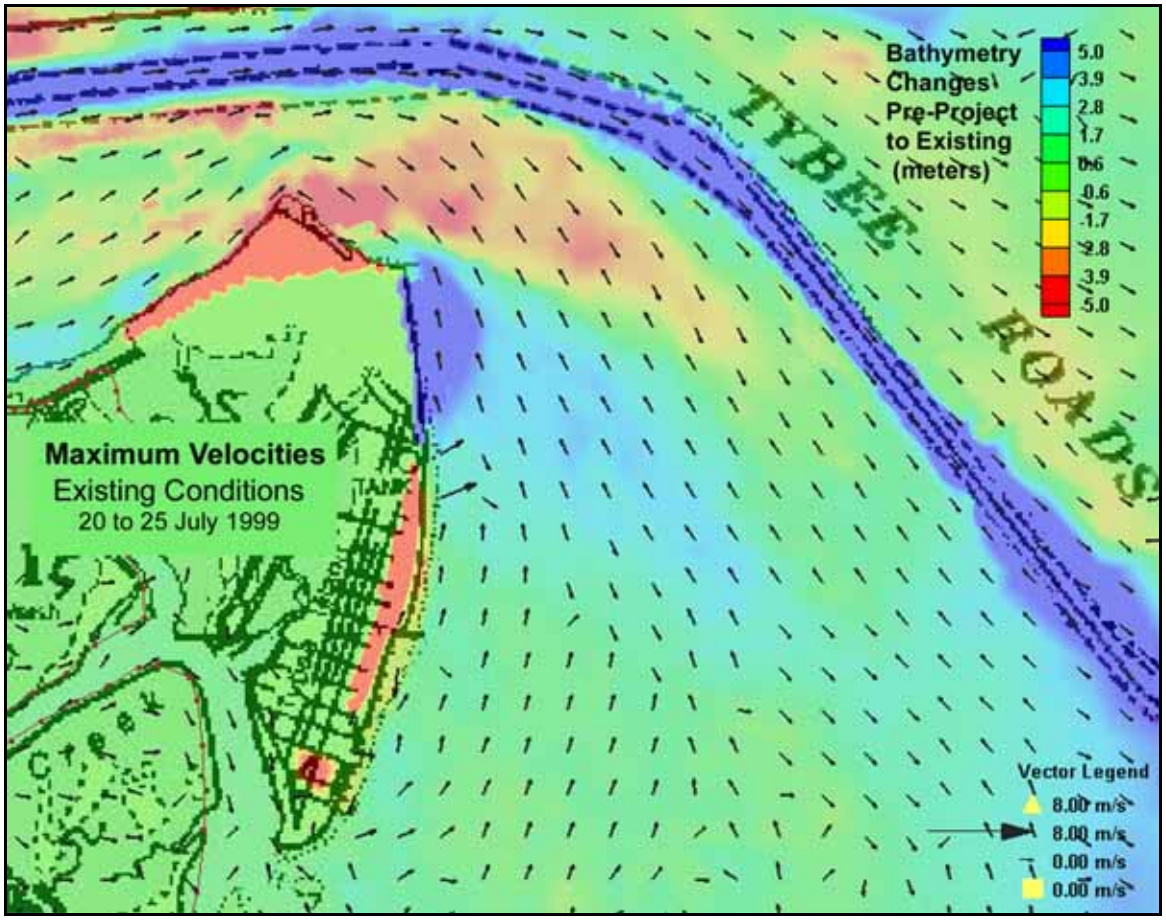

Figure 3-24. Maximum velocities 20–25 July 1999, existing conditions.

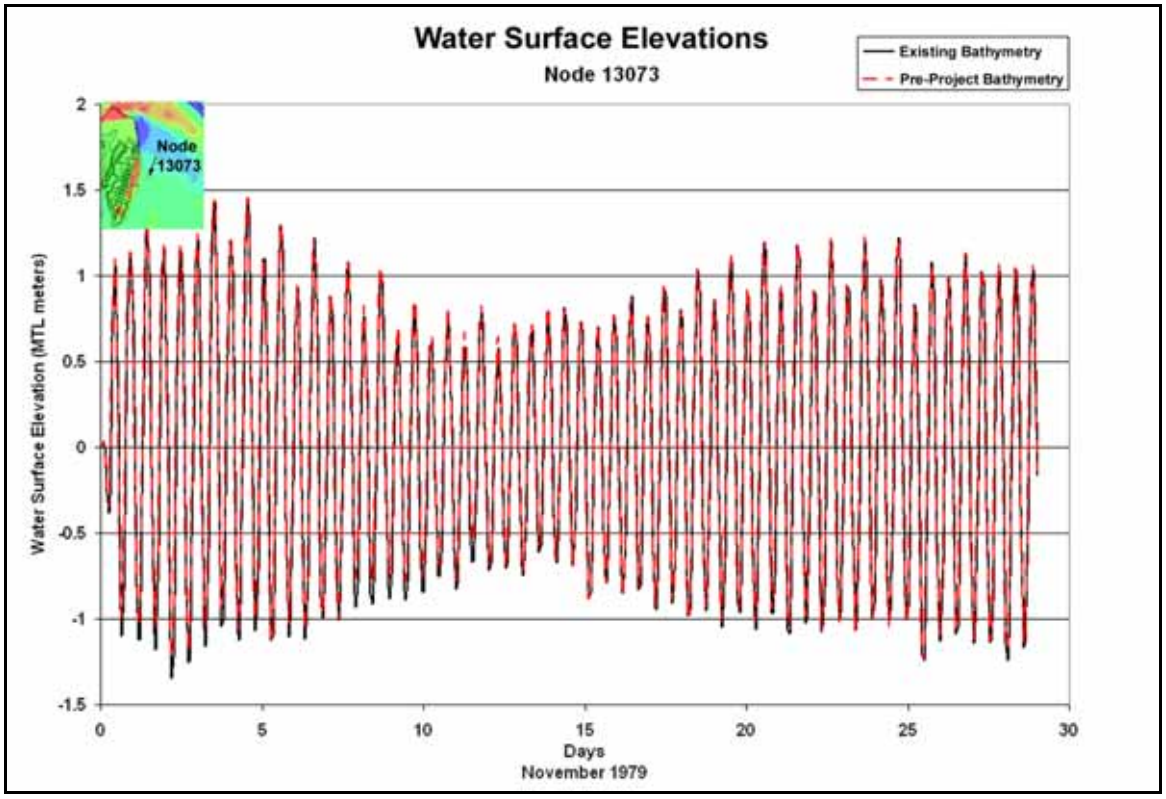

Figure 3-25. Existing and pre-project predicted water surface elevations 1–29 November 1979.

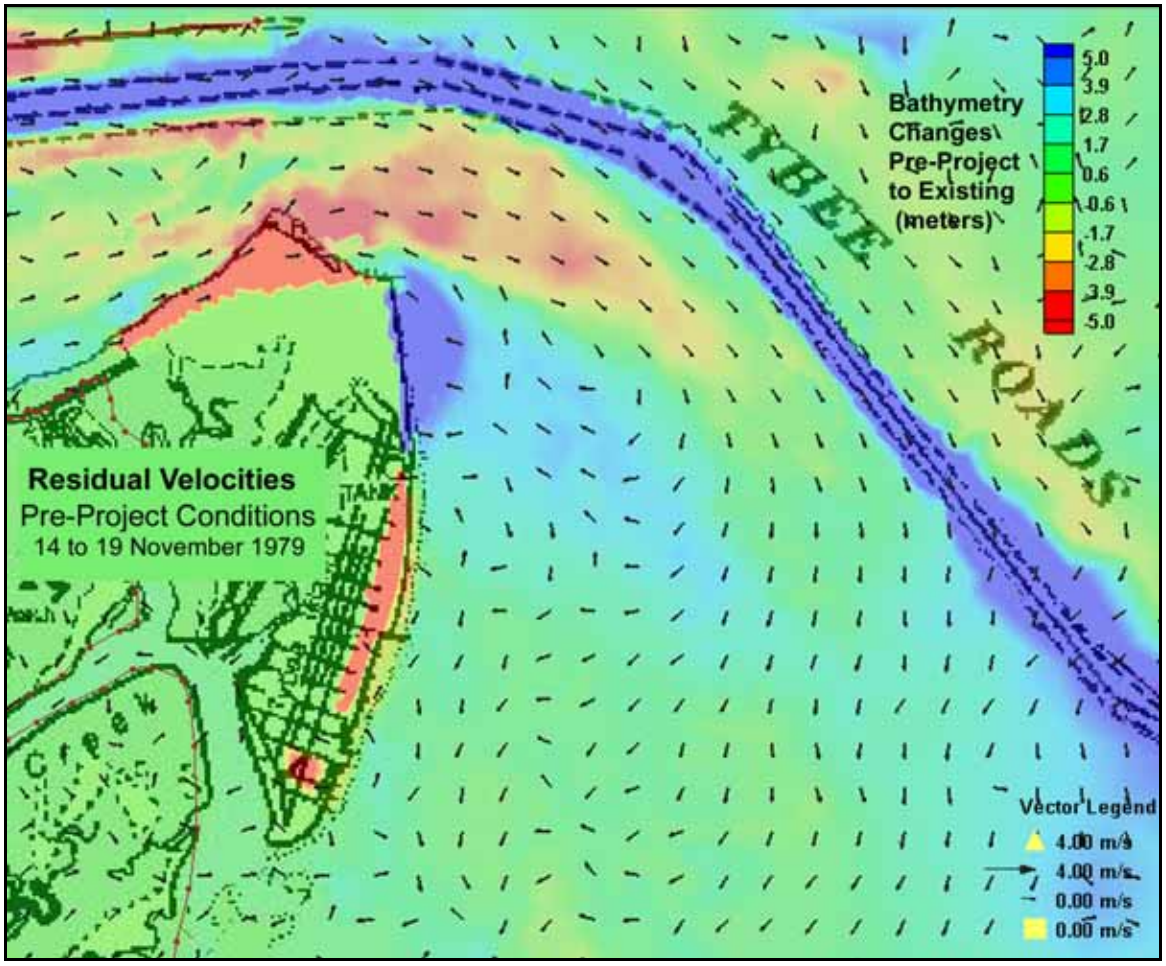

Figure 3-26. Residual velocities 14–19 November 1999, pre-project conditions.

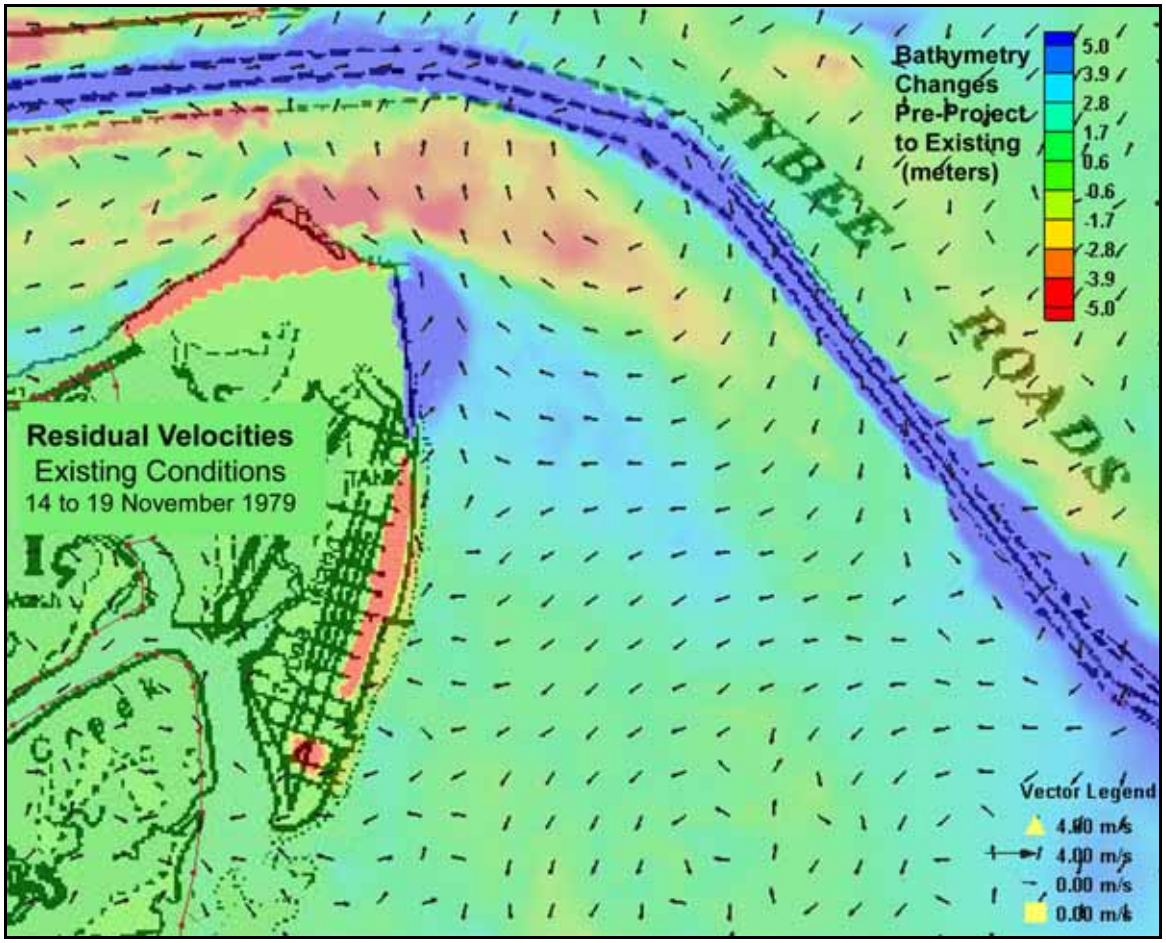

Figure 3-27. Residual velocities 14–19 November 1999, existing conditions.

Difference in peak velocity magnitude differences between the pre-project condition simulations and the existing condition simulations around Tybee Island for the active storm period of November 1979 vary between plus or minus 0.5 m/sec (1.6 ft/sec) (Figures 3-28 to 3-33). The velocity magnitudes north of Tybee Island are greater for existing conditions as was the case for the July 1999 simulations (Figure 3-28). This is due to the shallower depths in this area for the existing condition. Likewise, in Figure 3-29, the pre-project condition has greater velocity magnitudes for Node 15435, on the northeast side of Tybee Island. Fewer of the observation nodes east of Tybee Island have higher peak velocity magnitudes with the existing conditions for the November 1979 simulations than for the July 1999 simulations. These velocity magnitude differences are due to the complex interaction of changes to the overall flow pattern with the most observable changes being in the north. On the south end of Tybee, pre-project currents are generally stronger to the south (Figures 3-32 and 3-33), but there is significant spatial variability in both the pre-project and

existing simulations in this area. The decrease in current magnitude is due to the southward migration of Tybee Creek between 1854 and 2007.

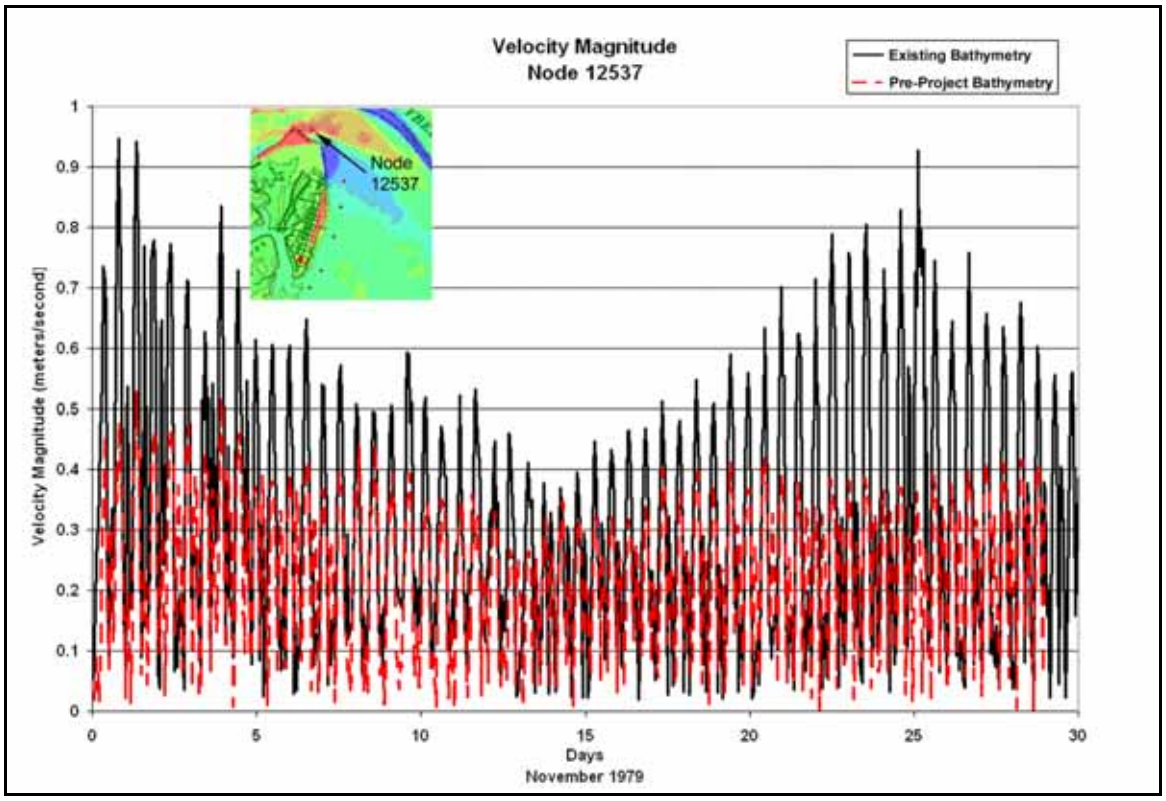

Figure 3-28. Velocity magnitudes for existing and pre-project conditions November 1979, Node 12537.

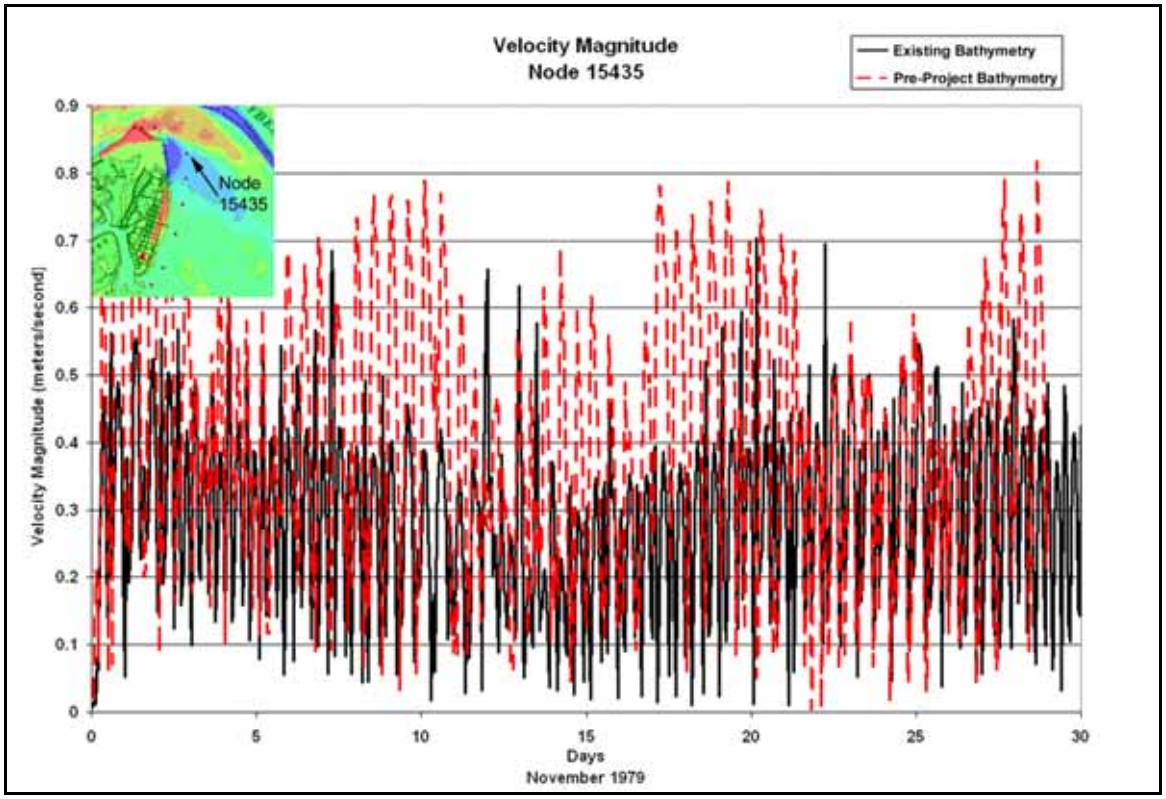

Figure 3-29. Velocity magnitudes for existing and pre-project conditions November 1979, Node 15435.

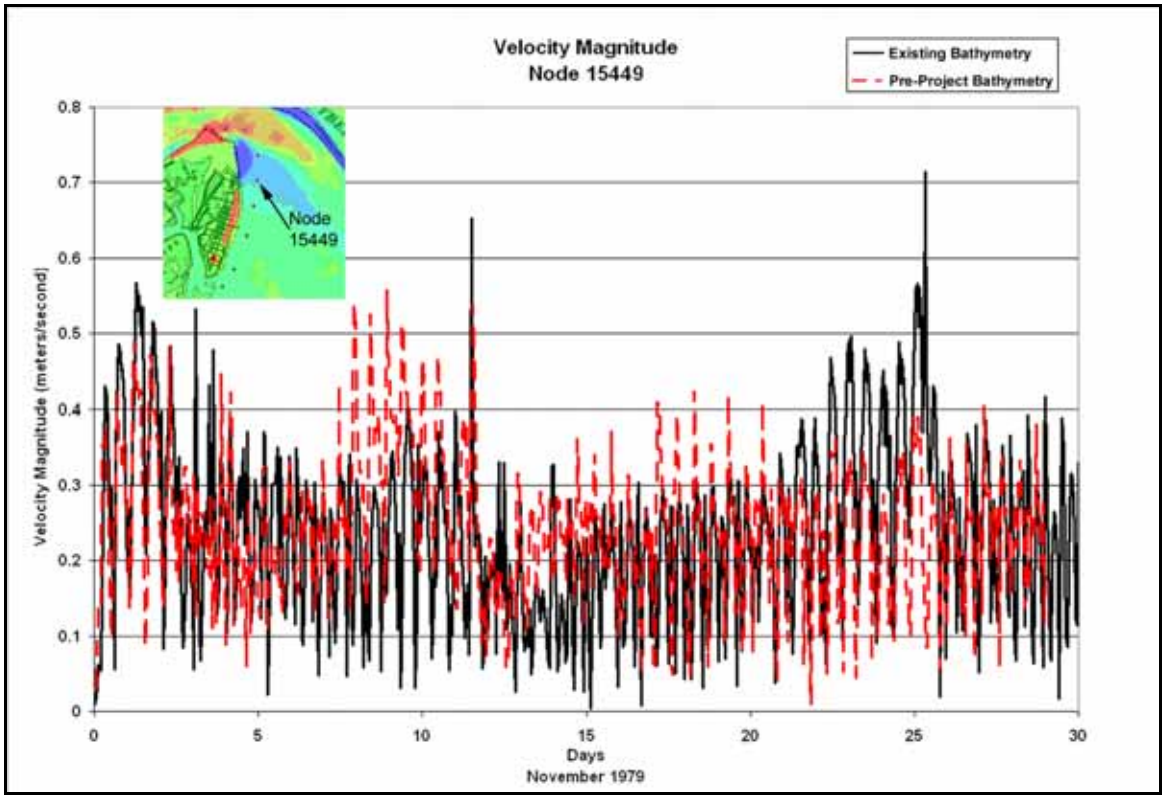

Figure 3-30. Velocity magnitudes for existing and pre-project conditions November 1979, Node 15449.

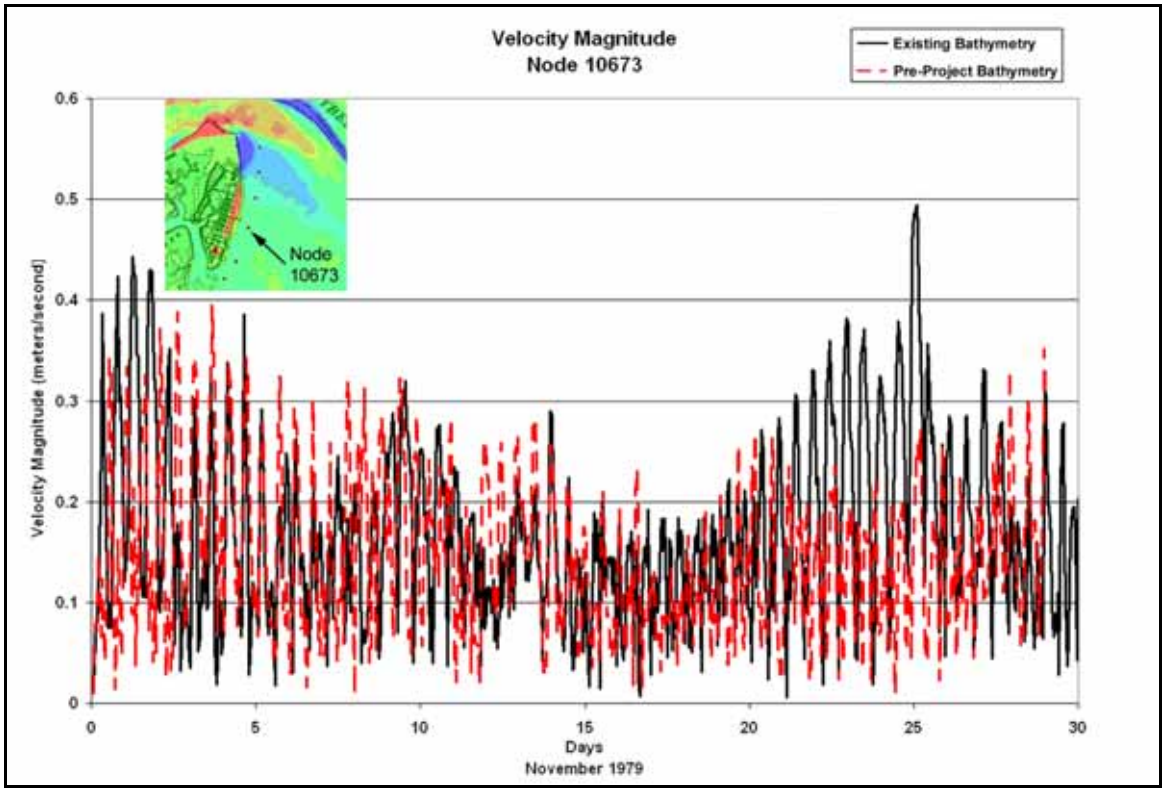

Figure 3-31. Velocity magnitudes for existing and pre-project conditions November 1979, Node 10673.

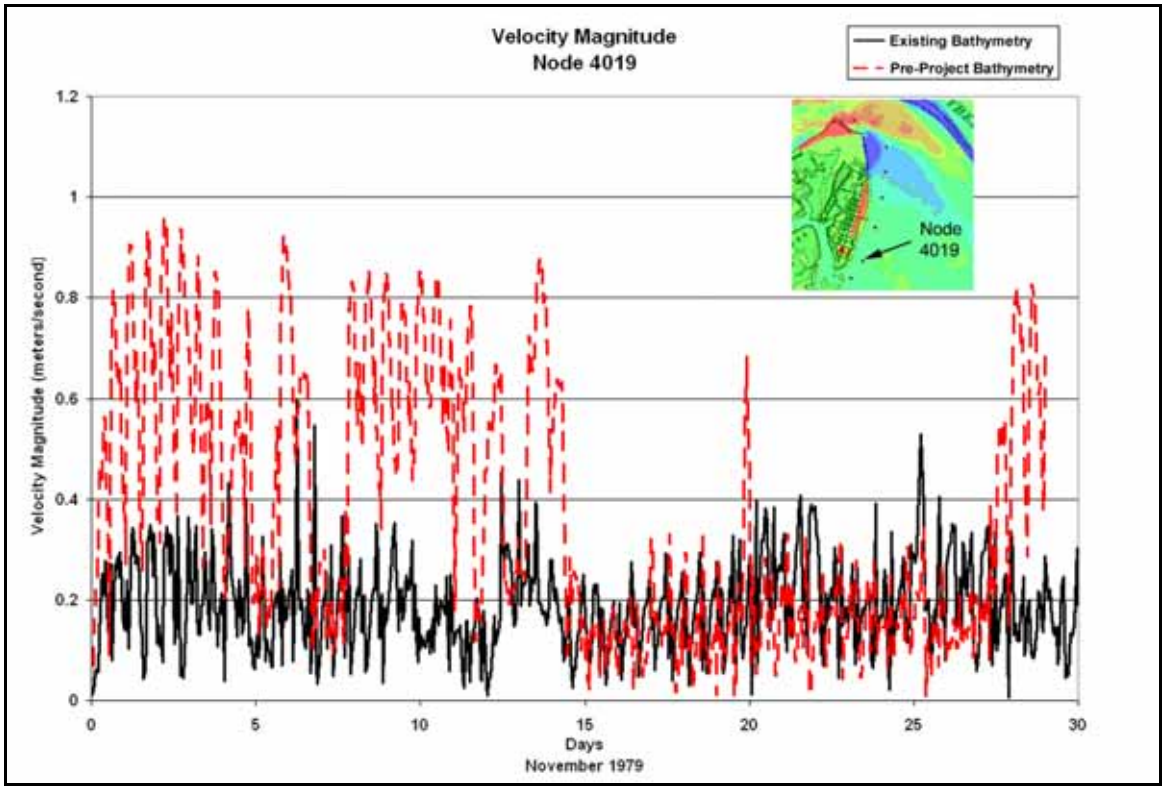

Figure 3-32. Velocity magnitudes for existing and pre-project conditions November 1979, Node 4019.

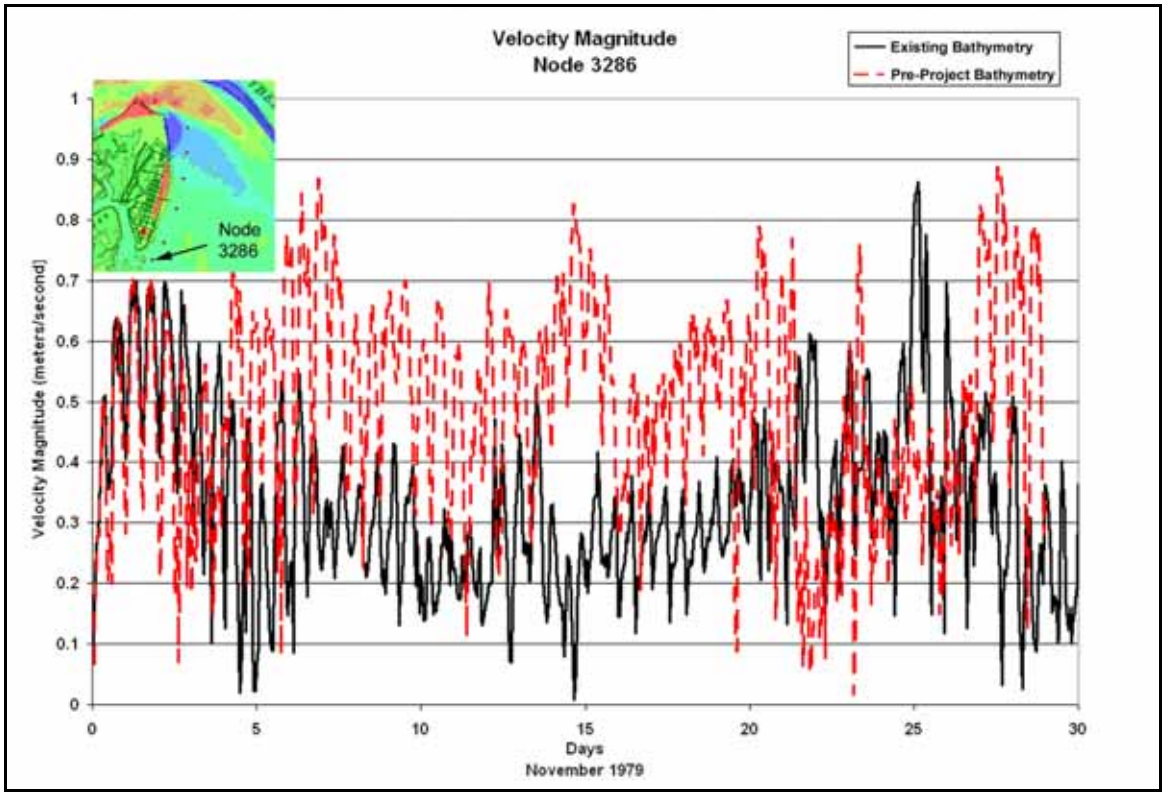

Figure 3-33. Velocity magnitudes for existing and pre-project conditions November 1979, Node 3286.

The direction of the maximum velocities for the 14–19 November 1979 simulation period with pre-project conditions is to the east for velocities north of Tybee Island and peak velocity vectors form an eddy pattern east of Tybee Island (Figure 3-34). The direction of the maximum velocities for the 14–19 November simulation period with existing conditions is northerly for velocities north of Tybee Island and the peak velocity vectors east of Tybee Island have a more uniform distribution with a northerly direction (Figure 3-35).

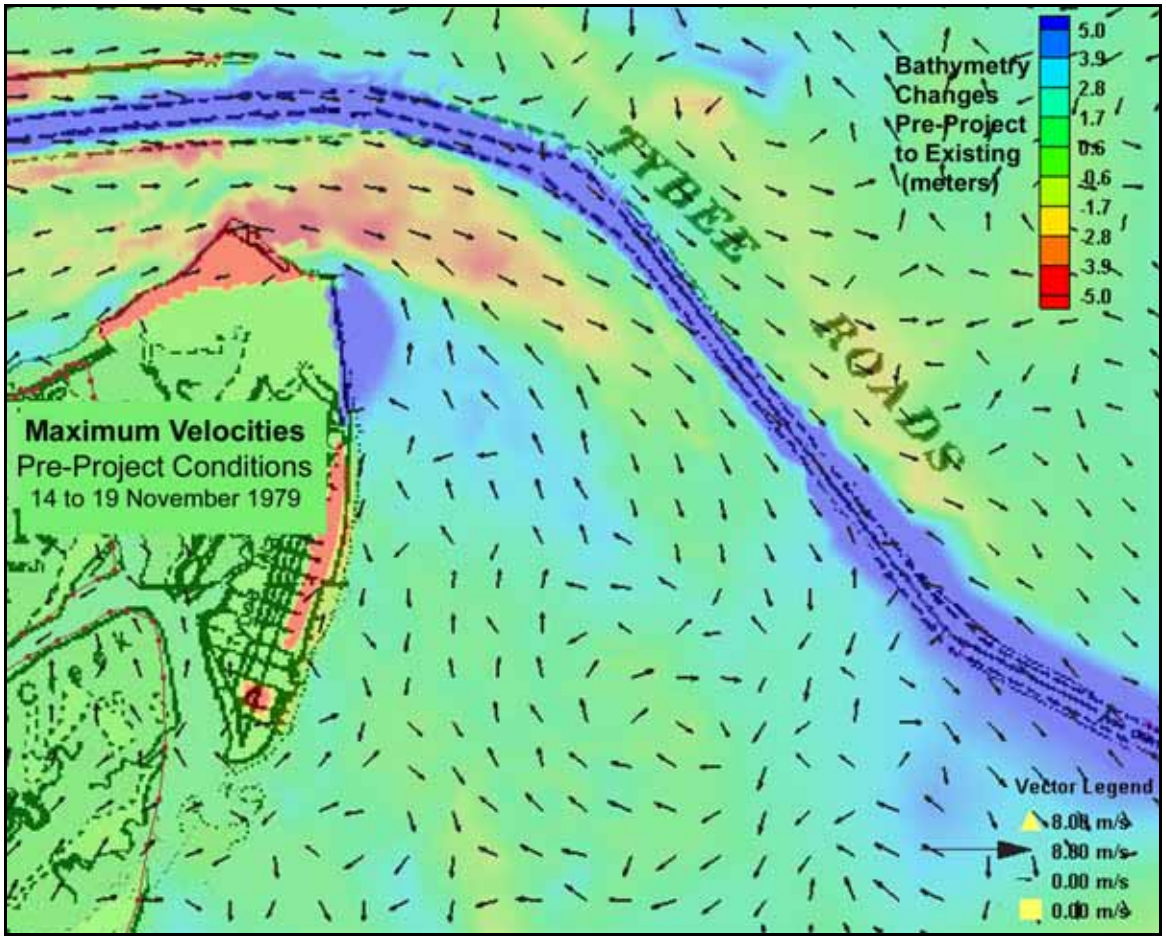

Figure 3-34. Maximum velocities 14–19 November 1979, pre-project conditions.

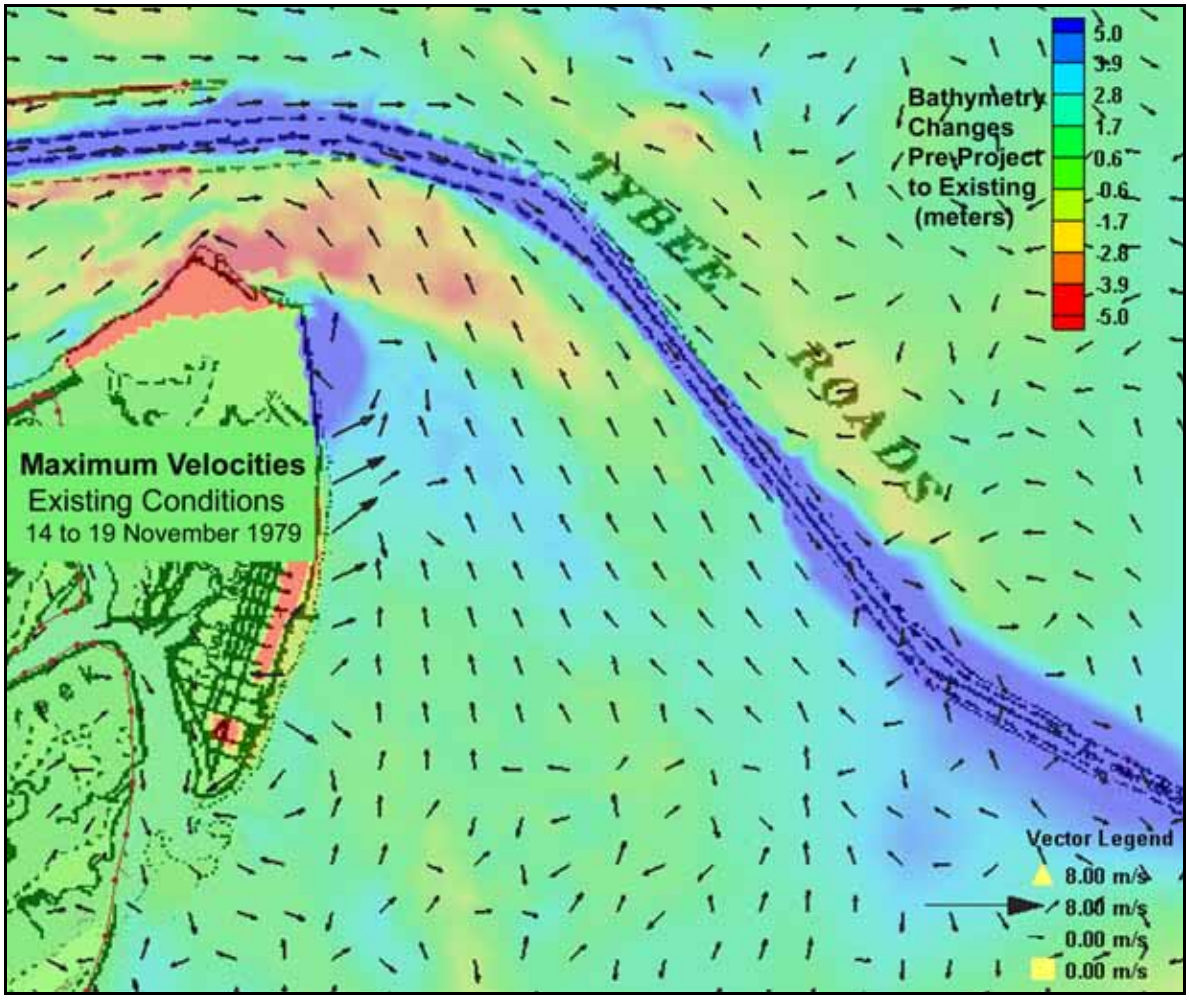

Figure 3-35. Maximum velocities 14–19 November 1979, existing conditions.

September 1989 simulations

Water surface elevation calculations for simulations of the time period 14–22 September 1989 with Hurricane Hugo retracked to impact the Tybee Island area indicate no difference in storm surge elevation between simulations with pre-project bathymetry and simulations with existing bathymetry, except for minor difference in calculated low water levels (Figure 3-36).

The plots of residual velocities for the tidal cycle that represents a retracked Hurricane Hugo indicate the same northward shift of the eddy pattern northeast of Tybee Island that was observed in the July 1999 and November 1979 simulations (Figures 3-37 and 3-38).

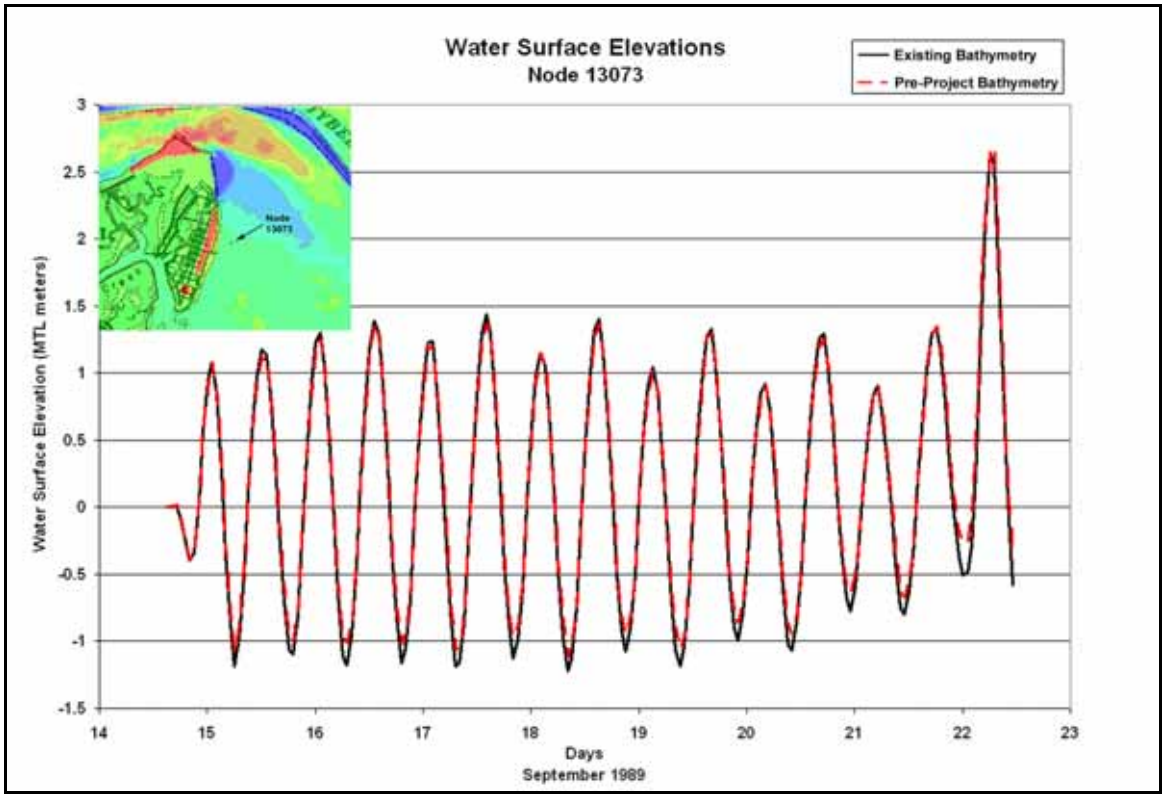

Figure 3-36. Existing and pre-project predicted water surface elevations 14–22 September 1989.

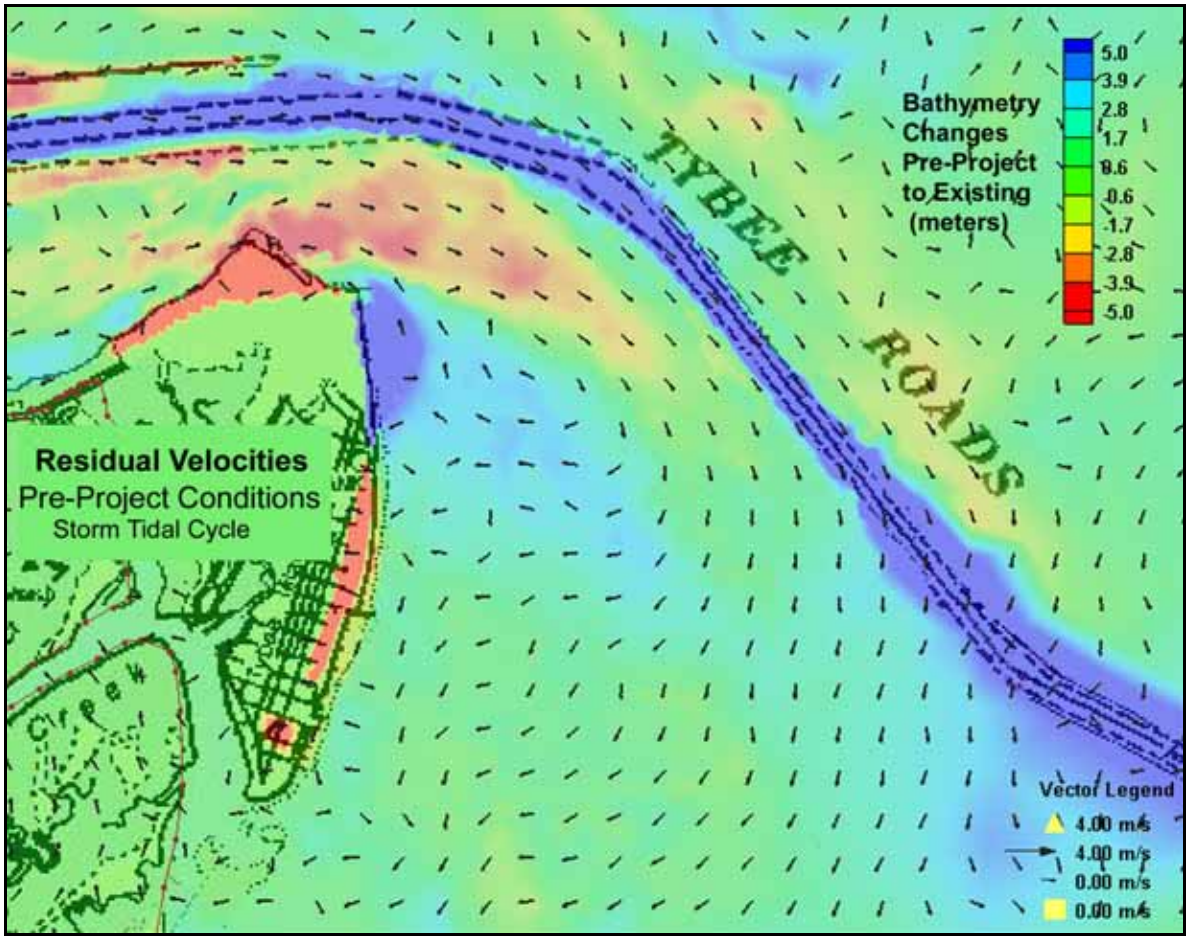

Figure 3-37. Residual velocities for the retracked Hurricane Hugo, pre-project conditions.

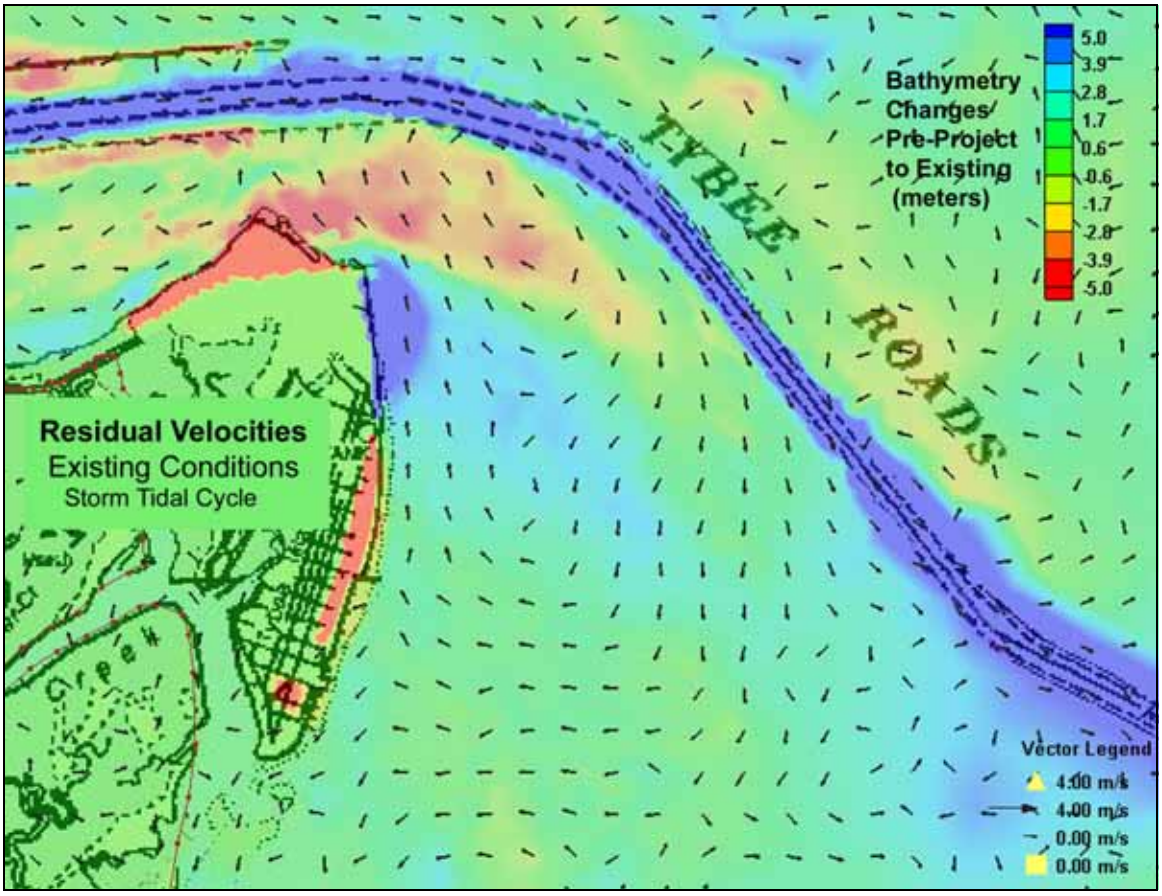

Figure 3-38. Residual velocities for the retracked Hurricane Hugo, existing conditions.

Examination of velocity magnitude plots reveals an increase in the peak storm velocity magnitude of 0.4 m/sec (1.3 ft/sec) for existing conditions north of Tybee Island (Figure 3-39) due to the shallower bathymetry. Northeast of Tybee Island there is a large (1.0 m/sec (3.3 ft/sec)) reduction in the velocity magnitude for existing conditions (Figure 3-40). The larger pre-project velocity magnitude northeast of Tybee Island was due to flows being confined by the northeast corner of Tybee Island which has since eroded away (Figures 3-39 and 3-40). The reduction in velocity magnitude for existing conditions diminishes at the observation nodes proceeding to the south (Figures 3-41 and 3-45) because the pre-project and existing bathymetries are more similar than in the north.

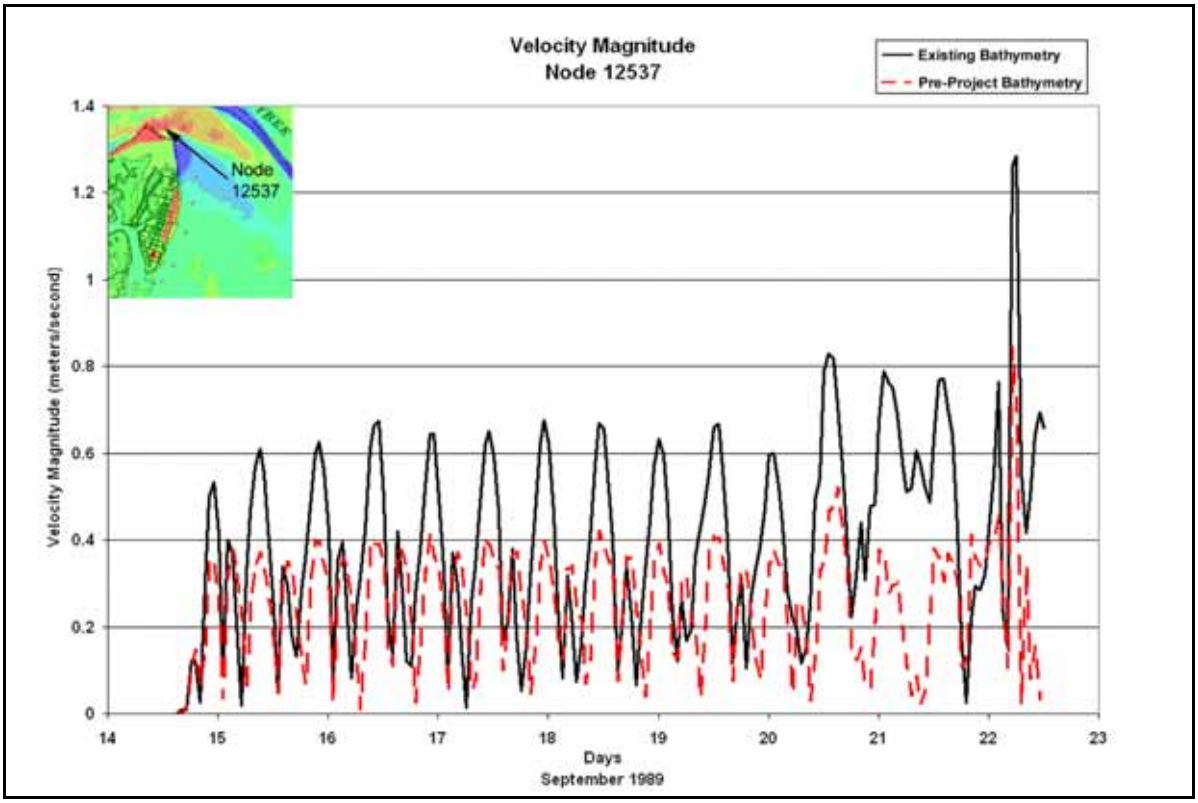

Figure 3-39. Velocity magnitudes for existing and pre-project conditions September 1989, Node 12537.

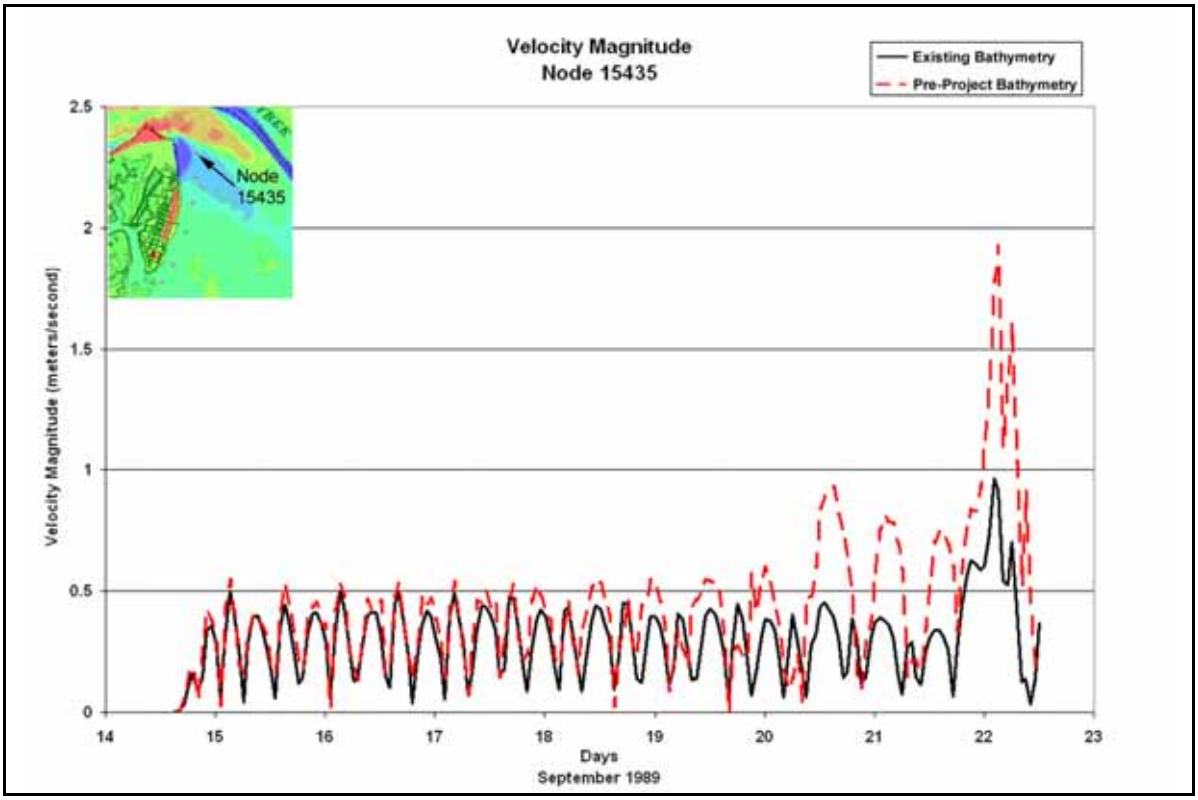

Figure 3-40. Velocity magnitudes for existing and pre-project conditions September 1989, Node 15435.

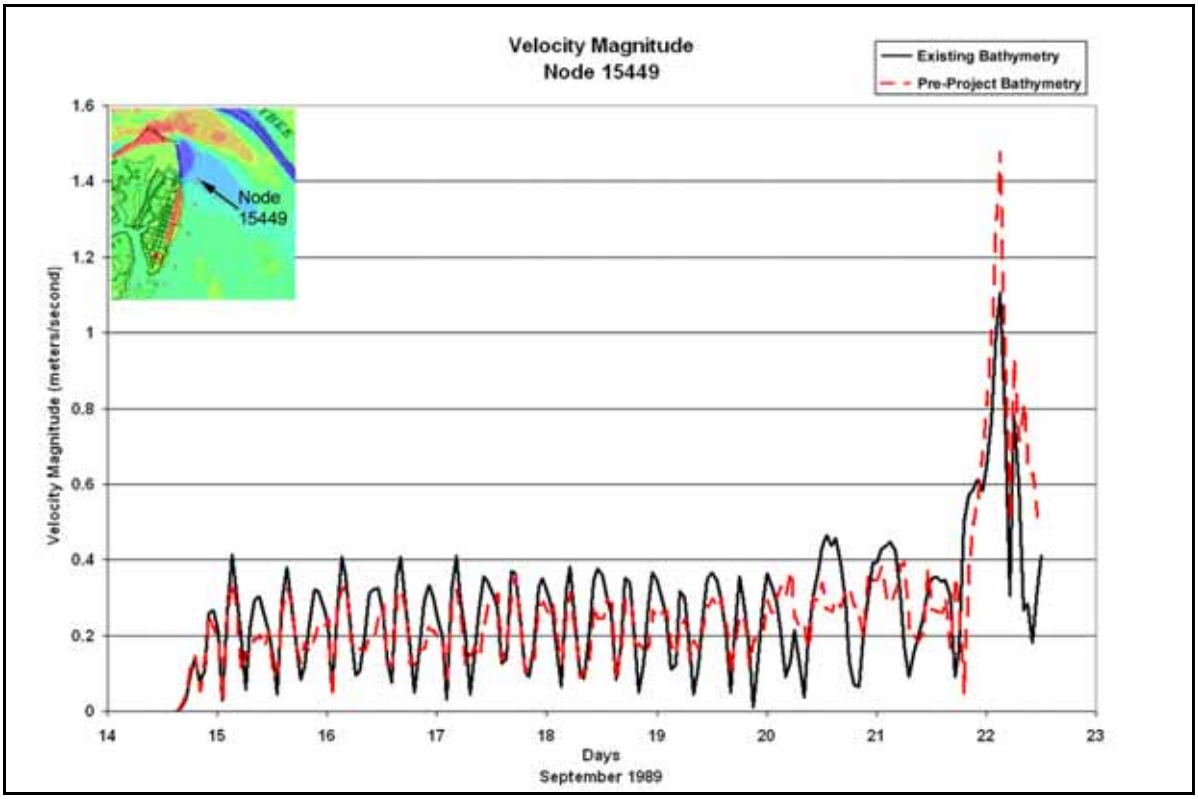

Figure 3-41. Velocity magnitudes for existing and pre-project conditions September 1989, Node 15449.

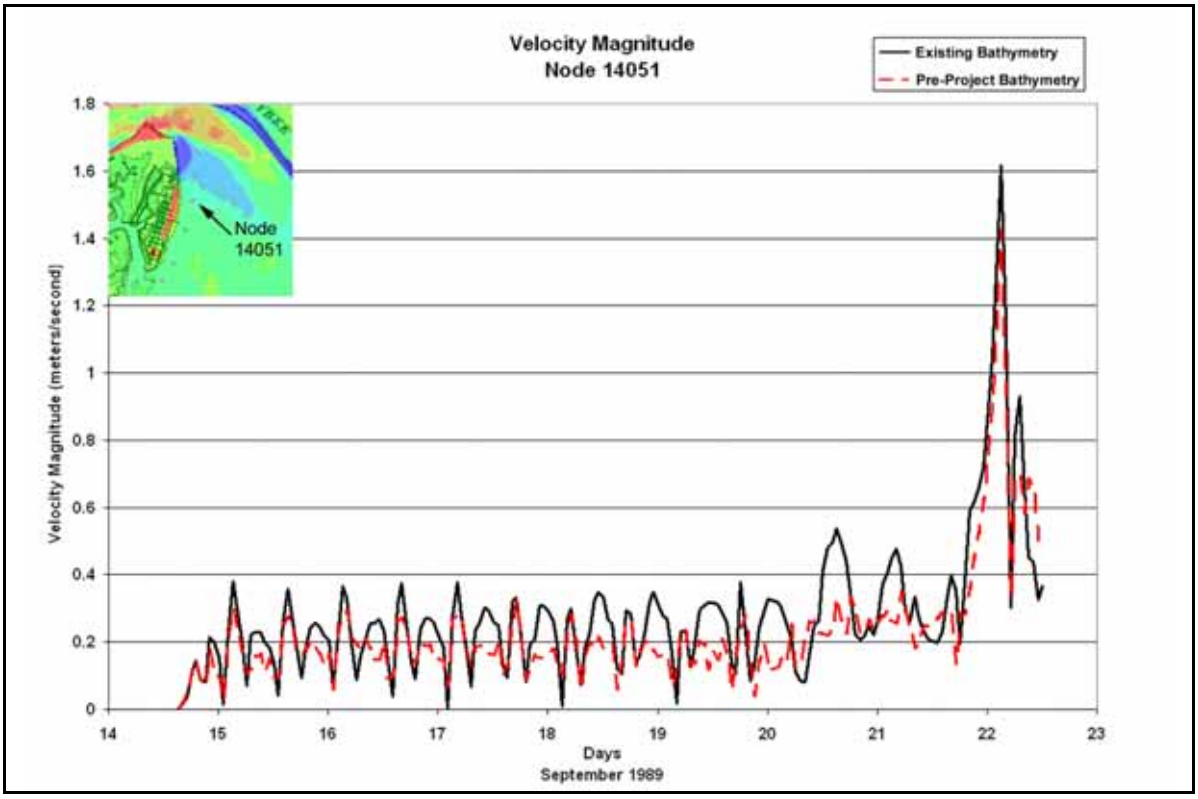

Figure 3-42. Velocity magnitudes for existing and pre-project conditions September 1989, Node 14051.

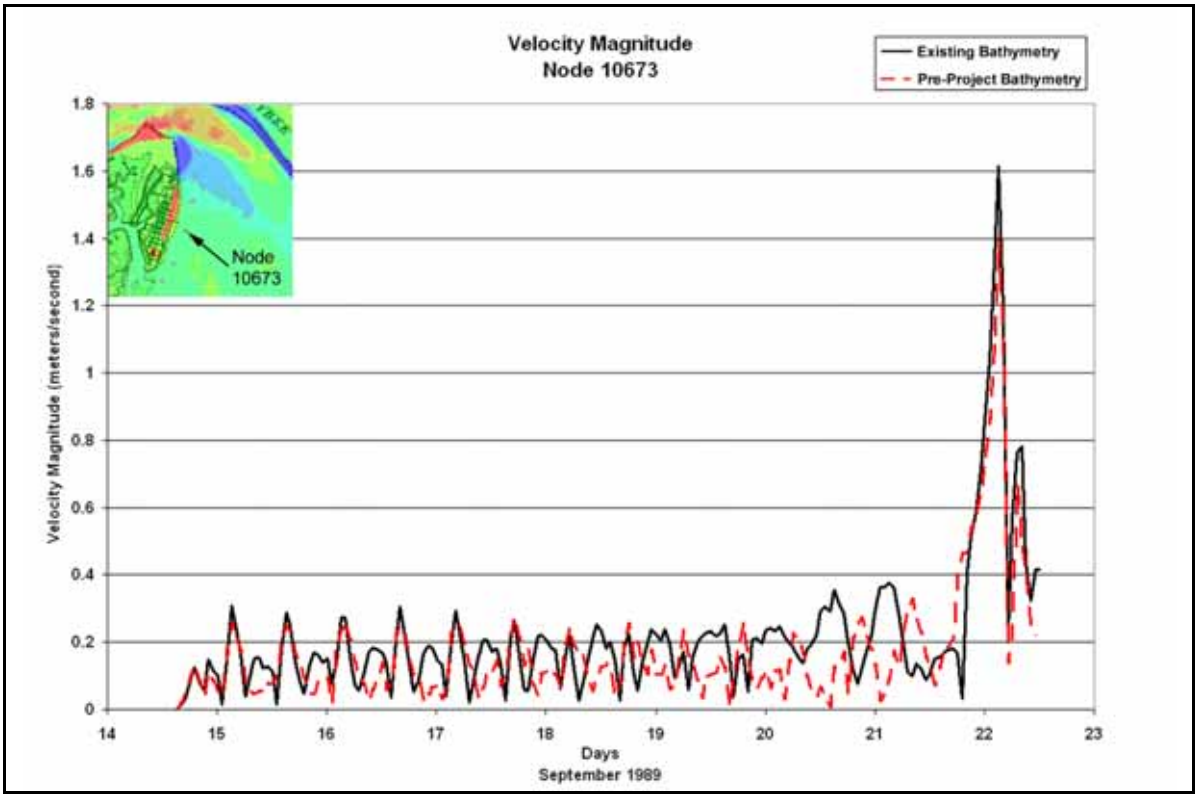

Figure 3-43. Velocity magnitudes for existing and pre-project conditions September 1989, Node 10673.

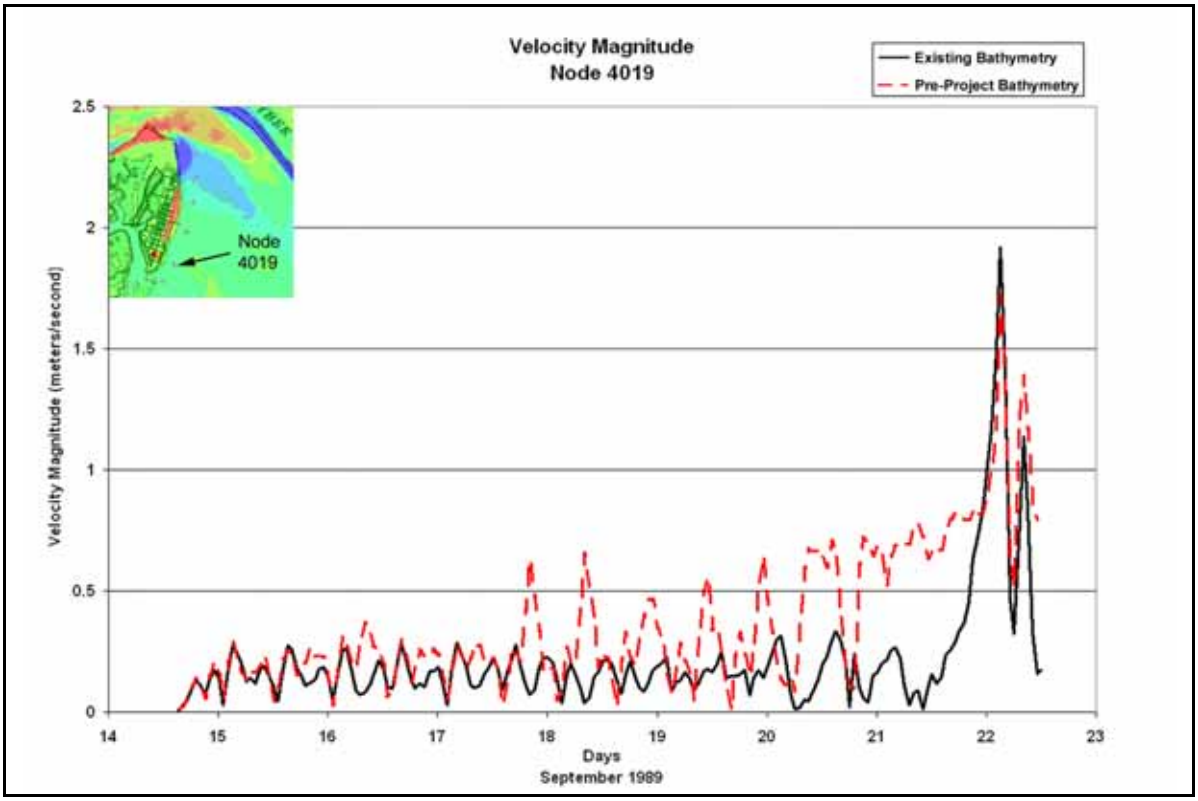

Figure 3-44. Velocity magnitudes for existing and pre-project conditions September 1989, Node 4019.

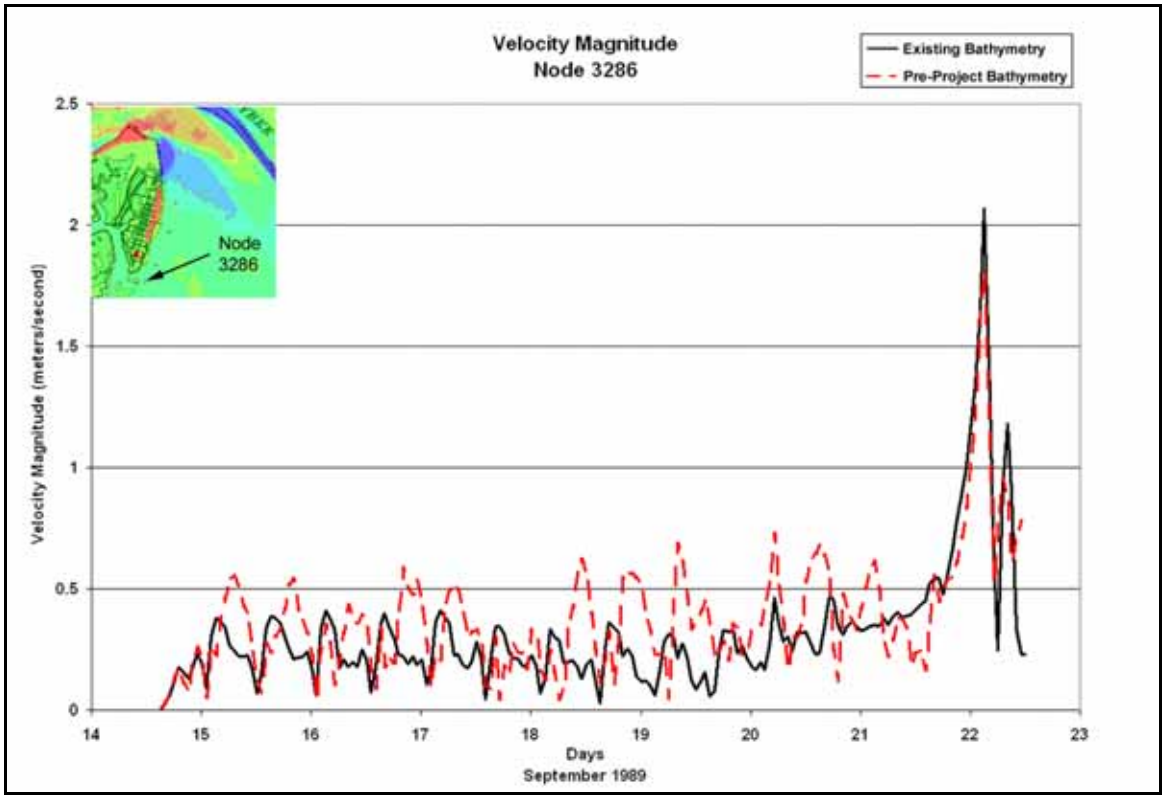

Figure 3-45. Velocity magnitudes for existing and pre-project conditions September 1989, Node 3286.

Plots of the maximum velocity fields reveal a shift of the direction of the maximum velocity vectors in the area northeast of Tybee Island. The maximum velocity vectors have a more southerly direction for the existing condition simulation than for the pre-project simulation. This southerly shift in direction is related to the removal of the northeast corner of the island (the bulge) due to erosion (Figures 3-46 and 3-47).

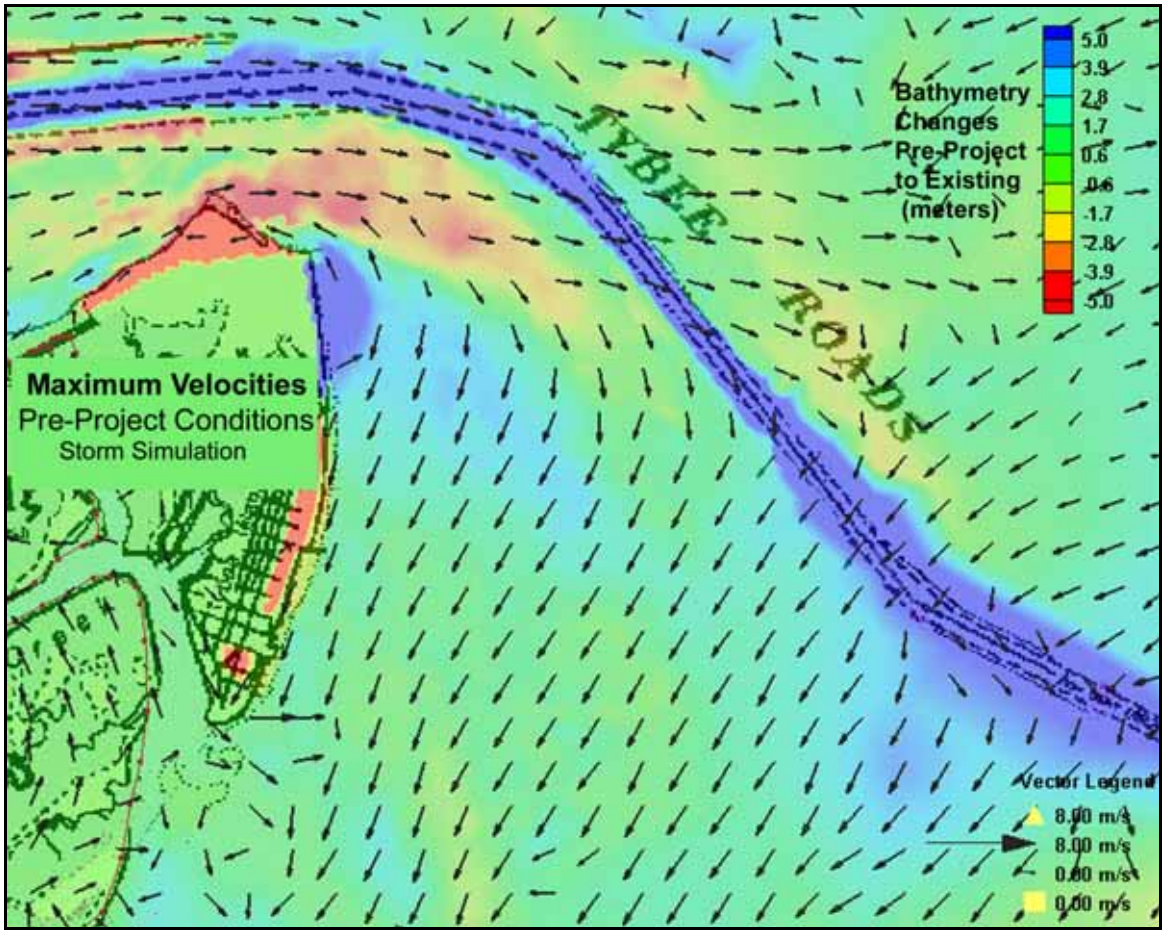

Figure 3-46. Maximum velocities September 1989 with retracked Hurricane Hugo, pre-project conditions.

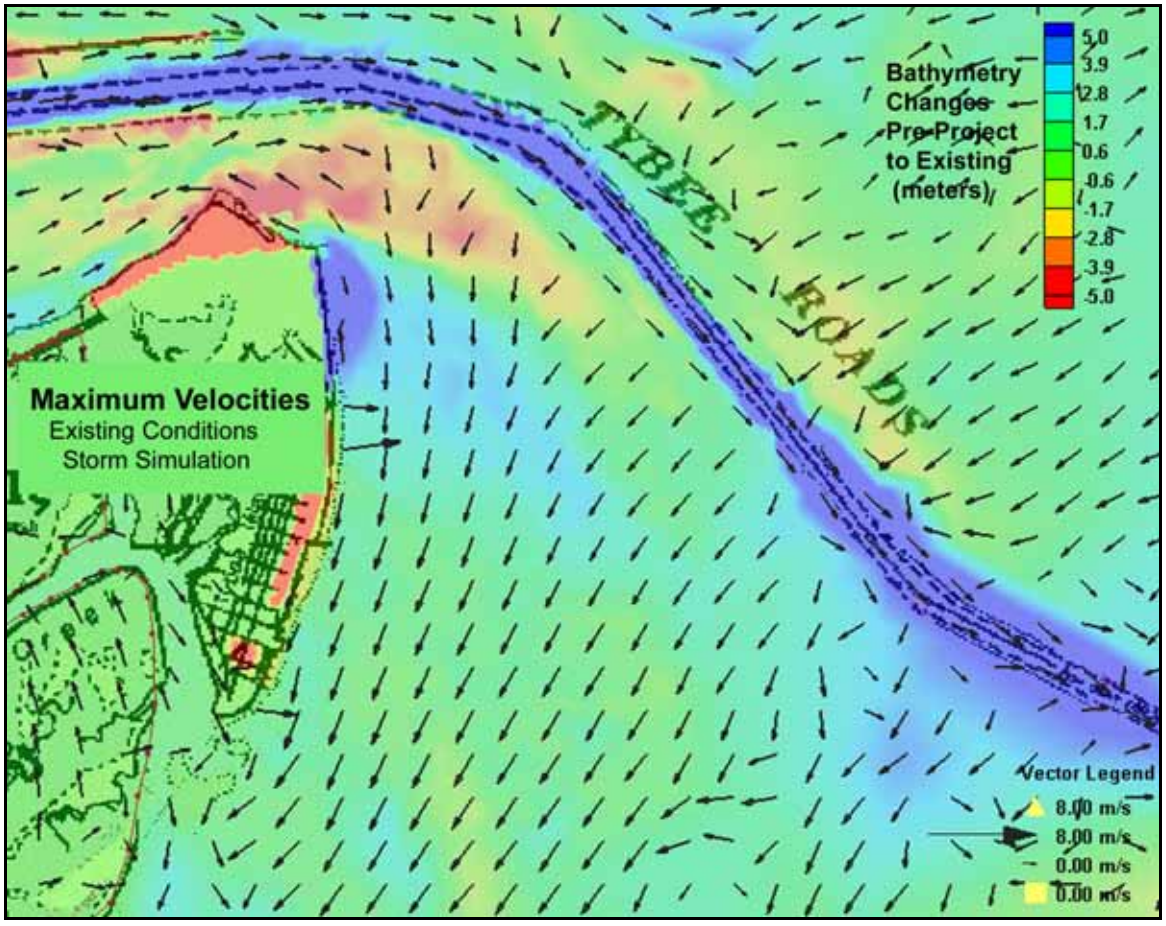

Figure 3-47. Maximum velocities September 1989 with retracked Hurricane Hugo, existing conditions.

Summary of circulation results

Changes in the bathymetry from pre-project (historic) to existing conditions have not increased the tidal or storm surge water surface elevations in the vicinity Tybee Island. Velocity magnitudes north of Tybee Island have increased while velocity magnitudes along the east side of Tybee Island increase or decrease in response to specific meteorological events. The center of a residual velocity eddy located northeast of Tybee Island has shifted to the north for simulations with existing bathymetric conditions as compared to simulations with the pre-project (historic) bathymetry. The shift of the location of the residual velocity eddy is in response to increased velocities in the navigation channel and accretion of the North Tybee Shoal. The area where the residual velocity eddy has shifted is an area of bathymetric change (deepened navigation channel and accreted North Tybee Shoal).

4 Wave Modeling

Waves, together with tidal currents, drive sediment transport in the areas adjacent to Tybee Island. Numerical model simulations of wave transformation were required to evaluate changes in the magnitude and spatial variation of wave parameters due to changes in the bathymetry and topography of the surrounding area since the construction of the Savannah Harbor jetties and major improvements to the navigation channel. The wave results also serve as an input to sediment transport calculations described in Chapter 5. The steady-state spectral wave model STWAVE (Smith et al. 2001) was applied for wave transformation modeling. STWAVE was forced with directional wave spectra based on typical and storm waves hindcast by the WIS. The simulations include representative tide and surge water levels. This section describes the STWAVE wave transformation model, the model input, and model results.

STWAVE model description

The numerical model STWAVE was used to transform waves to the project site. STWAVE numerically solves the steady-state conservation of spectral action balance along backward-traced wave rays:

$$\begin{aligned}&(C_{ga})_x \frac{\partial}{\partial x}\frac{C_a C_{ga}\cos(\mu-\alpha)E(f,\alpha)}{\omega_r}\\&+(C_{ga})_y \frac{\partial}{\partial y}\frac{C_a C_{ga}\cos(\mu-\alpha)E(f,\alpha)}{\omega_r}\\&=\sum\frac{S}{\omega_r}\end{aligned} \tag{4-1}$$

where:

C_{ga} = absolute wave group celerity
x,y = spatial coordinates, subscripts indicate x and y components
C_a = absolute wave celerity
μ = current direction
α = propagation direction of spectral component
E = spectral energy density
f = frequency of spectral component

ω_r = relative angular frequency (frequency relative to the current)
S = energy source/sink terms

The source terms include wind input, nonlinear wave-wave interactions, dissipation within the wave field, and surf-zone breaking. The terms on the left-hand side of Equation 4-1 represent wave propagation (refraction and shoaling), and the source terms on the right-hand side of the equation represent energy growth or decay in the spectrum.

The assumptions made in STWAVE are as follows:

1. Mild bottom slope and negligible wave reflection
2. Steady waves, currents, and winds
3. Linear refraction and shoaling
4. Depth-uniform current

The version of STWAVE applied here is a half-plane model, meaning that only waves propagating toward the coast are represented. Waves reflected from the coast or waves generated by winds blowing offshore are neglected. Wave breaking in the surf zone limits the maximum wave height based on the local water depth and wave steepness:

$$H_{mo_{\max}} = 0.1 L \tanh kd \tag{4-2}$$

where:

$H_{mo_{\max}}$ = maximum zero-moment signficant wave height
L = wavelength
k = wave number
d = water depth

STWAVE is a finite-difference model and calculates wave spectra on a rectangular grid with square grid cells. The model outputs zero-moment wave height, peak wave period (T_p), and mean wave direction (α_m) at all grid points and two-dimensional spectra at selected grid points.

Wave model inputs

The inputs required to execute STWAVE are as follows:

1. Bathymetry grid (including shoreline position and grid size and resolution)
2. Incident frequency-direction wave spectrum on the offshore grid boundary
3. Current field (optional)
4. Tide plus surge elevation, wind speed, and wind direction (optional)

Bathymetry grids

Two STWAVE Cartesian grids were generated for this study, one to represent the topography and bathymetry at the time of this study (existing condition) and the other to represent the topography and bathymetry in place prior to major improvements of the Federal navigation channel and construction of the jetties and offshore submerged breakwater (pre-project condition). The existing condition (2007) STWAVE grid was created by merging several data sets as described in Chapter 3 for the ADCIRC model. Figure 4-1 provides the depth contours of the existing condition STWAVE grid (in meters relative to MTL). There were limited topographic and bathymetric data available for the time period prior to construction of the jetties. The bathymetry was compiled to represent conditions in 1854 as described in Chapter 3. Figure 4-2 provides the depth contours of the historic (pre-project) condition STWAVE grid (in meters relative to MTL).

In both cases, the grid origin is x = 538,104.6 m (1,765,435.0 ft) and y = 3,548,280.0 m (11,641,338.6 ft) in UTM NAD83 Zone 17, and the grid orientation is 140 deg (which is the orientation of the grid x-axis measured counterclockwise from East). The grid domain is 21.7 km (13.5 miles) (cross shore, 434 cells) by 31.6 km (19.6 miles) (alongshore, 631 cells) with a grid resolution of 50 m (164 ft). The grid extends seaward to approximately 12-15 m MTL water depth.

Examination of the STWAVE model grids represented in Figures 4-1 and 4-2 reveals significant topographic and bathymetric differences. The most obvious differences between the two model grids are evident in the configuration of the rivers, streams, and islands. Changes to Tybee Island and the adjacent offshore environment, in particular, the channels, shoals, and bars, will drive the changes in the wave conditions during the STWAVE modeling of these two scenarios (existing and pre-project).

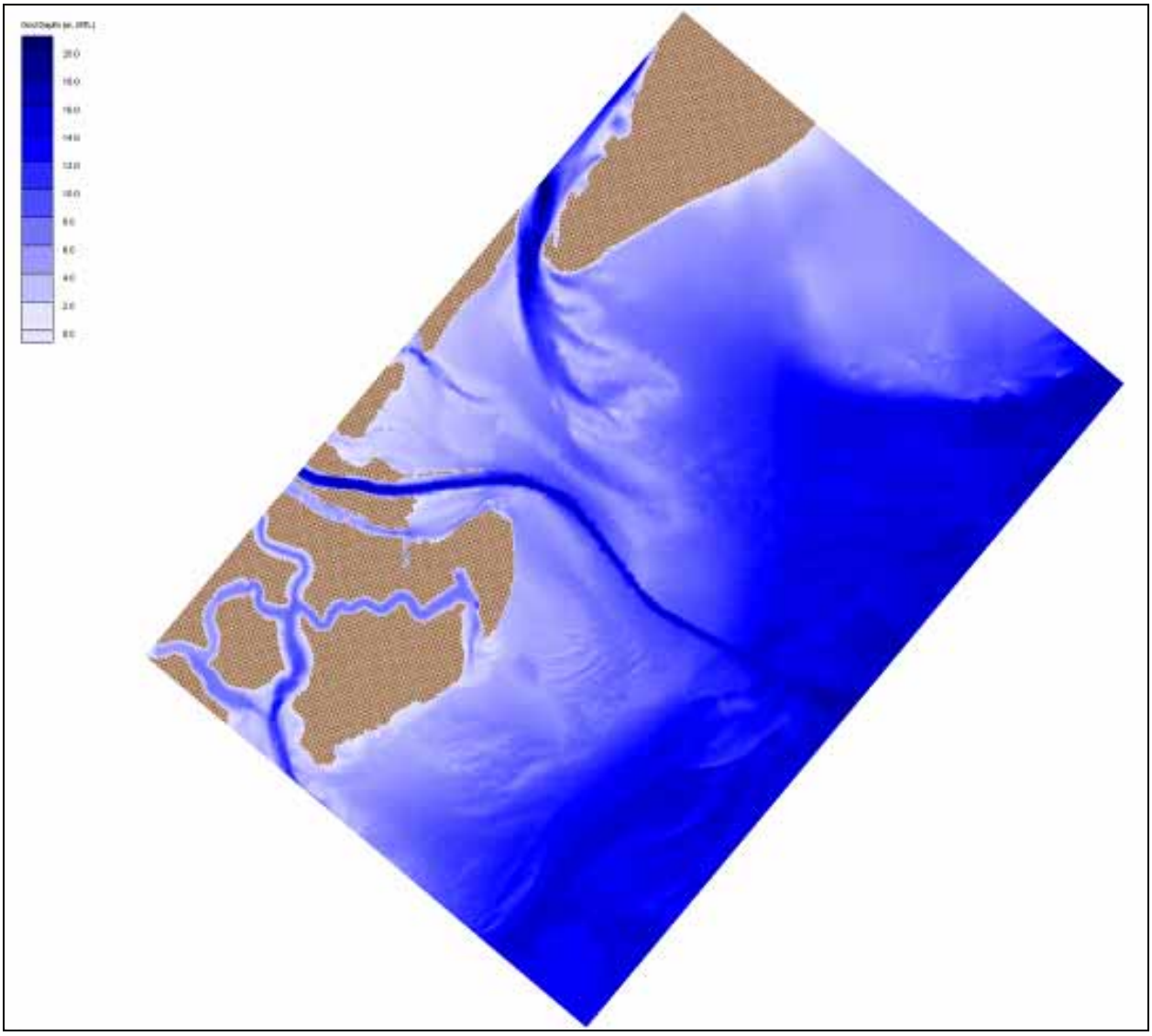

Figure 4-1. Existing condition grid (depths in meters, MTL). Land is shown in brown.

Tybee Island has become more elongated in the period since prior to the construction of the jetties. Significant volumes of sediment have been removed from the northern portion of Tybee Island, which was significantly larger and protruded farther into the Atlantic. Additionally, the southern portion of the island has migrated to the south. Other obvious differences between the two model grids may not be based on actual morphologic change, but rather a relative lack of data between the two time periods. For example, there is little doubt that the islands surrounding the navigation entrance channel have experienced morphologic changes between the two conditions (1854 to 2007), but there was a lack of data in the historic surveys to accurately define the topography of the shoals and islands in this area.

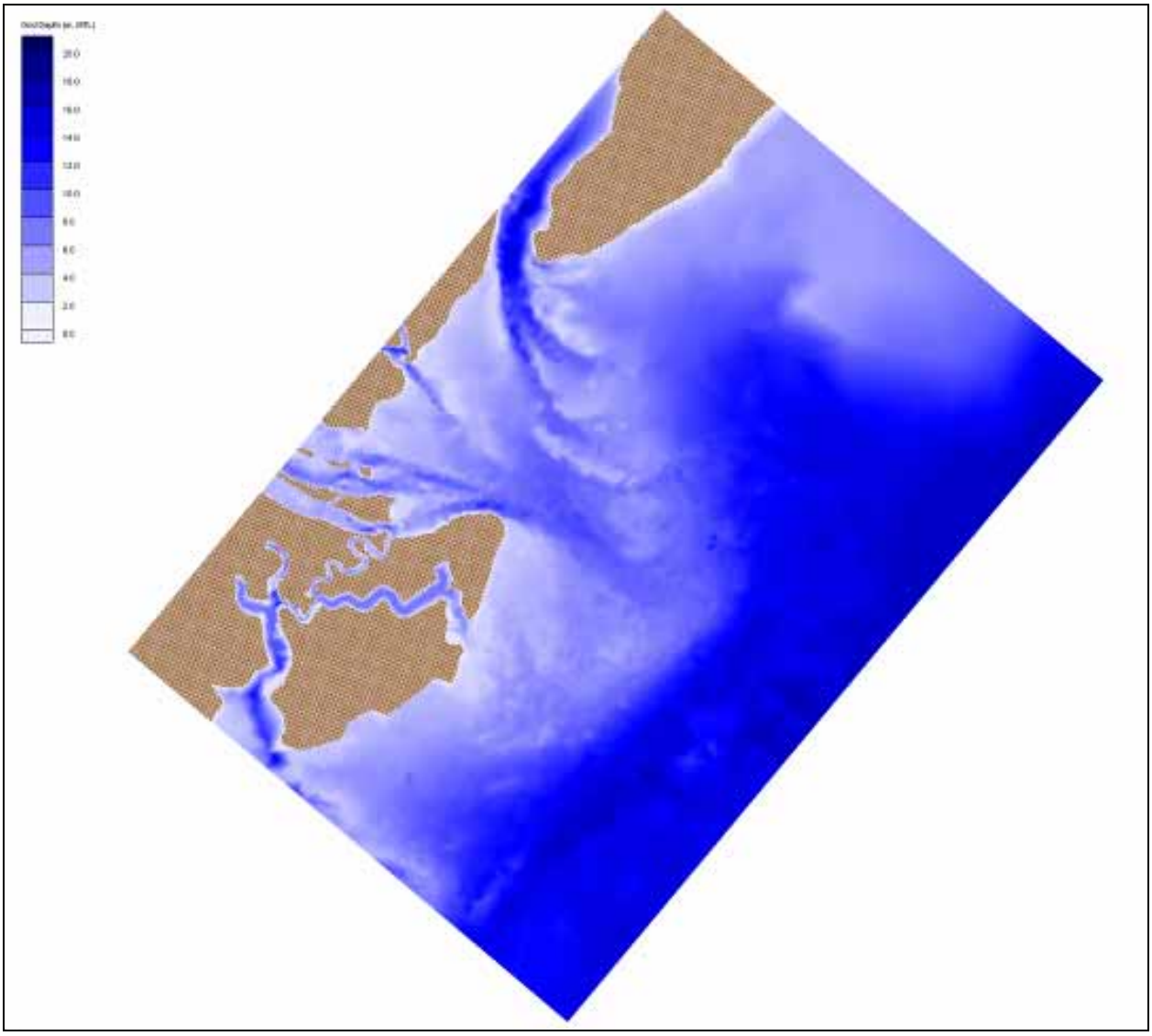

Figure 4-2. Pre-project condition grid (depths in meters, MTL). Land is shown in brown.

Some of the bathymetric changes are not easily seen by visually comparing the two model grids, so a difference plot was created to show how the depths differ from one time period to the next. Figure 4-3 represents these differences by showing positive changes (accretion) between the pre-project and existing conditions grids as blue areas and negative changes (erosion) as green areas. This plot is consistent with Figure 3-1 but is shown in the context of the STWAVE grid.

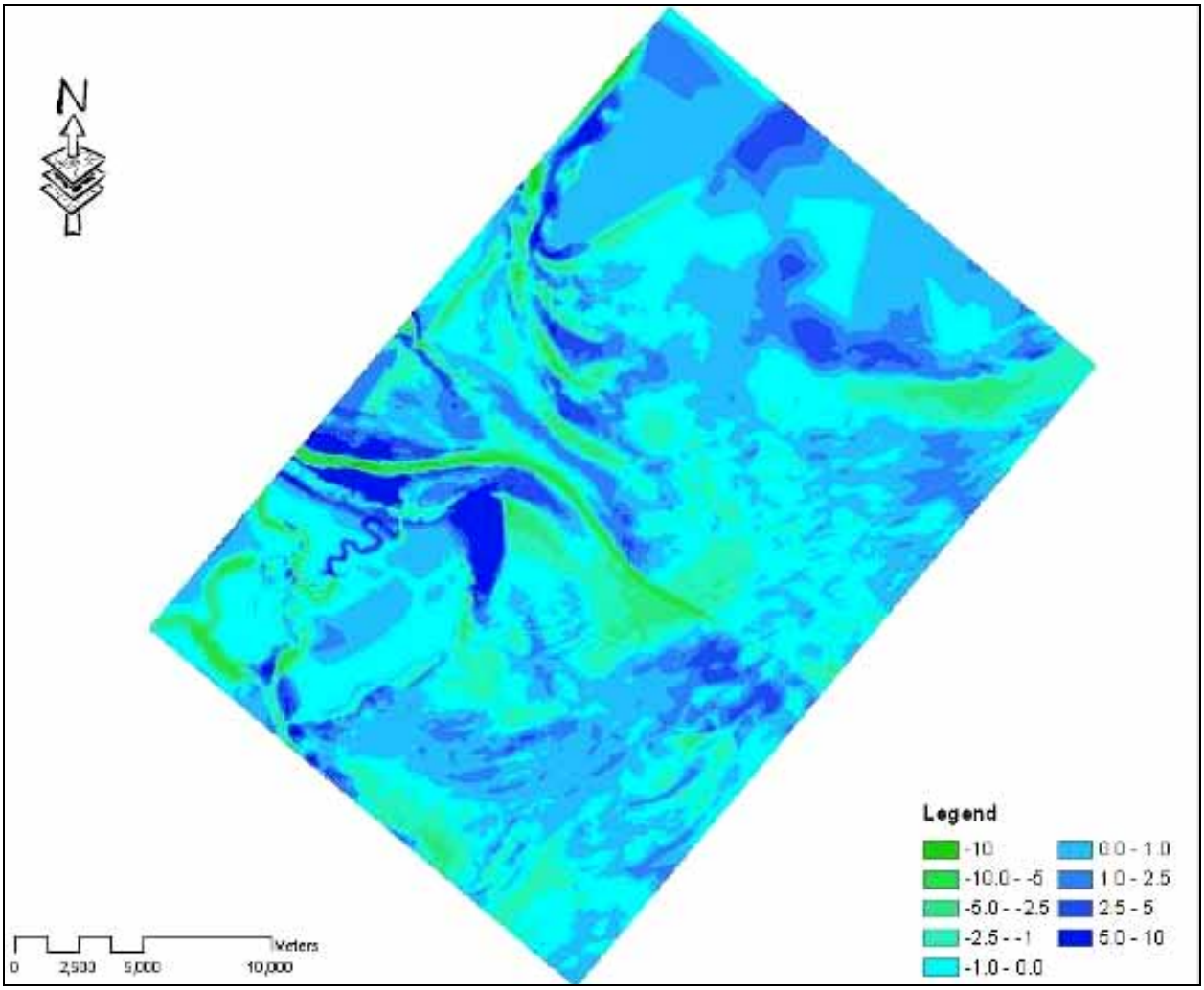

Figure 4-3. Depth differences (in meters) between pre-project and existing conditions grids.

Some areas in Figures 4-2 and 4-3 may not be representative due to a lack of data available to create the pre- and post-project STWAVE model grid. For example, the streams and creeks landward of Tybee and Little Tybee Island are not all well defined in either time period. Most of the subaerial portions of Tybee Island, Little Tybee Island, and Hilton Head Island in Figure 4-3 are not realistic due to lack of data coverage. The large accretion depicted across Tybee Island is an artifact of the data sets and should not be interpreted as actual growth in the elevation of the island.

Morphologic changes of importance to the wave modeling include deflation offshore of the northern half of Tybee Island and another deflation immediately south of Tybee and offshore of Little Tybee Island. There is also widespread deflation farther offshore and adjacent to the Tybee Range portion (both north and south) of the channel. Other changes are

evident and outlined in previous portions of this report. For the purpose of wave transformation modeling, these are the most important.

Input wave conditions

Three time periods were selected for wave simulation: a) a retracked Hurricane Hugo (tracked to hit near Savannah), 14–22 September 1989, was simulated to represent an extreme storm event; b) November 1979, which included a number of storms, was simulated to represent a stormy month; and c) July 1999 was simulated to represent a typical summer month. The offshore wave information for all these simulations were hindcast by the WIS using the wave generation and propagation model WISWAVE (Hubertz 1992). For the July 1999 simulation, hourly offshore wave conditions were taken from the latest WIS hindcast (1980–1999) at Station 368 (http://frf.usace.army.mil/cgi-bin/wis/atl/atl_main.html). WIS Station 368 is located at 32.0 deg North, 80.58 deg West in a water depth of approximately 15 m which is approximately on the offshore boundary of the STWAVE grids. The November 1979 time period is not included in the most recent WIS hindcast period, so it was necessary to use the 3-hourly data from the previous WIS study (Brooks and Brandon 1995) at Station 33 located at 32.0 deg North, 80.5 deg West in a water depth of approximately 13 m. Hurricane Hugo struck Charleston in September 1989 as a Category 4 storm. To evaluate the impact of an intense tropical storm, the Savannah Harbor nearshore placement of dredged material study (Gailani et al. 2003a) simulated a hypothetical retracked Hurricane Hugo striking Savannah. The offshore waves for the retracked Hugo were generated using the WIS methodology. These same retracked Hugo offshore waves were used in this study. The retracked Hurricane Hugo wave information was available at 3-hour intervals. The simulation start and end times are summarized in Table 4-1.

Table 4-1. Start and end times for STWAVE model simulations.

Simulation	Start Date/Time (yyyymmddhh)	End Date/Time (yyyymmddhh)	Interval (hours)
Nov. 1979	1979110100	1979113021	3
Sept. 1989	1989091414	1989092209	3
July 1999	1999070101	1999073100	1

Figures 4-4 to 4-6 show the time histories of offshore significant wave height, peak wave period, and mean wave direction for the three simulation time periods. Wave direction is reported in meteorological convention with waves from the north at 0 deg and waves from the east at 90 deg. The November 1979 simulation has offshore wave heights exceeding 3 m and the retracked Hurricane Hugo has a maximum offshore wave height of 8 m (which is near depth-limited breaking at the offshore STWAVE grid boundary). Summary statistics of the offshore wave parameters are given in Table 4-2.

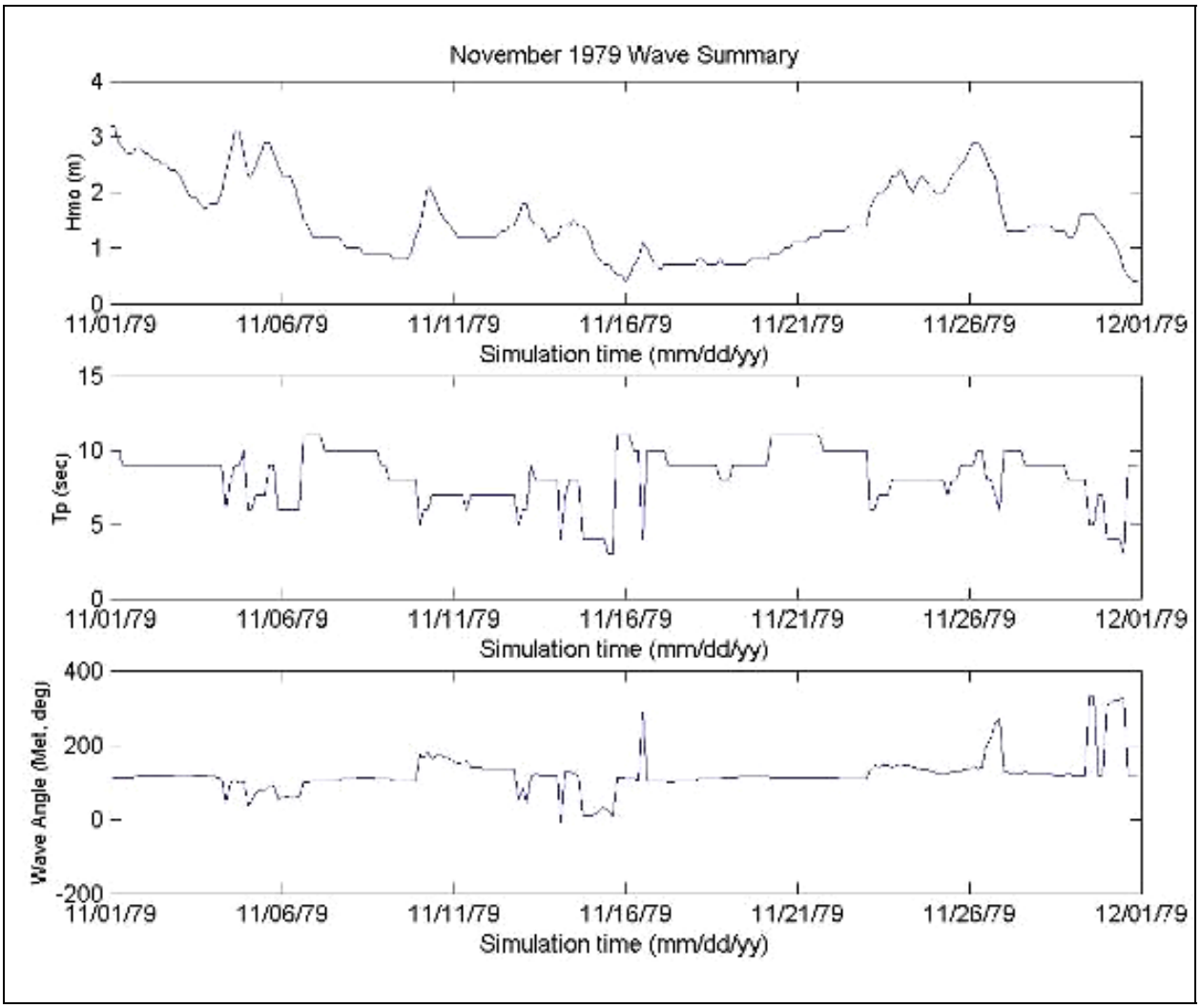

Figure 4-4. Offshore wave conditions for November 1979 at WIS Station 33.

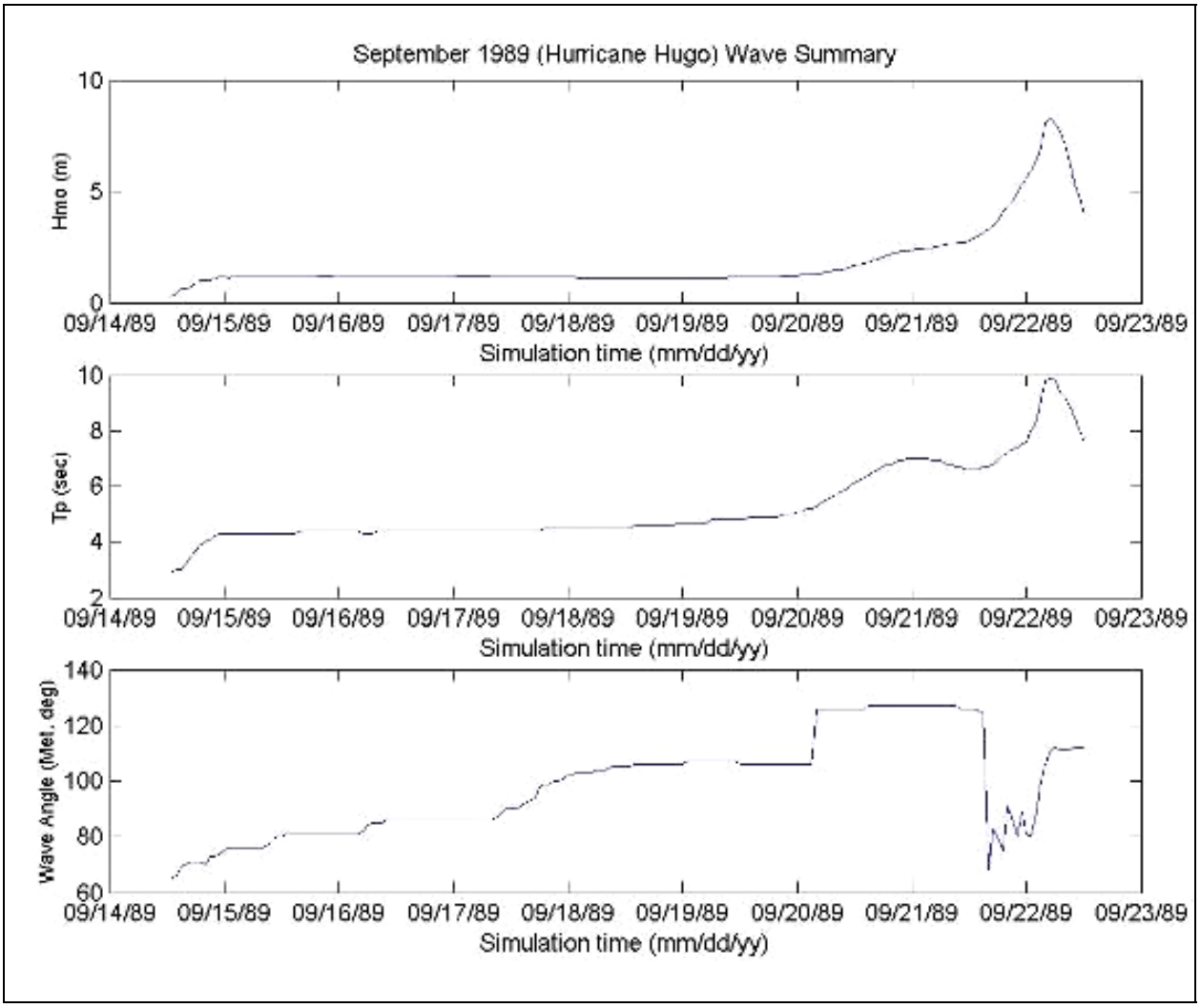

Figure 4-5. Offshore wave conditions for retracked Hurricane Hugo, September 1989.

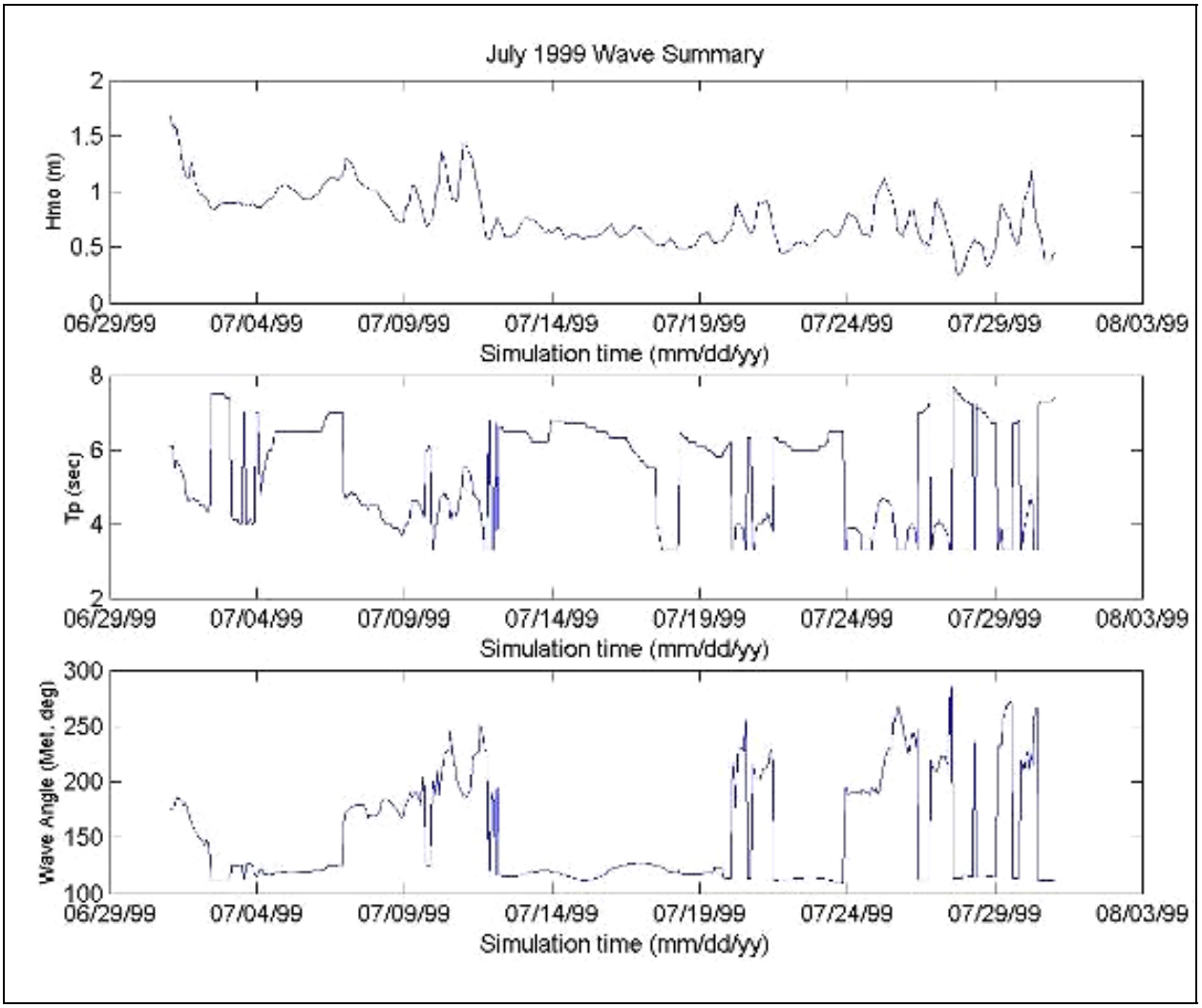

Figure 4-6. Offshore wave conditions for July 1999 at WIS Station 368.

Table 4-2. Statistical summary of offshore (WIS) hindcast wave characteristics.

Simulation	Max Wave Height m	Mean Wave Height m	Median Wave Height m	Min Wave Height m	Max Wave Period sec	Mean Wave Period sec	Median Wave Period sec	Min Wave Period sec
Nov. 1979	3.20	1.51	1.30	0.40	11.00	8.32	9.0	3.0
Sept. 1989	8.01	1.81	1.18	0.43	10.00	7.78	6.0	3.0
July 1999	1.68	0.78	0.72	0.26	7.69	5.41	5.93	3.33

Input wave spectra are required to drive STWAVE on the offshore grid boundary. Parametric spectral shapes were used to generate the input spectra from the offshore wave parameters. The wave energy is distributed in frequency using the TMA spectral shape with a spectral peakedness parameter of 3.3 to 7 (Bouws et al. 1985) and in direction using a $\cos^{nn}(\alpha-\alpha_m)$ distribution, where α_m is the mean wave direction, with *nn* of 4 to 26. The input spectra for all cases except the retracked Hurricane Hugo have 30 frequencies, starting with 0.04 Hz and incrementing by 0.01 Hz. For the retracked Hurricane Hugo, 20 frequencies were used starting at 0.04167 Hz and incrementing exponentially to 0.333 Hz. The directional resolution for all simulations is 5 deg.

Water level

The water levels (combination of tide and storm surge) applied in STWAVE were determined by the ADCIRC model simulations (Chapter 3). The water levels were extracted from ADCIRC at the STWAVE boundary (WIS station location) and applied over the entire grid. The water level was updated with each new wave boundary condition (either every 1 or 3 hr).

Winds and currents

Local wind wave generation within the STWAVE domain was not included in these simulations. A sensitivity analysis of the importance of wave-current interaction (current-induced shoaling and refraction) within the model domain was conducted during the previous study (Smith et al. 2006) in this area with the same environmental forcings. The sensitivity analysis concluded that wave-current interaction was not a significant enough contributor to warrant its inclusion and it was, therefore, omitted from this study as well.

A spectral wave model was selected for these simulations to realistically include the directional and frequency spread of wave energy in this open coastal setting (in contrast, monochromatic models generally have sharp gradients in wave parameters that are not seen in nature). These simulations include variations in water level (tide and surge), but neglect wave-current interaction because the impact is small and localized in the channel. Bottom friction was also neglected. The wave simulations were run for extended time periods (Table 4-1), which include a large range of incident conditions (wave heights, periods, directions, and water levels). STWAVE output is used to examine the morphologic changes between the two time

periods on the waves, to provide radiation stress gradients to force wave-driven currents in the circulation model (Chapter 3), and to provide input to the sediment transport modeling (Chapter 5).

Wave model results

Some sample STWAVE results are shown in this section to illustrate the range of conditions simulated and the impact of the changes that have occurred since approximately 1854. Figures 4-7 and 4-8 show the wave heights at the peak of the retracked Hugo simulation over the existing and pre-project bathymetry, respectively. Offshore wave heights exceeded 8 m (26 ft) at the grid boundary and the peak period was 10 sec. These are the most severe wave conditions simulated during any of the three model simulation periods. The wave heights decreased toward the shore due to depth-limited wave breaking. These boundary conditions resulted in wave heights along the Atlantic shoreline of Tybee Island in the range of 2.5 to 3.5 m (8.2 to 11.5 ft) under existing conditions and 2 to 3 m (6.6 to 9.8 ft) under the pre-project conditions. Figure 4-9 shows the differences in wave heights (existing condition minus the pre-project condition) at the peak of the storm (22 September 0600 UTC). Areas with larger wave heights under existing conditions than pre-project conditions are depicted by yellows and reds, while areas with reduced wave heights are depicted by blues, and areas with no change in wave height are white. Examination of the relationship between bathymetric changes and wave height differences reveals that erosion of nearshore morphology since project construction, depicted by green areas in Figure 4-3, allows larger wave heights closer to shore during storm events, depicted by areas of yellow and red in Figures 4-9 and 4-10. When examining the wave height differences in Figures 4-9 and 4-10, it is important to remember the previous discussion concerning topographic changes between the two time periods. For example, the dark red area on the northern end of Tybee Island actually represents an area that was land during the period prior to the jetties and is presently intertidal and subaqueous. Therefore, the difference contours are somewhat deceiving because this is an area where waves would not have been present in the past and the magnitude of change should be interpreted as such.

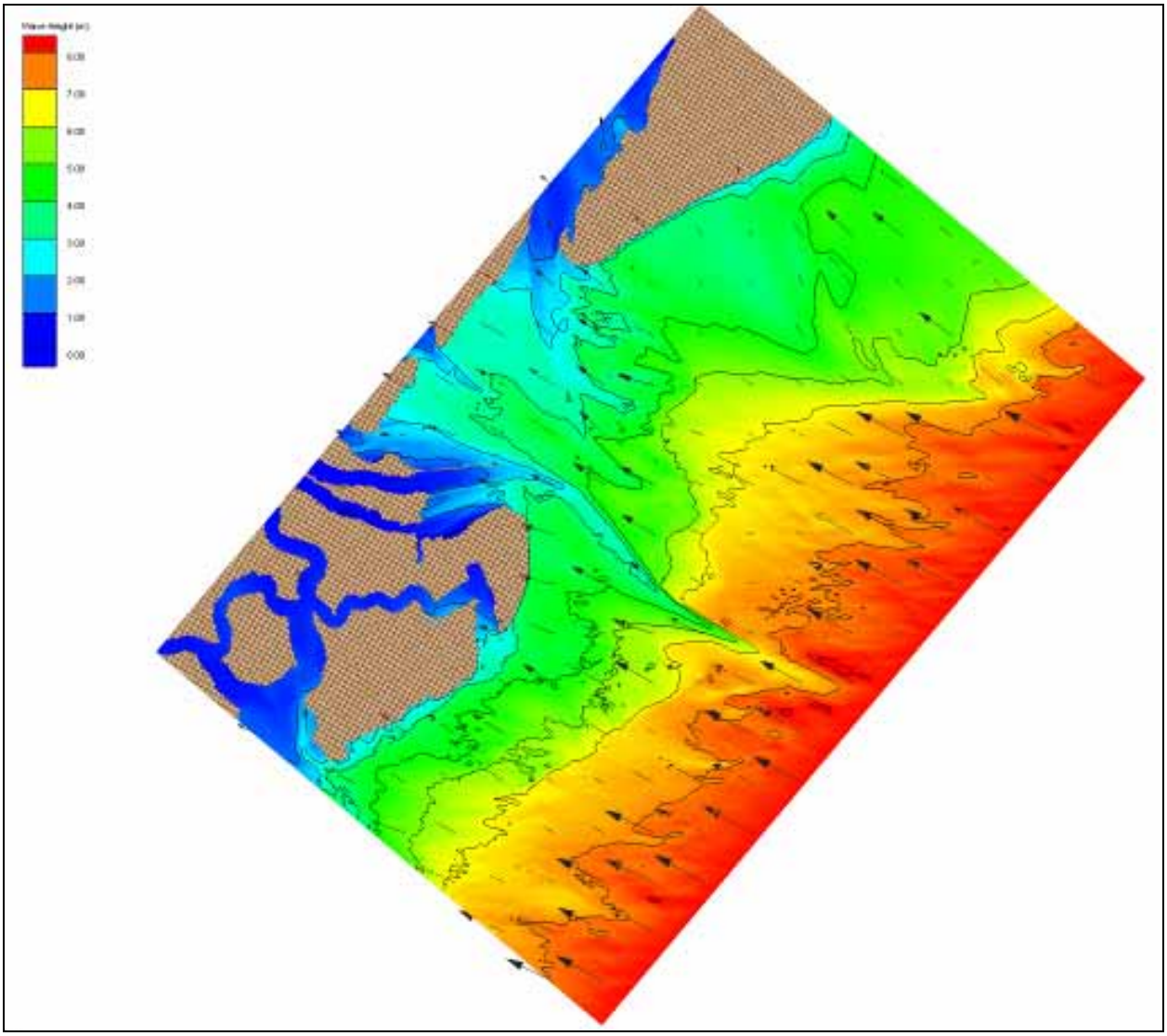

Figure 4-7. Wave height for existing bathymetry at peak of hypothetical retracked Hurricane Hugo, 22 September 1989.

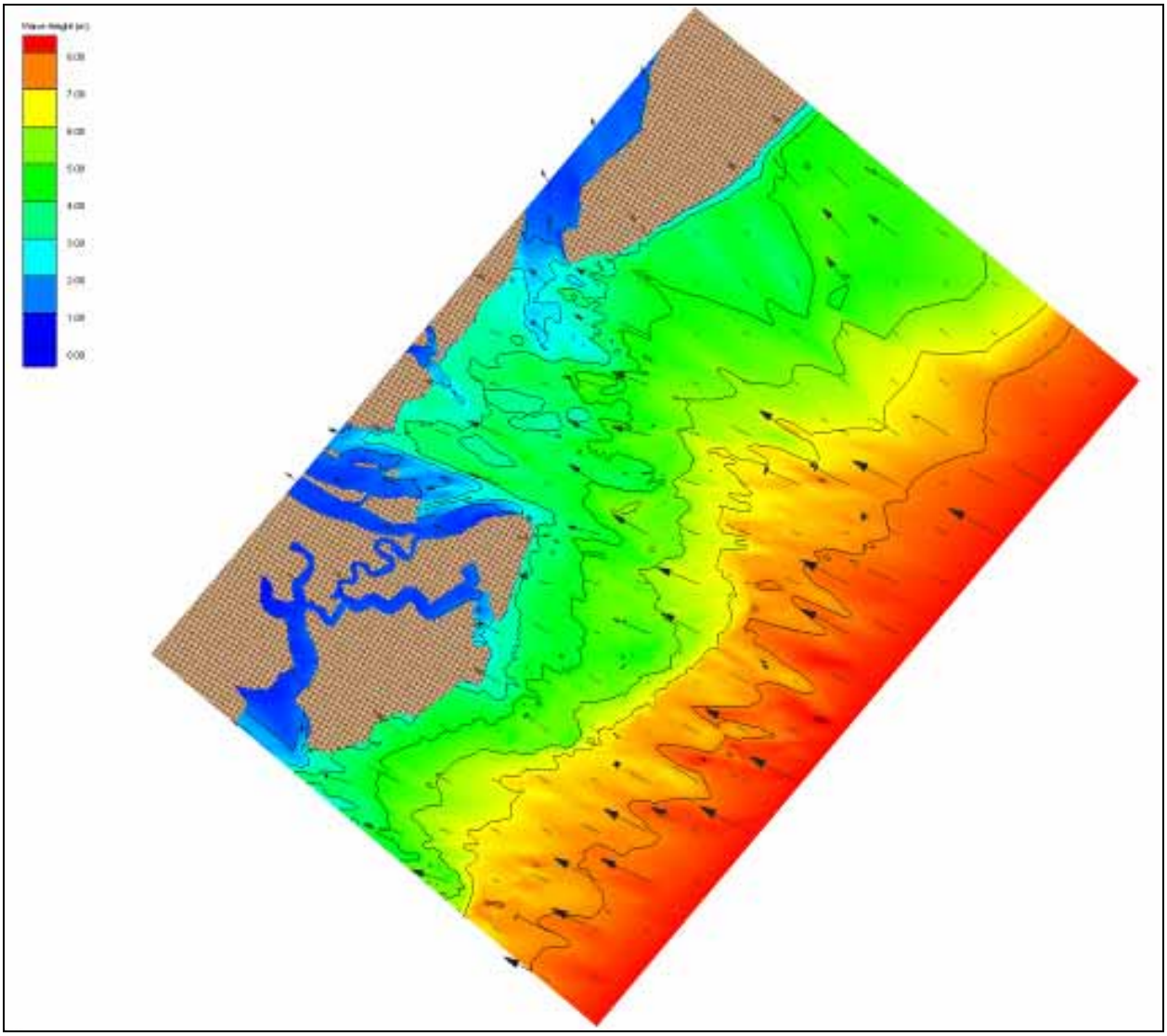

Figure 4-8. Wave height for pre-project bathymetry at peak of hypothetical retracked Hurricane Hugo, 22 September 1989.

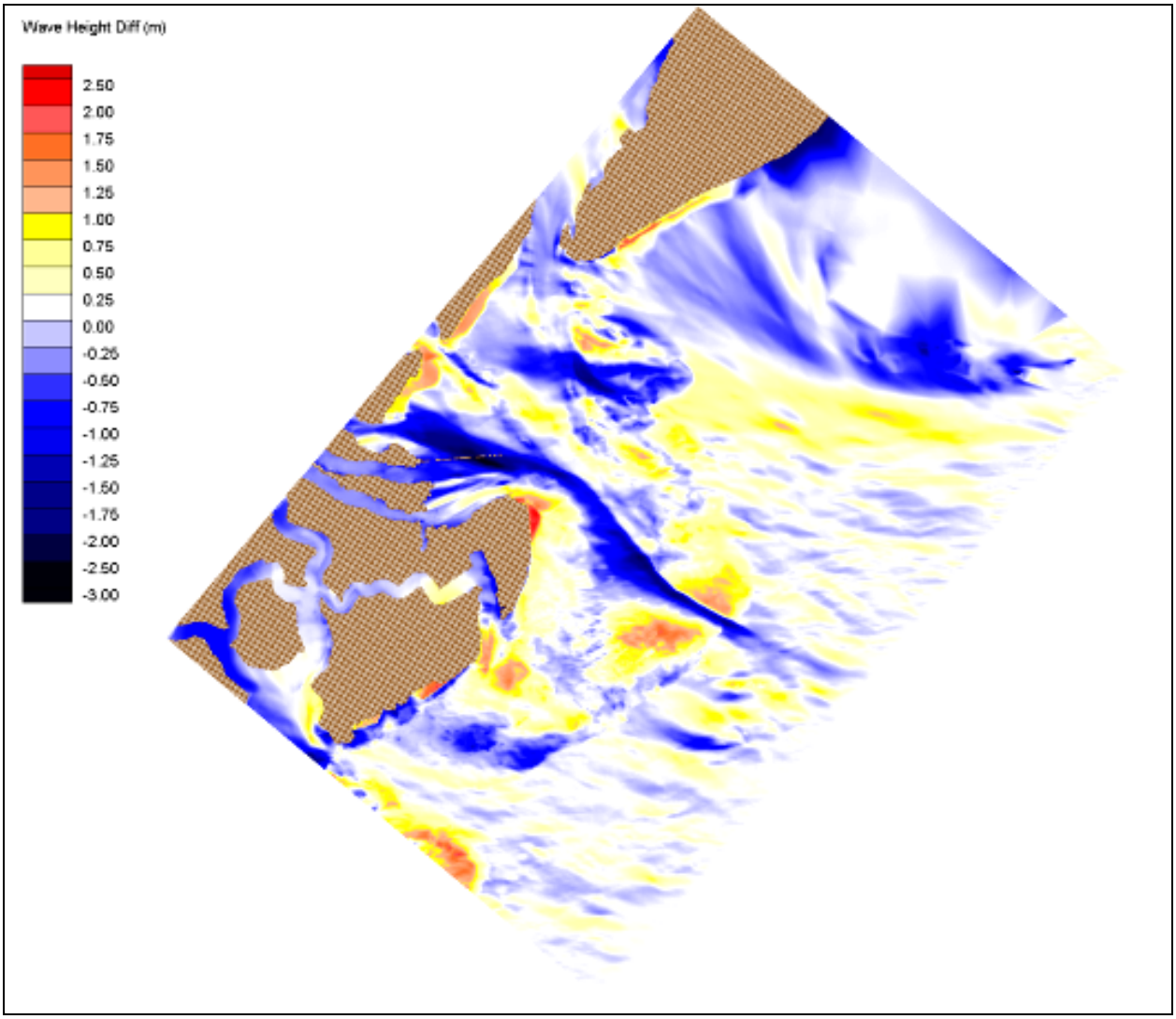

Figure 4-9. Wave height differences (existing minus pre-project condition) at peak of hypothetical retracked Hurricane Hugo, 22 September 1989.

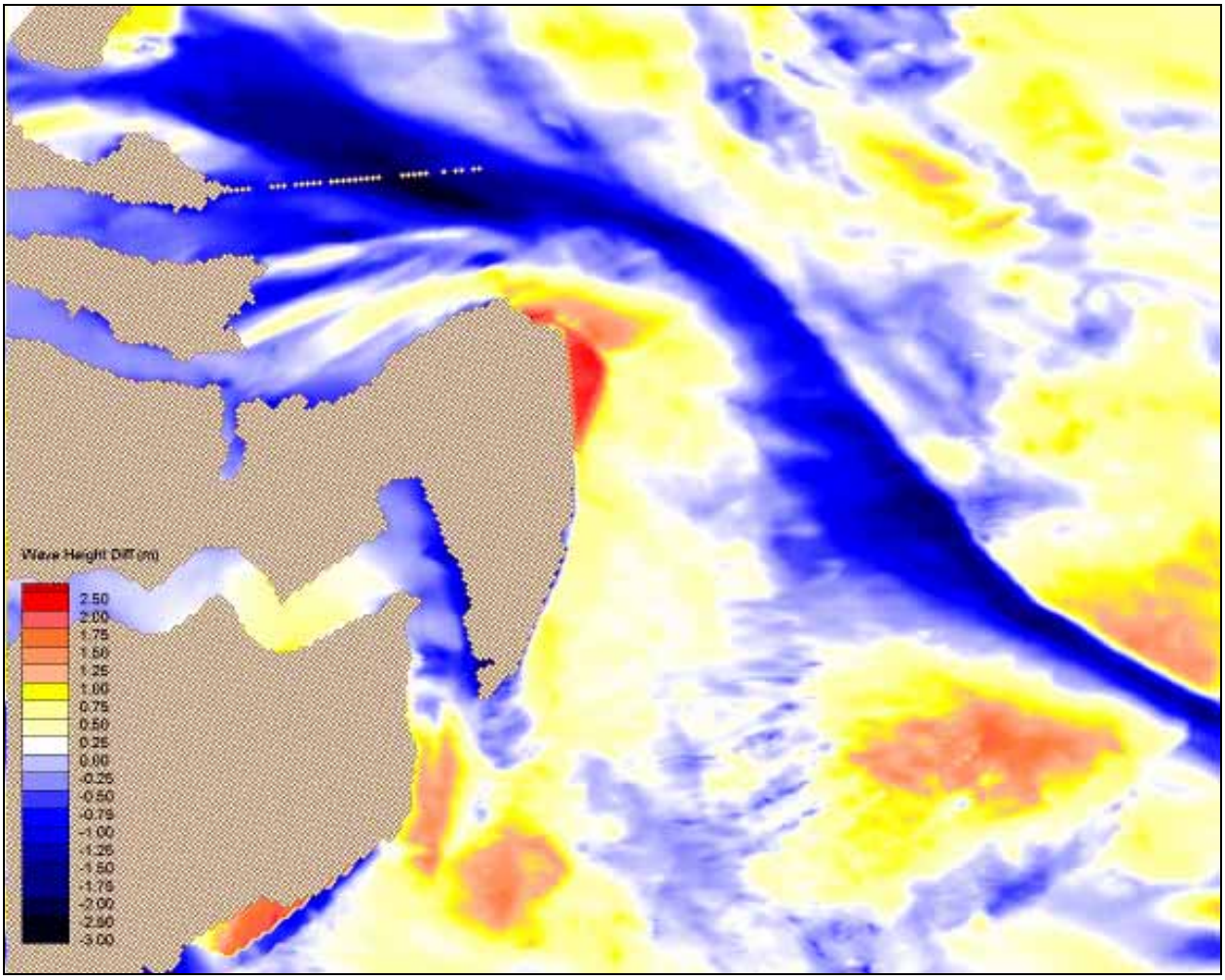

Figure 4-10. Zoomed in view of wave height differences (existing minus pre-project condition) at Tybee Island at peak of hypothetical retracked Hurricane Hugo, 22 September 1989.

In order to more concisely represent the wave height changes surrounding Tybee Island, discrete points were established where wave height differences could be determined without the potential for mistakenly including areas that used to be dry land. The layout and ID numbers of these wave observation points, which are subsequently divided into two subsets (northern and eastern), is provided in Figure 4-11. The northern subset consists of observation points 1 through 34 and the eastern subset includes points 35 through 89. Establishing these points enables wave height difference statistics to be summarized over the entire STWAVE model simulation time series. Figures 4-12 and 4-13 present the minimum, maximum and mean wave height differences for the observation points for 14–22 September 1989 for the northern and eastern observation point subsets (see Figure 4-11), respectively. The top portion of the figure shows

the distribution of the points from west to east and north to south and the bottom portion provides the corresponding wave statistics.

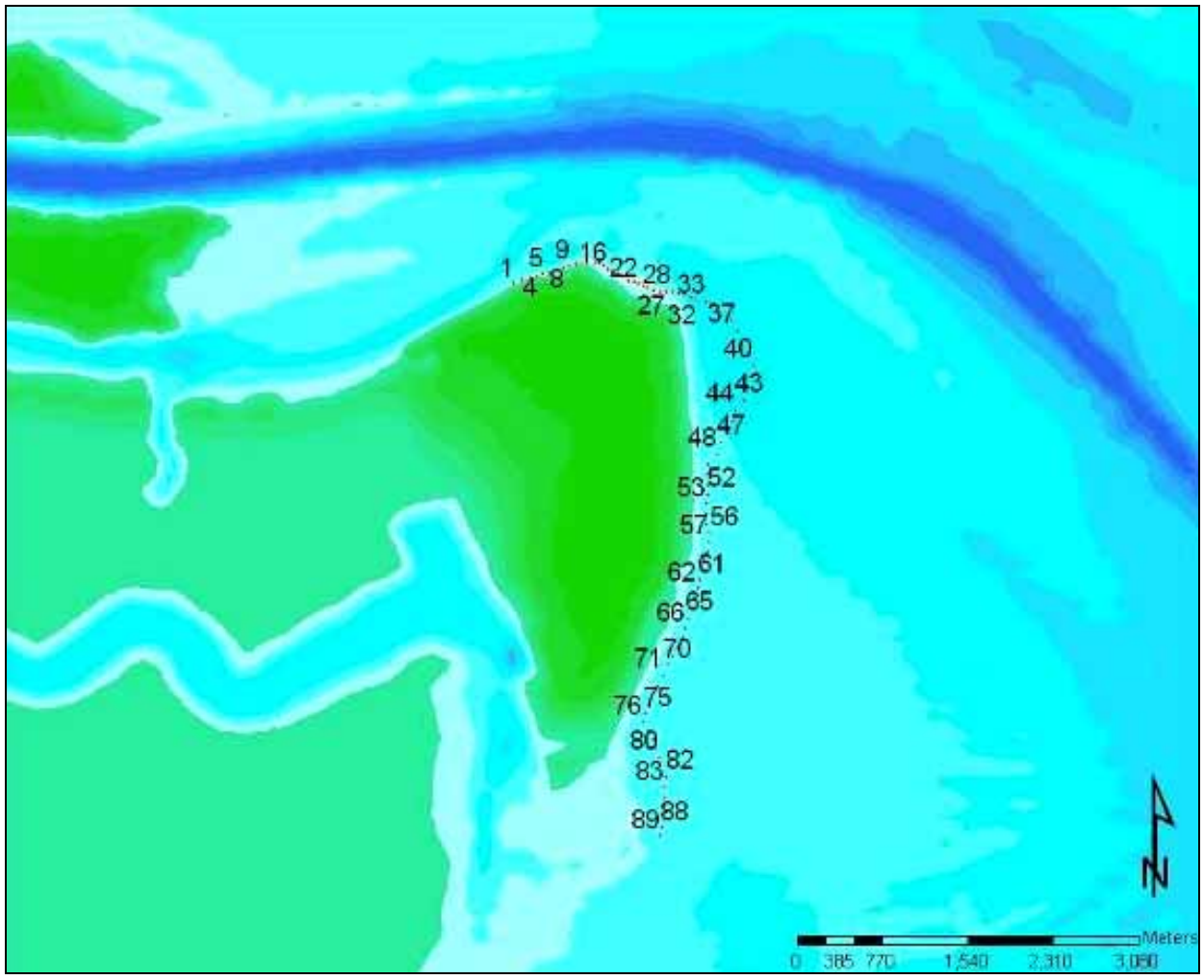

Figure 4-11. Location and distribution of observation points for wave height and direction difference comparisons.

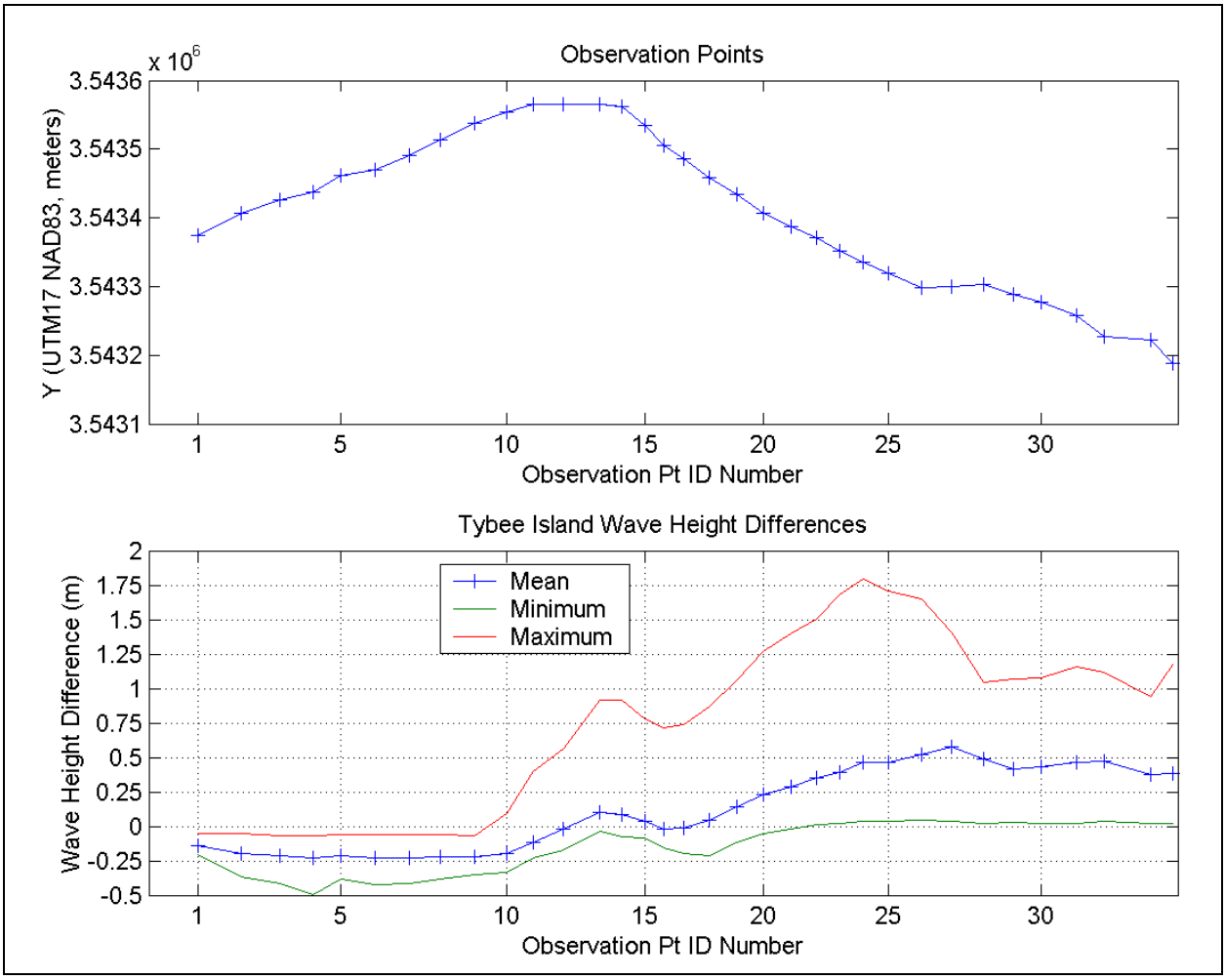

Figure 4-12. Wave height differences at northern Tybee observation points for 9–22 September 1989 (hypothetical retracked Hurricane Hugo).

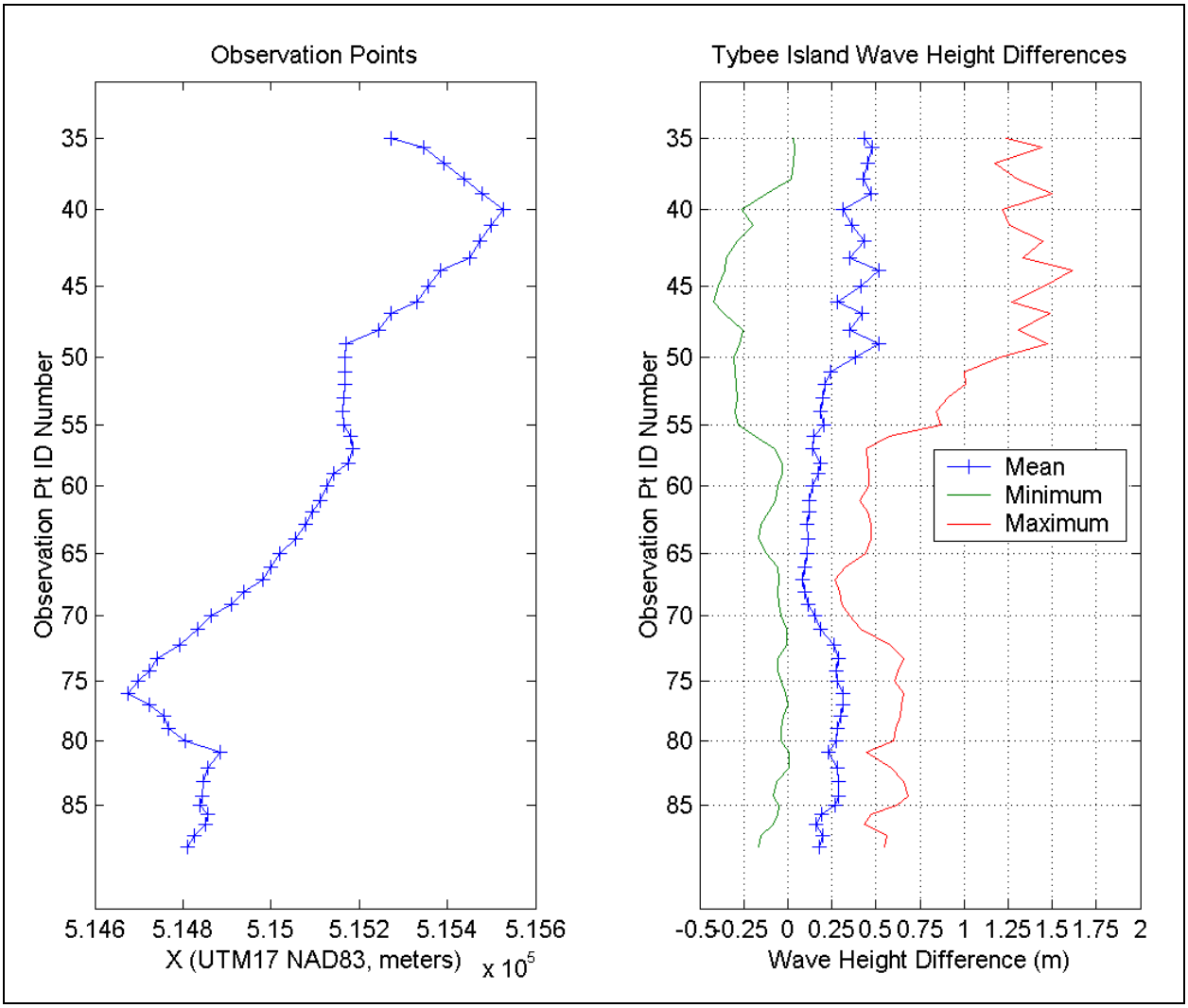

Figure 4-13. Wave height differences at eastern Tybee observation points for 9–22 September 1989 (hypothetical retracked Hurricane Hugo).

The interior portion of the northern edge of the island (points 1–10) exhibits a clear trend towards a decrease in wave heights (Figure 4-12), with the maximum wave height increase at or near zero and the mean difference approximately -0.25 m (-0.8 ft). This transitions to an area of marked increase in wave height along the northern shoreline closer to the Atlantic (points 20–34 in Figure 4-12) and along the northern half of the east facing Atlantic shoreline (points 35–55 in Figure 4-13). These increases are dominated by the large wave heights experienced during the peak of the retracked Hugo event and are influenced by the increased water depths close to the northern end of the island (Figure 4-3), which produced wave height differences of between +1 and +1.75 m (3.3 to 5.7 ft) during the peak of the storm event and an average of approximately +0.5 m (1.6 ft) over the duration of the 8-day simulation. The southern half of the Atlantic shoreline

(points 56–89 in Figure 4-13) experiences more uniform changes in the magnitudes of the wave height increases, resulting in a mean wave height difference of between approximately +0.1 and +0.25 m (0.3 to 0.8 ft).

The mean wave directions of the existing and pre-project simulations were also computed at the observation points shown in Figure 4-11. Figures 4-18 through 4-22 show mean wave vectors for both the existing (blue) and pre-project (red) simulations of the retracked Hugo event. The lengths of the vectors represent a scaled version of the mean wave height at each observation point, but the emphasis should be on the similarities and differences between the mean wave directions at each of the observation points. As can be seen in Figure 4-18, significant differences in mean wave direction exist over large portions of the northern Tybee observation domain. This is particularly true for observation points 1 through 15 and 25 through 34. The largest differences in mean direction are from points 28 to 34, which coincide with the area of large bathymetric change at the northeast corner of the island. The magnitudes of the differences decrease as the observation point numbers increase and move around the area of large bathymetric change and toward southern end of the island along the Atlantic shoreline. Points 55 through 57 (Figure 4-20), in the vicinity of the middle of the island, depict an area of localized increase in the magnitude of mean wave direction change. Changes in mean wave direction remain relatively mild until reaching the southern tip of the island at observation points 82 through 88 (Figure 4-22).

Although the highest rate of sediment transport occurs during storms, it is important to investigate a large range of incident wave conditions. In addition to the retracked Hurricane Hugo, two months were simulated which include both winter and summer conditions with a large range of incident wave height, period, and direction (Table 4-2, and Figures 4-5 and 4-6). November 1979 was selected to represent winter conditions and included multiple storm events. Figures 4-14 and 4-15 present wave height difference statistics for the month of November at the northern and eastern observation point subsets, respectively. The interior portion of the northern edge of the island (points 1–10) exhibits a clear trend towards a decrease in wave heights (Figure 4-14), with the maximum wave height increase near zero with the mean difference slightly less than -0.25 m (0.8 ft).

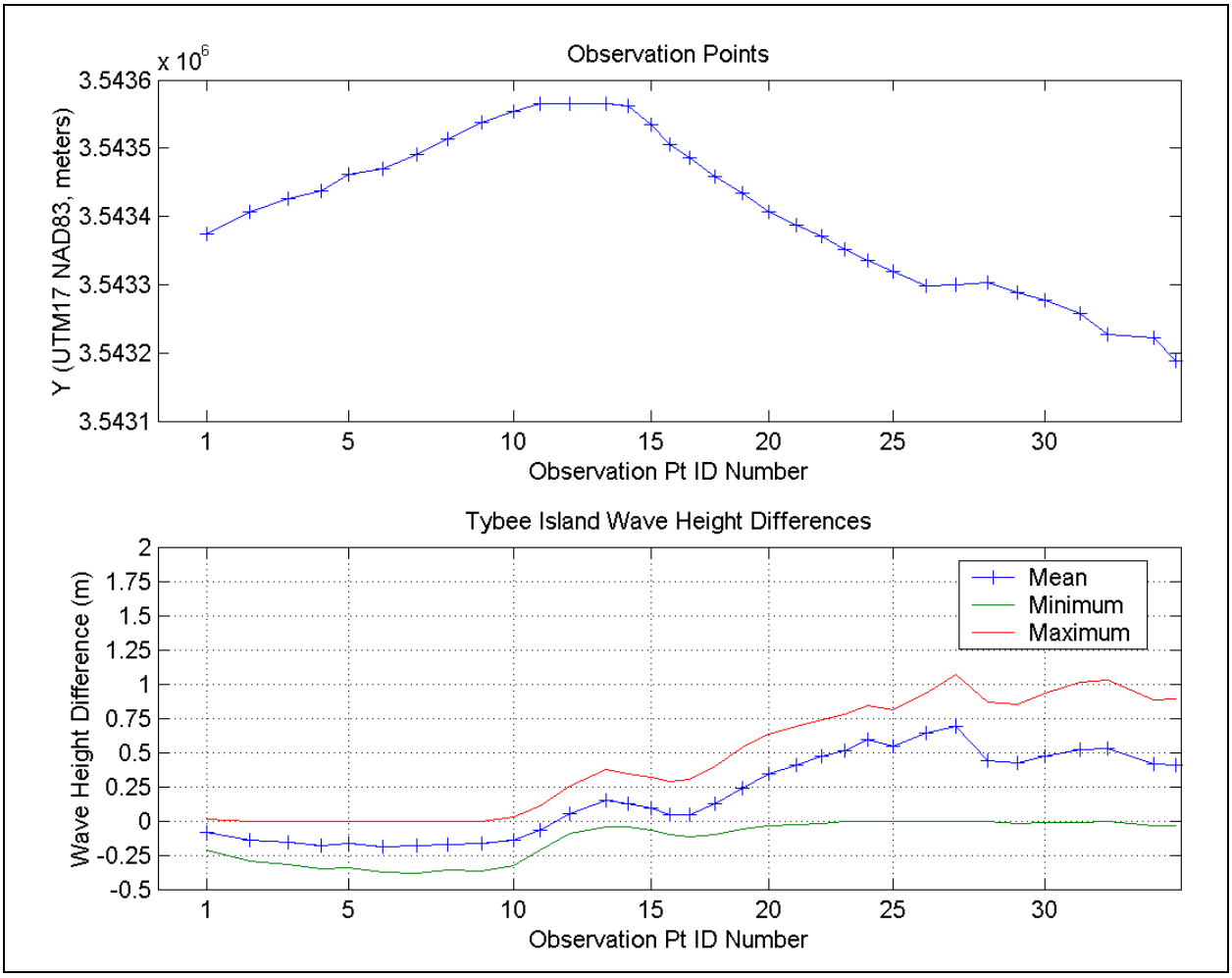

Figure 4-14. Wave height differences at northern Tybee observation points for 1–30 November 1979.

This transitions to an area with significantly increased wave heights along the northern shoreline closer to the Atlantic (points 20–34 in Figure 4-14) and along the northern half of the east facing Atlantic shoreline (points 35–55 in Figure 4-15). These increases are dominated by the periodic storm events during the month and are influenced by the increased water depths close to the northern end of the island (Figure 4-3). The maximum wave height differences in this area vary between +0.75 and +1.25 m (2.5 to 4.1 ft), while the mean difference is approximately +0.5 m (1.6 ft). The southern half of the Atlantic shoreline (points 56–89 in Figure 4-15) experienced more uniform changes in the magnitudes of the wave height differences, resulting in a mean difference of between approximately +0.1 and +0.4 m (0.3 to 1.3 ft).

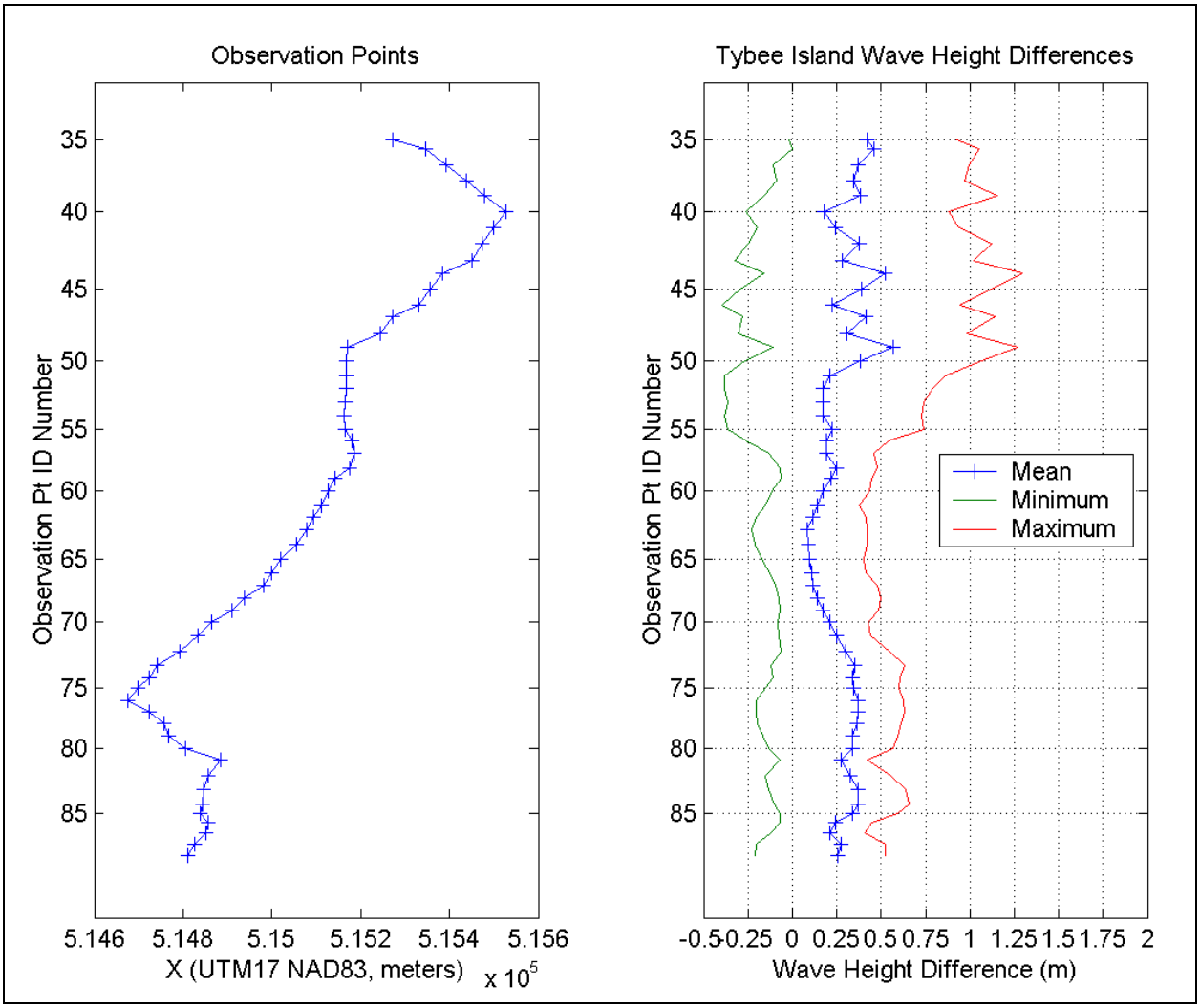

Figure 4-15. Wave height differences at eastern Tybee observation points for 1–30 November 1979.

Changes in mean wave direction for the November 1979 simulation are presented in Figure 4-23 through 4-27. The locations of significant differences in mean wave direction and the magnitude of those differences are very similar to those described for the retracked Hugo simulation.

July 1999 was selected to represent a relatively calm summer condition. Figures 4-16 and 4-17 present wave height difference statistics for the month of July at the northern and eastern observation point subsets, respectively. The relatively calm summer conditions of July 1999 produced a more equitable mix of wave height increases and decreases in close proximity to Tybee Island than either of the other two simulations. In fact, with the exception of the inlet exposed northern tip of the island, the mean wave height differences trended towards null. Mean wave height differences for the interior half of the northern shoreline varied only slightly on

either side of zero (points 1–17 in Figure 4-16). The northeastern corner of the island (points 20–34 in Figure 4-16 and points 35–40 in Figure 4-17) experienced slightly larger increases in wave heights and relatively no wave height decreases during the month, raising the mean difference to approximately +0.25 m. Variability between positive and negative wave height differences served to lower the mean difference to roughly zero along the remainder of the Atlantic shoreline (points 41–89 in Figure 4-17).

Changes in mean wave direction for the July 1999 simulation are presented in Figure 4-28 through 4-32. The locations of significant differences in mean wave direction are very similar to those described for previous simulations. However, the magnitudes of the differences are generally less than both the retracked Hugo and November 1979 simulations, especially for observation points 48 to 66.

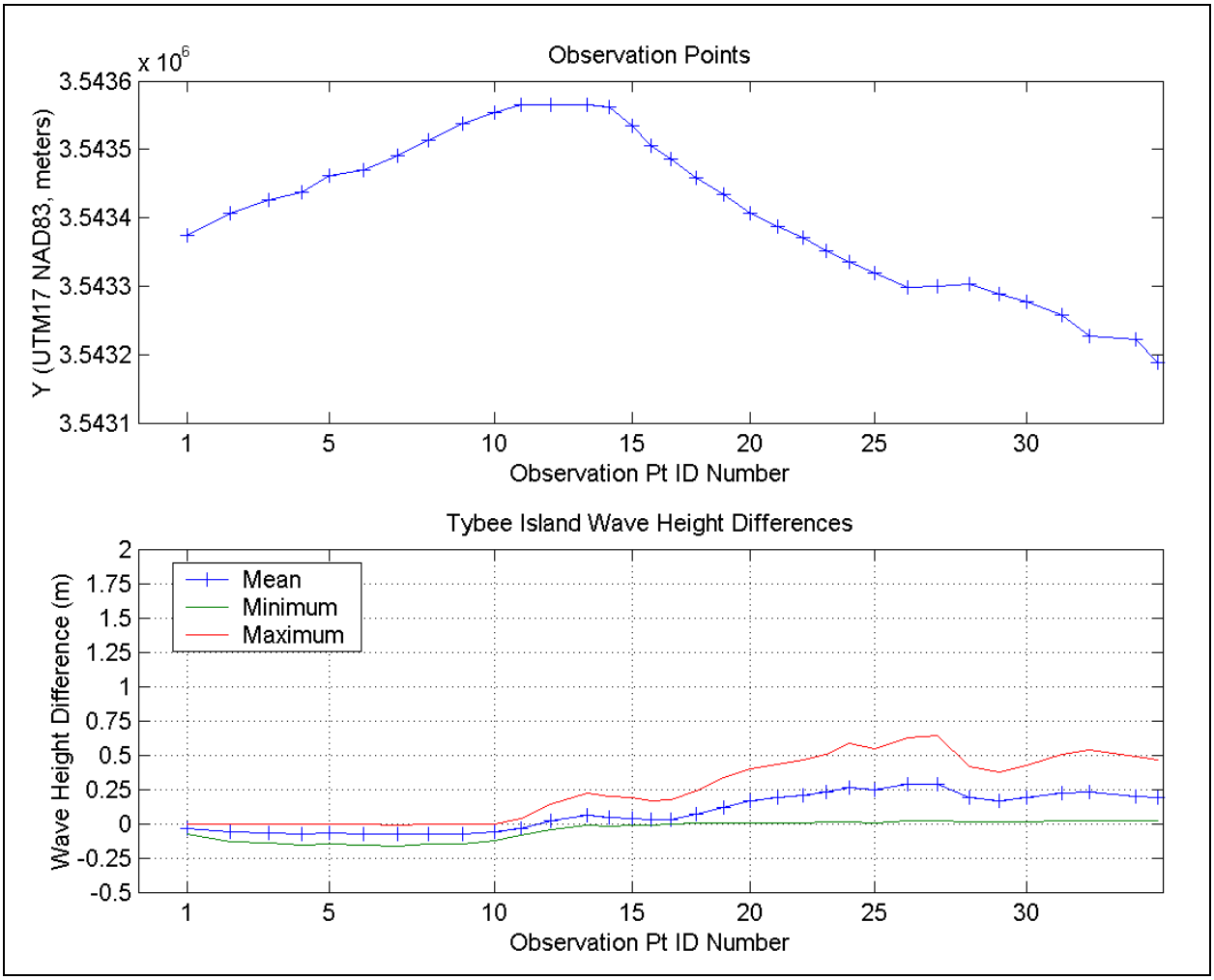

Figure 4-16. Wave height differences at northern Tybee observation points for 1–31 July 1999.

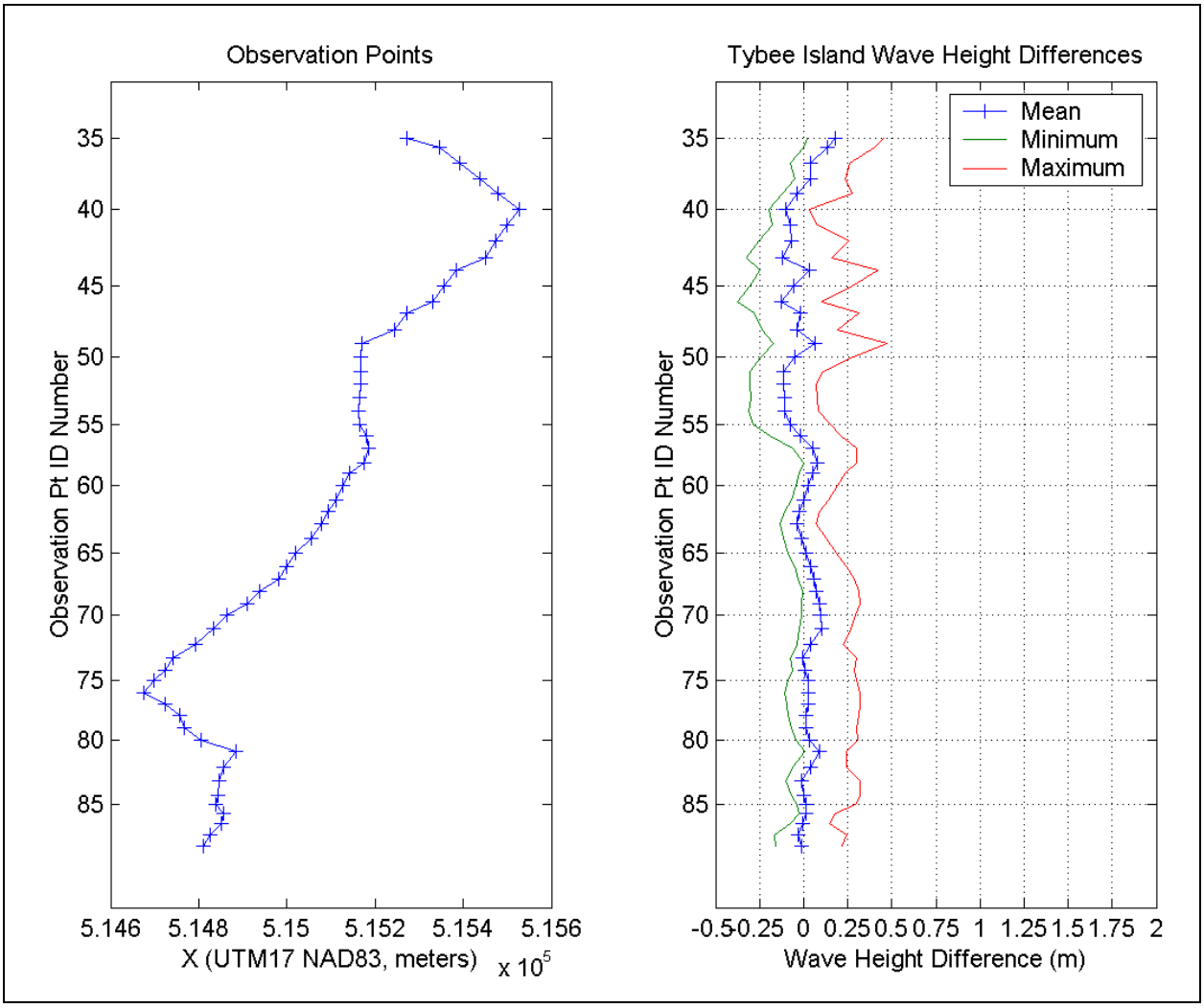

Figure 4-17. Wave height differences at eastern Tybee observation points for 1–31 July 1999.

Summary of wave results

Waves are one of the primary drivers of sediment transport. The impacts of the topographic and bathymetric change, since before the construction of the Savannah Harbor jetties and major improvements to the navigation channel, were investigated by applying the STWAVE wave model. Model simulations were made for the existing conditions and the pre-project conditions for two historical time periods (November 1979 and July 1999) and a hypothetical extreme event (Hurricane Hugo retracked to strike Savannah). These simulations cover a large range of incident wave height, period, and direction and water levels. Comparing the wave heights between the two conditions for all three simulations reveals how different incident waves are influenced by the relative differences in the bathymetry of the two model grids.

The large hypothetical waves during the retracked Hugo event produced extreme wave height differences in areas with large bathymetric differences. These differences were explored in detail for the shoreline of Tybee Island (Figures 4-10, 4-12, and 4-13). The offshore and nearshore changes in bathymetry close to the northern end of the island produced wave height differences of between +1.5 and +1.75 m (4.9 to 5.7 ft) during the peak of the storm event and an average of approximately +0.5 m (1.6 ft) over the duration of the 8-day simulation. The November 1979 simulation was also dominated by several storm events of lesser magnitude and produced mean wave height differences of between +0.25 and +0.5 m (0.8 to 1.6 ft) for the northern portion of Tybee Island. The relatively calm summer conditions of July 1999 produced a more equitable mix of wave height increases and decreases in close proximity to Tybee Island. In fact, with the exception of the exposed northern tip of the island, the mean wave height differences trended towards null.

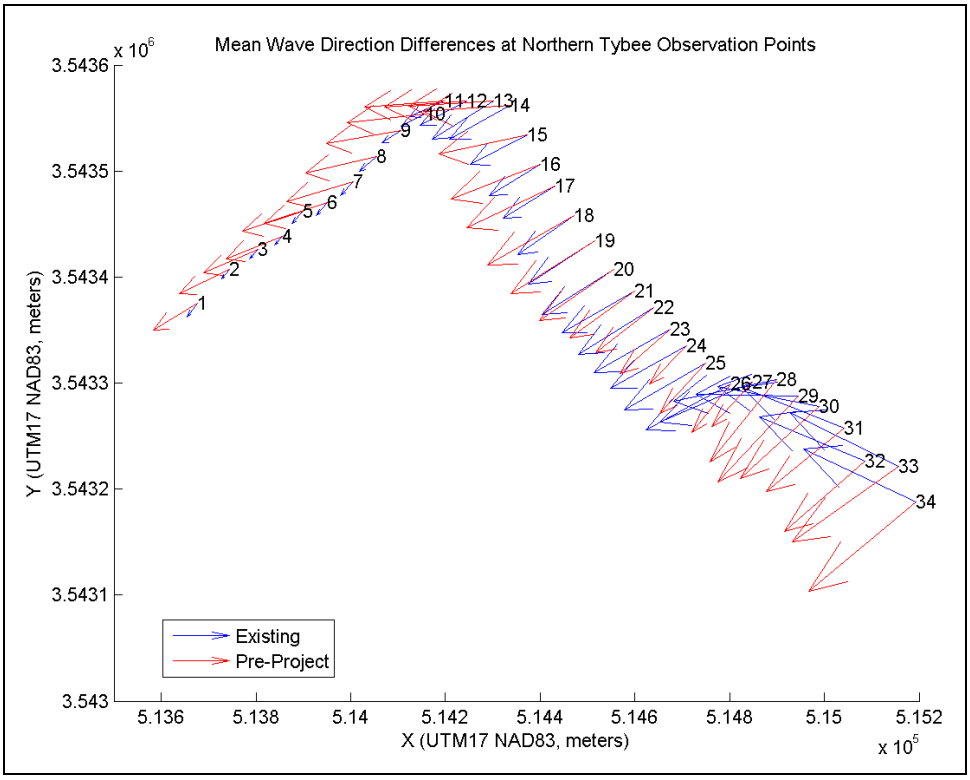

Figure 4-18: Vectors of mean wave height direction at the northern Tybee observation points for 9–22 September 1989 (hypothetical retracked Hurricane Hugo).

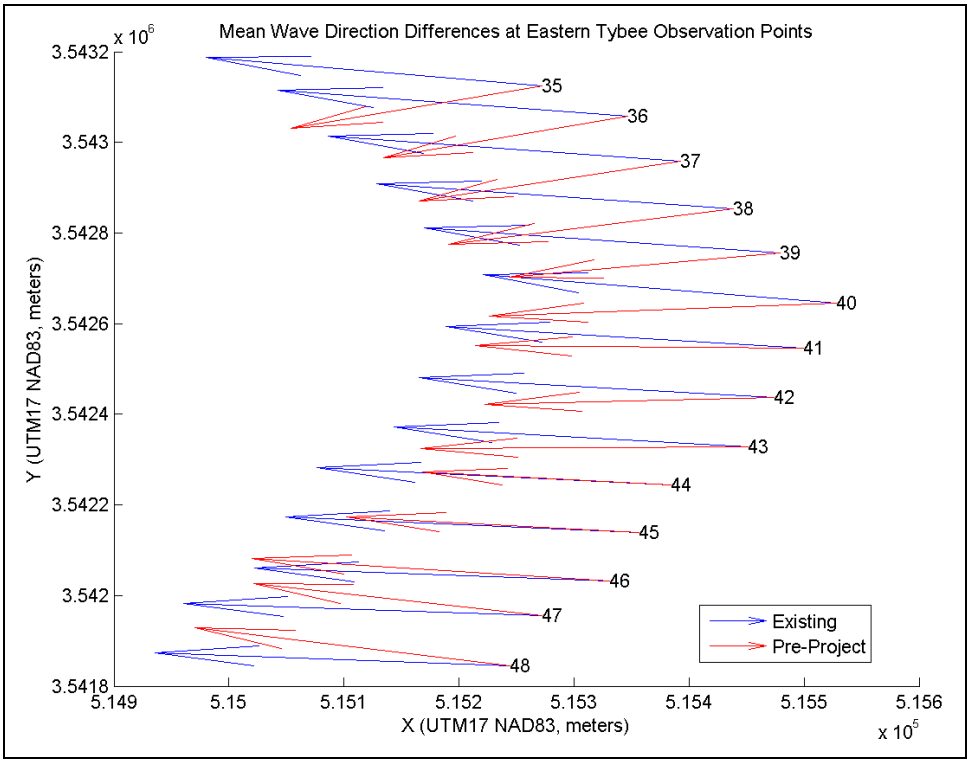

Figure 4-19: Vectors of mean wave height direction at the eastern Tybee observation points for 9–22 September 1989 (hypothetical retracked Hurricane Hugo).

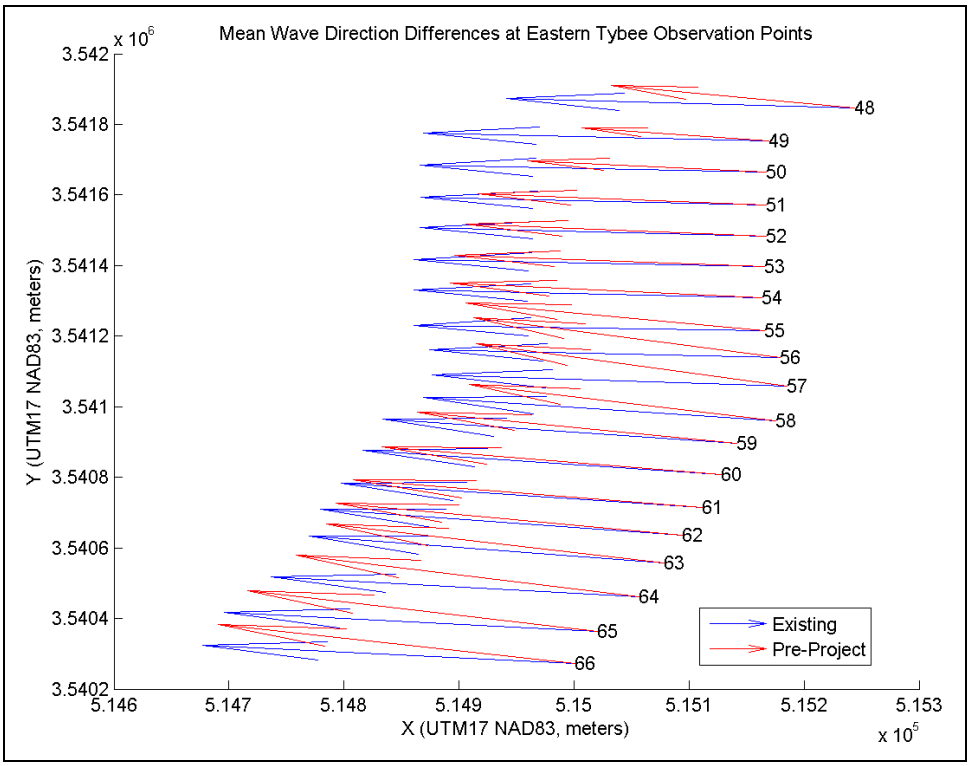

Figure 4-20: Vectors of mean wave height direction at the eastern Tybee observation points for 9–22 September 1989 (hypothetical retracked Hurricane Hugo).

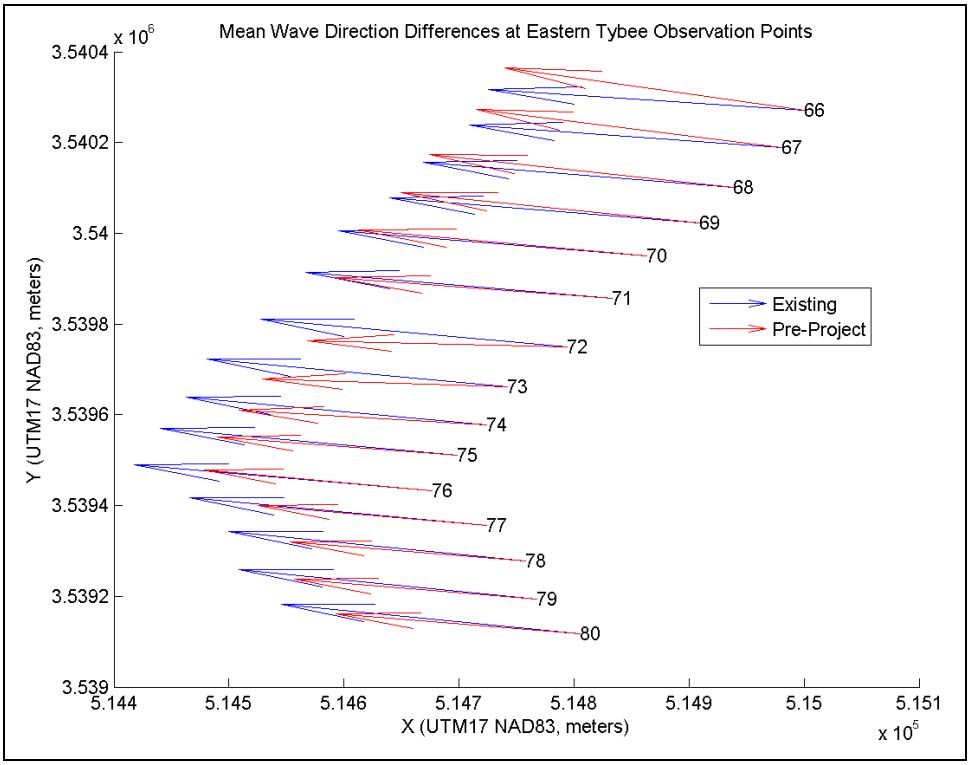

Figure 4-21: Vectors of mean wave height direction at the eastern Tybee observation points for 9–22 September 1989 (hypothetical retracked Hurricane Hugo).

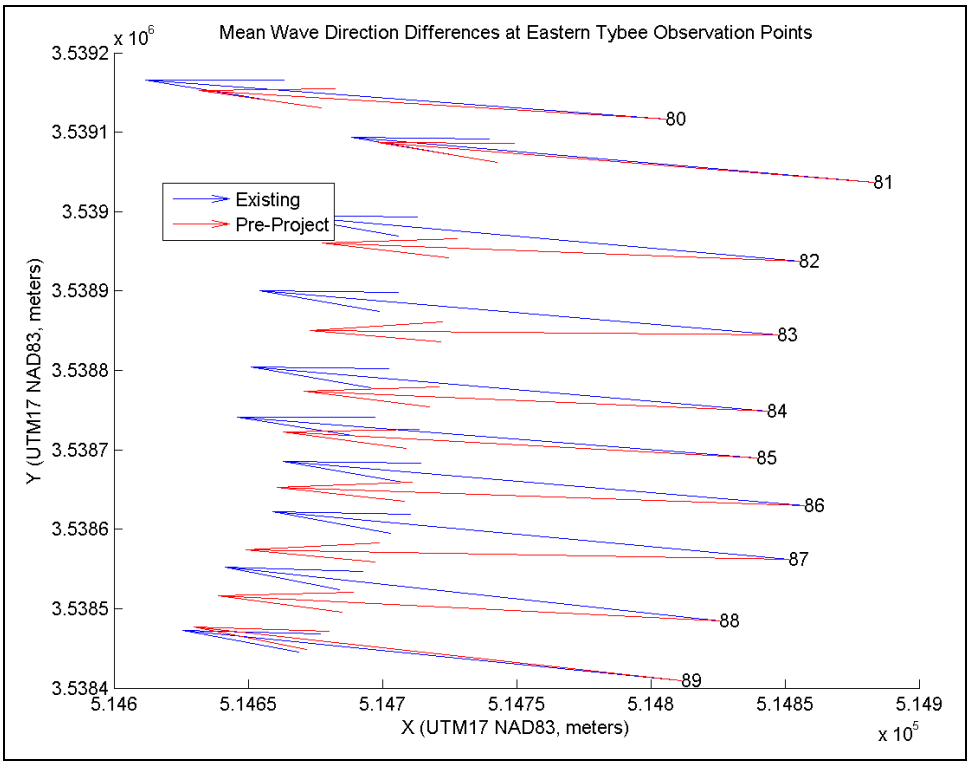

Figure 4-22: Vectors of mean wave height direction at the eastern Tybee observation points for 9–22 September 1989 (hypothetical retracked Hurricane Hugo).

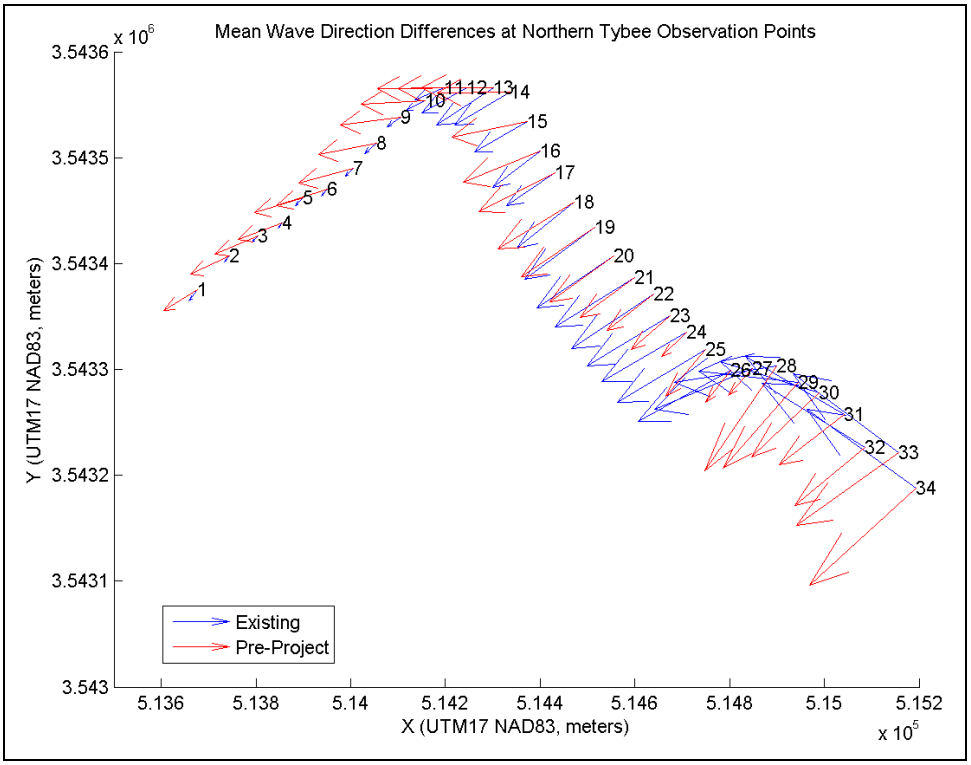

Figure 4-23: Vectors of mean wave direction at the northern Tybee observation points for 1–30 November 1979.

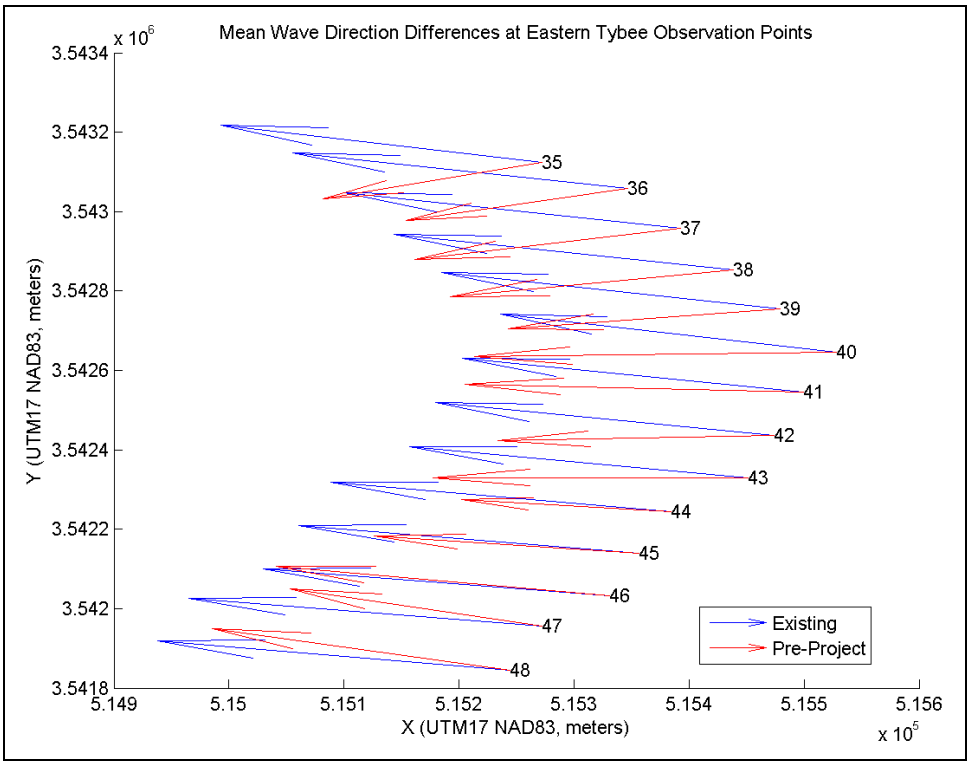

Figure 4-24: Vectors of mean wave direction at the eastern Tybee observation points for 1–30 November 1979.

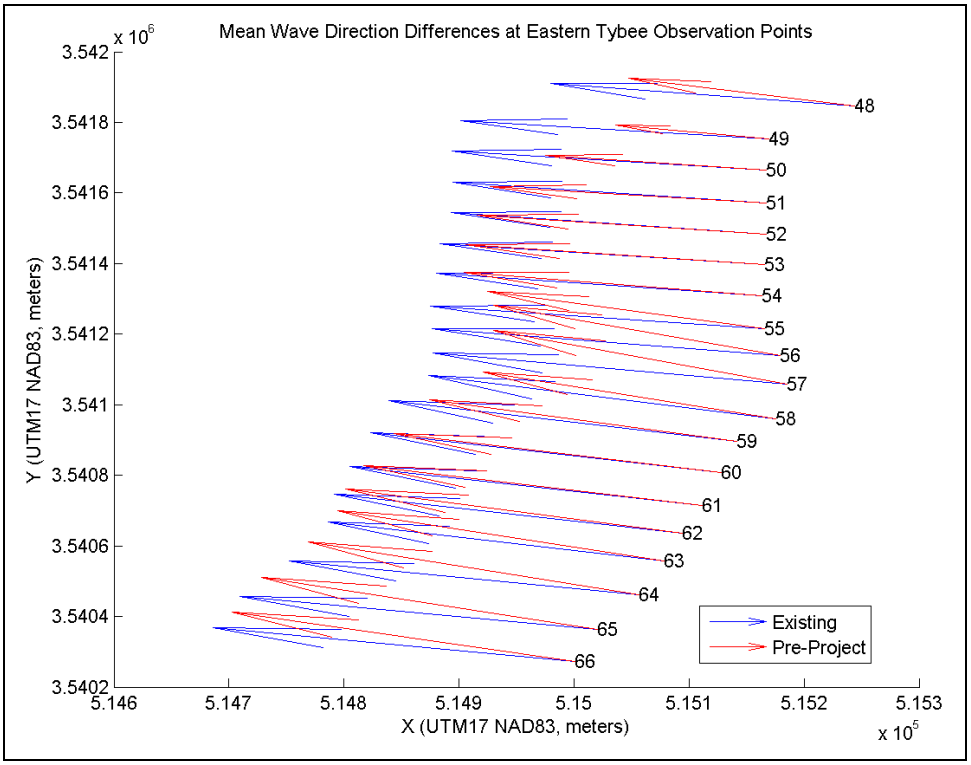

Figure 4-25: Vectors of mean wave direction at the eastern Tybee observation points for 1–30 November 1979.

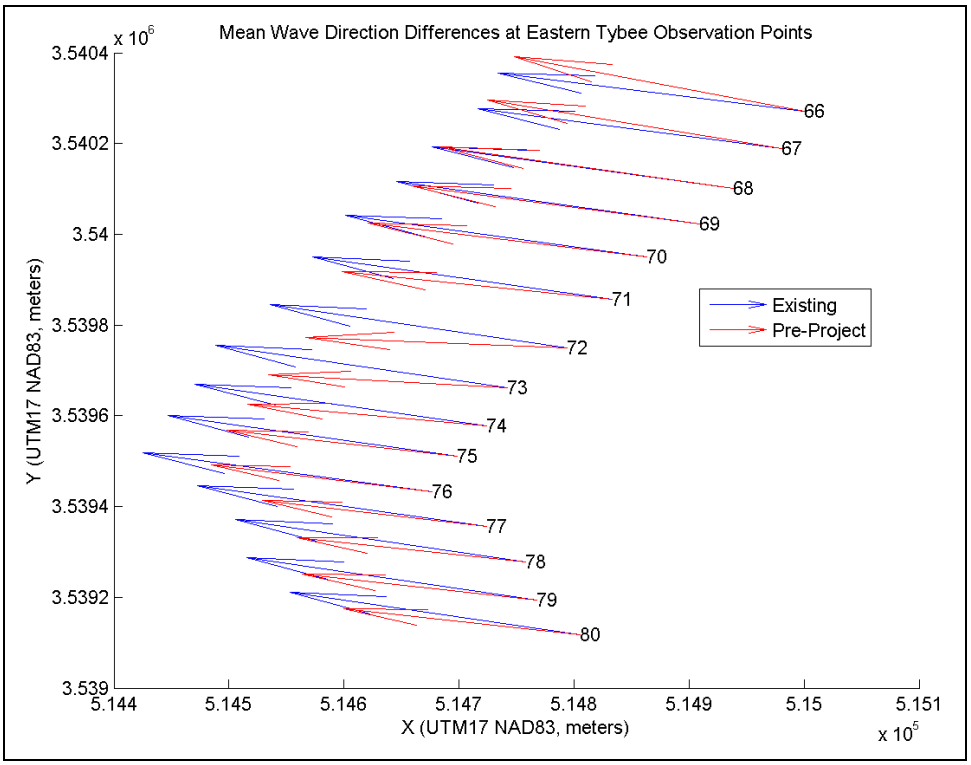

Figure 4-26: Vectors of mean wave direction at the eastern Tybee observation points for 1–30 November 1979.

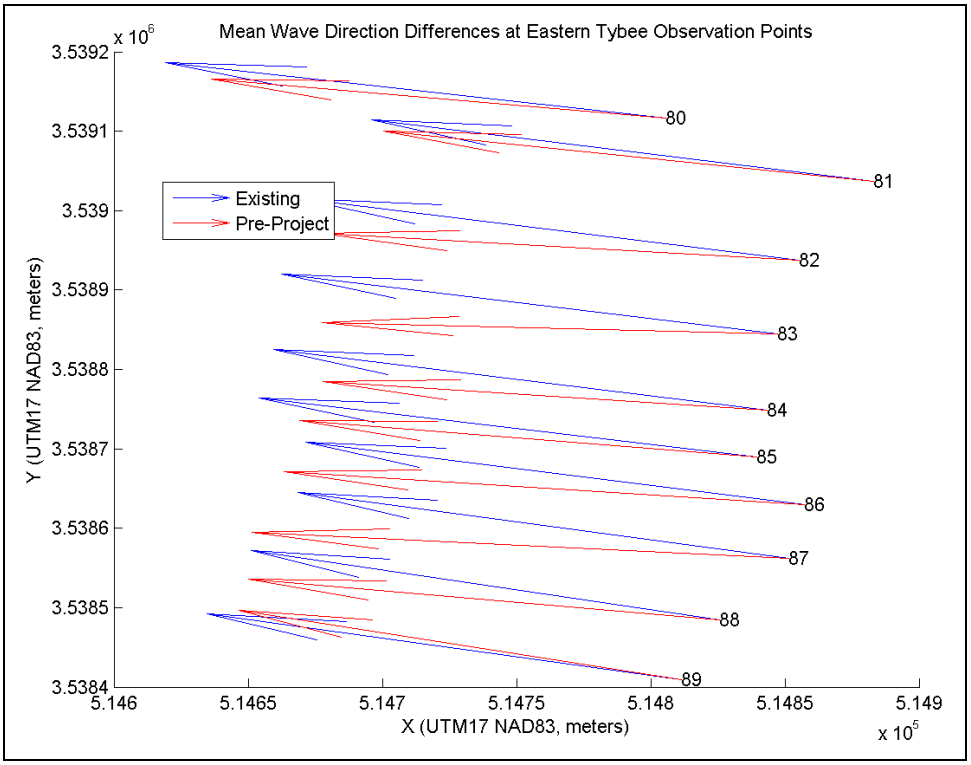

Figure 4-27: Vectors of mean wave direction at the eastern Tybee observation points for 1–30 November 1979.

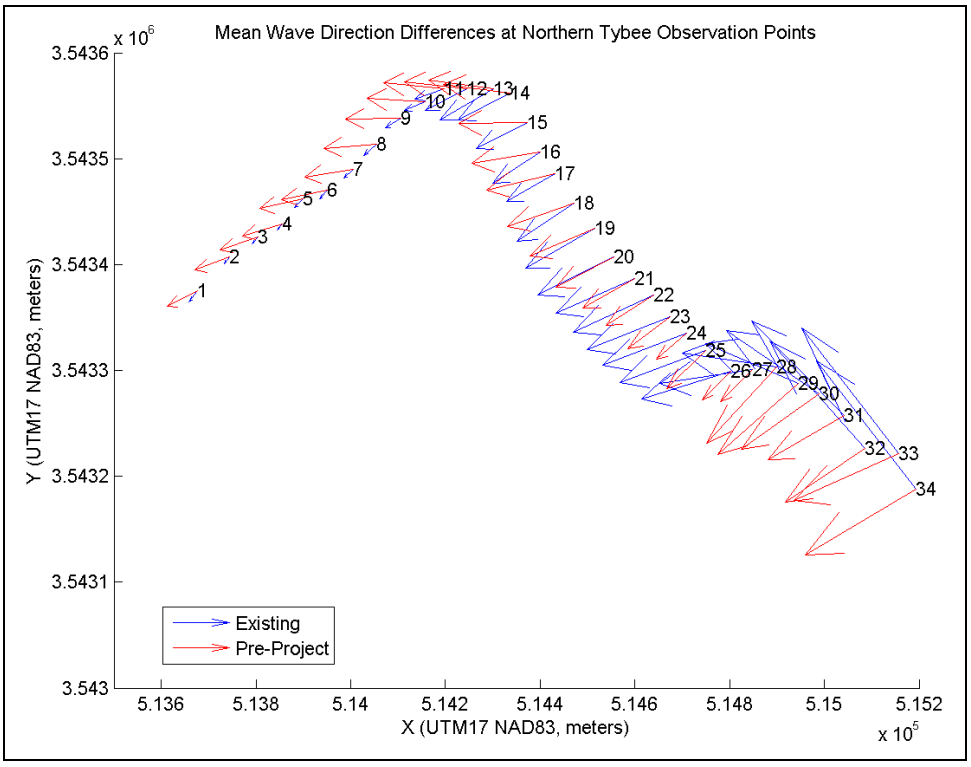

Figure 4-28: Vectors of mean wave height direction at the northern Tybee observation points for 1–31 July 1999.

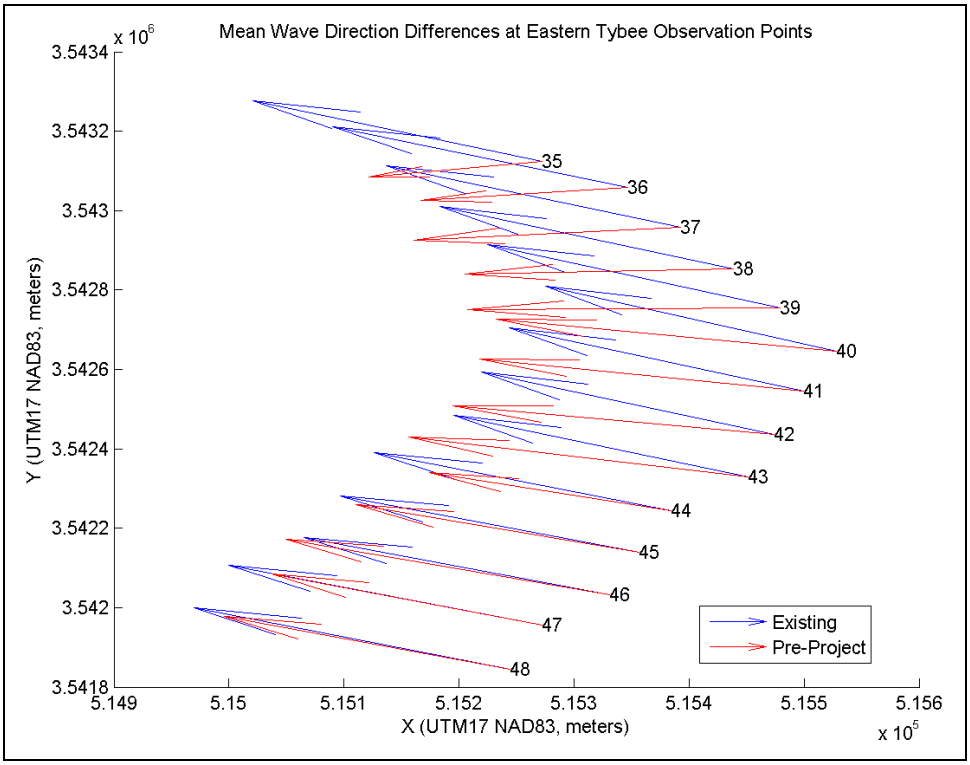

Figure 4-29: Vectors of mean wave height direction at the eastern Tybee observation points for 1–31 July 1999.

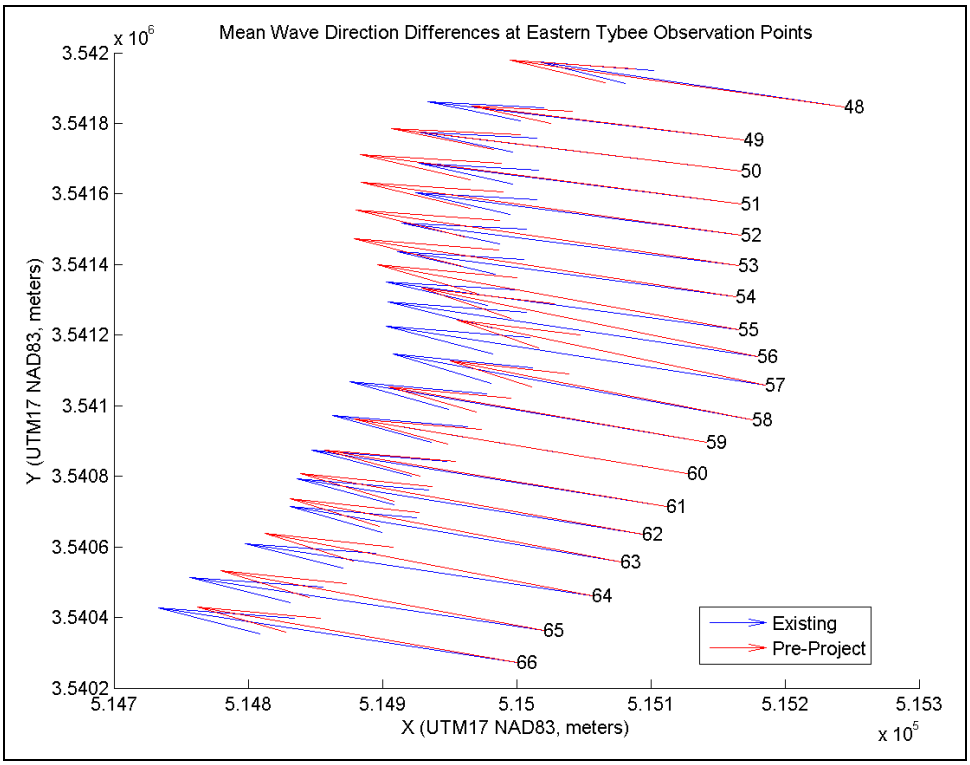

Figure 4-30: Vectors of mean wave height direction at the eastern Tybee observation points for 1–31 July 1999.

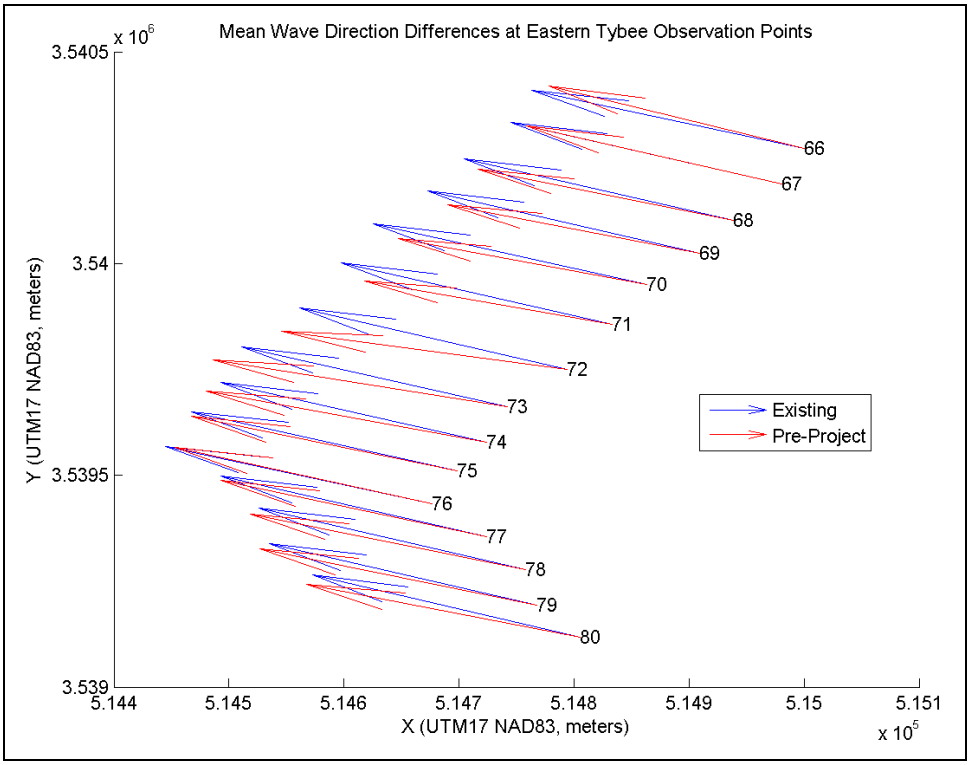

Figure 4-31: Vectors of mean wave height direction at the eastern Tybee observation points for 1–31 July 1999.

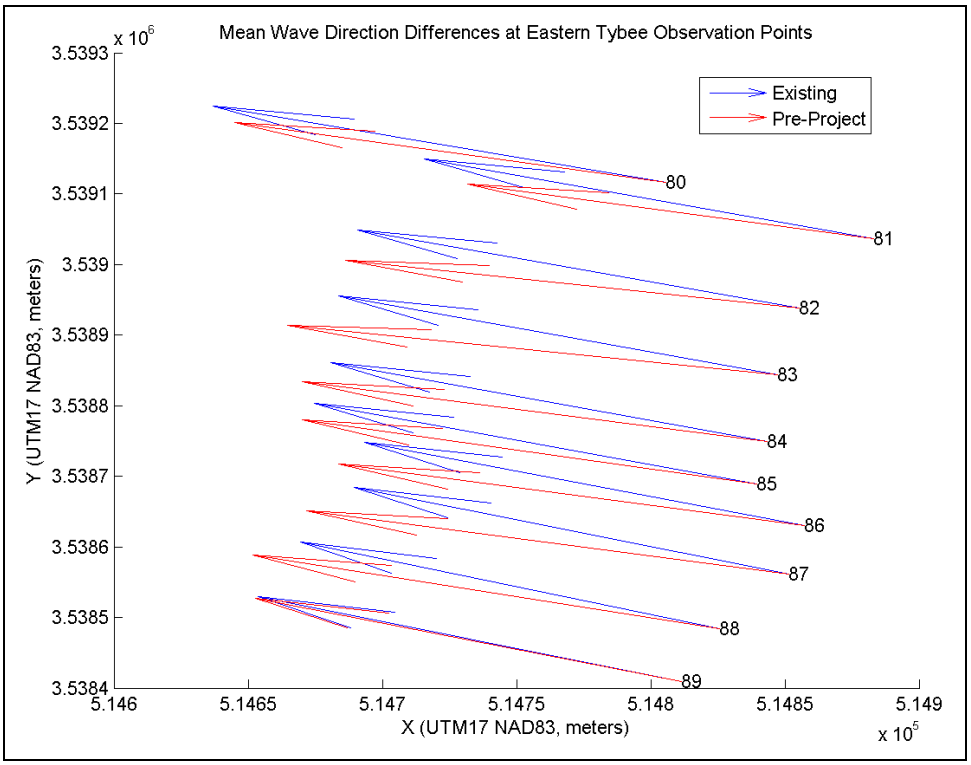

Figure 4-32: Vectors of mean wave height direction at the eastern Tybee observation points for 1–31 July 1999.

5 Sediment Transport Modeling

This chapter describes modeling efforts to estimate sediment transport rates and the changes in transport rates and patterns due to historical improvements to the Savannah navigation channel, including channel deepening and construction of the jetties and the offshore breakwater (see Figure 1-1). The simulations of sediment transport described in this chapter rely on the estimated environmental conditions at the site, specifically the ADCIRC circulation simulations (Chapter 3) and STWAVE wave simulations (Chapter 4). The first part of this section describes GTRAN (Jensen et al. 2002) simulations of sediment transport patterns over the entire nearshore. The second part analyzes the patterns of the existing conditions and pre-project model runs for potential changes in sediment transport patterns.

Nearshore sediment transport model

To estimate the transport in the nearshore, predictive techniques are applied with available knowledge of the environmental conditions and sediment properties. The sediment transport model GTRAN applied currents, water levels, and waves calculated by ADCIRC and STWAVE to predict transport magnitudes and pathways in the study area. GTRAN is a point model, which estimates potential transport and does not solve continuity of mass, i.e., it is a local transport model and it assumes unlimited sediment is available. GTRAN includes effects of waves and current on transport of non-cohesive sediment. Tidal-, wind-, and wave-generated circulation and wave parameters are provided to GTRAN through the external simulations with ADCIRC and STWAVE. Sediment properties of the bed in the study area were determined from information available from USACE, NOAA, the Skidaway Institute, and others. These data sources are discussed in more detail in Smith et al. (2006). From input hydrodynamic, wave, and sediment bed conditions, GTRAN calculates sediment transport through a collection of sediment transport methods. A detailed description of the GTRAN sediment transport methods, including sediment transport equations, is provided in Appendix A.

To calculate sediment transport, simplifying assumptions and representations of the natural processes are applied. Making such approximations is standard practice in the field of numerical modeling and is not unique to

sediment transport models. The following discussion of the approximations used for estimating transport rates is limited to general descriptions of the approximations applied.

Wave-generated current and transport

ADCIRC simulations included currents driven by the tide, wind, waves, and river. Wave-generated currents (longshore currents and undertow) and asymmetry in the wave orbital motions are a significant or dominant factor in nearshore hydrodynamics at many sites and must be considered in nearshore transport studies. This section will address the treatment of wave-induced hydrodynamics included in this study and the implications of neglecting certain components of the hydrodynamic forcing on GTRAN model results.

Longshore current

Longshore transport is defined as the quantity of nearshore sediment transport generated along the coast by breaking waves and the associated longshore currents. At Savannah, the shore parallel tidal and wind-driven currents augment this transport. The distinction between transport in the nearshore region and offshore (deep water) region is primarily in the transport processes of the two regions. For sediment transport in the offshore zone, waves produce additional bottom shear stresses and increase turbulence that suspends sediment near the bottom. Surface waves contribute little to transport direction. Ocean circulation currents transport the suspended sediment (and sediment near the bed). In the most general terms, the waves act as a stirring mechanism, and the currents transport the sediment. In the case of nearshore transport, breaking waves also impart an increased shear stress and turbulence on the bottom sediments. In addition, breaking waves exert a stress that generates longshore currents and transport along with tidal and wind-driven currents. Depth-averaged wave-generated longshore currents are included in the ADCIRC simulation through forcing by gradients in radiation stresses calculated by STWAVE (see Chapters 3 and 4).

Undertow

In addition to longshore currents, waves generate an offshore-directed current or “undertow” near the bottom to balance the shoreward mass flux that occurs above wave troughs. Undertow is a primary factor in offshore

sediment transport in the surf zone during storms (Miller et al. 1999). Undertow exists in the lower water column, influencing the sediment bed and is, therefore, a dominant mechanism for offshore sediment transport during large wave events.

A simple estimation of undertow derived through mass balance was implemented in the GTRAN simulations. The undertow estimate (called stokes velocity), U_{Stokes} as described by Nielsen (1992) is:

$$U_{Stokes} = -\frac{gH^2}{8cD}$$

where:

g = gravitational acceleration
H = wave height
c = wave celerity
D = water depth

Wave asymmetry

Wave asymmetry is the imbalance of forward (onshore) and backward (offshore) components of the bottom orbital velocities resulting from the nonlinearity of surface waves in shallow water. Wave asymmetry becomes a mechanism for shoreward sediment transport primarily during milder wave conditions (when undertow is small). In deep water, waves have a sinusoidal form and generate equal backward and forward bottom velocities. As the waves approach shallow water, wave crests become short and steep, while the troughs become long and flat. Near the bottom, orbital velocities include short bursts of strong, onshore velocity under the steep wave crest and weaker, longer duration offshore velocity under the trough. These onshore bursts generally move more sand than the longer duration, lower magnitude offshore velocities. The transport methods in GTRAN include the effect of wave asymmetry on transport.

Bed sediment characteristics

In addition to the ADCIRC and STWAVE model output previously discussed, GTRAN requires bed sediment information. Areas with similar sediment qualities must be defined spatially and characterized by a median grain size diameter and sorting parameter.

The GTRAN model runs rely on sediment sample information compiled during the sediment budget analysis. The samples were collected within the navigation channel and immediately offshore of Tybee Island. Figure 5-1 provides the location of and mean grain size information for sediment samples taken by USACE, NOAA, the Skidaway Institute, and others. Mean grain sizes are given in millimeters and in phi (φ) units. The phi unit can be related to the grain size using Equation 5-1 below.

$$\varphi = -\log_2(d) \tag{5-1}$$

Conversely, the grain size (d) in millimeters can be determined from phi units using Equation 5-2.

$$d = 2^{-\varphi} \tag{5-2}$$

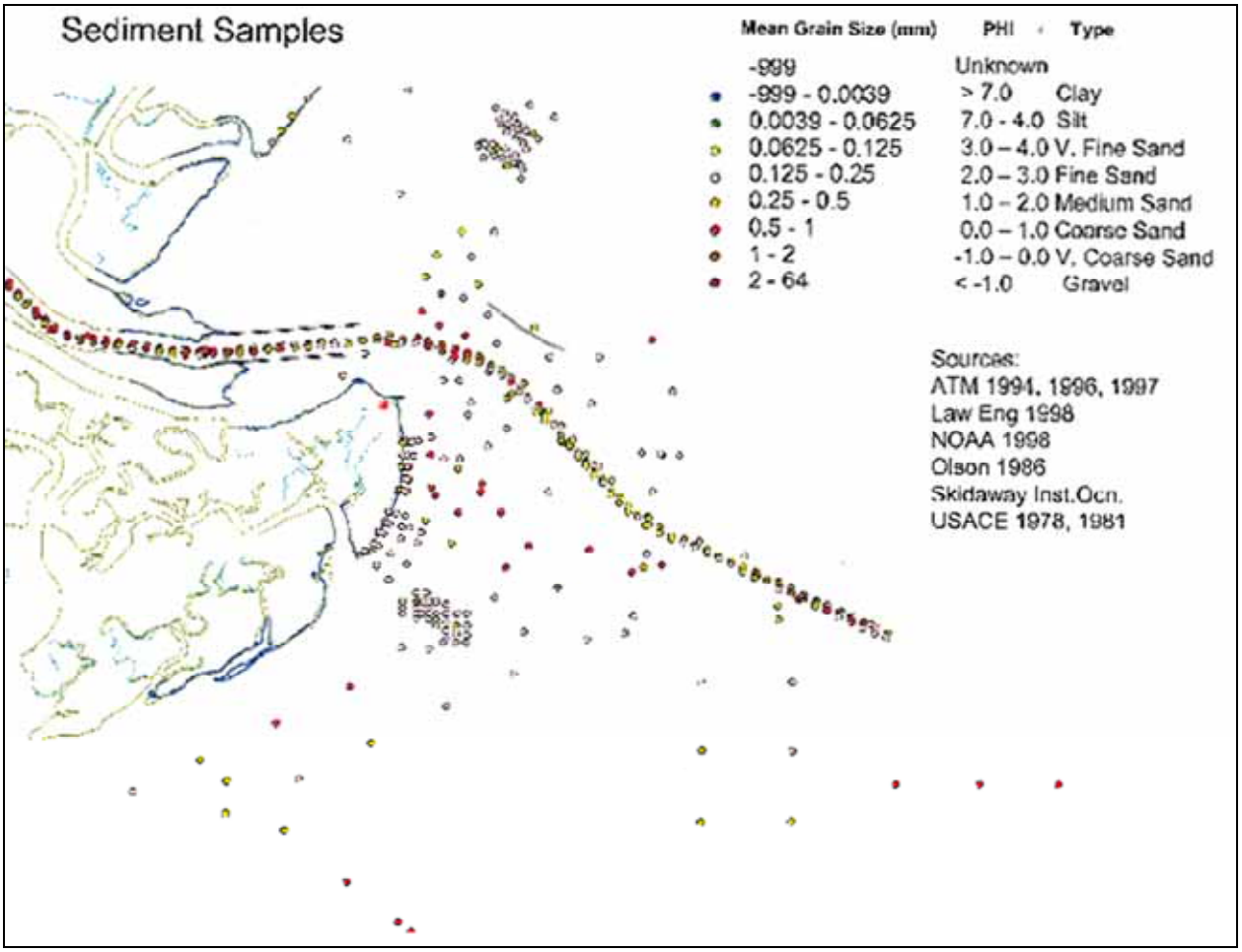

Figure 5-1. Locations and mean grain sizes of sediment samples taken within and around the Federal navigation channel and Tybee Island.

Another sediment quality required to generate a grain size distribution is the sediment sorting. The sorting of a sediment sample refers to the range of grain sizes present. A perfectly sorted sample contains sediment of a uniform diameter, while a poorly sorted sample contains widely varying sizes.

In order to incorporate the available data and best represent the sediment transport pathways in the study area, a spatially uniform mean grain size of 0.2 mm (2.25 phi) was selected to characterize the area's bed sediment. The sediment was also selected as moderately to poorly sorted, with a sorting parameter of 1.0. Figure 5-2 provides the grain size distribution generated from the selected sediment parameters.

Figure 5-2. Grain size distribution of spatially uniform bed characteristics for GTRAN modeling.

Sediment transport patterns

GTRAN is a point model, and it requires X, Y, and Z coordinates for each location where sediment transport is to be calculated. The computational domain of the model was defined by 339 discrete points whose primary emphasis was on capturing the Tybee nearshore, the Tybee Island shelf, and the navigation channel. Secondary emphasis was placed on the Daufuskie/Turtle Island shelf and the breakwater lee shoal. The Calibogue Sound channel and Barrett Shoals areas received the fewest number of GTRAN points. Figure 5-3 illustrates the calculation locations selected for this study.

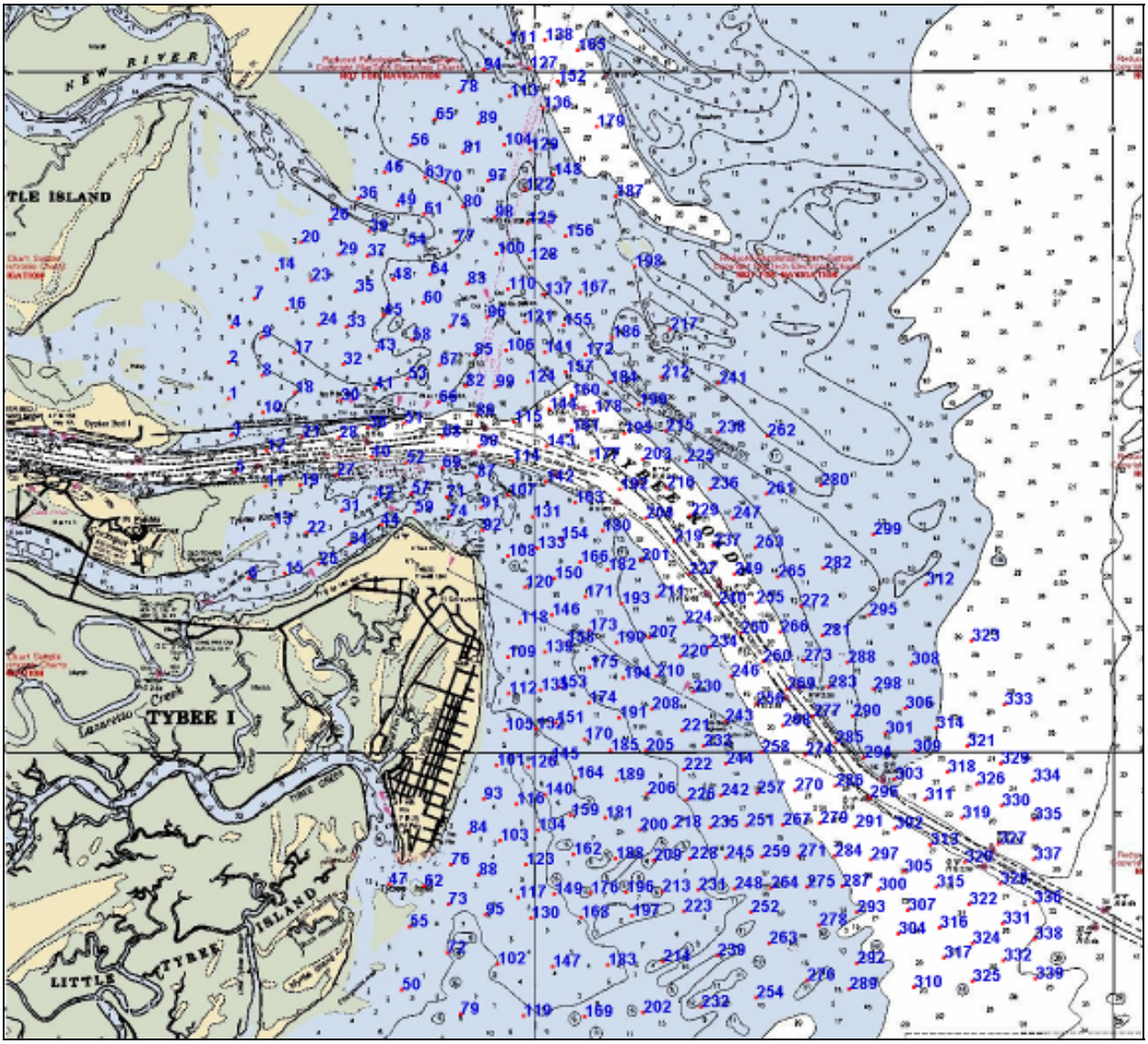

Figure 5-3. GTRAN calculation locations.

Three distinct time periods were modeled in ADCIRC and STWAVE prior to the GTRAN modeling. Two of the time periods, November 1979 and July 1999, were month-long simulations, while September 1989 represented only eight days surrounding a retracked Hurricane Hugo simulation. All of these time periods were modeled with the existing bathymetry and the pre-project bathymetry.

Cumulative sediment transport vectors (representing the integral of the point transport over the simulation period) at the calculation points are presented in Figures 5-5 through 5-10 in this section and rose plots (directional distribution of transport) are presented in Appendix B. The cumulative sediment transport vectors for each modeling scenario are plotted on a background of the corresponding bathymetry. The bathymetry changes discussed in Chapter 2 should also be considered for a more complete picture of the transport processes. The reader should pay special attention to the vector scale for each simulation period, as the scales vary between plots. The scale is based on the maximum cumulative sediment transport for each specific simulation. Therefore, the scale for the November 1979 simulation is different than the scale for the September 1989 simulation. The discussion of cumulative sediment transport vector patterns will reference the sediment budget cell designations as presented in Chapter 2 and Figure 5-4. The orange dots in Figure 5-4 correspond to the GTRAN calculation points.

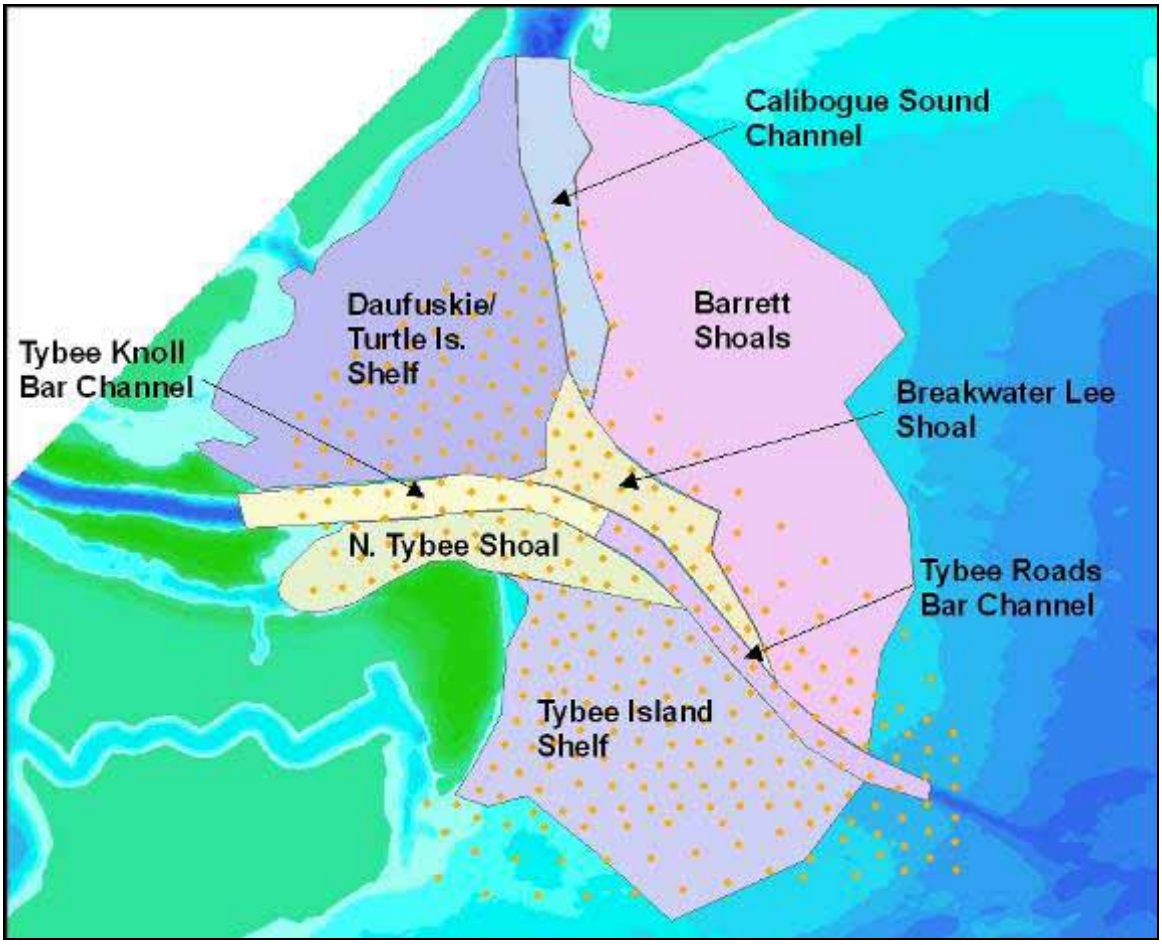

Figure 5-4. Summary of regions used in Table 5-1.

November 1979

Cumulative potential sediment transport (integral of point sediment fluxes over the month) in the existing condition November 1979 simulation is characterized by ebb dominated transport within the Tybee Knoll and Tybee Roads Bar Channels (Figure 5-5). The largest cumulative sediment transport magnitude is approximately 270 m^3/m (2,900 ft^3/ft) and is located within the navigation channel at calculation point 68. The five largest cumulative sediment transport magnitudes and six of the seven points of more than 100 m^3/m (1080 ft^3/ft) are located within the navigation channel. None of the remaining areas can be characterized by a single transport direction. Transport within the western portion of the Tybee Island shelf is largely directed onshore and in the northern portion of the cell the transport is to the northwest. There is more variability in the net transport direction closer to the channel and along the southern shelf boundary. Offshore transport is seen on the offshore boundary of the Tybee Island shelf. Net transport within the eastern half of the north

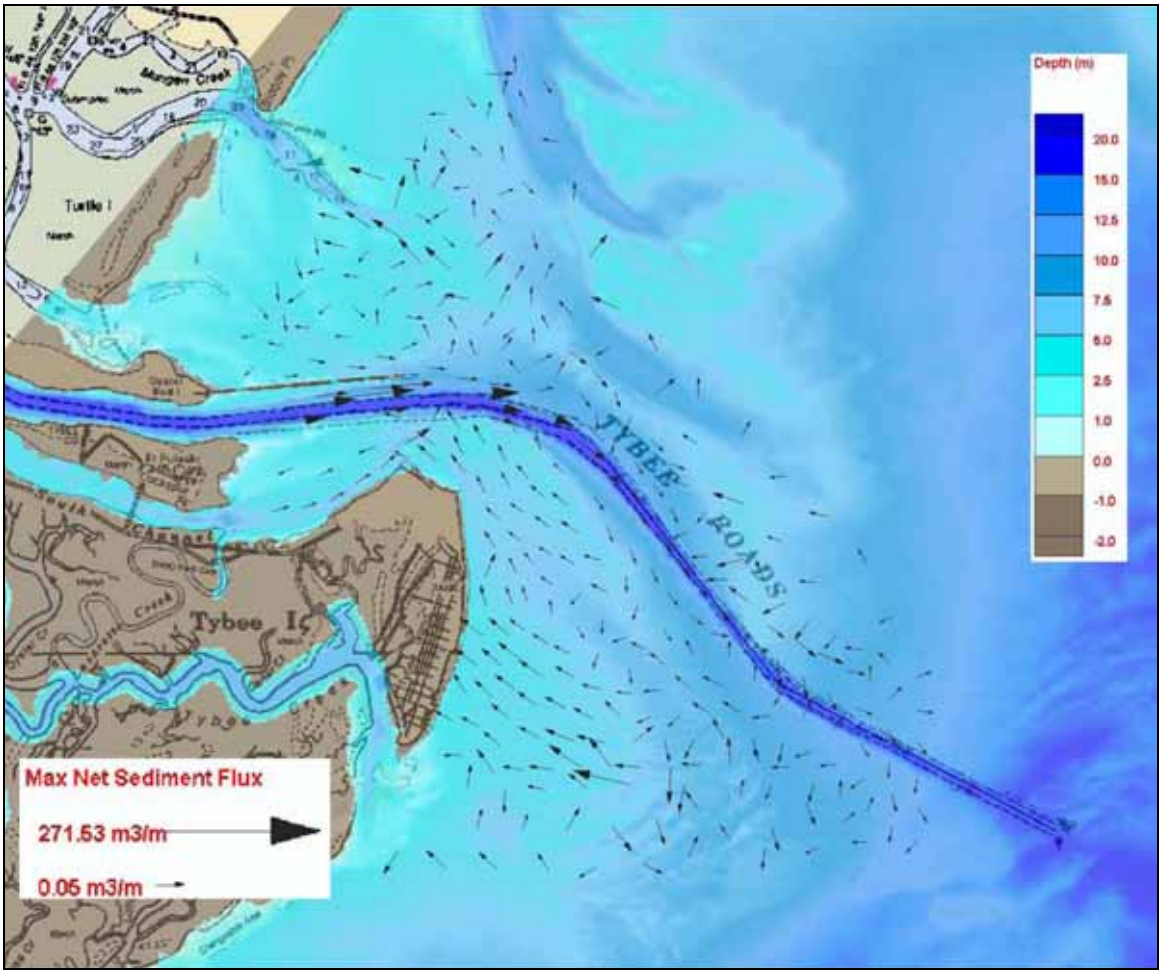

Figure 5-5. Cumulative potential sediment transport vectors for November 1979 existing conditions GTRAN simulation.

Tybee shoal area is uniformly directed toward the northwest, while transport in the western half is directed both towards the Tybee Knoll Bar Channel (northeast) and the South Channel (southwest). Transport within the Daufuskie/Turtle Island shelf just offshore from the New River channel is flood dominated, and transport within the Breakwater Lee Shoal area enters the area on the north and east and exits into the channel. Transport on the southern end of Barrett Shoals is directed toward the channel and offshore.

Cumulative sediment transport patterns in the November 1979 pre-project simulation are similar to the existing condition in that offshore transport is dominant in the channels (which were shallower and broader than the existing condition) and onshore transport is dominant on the shoals

(Figure 5-6). However, the magnitudes of the cumulative transport are more balanced than in the existing condition, where transport rates were significantly larger in the main channel. The largest cumulative sediment transport magnitude is 360 m^3/m (3,880 ft^3/ft) and is located on the western edge of Barrett Shoals near the Calibogue Sound channel (calculation point number 179). An area where the transport patterns differ from the existing condition is the eastern part of the north Tybee shoal and the northern part of the Tybee Island shelf. In the existing condition, transport is to the northwest, directed toward the Tybee Knoll channel. In the pre-project condition, transport patterns show a clockwise circulation around the northern edge of the shelf and feeding back onto the shelf. Transport within the offshore portion of Tybee Roads is directed to the offshore portions of the Tybee Island shelf, and there is somewhat more of the trend towards transport along the southeast edge of the Tybee Island shelf (less offshore), than in the existing condition.

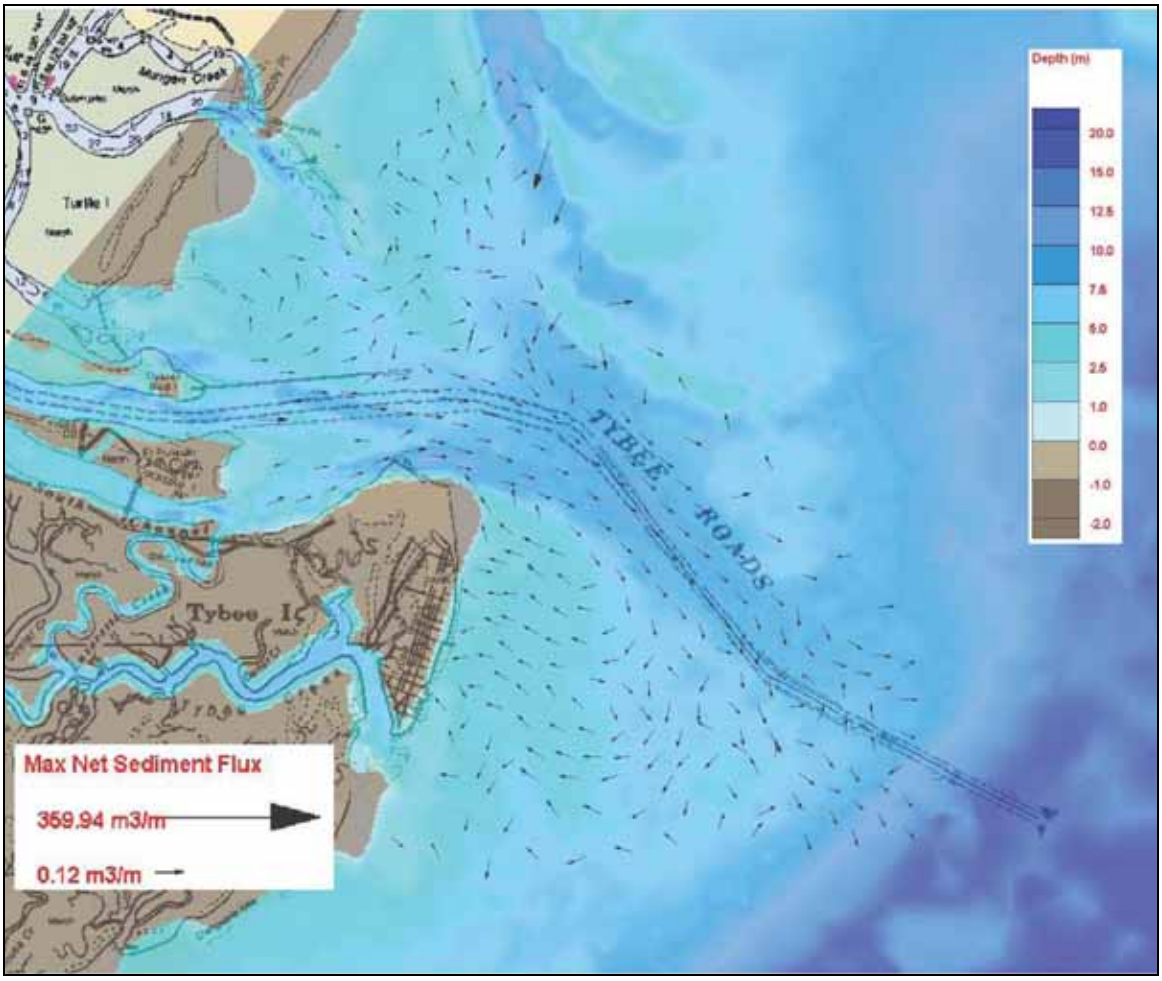

Figure 5-6. Cumulative potential sediment transport vectors for November 1979 pre-project GTRAN simulation.

Figures B-1 through B-8 provide the sediment transport rose plots. Rose plots show the full distribution of transport over the simulation.

September 1989

The September 1989 simulations differ from the November 1979 and July 1999 simulations. The simulation is much shorter (8 days instead of a full month) and contains a single, very large event. With the exception of a couple of outlying points, the existing condition results of the September 1989 (retracked Hurricane Hugo) simulation are like November 1979 in that the largest cumulative sediment transport magnitudes (195 to 75 m^3/m (2,100 to 810 ft^3/ft)) are located within the navigation channel. More specifically, the Tybee Knoll Bar Channel and Tybee Roads Bar Channel areas are responsible for the large, ebb-directed cumulative transport magnitudes (Figure 5-7). Unlike the November 1979 results, transport on the eastern half of the north Tybee shoal is not uniform, it is directed both offshore (southeast) and onshore (west northwest). In addition, most of the transport within the Tybee Island shelf is directed away from Tybee Island via a pathway that first follows the navigation channel offshore and then curves to the southeast, along Little Tybee Island.

The pre-project cumulative transport vectors for September 1989 are similar to those from the existing in that there is a general trend towards moving more sediment away from Tybee Island (Figure 5-8). However, transport on the north Tybee shoal (25.5 m^3/m (274 ft^3/ft) average) is larger in magnitude than the existing September 1989 (8.7 m^3/m (94 ft^3/ft) average) and is more uniformly directed offshore. Other than transport on the northeast Tybee shoreline pushing sediment onshore and toward the north Tybee shoal, transport on the Tybee Island shelf is offshore and to the south. The largest magnitudes of cumulative sediment transport are more scattered than the existing condition and occur in the north Tybee shoal (84 m^3/m (900 ft^3/ft)), Tybee Knoll (113 m^3/m (1,200 ft^3/ft)) and Tybee Roads Bar Channels (60 m^3/m (650 ft^3/ft)), Breakwater Lee Shoal (57 m^3/m (610 ft^3/ft)), and Barrett Shoals (140 m^3/m (1,500 ft^3/ft)) areas.

Figures B-9 through B-16 provide the sediment transport rose plots for September 1989.

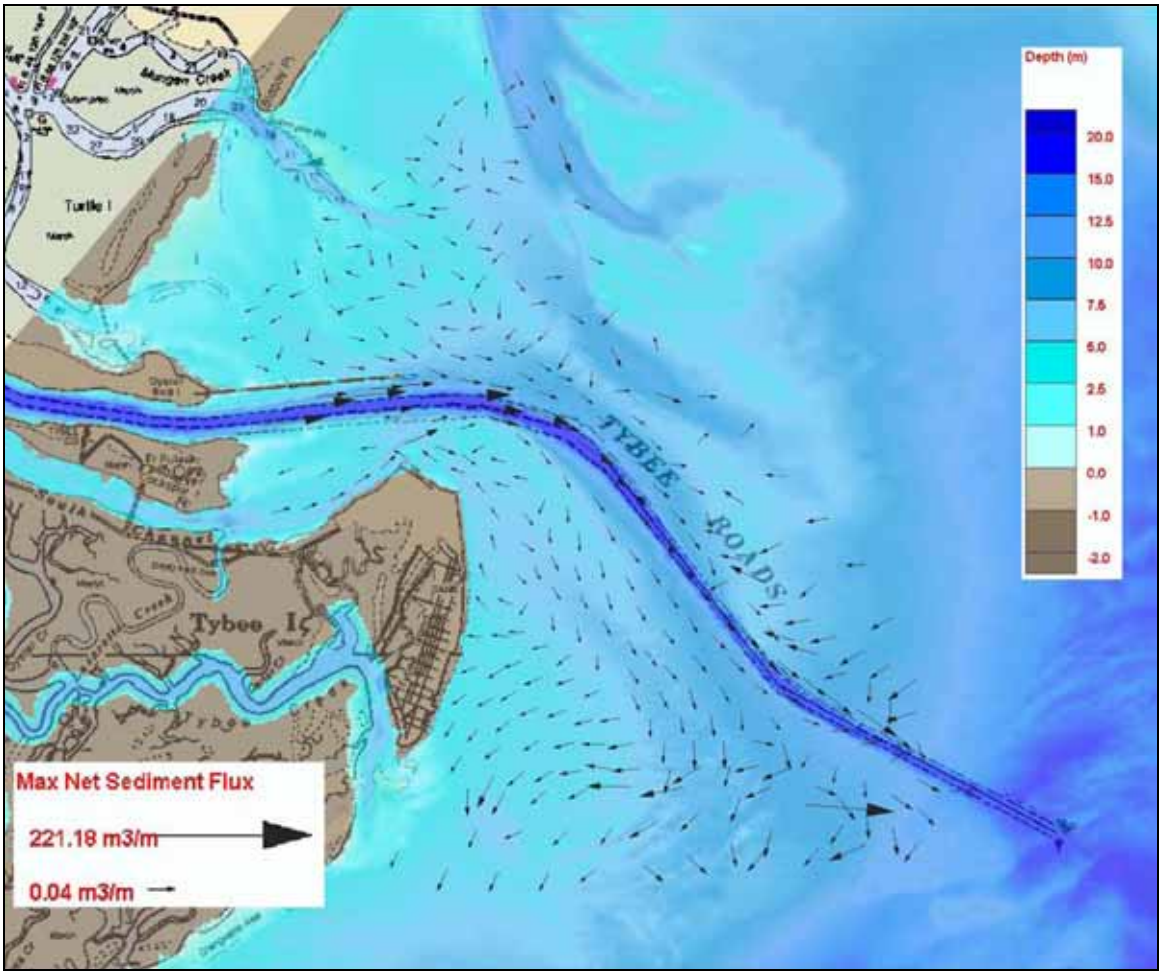

Figure 5-7. Cumulative potential sediment transport vectors for September 1989 (Hugo) existing conditions GTRAN simulation.

July 1999

Like the November 1979 and September 1989 existing simulations, the July 1999 existing results show that the largest magnitudes (300 to 85 m^3/m (3,200 to 910 ft^3/ft)) of cumulative transport are within the navigation channel and ebb-directed (offshore). However, the remaining areas are unlike the previous two existing simulations in that there is little variability in the average transport direction. Outside of the navigation channel the transport is almost uniformly directed onshore and to the northwest (Figure 5-9). Transport convergence can be seen where the South Channel (northeast directed transport) and north Tybee shoal meet (northwest directed transport), resulting the growth of the shoal and filling of the channel.

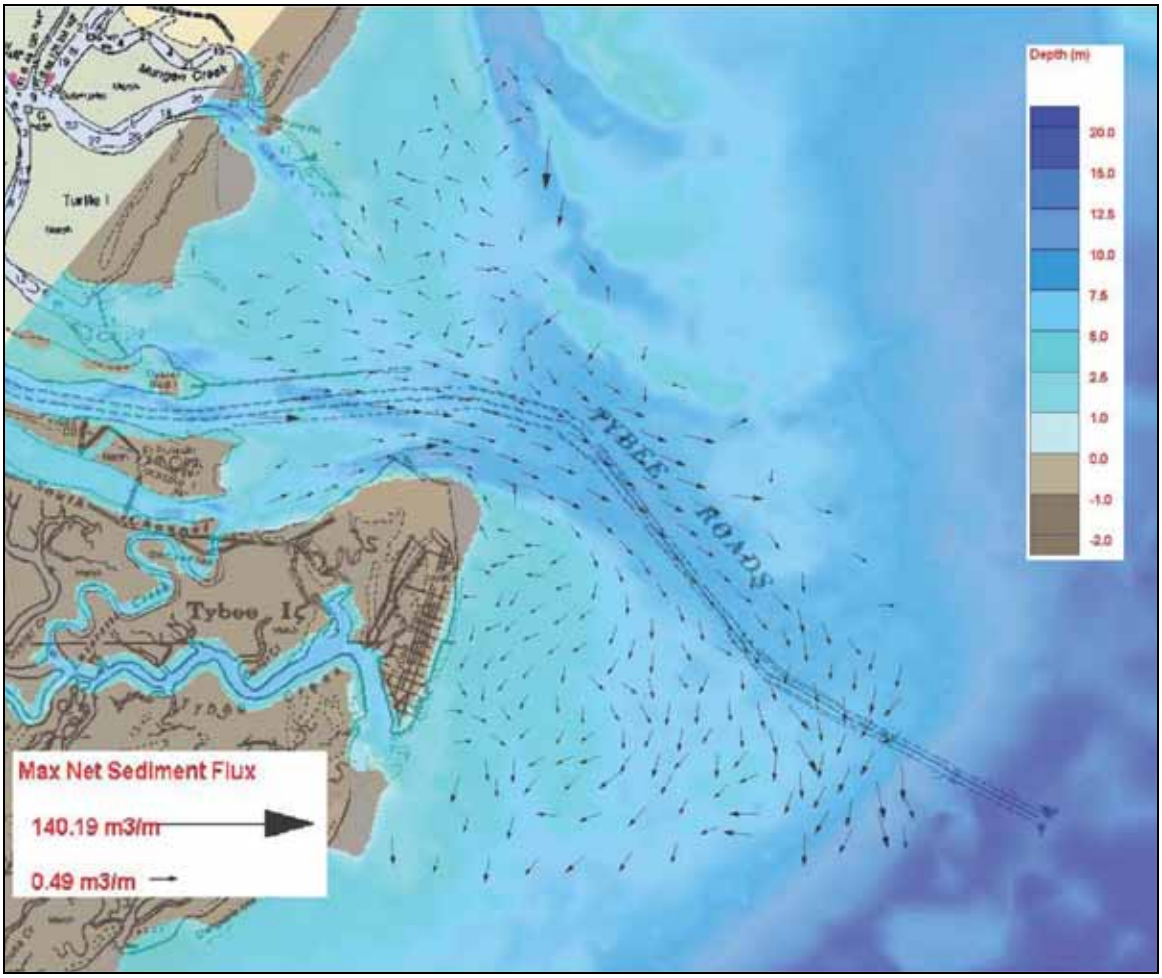

Figure 5-8. Cumulative potential sediment transport vectors for September 1989 (Hugo) pre-project GTRAN simulation.

The pre-project July 1999 simulation resulted in lower cumulative sediment transport magnitudes across the entire domain. The largest magnitudes (207 to 40 m^3/m (2,200 to 430 ft^3/ft)) were found along the southern edge of the Tybee Knoll Bar Channel area and the northern edge of the north Tybee shoal area. The prevailing transport direction was still onshore and to the northwest; however, there were small areas where this was not the case (Figure 5-10). The Tybee Knoll Bar Channel and the north Tybee shoal were both directed primarily offshore. Similar to the existing simulation, there is a convergence of transport where the South Channel and northern Tybee Island shelf meet (although further to the east than in the existing condition). This shoaling area correlates to sediment accumulation in the bathymetry change figure (Chapter 2).

Figures B-17 through B-24 provide the sediment transport rose plots for the two July 1999 simulations.

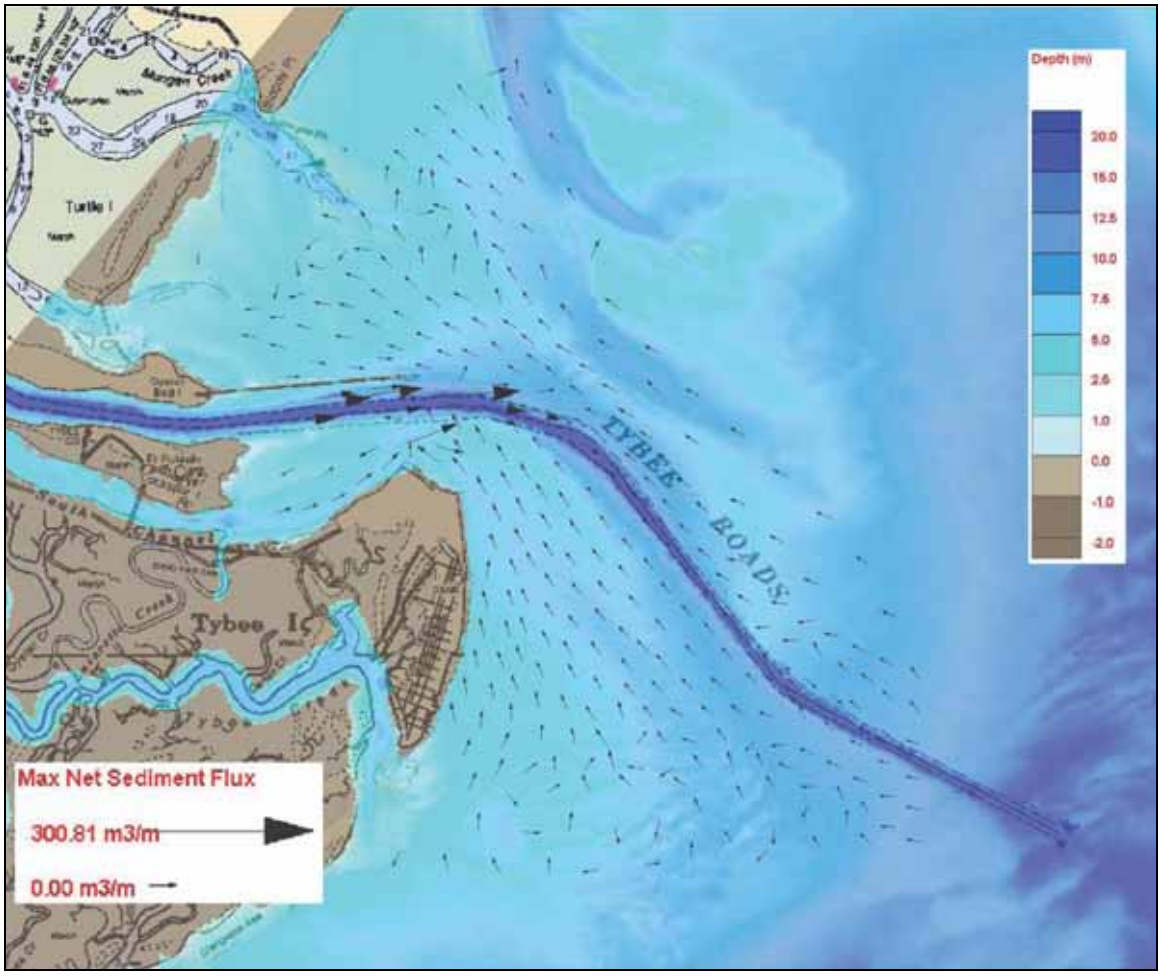

Figure 5-9. Cumulative potential sediment transport vectors for July 1999 existing conditions GTRAN simulation.

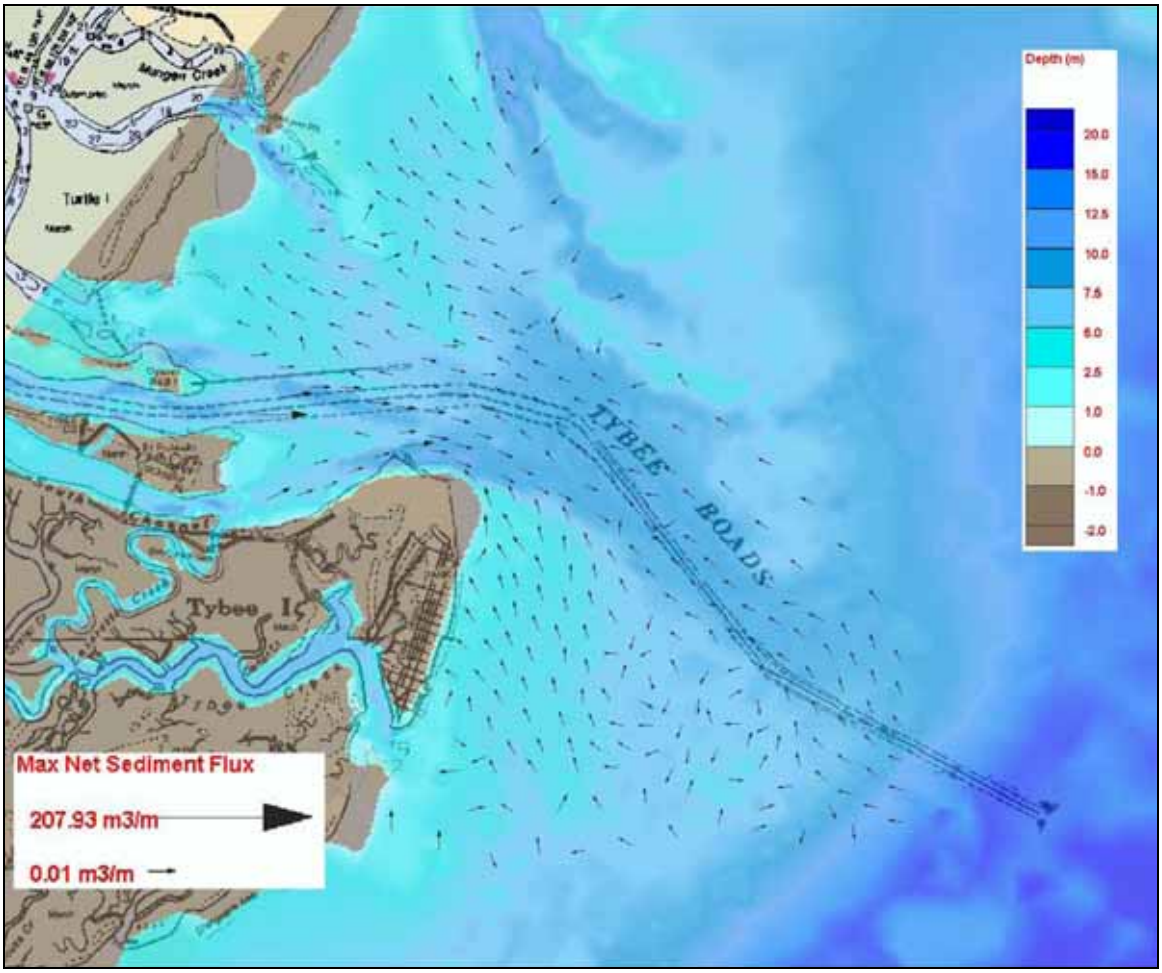

Figure 5-10. Cumulative potential sediment transport vectors for July 1999 pre-project GTRAN simulation.

Changes to sediment transport patterns

Changes in cumulative sediment transport (differences between integrals of point sediment fluxes over the simulation period) due to historic navigation improvements were determined from the differences in cumulative sediment transport from the existing condition and pre-project GTRAN model runs for each of the simulation periods. Differences were calculated by subtracting the existing conditions results from the pre-project conditions results. Figures 5-11, 5-12, and 5-13 present the changes in cumulative sediment transport vectors between the pre-project and existing conditions for November 1979, September 1989 (retracked Hurricane Hugo), and July 1999 simulations, respectively. Bathymetry change contours from the pre-project to existing model grid are used as background for the figures in the appendix. Positive values of bathymetry change reflect eroded areas and negative values represent areas of accretion. Again, the vector

scales differ for each simulation period. The transport differences are generally in the areas of bathymetry differences.

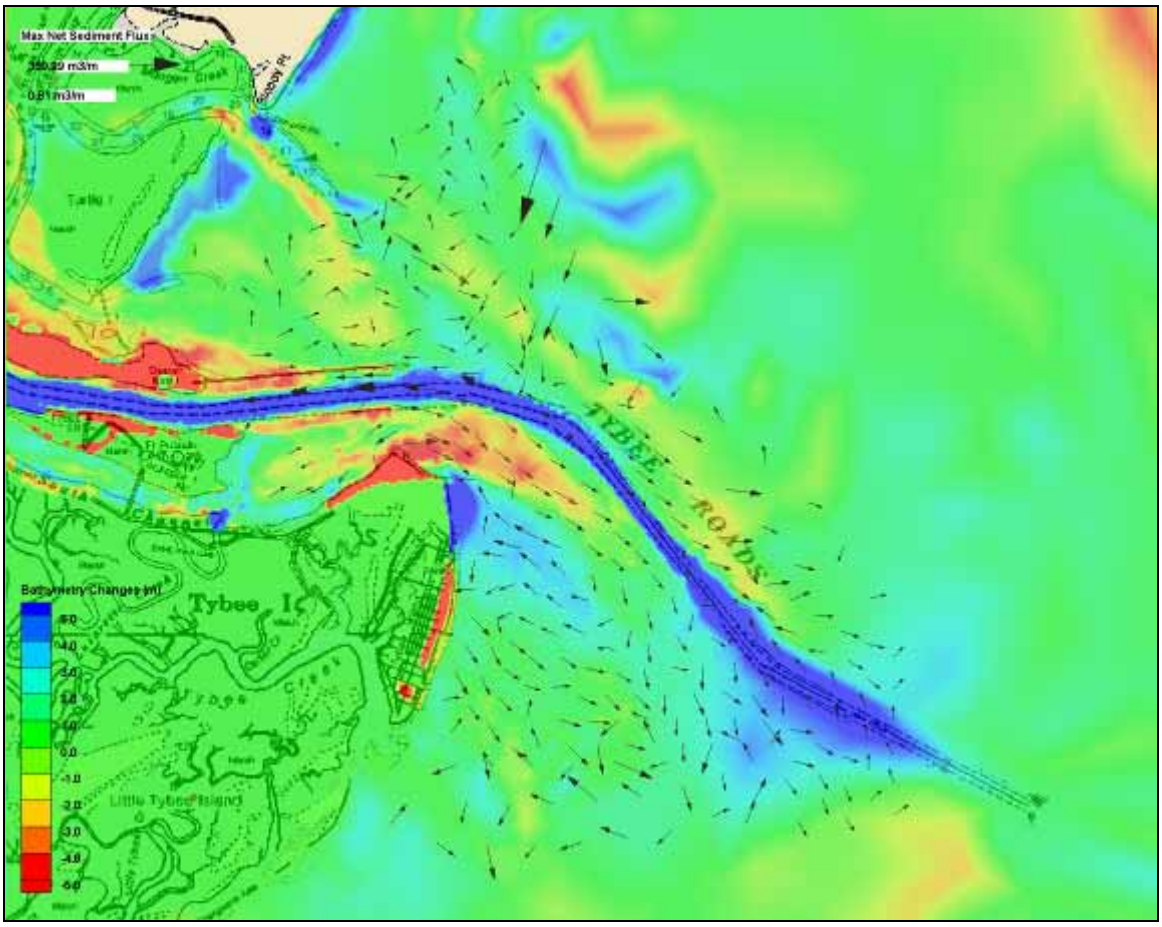

Figure 5-11. Change in cumulative sediment transport vectors (pre-project minus existing) for November 1979 GTRAN simulation.

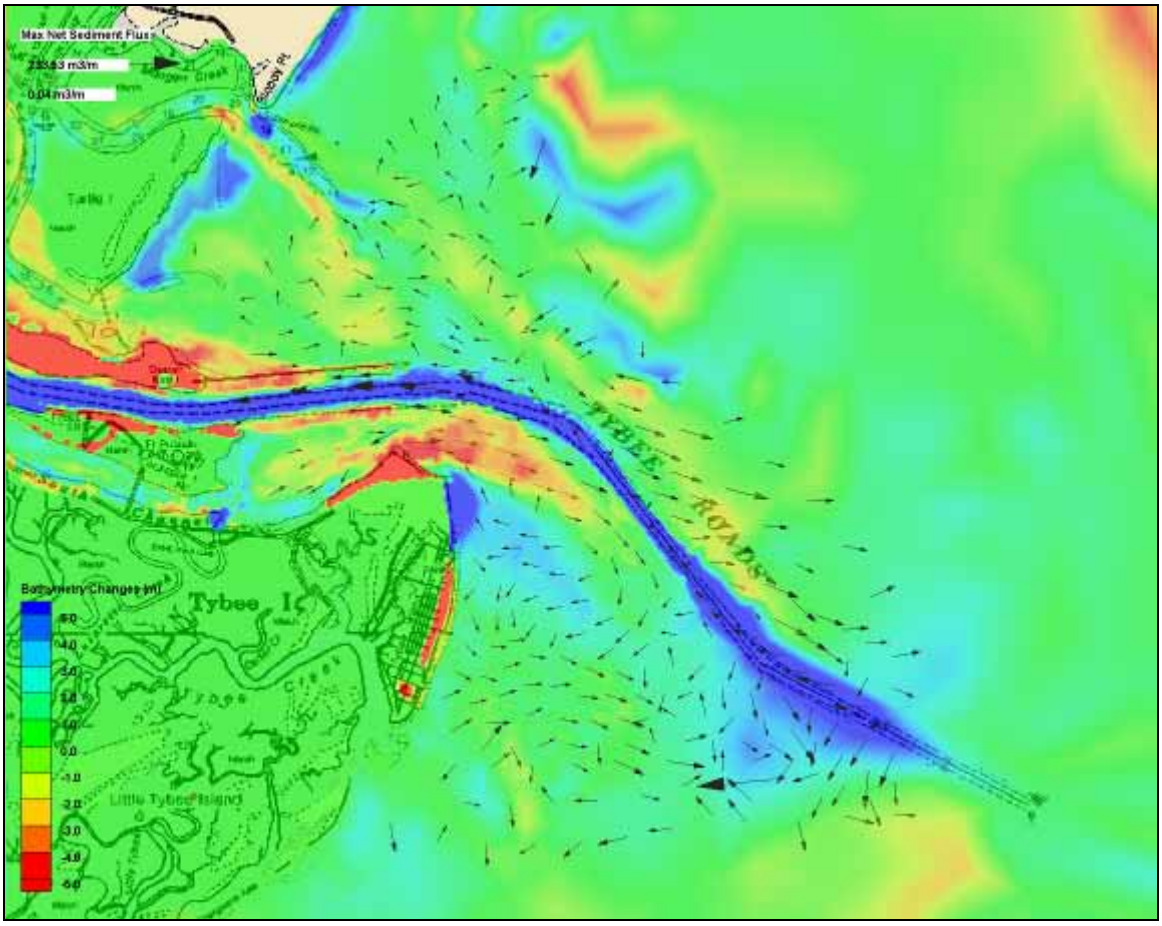

Figure 5-12. Change in cumulative sediment transport vectors (pre-project minus existing) for September 1989 GTRAN simulation.

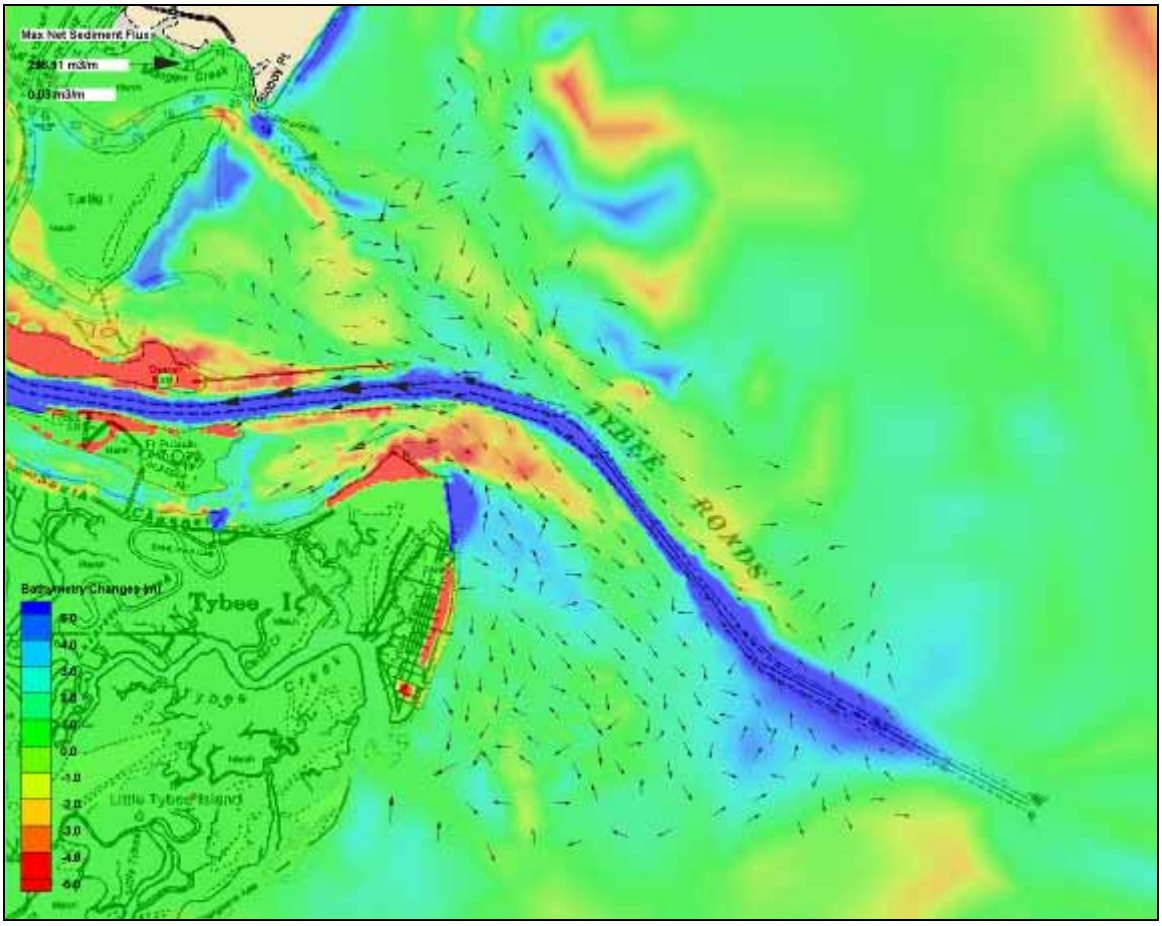

Figure 5-13. Change in cumulative sediment transport vectors (pre-project minus existing) for July 1999 GTRAN simulation.

All three of the simulation periods show widespread differences in cumulative sediment transport. Not only are the magnitudes different, but there are differences between the transport directions. Table 5-1 is useful for quickly and simply comparing the differences in cumulative transport magnitudes by sediment budget cell. The table provides the pre-project (Q_{pre}) and existing (Q_{exist}) cumulative transport magnitudes averaged (columns) over each sediment budget cell area (rows). According to these spatially averaged cumulative magnitudes, transport decreased during relatively stormy conditions (Nov. 1979 and Sept. 1989) on the Tybee Island shelf, north Tybee shoal, Breakwater Lee Shoal, Barrett Shoals, and Calibogue Sound Channel. On the contrary, transport increased on the Tybee Knoll Bar Channel, Tybee Roads Bar Channel, and the Daufuskie/ Turtle Island shelf (during Nov. 1979 only). During the relatively calm conditions of the July 1999 simulations, transport magnitudes increased in each area.

Table 5-1. Average cumulative transport rates per cell.

Location	Nov 1979		Sep 1989		Jul 1999	
	Q_{pre} (m^3/m)	Q_{exist} (m^3/m)	Q_{pre} (m^3/m)	Q_{exist} (m^3/m)	Q_{pre} (m^3/m)	Q_{exist} (m^3/m)
Tybee Island Shelf	27.69	23.91	19.28	17.54	6.64	8.38
North Tybee Shoal	21.55	17.11	25.54	8.69	15.88	24.24
Tybee Knoll Bar Channel	33.17	111.53	31.83	91.63	33.76	129.68
Tybee Roads Bar Channel	19.02	27.96	33.80	39.70	2.10	9.57
Breakwater Lee Shoal	18.16	8.76	25.04	9.83	1.84	6.77
Barrett Shoals	42.75	25.32	32.35	26.55	7.13	7.61
Calibogue Sound Channel	9.59	7.28	6.81	3.80	1.87	4.09
Daufuskie/Turtle Island Shelf	12.53	16.94	6.11	5.57	6.48	10.00
Note: Q_{pre} = sediment flux for pre-project bathymetry, Q_{exist} = sediment flux for existing bathymetry.						

All three simulation periods (Figures 5-6, 5-8, and 5-10) clearly show ebb dominant transport in the shallower and broader channels through the Tybee Knoll Bar Channel and north Tybee shoal areas of the pre-project bathymetry. In contrast, the existing conditions simulations only show uniform ebb dominance within the Federal navigation channel (Figures 5-5, 5-7, and 5-9). The areas of ebb dominance within the north Tybee shoal during pre-project simulations exhibit onshore (northwest) transport during November 1979 and July 1999 and a combination of onshore (west northwest) and offshore (southeast) during September 1989 for existing conditions. This is an important difference, in particular for the pre-project November 1979 simulation, because it contributes to a clockwise circulation around the northern edge of the Tybee Island shelf and feeding back onto the shelf. Another significant difference in the sediment transport patterns between the pre-project and existing conditions simulations occurs on Barrett Shoals, the Tybee Roads Bar Channel, and Tybee Island shelf for both November 1979 and September 1989. There is a stronger signal for transport from the offshore portions of Barrett Shoals and Tybee Roads Bar Channel onto the offshore portion of Tybee Island shelf for the pre-project simulations as opposed to the existing conditions.

Sediment transport summary

Sediment transport patterns observed by studying the GTRAN output and subsequent cumulative sediment transport plots are consistent with the observations made in the sediment budget analysis. For example, storm conditions generate significantly more transport in the Breakwater Lee Shoal area under pre-project simulations than during existing simulations. In addition, the transport convergence at the intersection of the South Channel and north Tybee shoal during the existing July 1999 simulation, and to a lesser degree during the other two existing conditions simulations, support the observed trend for the north tip of Tybee Island to migrate northward into the southern channel of the Savannah River. Finally, the overall sediment transport trends are consistent with the deflation of the northern portion of the Tybee Island shelf and the growth of the north Tybee shoal discussed in Chapter 2.

The pre-project simulations for all of the study periods tend to keep more transport within the Tybee Island Shelf and the north Tybee shoal areas than the existing simulations. This is especially evident in the north Tybee shoal during simulations with the existing bathymetry. All three existing simulations show more transport directed into the Tybee Knoll Bar Channel from the north Tybee shoal than during pre-project simulations. There is also more transport from Barrett Shoals and the Tybee Roads Bar Channel onto the offshore portions of the Tybee Island shelf during pre-project simulations than during existing conditions. The existing simulations show more material being lost to the Tybee Roads Bar Channel than during pre-project.

From Table 5-1, it is also clear that the average magnitude of transport within the Tybee Knoll and Tybee Roads Bar Channels is much higher during existing simulations than during pre-project. Under pre-project conditions, sediment is capable of moving from the Tybee Knoll Bar Channel area to the north Tybee shoal, but existing conditions create a reversal whereby sediment moves from the north Tybee shoal into the Tybee Knoll and is essentially lost to the system.

6 Impact Assessments

The Federal Navigation project at the Savannah River entrance includes construction of two jetties and an offshore breakwater and dredging of the navigation channel. The purpose of this study is to assess the impacts of the project on Tybee Island, including the beach and the Tybee shelf. This assessment was based on numerical modeling of circulation, waves, and sediment transport, and comparison of pre-project and post-project sediment budgets.

The numerical modeling focused on changes to the circulation, waves, and sediment transport based on simulations using a pre-project bathymetry from an 1854 survey and the existing bathymetry (composite from 2005–2007, with gaps filled with data from 1973–1995). The simulations included a stormy month (November 1979), a calm month (July 1999), and a hurricane (a hypothetical Hurricane Hugo retracked to hit Savannah, 14–22 September 1989). These simulations do not evolve the conditions over the past 153 years, but examine changes in the hydrodynamic and sediment patterns between the two snapshots in time.

The most significant change in the calculated circulation pattern was the increase in current speed through the navigation channel in the existing condition, as would be expected. The South Channel of the Savannah River entrance hugged the north end of the island in 1854, and there was a circulation cell that was centered on the south side of the channel (on the line between the north Tybee shoal and Tybee Island shelf sediment budget cells). This gyre would naturally circulate sediment onto the Tybee Island shelf. In the existing condition, the gyre is shifted north to the south edge of the Tybee Knolls Channels. It has the potential to push sand off the Tybee Island shelf and into the north Tybee shoal. Tidal and storm surge levels were not significantly impacted by the project. Current magnitudes tended to increase for the existing bathymetry on the north end of Tybee Island, and both increased and decreased along the rest of the island, depending on the meteorological condition and location.

Waves were simulated for the same bathymetries (1854 and 2005–2007) and the same forcing conditions as the circulation (November 1979, July 1999, and September 1989). Water levels were provided by the

circulation model. The deepening of the bathymetry along the Tybee shoreline allowed larger waves to propagate closer to shore. The maximum increase in wave heights (based on the 2 to 2.5 m contour of the pre-project bathymetry) ranged from 1.5 to 1.75 m during the peak of the retracked Hugo. The maximum increases were on the northern end of Tybee. For the retracked Hugo, the average increase in wave height was 0.5 m; for November 1979 (stormy month), the average increase was 0.25 to 0.5 m; and there was no increase in the mean wave heights for July 1999 (fair weather month). Storm waves tended to increase in the nearshore at Tybee due to increased depth along the shelf and due to focusing on the north Tybee shoal for the existing condition bathymetry relative to the pre-project condition.

The simulated waves, currents, and water levels were used to estimate point sediment transport for the 1854 and 2005–2007 bathymetry and the three simulation periods. Point sediment transport estimates were integrated over the simulation periods to give cumulative transport rates over 339 calculation points and averaged over each of the sediment budget cells. Calculated potential transport increased in the channel for the existing condition (compared to pre-project), as expected from the circulation pattern. Also, the transport pattern on the North Tybee Shoal changes (as the sediment has filled the South Channel along the shoreline). For the existing condition, calculated sediment transport was directed north along the north Tybee shoal and toward the Tybee Knoll Channel, with very little recirculating to the Tybee Island shelf. In the pre-project simulations, transport patterns showed recirculation onto the shelf from the margins of the South Channel. The sediment transport results also indicated more transport in the Breakwater Lee Shoal area under pre-project conditions than existing conditions. The existing condition also shows more of a tendency for offshore transport on the outer edges of the Tybee Island shelf. The average magnitude of the cumulative transport in the Tybee Knoll and Tybee Roads Bar Channels was larger for all existing condition simulations (3–4 times larger than pre-project for Tybee Knoll Channel). In the other areas, cumulative transport was generally comparable between existing and pre-project conditions. In general, it was not the magnitudes of transport that changed due to the project (with the exception of the Tybee Knoll Channel), but the pathways.

The sediment pathways are best expressed through the sediment budget. The budget was developed based on historical volume changes in five

sediment budget cells, shoreline change rates on Tybee Island, beach nourishment volumes, dredging volumes, and pathways, and relative rates provided by the numerical sediment transport modeling. The directions of the exchange between each of the cells is important for evaluating the impact of the navigation project on Tybee, but the exact numbers are less important. For example, sediment leaving Barrett Shoals to the south and east in the budgets may cycle through the Tybee Roads Channel or be lost offshore, directly. The connections between cells are shown as one way, representing the net transfer between cells (although there may actually be transport going in both directions through time (seasonal or storm related cycles) or space).

There are two important points to glean from the sediment budget. First, there was deflation of the Tybee Island Shoal and shoreline erosion prior to the project. Thus, some of the erosion experienced on the shoal and shoreline is part of the natural process. Second, the post-project budget shows only pathways leaving the Tybee Island Shoal (with the exception of the beach fills). As a result, the Tybee Island Shoal and shoreline can only be losing sand. The primary change in the pre-project and post-project budgets for the Tybee Island Shoal is the loss of bypassing from Barrett Shoals, through the Tybee Roads Channel. For pre-project conditions, this bypassing would have occurred through migration of the channel and shoal to the south, and then a break through of a more efficient, straight channel. The break through would leave the shoal on the south side of the channel to feed the Tybee Island Shoal. The project dredging maintains the channel position for navigation safety and efficiency but cuts off the natural bypassing mechanism. Construction of jetties and channel dredging generally causes deflation of the ebb shoal and eventual downdrift erosion. Figure 6-1 shows a cumulative volume change from each of the sediment budget cells over the study period. The Tybee Island shoal platform shows the increasing deflation of that cell. The north Tybee shelf shows a general increase in sediment volume over time as the north shoreline bulge has eroded and the shelf has gained sediment. Due to the dredging events the Tybee Knoll and Tybee Roads Bar channels have also lost sediment volume. The cells on the north side of the sediment budget study (Daufuskie/Turtle Shoal, Calibogue Sound, and Barrett Shoals) all show a net cumulative volume change that is close to the original volume indicating that the net change is small in these cells.

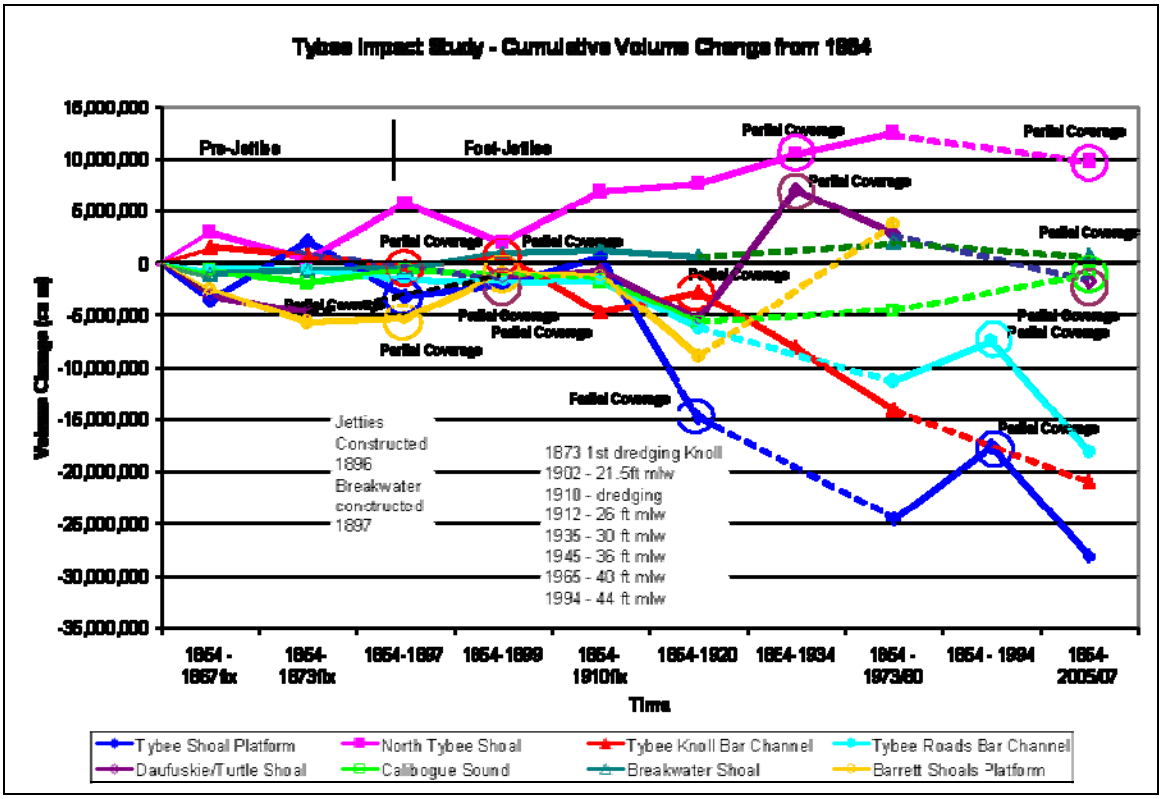

Figure 6-1. Cumulative volume change for each cell in sediment budget.

Two morphologic models observed at other simpler single inlet systems may help explain how the Tybee Roads complex of five inlets interact and affect the ebb shoal and sediment budget. An ebb-tidal breaching model may explain the evolution of the Calibogue Sound ebb shoal and its related four channels. This model explained by Fitzgerald et al. (1978) shows that the main flow out of an inlet changes orientation over time as the channels evolve through the ebb shoal (Figure 6-2). Closely associated by location are the Savannah River entrance/Wright River/South Channel complex, which before the construction of the two jetties could be considered a stable inlet based on the Fitzgerald et al. (1978) model. After construction of the jetties, the ebb shoal (in the form of the Tybee Island Shoal platform) has behaved similar to a typical single inlet downdrift ebb shoal that has collapsed and deflated as in the model described by Hansen and Knowles (1988). In the case of a single inlet, the downdrift ebb shoal deflated and migrated onshore as the jetties funneled the tidal flow further offshore. The Savannah River entrance is much more complex with the three channels (instead of one) where only one channel was modified by the construction of jetties.

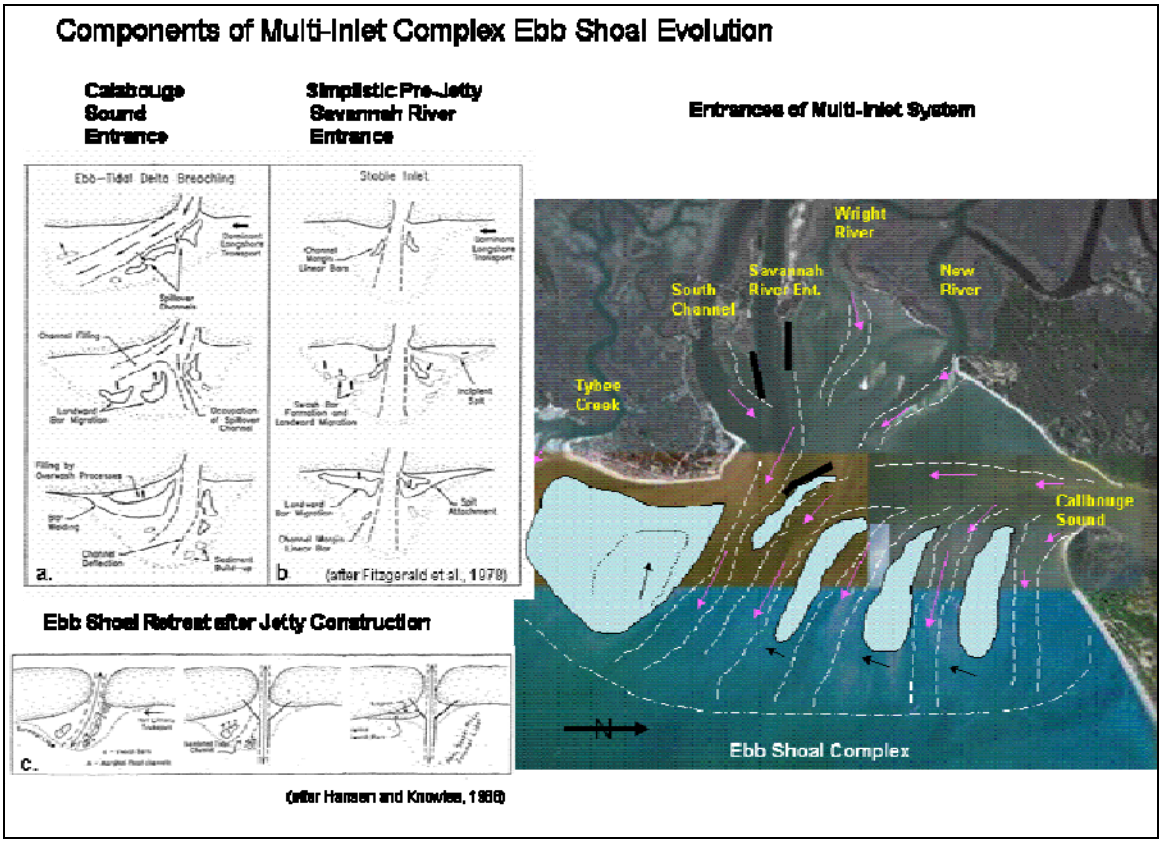

Figure 6-2. Morphologic model of changes at the Tybee Roads area.

The jetties and dredging of the Savannah River entrance have made this channel the dominant channel, while the Wright River entrance and the South Channel have shoaled and lost some of their influence on sediment transport and morphological evolution of this system. Deflation of the Tybee Island Shoal cell could be likened to the collapse of the model down-drift ebb shoal which is now starved of sediment. A typical inlet has the downdrift jetty attached to the shore and the shoal deflates and migrates directly onshore. In this case, the jetty is attached to Cockspur Island, and the collapse of the shoal and migration onshore are complicated by the interaction with the South Channel and resulting change to the northern Tybee shoreline. Sediment is now transported north into the north Tybee Island shoal area. The north terminal groin on Tybee Island is in the place where an inlet jetty typically would be, but it is much shorter and allows transport onto the north Tybee shoal.

The impact of the navigation project on the Tybee Island shoreline and shelf is estimated directly from the sediment budget. The impact is defined as volume change rate to the Tybee Island shoal and shoreline normalized by the post-project change rate:

$$impact = \frac{\left(\Delta V_{TybeeIslandShelf} + \Delta V_{ShorelineChange}\right)_{post-project} - \left(\Delta V_{TybeeIslandShelf} + \Delta V_{ShorelineChange}\right)_{pre-project}}{\left(\Delta V_{TybeeIslandShelf} + \Delta V_{ShorelineChange}\right)_{post-project}} \quad 6\text{-}1$$

The shoreline change volume rates were not included in the cell volume changes, but they were applied as source or sink terms in the budget. For example, the post-project shoreline change volume rate was subtracted from the Tybee Island Shoal cell (sediment went from the shelf to the shoreline), so by adding the volume change rate back in, the shoreline change is included in the impact. The estimated impact is calculated as:

$$impact = \frac{\left(-250+15\right)_{post-project} - \left(-42-20\right)_{pre-project}}{\left(-250+15\right)_{post-project}} = 0.736 \quad 6\text{-}2$$

or, 73.6 percent of the erosion on the Tybee Island shelf and shoreline is due to the navigation project. This impact calculation includes the effect of beach fill placement. If the beach fill is removed from the calculation, the impact is:

$$impact = \frac{\left(-250+15-54\right)_{post-project} - \left(-42-20\right)_{pre-project}}{\left(-250+15-54\right)_{post-project}} = 0.785 \quad 6\text{-}3$$

or, 78.5 percent of the erosion on the Tybee Island shelf and shoreline is due to the navigation project. Additionally, the beach fill (54 m^3/yr) has mitigated 23.8 percent of the project-induced erosion (post-project volume change rate minus pre-project change rate: 289 m^3/yr – 62 m^3/yr).

Volume change rate estimates of the project impact can be expressed several ways. First, the volume change rate for the Tybee Island shelf and shoreline due to the project excluding the beach fill is -227,000 m^3/yr (numerator of Equation 6-3) or including the beach fill is -173,000 m^3/yr (numerator of Equation 6-2). The impact can also be estimated as the reduction in bypassing to the Tybee shelf cell as estimated from the sediment budget. The reduction of bypassing from the north to the Tybee shelf is estimated as -207,000 m^3/yr. The volume change rates north of the channel (Barrett Shoals, Calibogue Sound, Breakwater Lee, Daufuski and Turtle Island Shelves) have changed from -76,000 m^3/yr to +76,000 m^3/yr (total change of +152,000 m^3/yr), indicating the impact north of the channel is net accretion. Similarly, the net volume change rate south of the channel went from +101,000 m^3/yr to -220,000 m^3/yr

(north Tybee shoal and Tybee Island shelf, neglecting shoreline changes), indicating net erosion. The net accretion in the pre-project period is due to accretion in the north Tybee shoal as the Savannah entrance channel filled and migrated towards the Tybee Knoll Channel.

The volume change estimates in the sediment budgets (Figures 2-48 and 2-49) include uncertainties. Carrying these uncertainties through the evaluation of the impact results in an uncertainty of approximately 45,000 m^3/yr (59,000 cu yd/yr), or approximately 20 percent. The impact assessment was based on the most reliable numbers available from the sediment budget. Additional factors do play a role in impact of the project but are difficult to quantify reliably and are expected to be relatively small compared to the volume loss on the Tybee Island shelf. For example, reduced sediment sources from the Savannah River would have increased erosion of the Tybee Island shelf and shoreline even if the project had not been constructed.

Coastal river entrances are complex environments with the interaction of river flows, tidal flows, waves, and sediments. The dynamic nature of these entrances often requires construction of structures and dredging of the channel to provide safe and reliable navigation. Such engineering activities can interrupt natural sediment bypassing and impact the downdrift shelf and beach. This study estimates that approximately 73.6 percent (including the effect of the beach fill placement) or 78.5 percent (excluding the effect of the beach fill placement) (±20 percent) of the erosion on the Tybee Island shelf and shoreline are due to the Savannah Navigation project, with the remainder of the erosion attributed to the natural processes.

References

Anders, F. J., D. W. Reed, and E. P. Meisbeurger. 1990. *Shoreline movements, Report 2, Tybee Island, Georgia to Cape Fear, North Carolina, 1851–1983*. Technical Report CERC-83-1. Vicksburg, MS: U.S. Army Engineer Waterways Experiment Station.

Applied Technology and Management, Inc. (ATM). 2001. Draft Savannah Harbor beach erosion study: Savannah Harbor Expansion Project. Prepared for the Georgia Port Authority. Charleston, SC.

Bouws, E., H. Gunther, W. Rosenthal, and C. L. Vincent. 1985. Similarity of the wind wave spectrum in finite depth waves; 1. Spectral form. *Journal of Geophysical Research* 90(C1):975–986.

Brooks, R. M., and W. A. Brandon. 1995. *Hindcast wave information for the U.S. Atlantic Coast: Update 1976–1993 with hurricanes*. WIS Report 33. Vicksburg, MS: U.S. Army Engineer Waterways Experiment Station.

Byrnes, M. R., J. L. Baker, and F. Li. 2002. *Quantifying potential measurement errors and uncertainties associated with bathymetric change analysis*. ERDC/CHL CHETN-IV-50. Vicksburg, MS: U.S. Army Engineer Research and Development Center.

Fitzgerald, D. M., D. K. Hubbard, and D. Nummendal. 1978. Shoreline changes associated with tidal inlets along the South Carolina coast. *Proceedings of Coastal Zone 78*, ASCE, 1973–1974.

Gailani, J. Z., S. J. Smith, and N. C. Kraus. 2003a. *Monitoring dredged material disposal at the mouth of the Columbia River, Washington/Oregon, USA*. ERDC/CHL TR-03-5. Vicksburg, MS: U.S. Army Engineer Research and Development Center.

Gailani, J. Z., S. J. Smith, L. Raad, and B. A. Ebersole. 2003b. *Savannah Harbor entrance channel: Nearshore placement of dredged material*. Draft technical report. Vicksburg, MS: U.S. Army Engineer Research and Development Center.

Gibbs, A. E., and G. Gelfenbaum. 1999. Bathymetric change off the Washington-Oregon Coast. *Proceedings, Coastal Sediments '99*, ASCE, 1627–1642.

Hansen, M., and S. C. Knowles. 1988. Ebb-tidal delta response to jetty construction at three South Carolina inlets. In *Hydrodynamics and Sediment Dynamics of Tidal Inlets, Lecture Notes on Coastal and Estuarine Studies*, V29. ed. D. G. Aubrey and L. Weishar, 364–381. New York: Springer Verlag.

Hubertz, J. M. 1992. *User's guide to the Wave Information Studies (WIS) wave model, Version 2.0*. WIS Report 27. Vicksburg, MS: U.S. Army Engineer Waterways Experiment Station.

Jensen, R., N. Scheffner, S. J. Smith, D. Webb, and B. A. Ebersole. 2002. *Engineering studies in support of Delong Mountain Terminal project*. ERDC/CHL TR-02-26. Vicksburg, MS: U.S. Army Engineer Research and Development Center.

Luettich, R. A., Jr., and J. J. Westerink. 2004. *Formulation and numerical implementation of the 2D/3D ADCIRC Finite Element Model Version 44.XX, Theory report and formulation*, http://www.marine.unc.edu/C_CATS/adcirc/adcirc_theory_2004_12_08.pdf

_____. 2005. *A (parallel) advanced circulation model for oceanic, coastal, and estuarine waters. On-Line User's Guide*. http://www.marine.unc.edu/C_CATS/adcirc/document/ADCIRC_title_page.html

Madsen, O. S., and P. N. Wikramanayake. 1991. *Simple models for turbulent wave-current bottom boundary layer flow*. Contract Report DRP-91-1. Vicksburg, MS: U.S. Army Engineer Waterways Experiment Station.

Meyer-Peter, E., and R. Müller. 1948. Formulas for bed-load transport. *Second International Association of Hydraulic Engineering and Research (IAHR) Congress, Stockholm, Sweden*. Delft, Netherlands: IAHR.

Miller, T. L., R. A. Morton, and A. H. Sallenger. 2005. *The national assessment of shoreline change: A GIS compilation of vector shorelines and associated shoreline change data for the U.S. Southeast Atlantic Coast*. USGS Open File Report 2005-1326. St. Petersburg, FL.

Miller, H. C., S. J. Smith, D. G. Hamilton, and D. T. Resio. 1999. Cross-shore transport processes during onshore bar migration. *Proceedings of Coastal Sediments '99*, ASCE, 1065–1080.

Nielsen, P. 1992. *Coastal bottom boundary layers and sediment transport*. World Scientific Publishing, Singapore, Advanced Series on Ocean Engineering, vol. 4.

Oertel, G. F., J. E. Fowler, and J. Pope. 1985. *History of erosion and erosion control efforts at Tybee Island, Georgia*. Miscellaneous Paper CERC-85-1. Vicksburg, MS: U.S. Army Engineer Waterways Experiment Station.

Sargent, F. E. 1988. *Case histories of Corps breakwater and jetty structures, Report 2 South Atlantic Division*. WES TR-REMR-Co-3. Vicksburg, MS: U.S. Army Engineer Waterways Experiment Station.

Smith, J. M., A. R. Sherlock, and D. T. Resio. 2001. *STWAVE: Steady-State Spectral Wave Model User's manual for STWAVE, Version 3.0*. ERDC/CHL SR-01-1. Vicksburg, MS: U.S. Army Engineer Research and Development Center. http://chl.wes.army.mil/research/wave/wavesprg/numeric/wtransformation/downld/erdc-chl-sr-01-11.pdf

Smith, J. M., D. Stauble, B. Williams, and R. Chapman. 2006. Impacts of Savannah Harbor Expansion Project. Report prepared for U.S. Army Engineer District, Savannah, Savannah, GA.

Soulsby, R. L. 1997. *Dynamics of marine sands.* London: Thomas Telford, 249 pp.

Van Rijn, L. C. 1984. Sediment transport: Part I: Bed load transport; Part II: Suspended load transport; Part III: Bed forms and alluvial roughness. *Journal of Hydraulic Engineering* 110(10):1431–1456; 110(11):1613–1641; 110(12):1733–1754.

Wikramanayake, P. N., and O. S. Madsen. 1994a. *Calculation of suspended sediment transport by combined wave-current flows*. Contract Report DRP-94-7. Vicksburg, MS: U.S. Army Engineer Waterways Experiment Station.

_____. 1994b. *Calculation of movable bed friction factors*. Contract Report DRP-94-5. Vicksburg, MS: U.S. Army Engineer Waterways Experiment Station.

Appendix A: GTRAN Sediment Transport Methods

This section describes the sediment transport methods incorporated into the sediment transport model. These descriptions aim to provide a general overview of the predictive techniques.

Transport methods

Algorithms that estimate sediment movement under specific wave and current conditions are referred to as transport methods. Presently there are no sediment transport methods that are universally applicable to all environments and sediment types. For instance, a transport method developed for cobbles and boulders in an alpine stream is not likely to correctly represent sediment transport in an estuary or open-coast application. To correctly and reliably estimate sediment transport, the transport method must represent the important transport processes within the region of application. A general description and overview will be given for each transport method applied.

Wikramanayake and Madsen

Under contract with the U.S. Army Corps of Engineers, Dredging Research Program (DRP), researchers at Massachusetts Institute of Technology developed non-cohesive sediment transport algorithms for combined wave-current environments. The algorithms include the effects of variation between current and wave directions. The methods are outlined in DRP reports (Madsen and Wikramanayake 1991; Wikramanayake and Madsen 1994a) and were specifically designed for nearshore transport in high-energy regions, although the initial validation and calibration were performed outside the surf zone. User input includes near-bottom orbital velocity, mean currents, bed slope, and grain size.

The method uses a time-invariant turbulent eddy viscosity model and a time-varying near-bottom concentration model to estimate suspended sediment transport fluxes. The method first calculates the bed roughness, using methods outlined by Wikramanayake and Madsen (1994b). Bed load and suspended sediment concentrations are then calculated using bottom

shear stress. Estimates of vertical variation in suspended sediment concentration are based on a non-dimensional, time-varying, near-bottom reference concentration, $C_r(t)$. This concentration can be estimated as:

$$C_r(t) = \frac{C_b \gamma_o [|\Psi^*(t)| - \Psi_{cr}]}{\Psi_{cr}} \tag{A-1}$$

where:

C_b = volume fraction of sediment in the bed
γ_o = empirical resuspension coefficient
$\Psi^*(t)$ = the Shield's parameter based on instantaneous, skin-friction shear stress
Ψ_{cr} = the critical Shield's parameter

Laboratory experiments have demonstrated that γ_o decreases with increasing Shield's parameter or wave skin friction shear stress. However, data were insufficient to develop empirical methods to relate the resuspension coefficient to Shield's parameter and constant values of γ_o are applied for rippled and flat beds, respectively. The Shield's parameters are defined by:

$$\Psi^*(t) = \frac{u^*(t)}{(s-1)g d_{50}} \tag{A-2}$$

$$\Psi_{cr} = \alpha_1 \tan(\varphi) \tag{A-3}$$

where:

$u^*(t)$ = bed shear velocity
s = specific gravity of sediment
g = gravitational acceleration
d_{50} = median grain diameter
α_1 = coefficient dependent on the local Reynolds number
φ = angle of repose of the sediment grains

The reference concentration is used to estimate vertically varying concentrations in the water column due to steady and oscillatory currents. The estimated suspended sediment concentration is coupled with the vertically varying velocities to estimate the total suspended sediment flux.

The Wikramanayake and Madsen model also includes a method for estimating the instantaneous bed-load flux based on the Meyer-Peter and Müller (1948) formula. This instantaneous bed-load flux, Q_b (cm³/cm·s), is estimated by:

$$\vec{Q}_b(t) = \frac{d_{50}\sqrt{(s-1)gd_{50}}}{2\pi} \frac{8(|\Psi^*(t)| - \Psi_{cr})}{1 + \tan\beta_L \frac{\cos(\Phi_t - \Phi_{sw})}{\tan\Phi_f}} \frac{\vec{\tau}_b'(t)}{|\vec{\tau}_b'(t)|} \tag{A-4}$$

where $\beta_L = h/6\delta$, h is the water depth, δ is the boundary layer length scale, Φ_t is the angle between the current and the wave direction, Φ_{sw} is the angle between the wave direction and bottom slope, and $\tau_b'(t)$ is the instantaneous skin friction shear stress.

Wikramanayake and Madsen (1994a) performed several tests to compare their results to field measurements in wave/current environments and found that the model accurately predicted the current-related and wave-related sediment fluxes and distributions in the water column. No verification was performed for the bed-load model estimates. Field verification of the transport method has been performed by CHL against data sets from the Columbia River mouth (Gailani et al. 2003a) and in the surf zone at the Field Research Facility, Duck, North Carolina, with favorable comparisons to field data. The Wikramanayake and Madsen transport method is unsuitable for conditions in which sediment suspension and/or wave-induced shear stresses are small, therefore other methods of approximating sediment transport were applied under bedload-dominated or current-dominated transport conditions.

Soulsby bedload transport method

Soulsby (1997) developed a formula for combined wave-current bedload by integrating the current-only bedload formula of Nielsen (1992) over a single sinusoidal wave cycle. The formula is expressed as follows:

$$\Phi_{x1} = 12\theta_m^{1/2}(\theta_m - \theta_{cr}) \tag{A-5a}$$

$$\Phi_{x2} = 12(0.95 + 0.19\cos 2\varphi)\theta_w^{1/2}\theta_m \tag{A-5b}$$

$$\Phi_x = \text{maximum of } \Phi_{x1} \text{ and } \Phi_{x2} \tag{A-5c}$$

$$q_{bx} = \Phi_x \left[g(s-1) d_{50}^3 \right]^{1/2} \quad \text{(A-5d)}$$

subject to $\Phi_x = 0$ if $\theta_{cr} \geq \theta_{max}$

where:

θ_m = mean Shield's parameter over a wave cycle
θ_{cr} = critical Shield's parameter for initiation of motion
φ = angle between current direction and direction of wave travel
θ_w = amplitude of oscillatory component of θ due to waves
q_{bx} = mean volumetric bedload transport rate per unit width
θ_{max} = maximum Shield's parameter from combined wave-current stresses

Soulsby's combined wave-current bedload transport method was applied when sediment suspension was estimated to be near zero.

Van Rijn current-dominated transport method

The Van Rijn (1984) current-only total transport method was parameterized from Van Rijn's comprehensive theory of sediment transport in rivers. Although the method was developed for sediment transport in the riverine environment, the method may also be appropriately applied in the marine environment under conditions for which waves contribute little to the bottom shear stress. The simpler, parameterized formulae presented here approximate the full theory within ±25 percent and were developed for water depths between 1 and 20 m, velocities between 0.5 and 5 m/s, d_{50} between 0.1 and 2 mm, and for fresh water at 15 deg C. The resulting parameterized method estimates transport by the following simpler formulation:

$$q_t = q_b + q_s \quad \text{(A-6)}$$

$$q_b = 0.005 \overline{U} h \left\{ \frac{\overline{U} - \overline{U}_{cr}}{\left[(s-1) g d_{50} \right]^{1/2}} \right\}^{2.4} \left(\frac{d_{50}}{h} \right)^{1.2} \quad \text{(A-7)}$$

$$q_s = 0.012 \overline{U} h \left\{ \frac{\overline{U} - \overline{U}_{cr}}{\left[(s-1) g d_{50} \right]^{1/2}} \right\}^{2.4} \left(\frac{d_{50}}{h} \right) (D_*)^{-0.6} \quad \text{(A-8)}$$

where:

$$\overline{U}_{cr} = 0.19(d_{50})^{0.1} \log_{10}\left(\frac{4h}{d_{90}}\right) \left\{ 0.1 \le d_{50} \le 0.5\ mm \right.$$

$$\overline{U}_{cr} = 8.50(d_{50})^{0.6} \log_{10}\left(\frac{4h}{d_{90}}\right) \left\{ 0.5 \le d_{50} \le 2.0\ mm \right.$$

$$D_* = \left[\frac{g(s-1)}{\nu^2}\right]^{1/3} d_{50}$$

q_b = bedload transport
q_s = suspended transport
$\overline{U}$ = depth-averaged current
h = water depth
d_{90} = sediment diameter for which 90 percent is finer by weight

Transport model

Sediment transport processes along the length of the channel vary both spatially and temporally. A prime example of this variation is the difference between transport inside and outside of the surf zone. Waves and currents inside and outside the surf zone are responsible for transporting the sediment, but the transport mechanisms are different. Inside the surf zone, breaking waves increase turbulence and enhance sediment suspension while the wave-generated longshore currents transport the suspended sediment. Outside the surf zone, turbulence is much smaller, but the waves may suspend sediment over bedforms and the larger-scale, ocean circulation transports the sediment. Clearly, it would be difficult to represent the sediment transport in both of these regions with one transport method. The sediment transport model selects the appropriate transport method, develops the required input conditions, and tracks the spatial relationships, sediment characteristics, environmental conditions, and estimated sediment transport.

With the initial bed conditions specified, the model next distributes environmental forcing conditions from large-domain wave and circulation models to each of the computational points. The temporal resolution of the wave and current information is 1-hr or 3-hr as is the time-step of the model. This resolution is adequate to define the temporal changes in wave and current conditions for representing sediment transport. With local wave and current conditions determined, the model proceeds to estimate

the combined wave-current bottom shear stresses and to estimate the depth of the active sediment layer. The active sediment layer is defined as the depth of the sediment bed that is mobilized by sediment suspension and bed-load movement. Bottom shear stresses and non-cohesive sediment characteristics are further evaluated to determine the regime of sediment transport and the appropriate sediment transport method is selected to estimate the sediment transport rates. Jensen et al. (2002) give additional information regarding model development and application.

Appendix B: GTRAN Sediment Transport Rose Plots

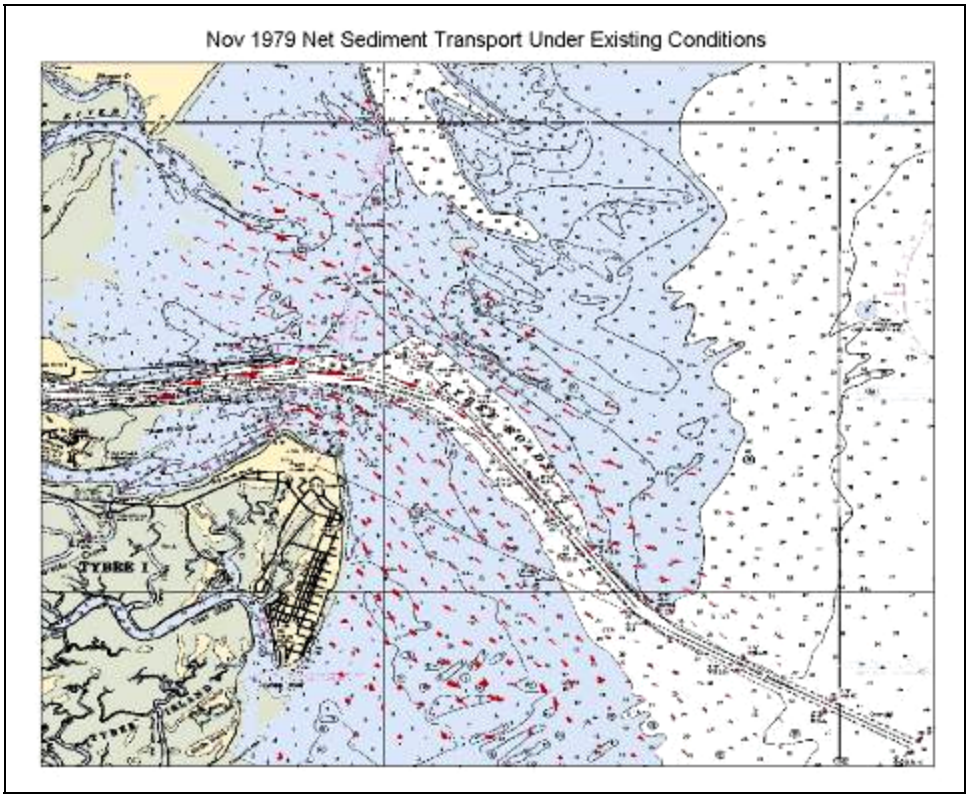

Figure B-1. Cumulative sediment transport rose plots for November 1979 existing conditions GTRAN simulation (full domain).

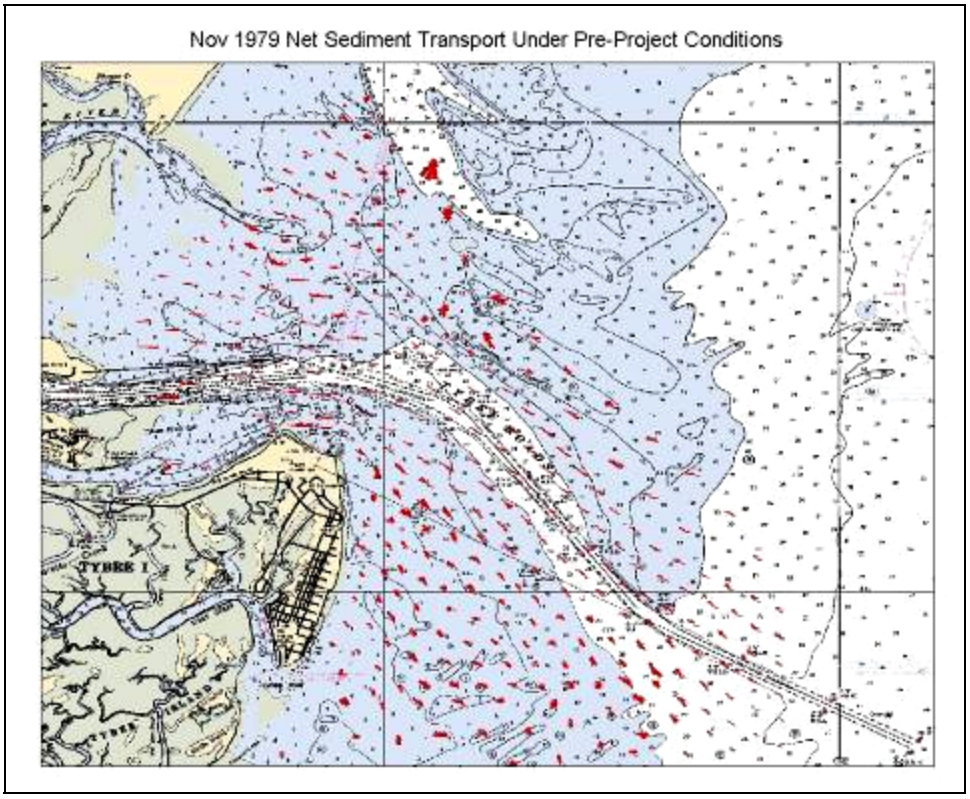

Figure B-2. Sediment transport rose plots for November 1979 pre-project GTRAN simulation (full domain).

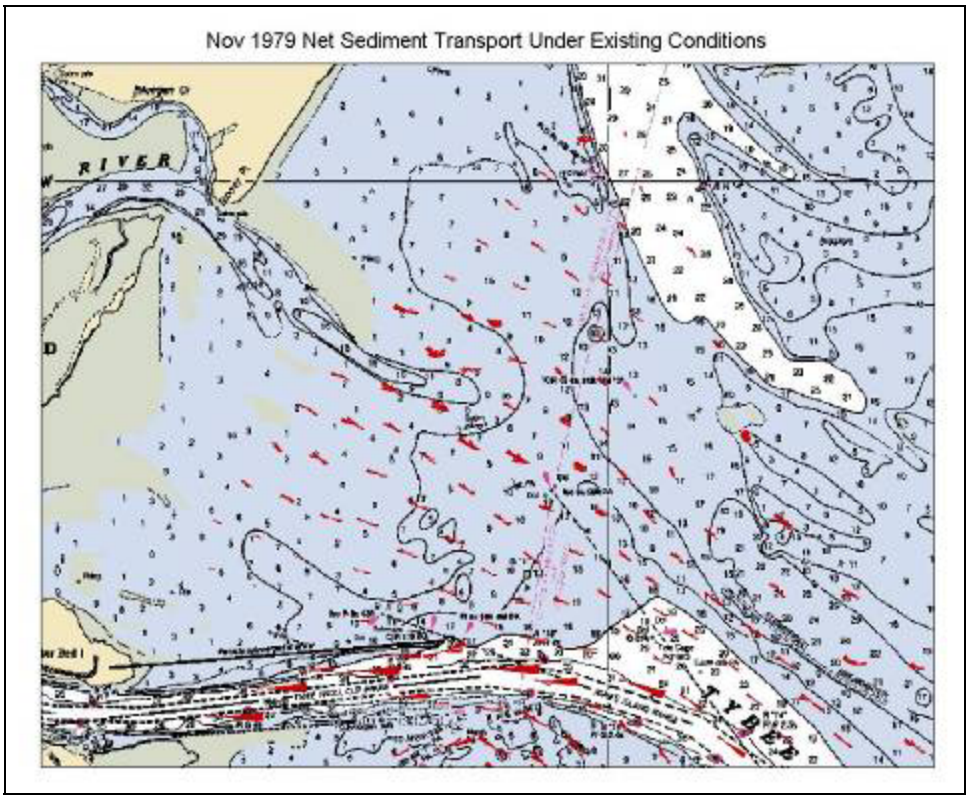

Figure B-3. Sediment transport rose plots for November 1979 existing conditions GTRAN simulation (northern domain).

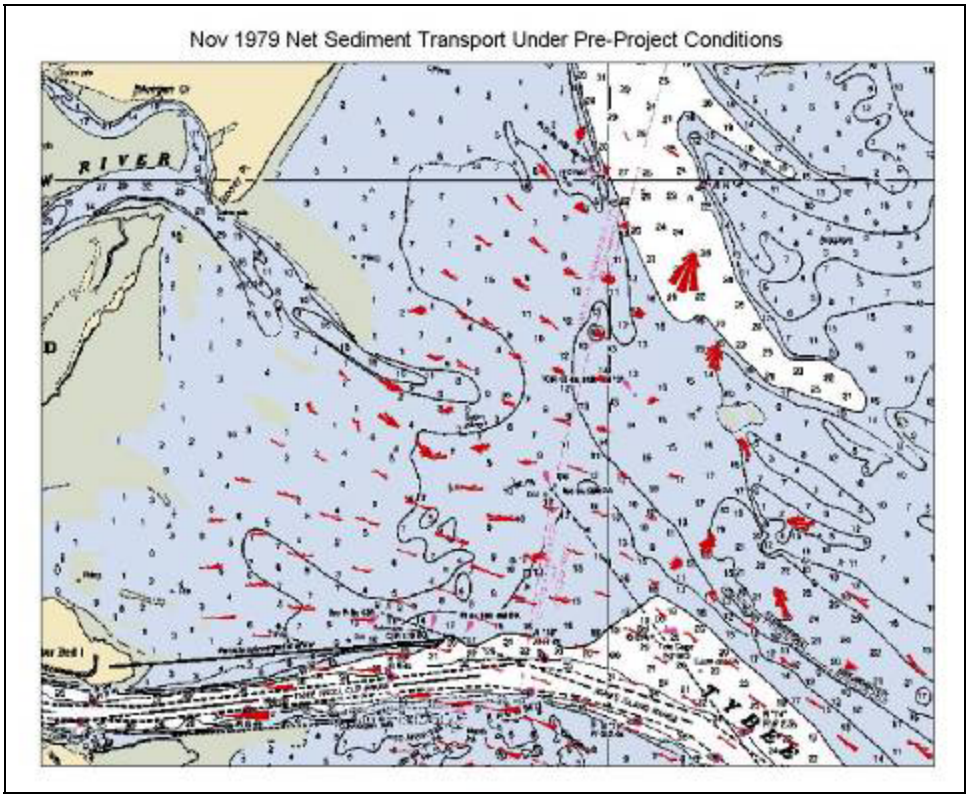

Figure B-4. Sediment transport rose plots for November 1979 pre-project GTRAN simulation (northern domain).

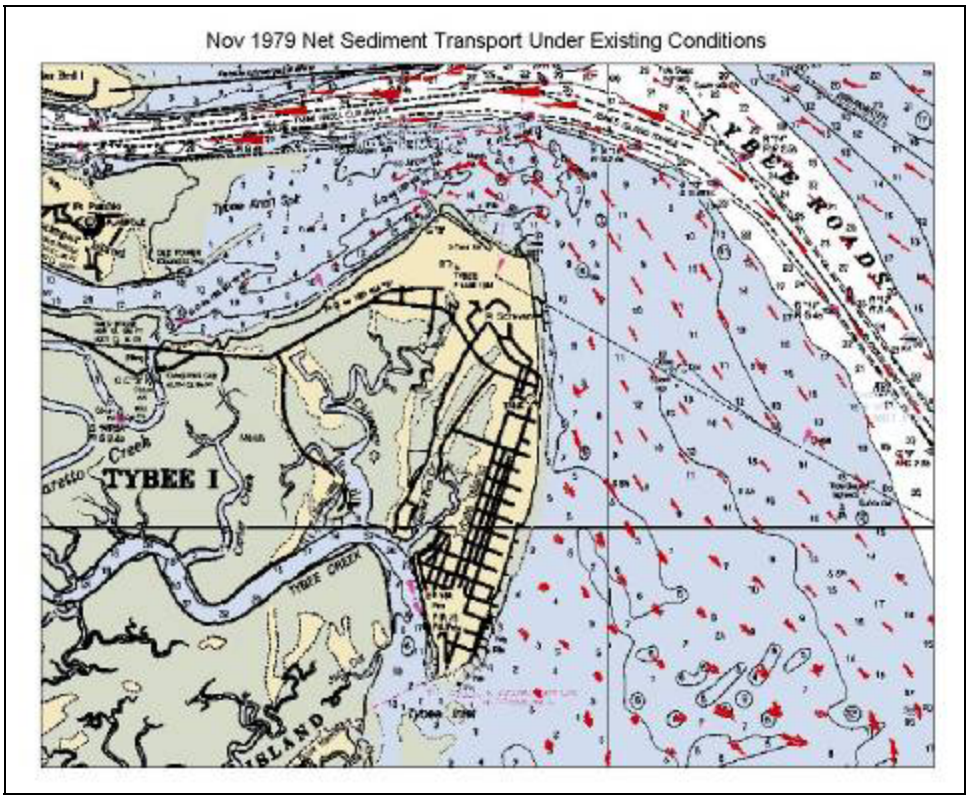

Figure B-5. Sediment transport rose plots for November 1979 existing conditions GTRAN simulation (southern domain).

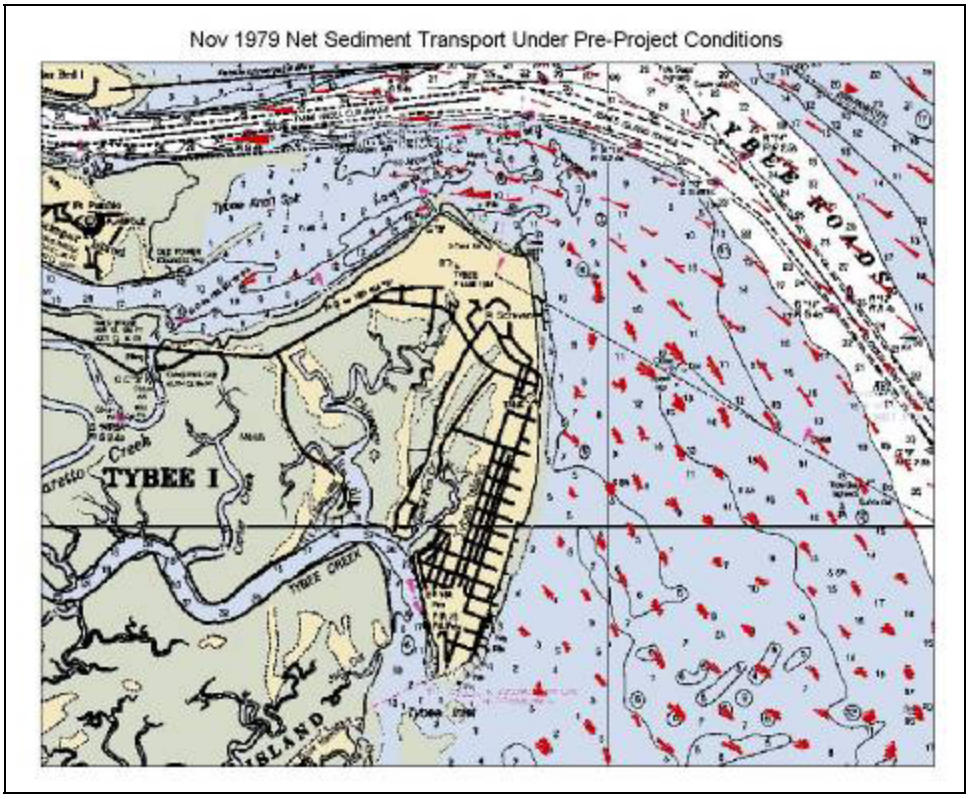

Figure B-6. Sediment transport rose plots for November 1979 pre-project GTRAN simulation (southern domain).

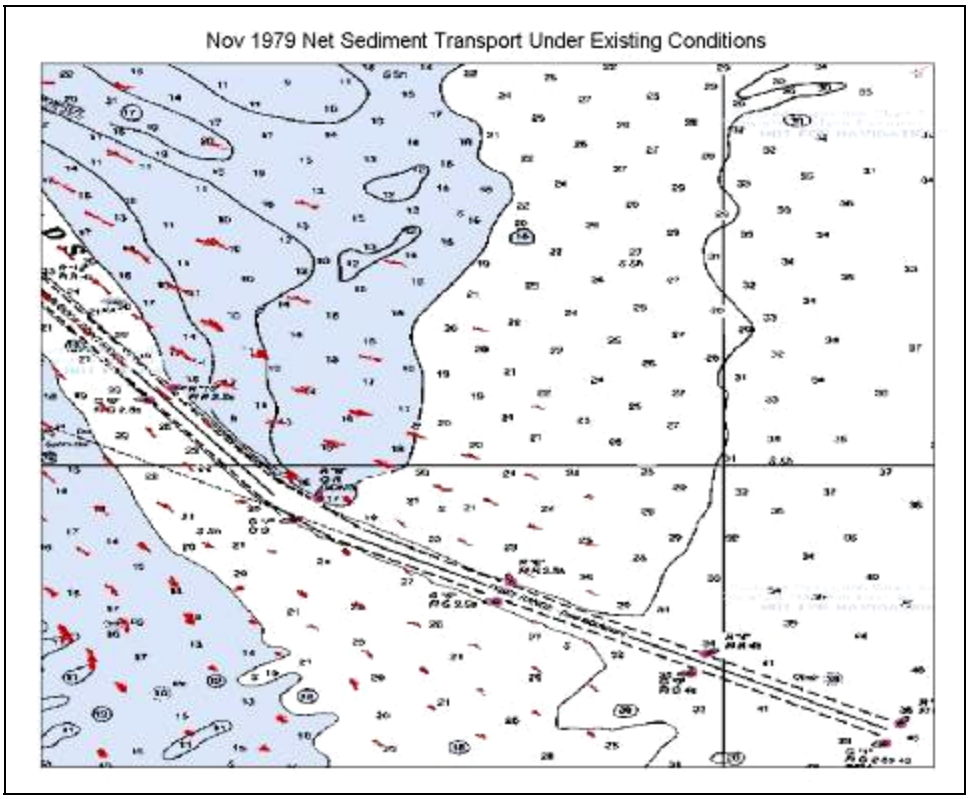

Figure B-7. Sediment transport rose plots for November 1979 existing conditions GTRAN simulation (southeastern domain).

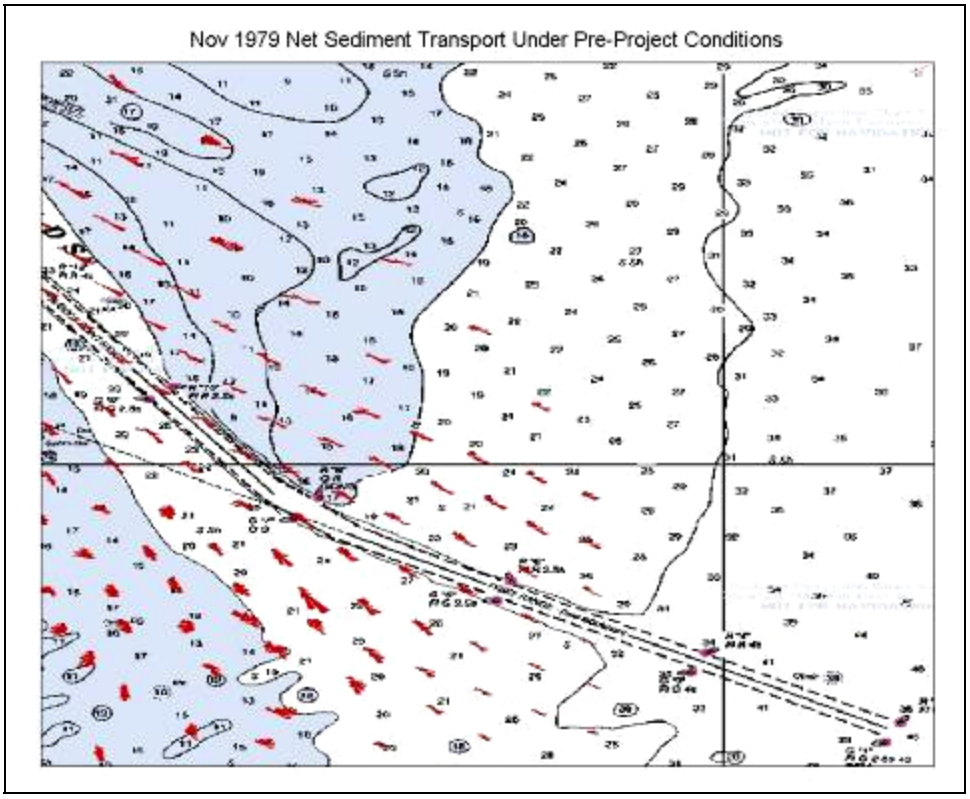

Figure B-8. Sediment transport rose plots for November 1979 pre-project GTRAN simulation (southeastern domain).

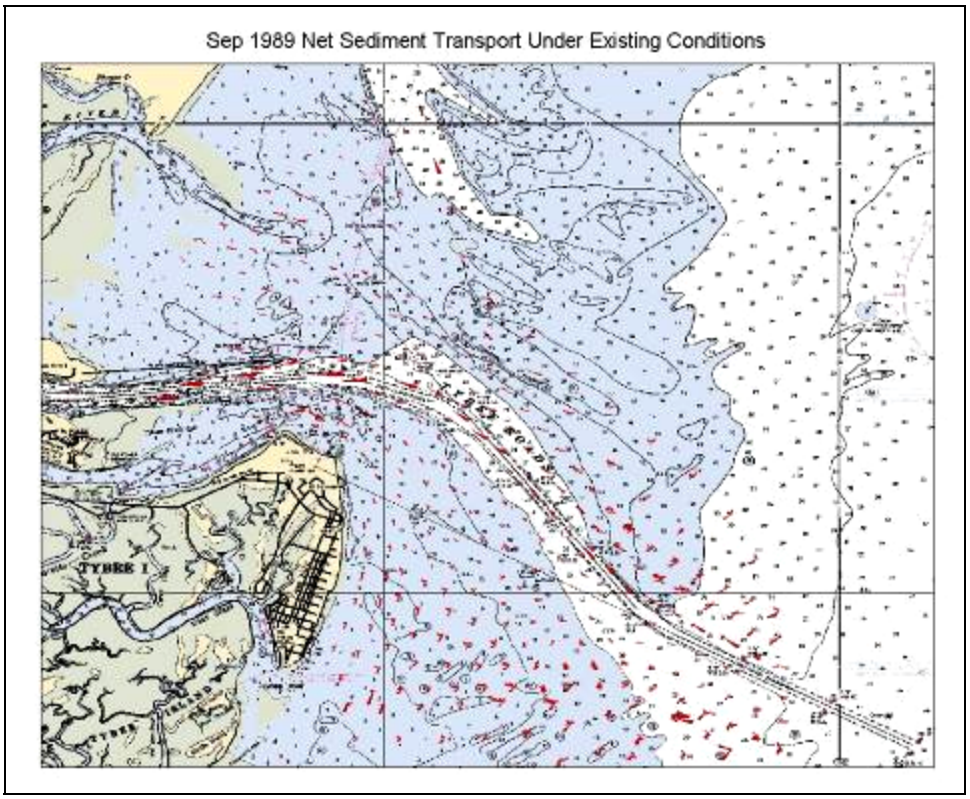

Figure B-9. Sediment transport rose plots for September 1989 (Hugo) existing conditions GTRAN simulation (full domain).

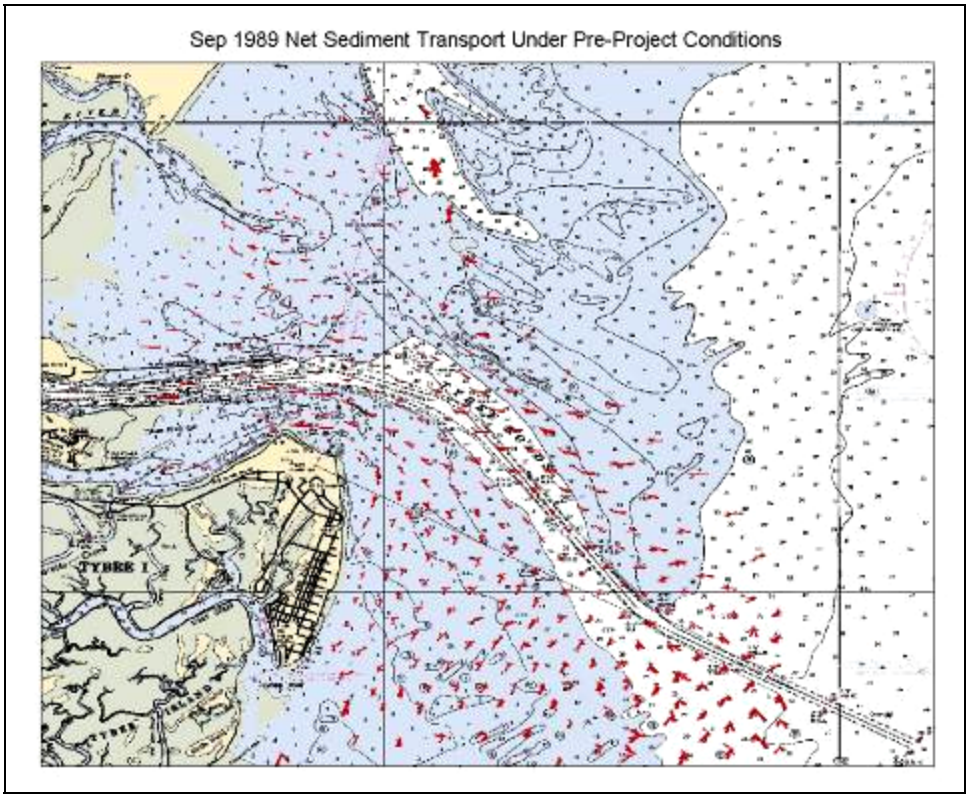

Figure B-10. Sediment transport rose plots for September 1989 (Hugo) pre-project GTRAN simulation (full domain).

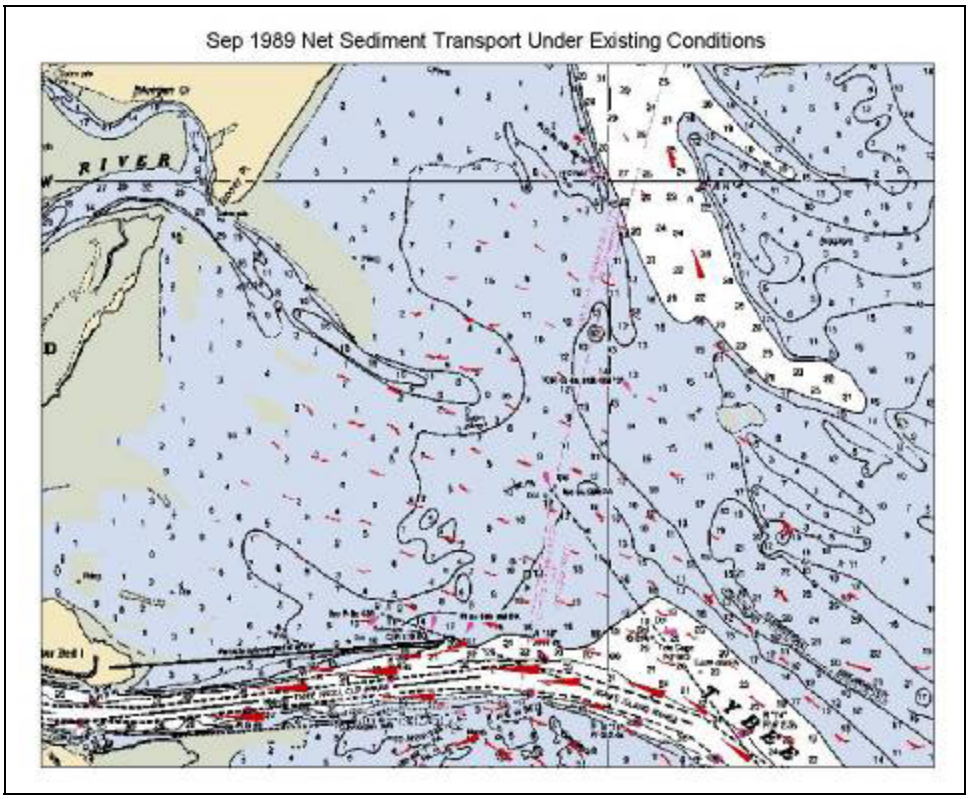

Figure B-11. Sediment transport rose plots for September 1989 (Hugo) existing conditions GTRAN simulation (northern domain).

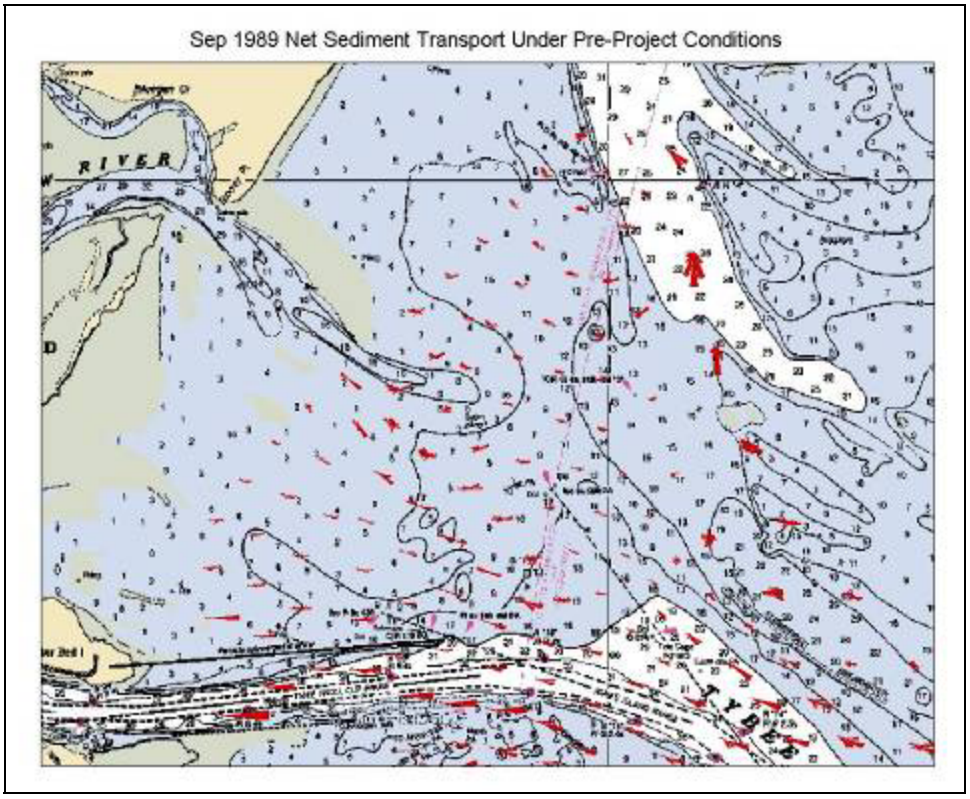

Figure B-12. Sediment transport rose plots for September 1989 (Hugo) pre-project GTRAN simulation (northern domain).

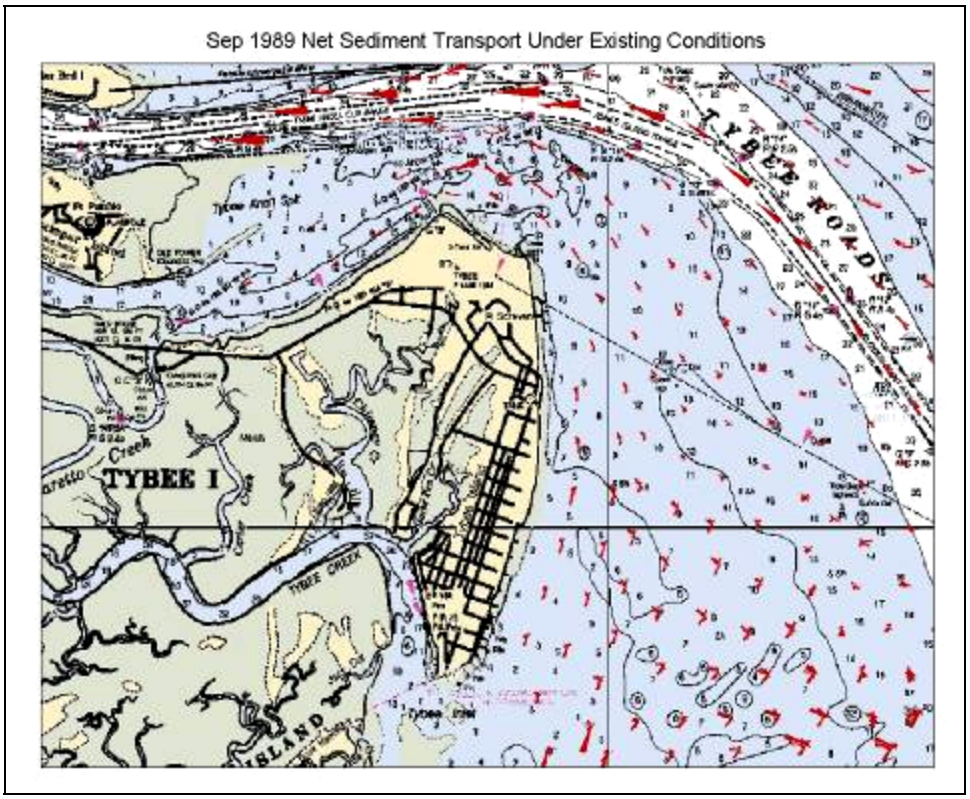

Figure B-13. Sediment transport rose plots for September 1989 (Hugo) existing conditions GTRAN simulation (southern domain).

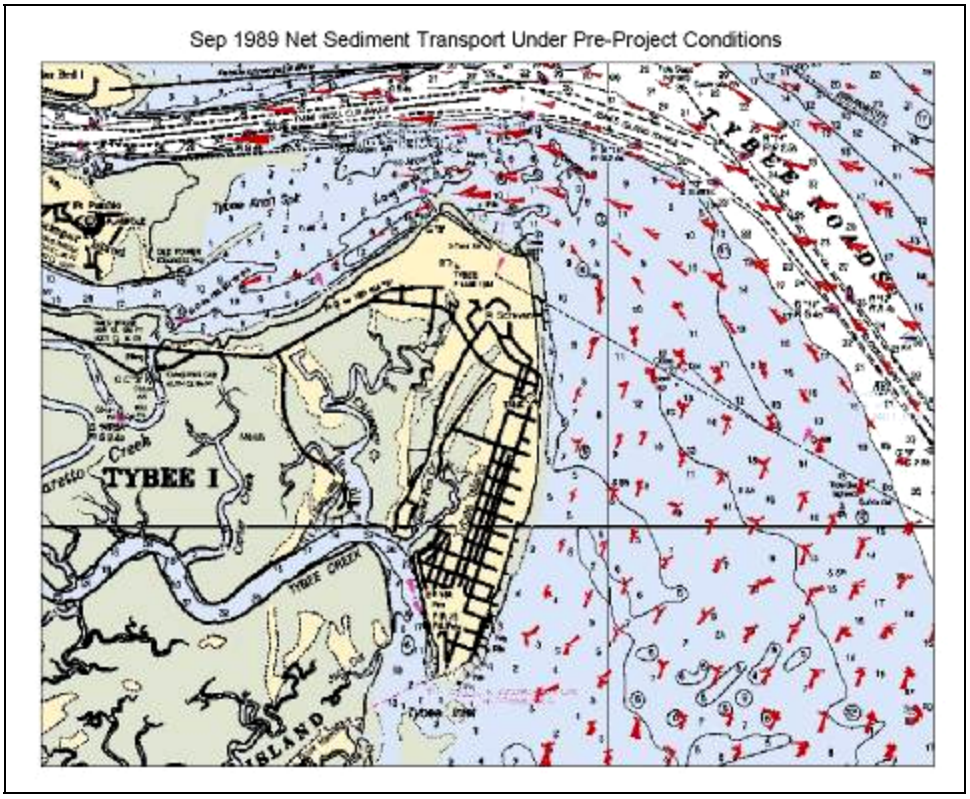

Figure B-14. Sediment transport rose plots for September 1989 (Hugo) pre-project GTRAN simulation (southern domain).

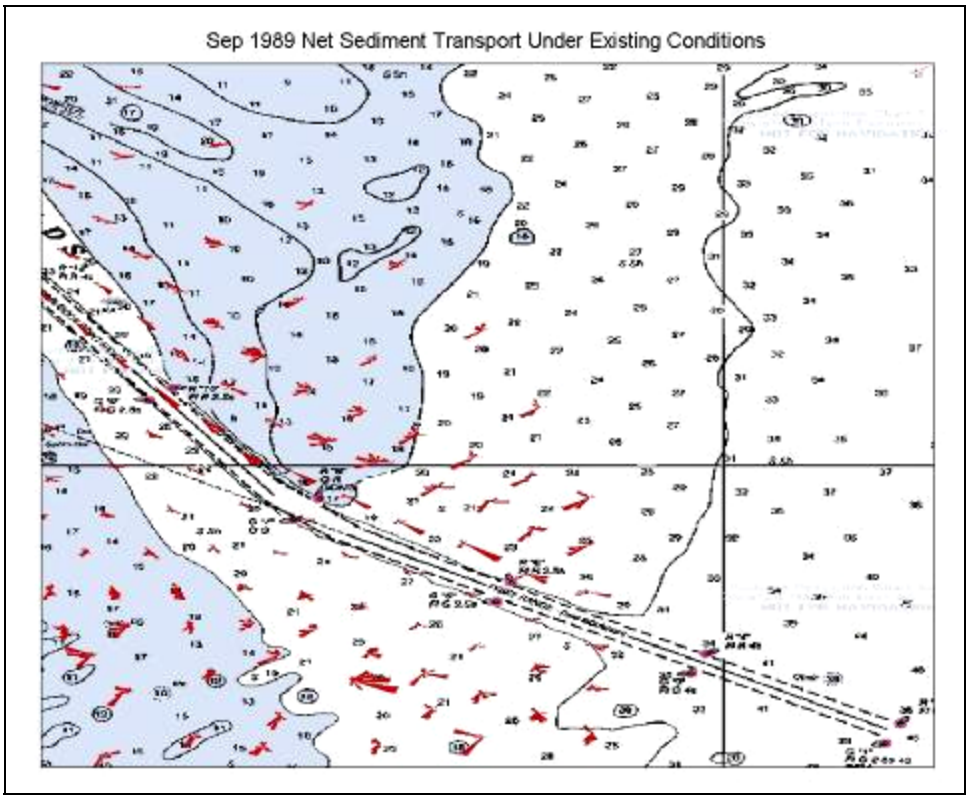

Figure B-15. Sediment transport rose plots for September 1989 (Hugo) existing conditions GTRAN simulation (southeastern domain).

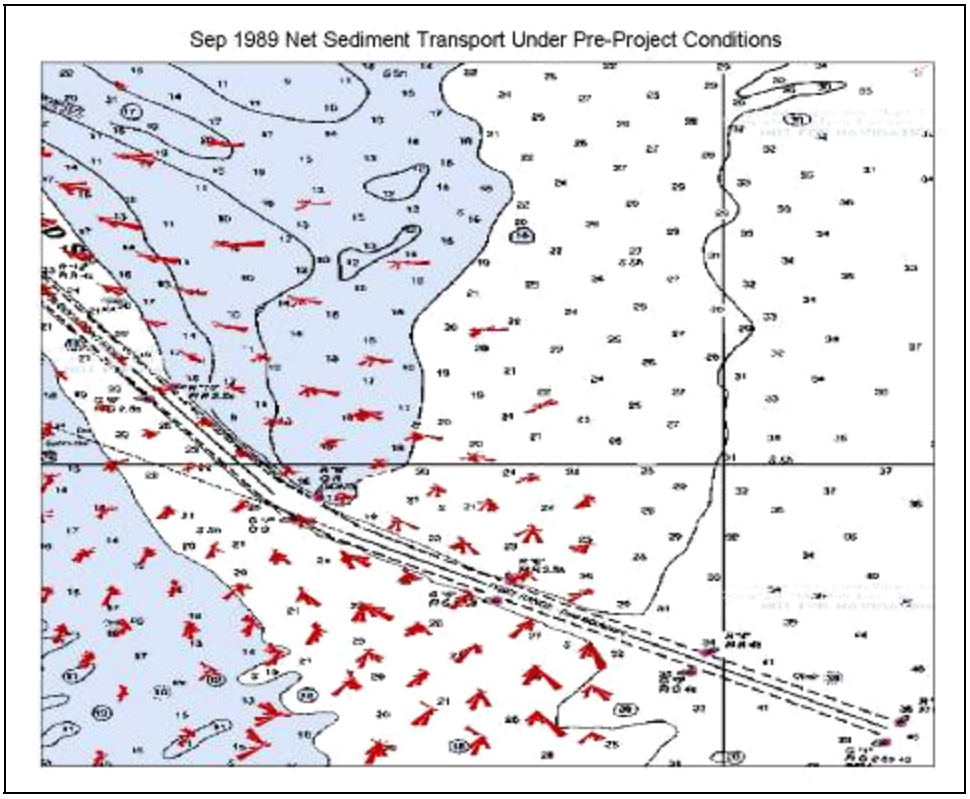

Figure B-16. Sediment transport rose plots for September 1989 (Hugo) pre-project GTRAN simulation (southeastern domain).

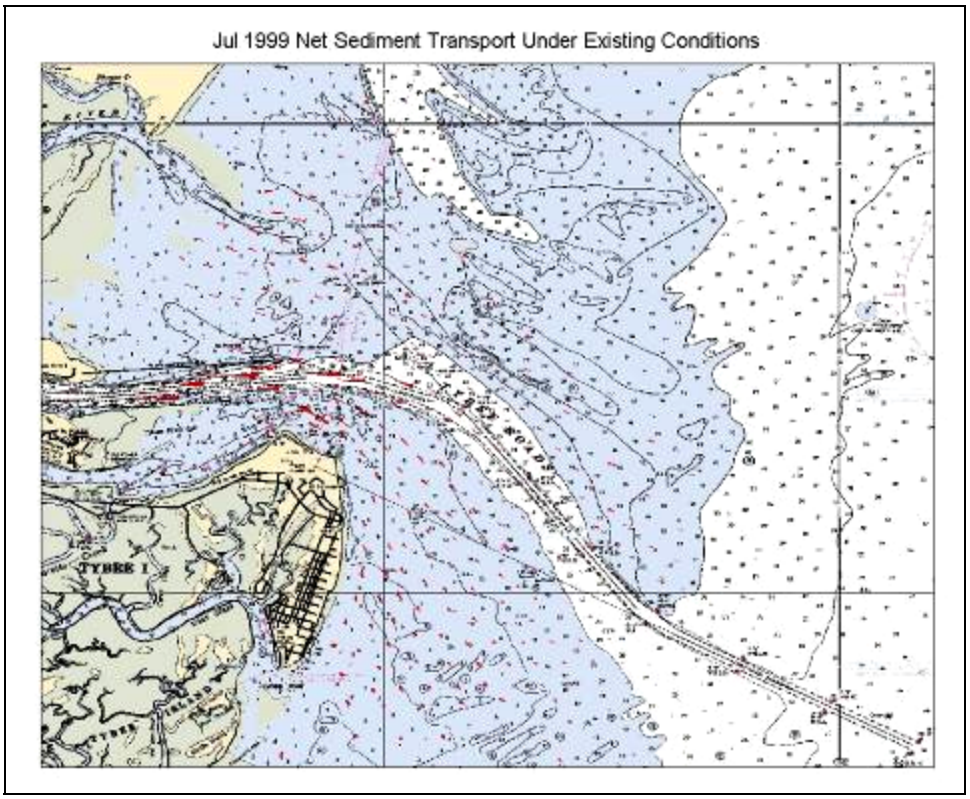

Figure B-17. Sediment transport rose plots for July 1999 existing conditions GTRAN simulation (full domain).

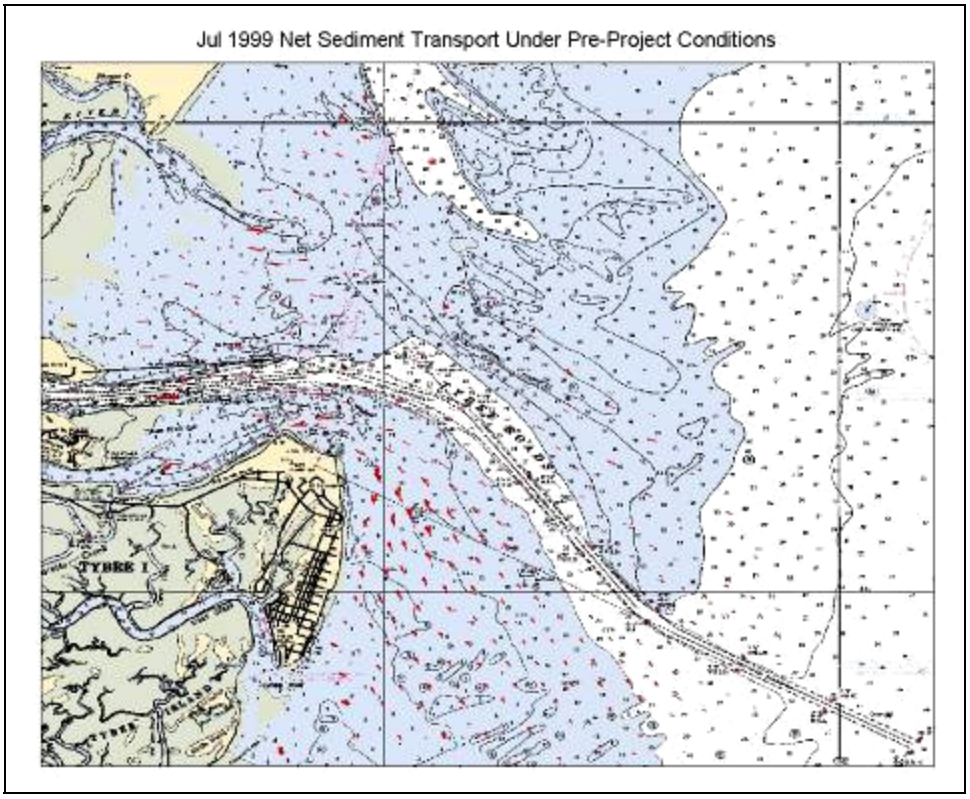

Figure B-18. Sediment transport rose plots for July 1999 pre-project GTRAN simulation (full domain).

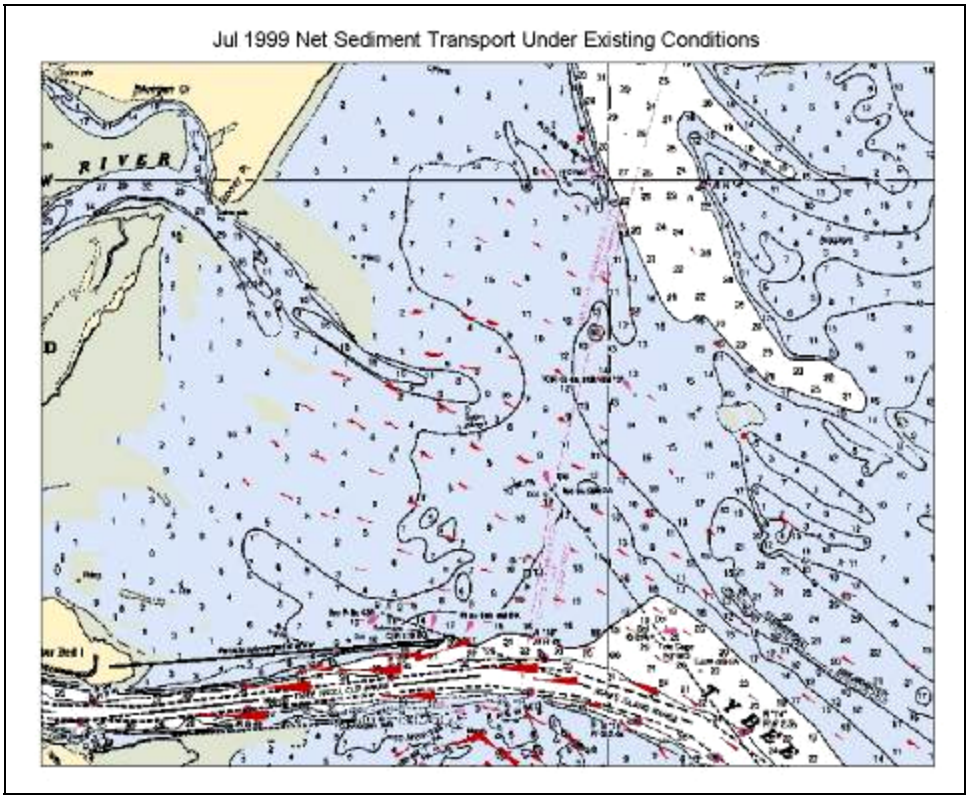

Figure B-19. Sediment transport rose plots for July 1999 existing conditions GTRAN simulation (northern domain).

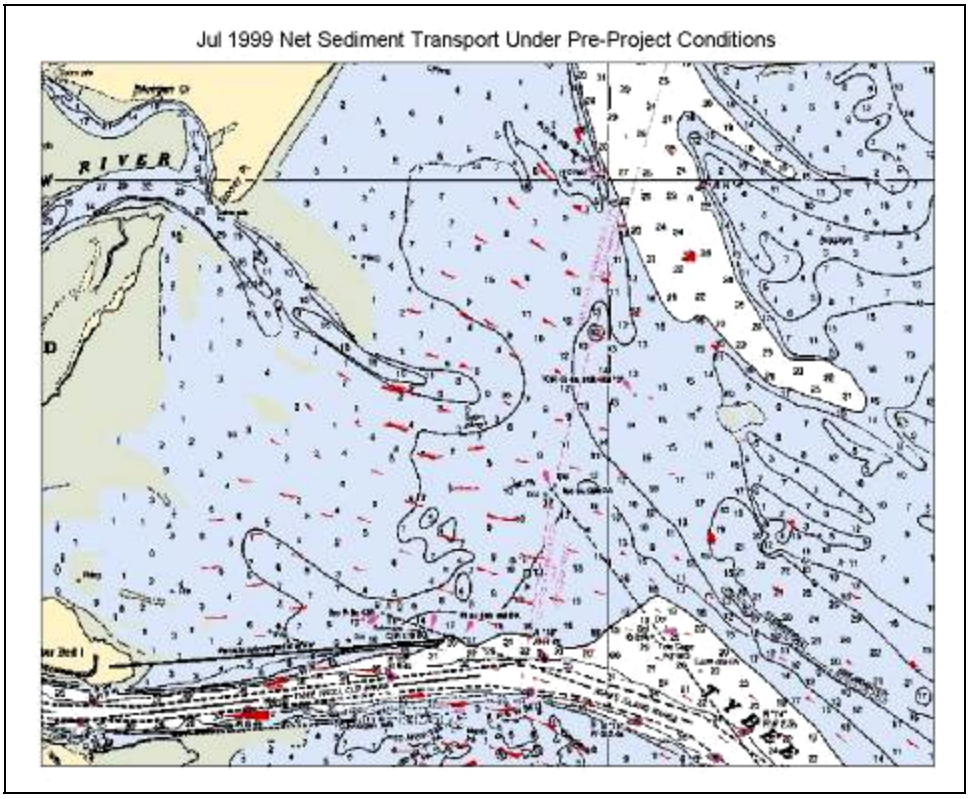

Figure B-20. Sediment transport rose plots for July 1999 pre-project GTRAN simulation (northern domain).

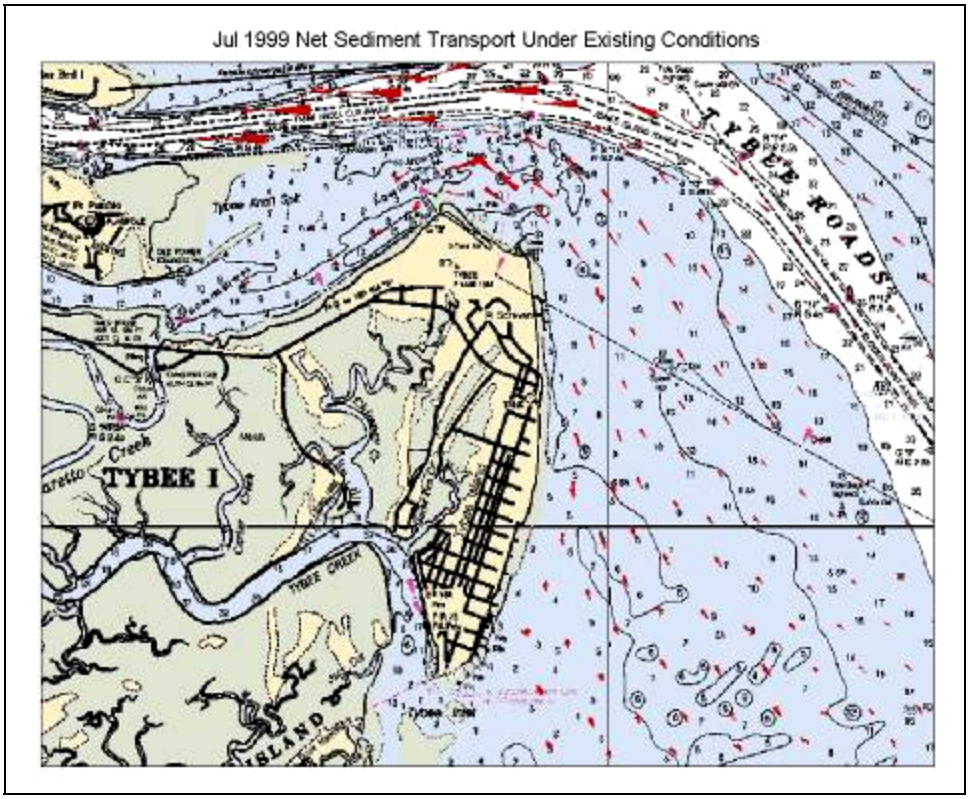

Figure B-21. Sediment transport rose plots for July 1999 existing conditions GTRAN simulation (southern domain).

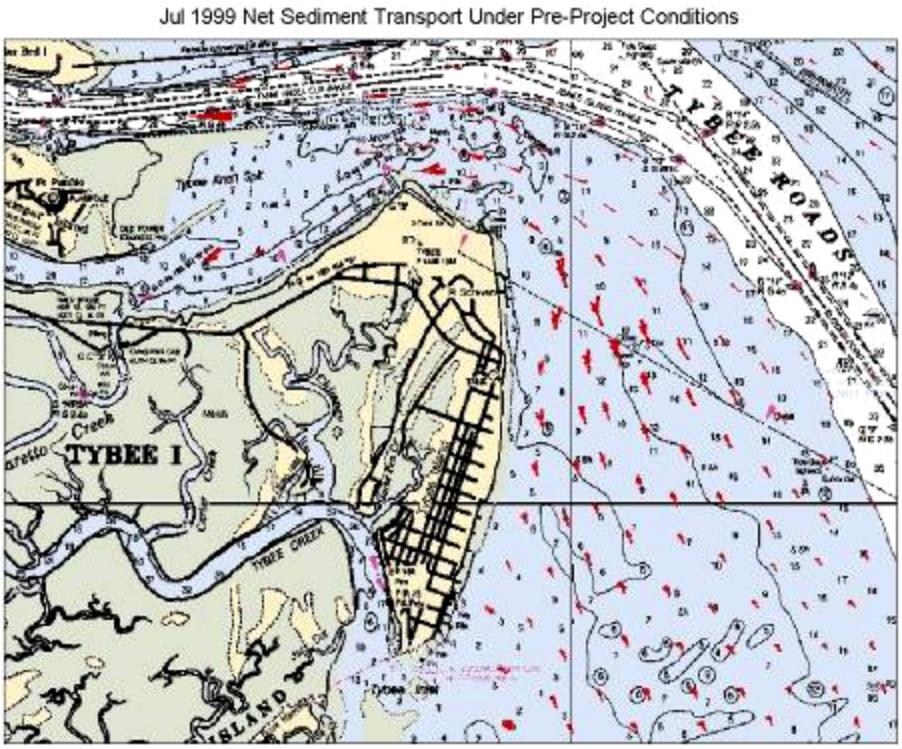

Figure B-22. Sediment transport rose plots for July 1999 pre-project GTRAN simulation (southern domain).

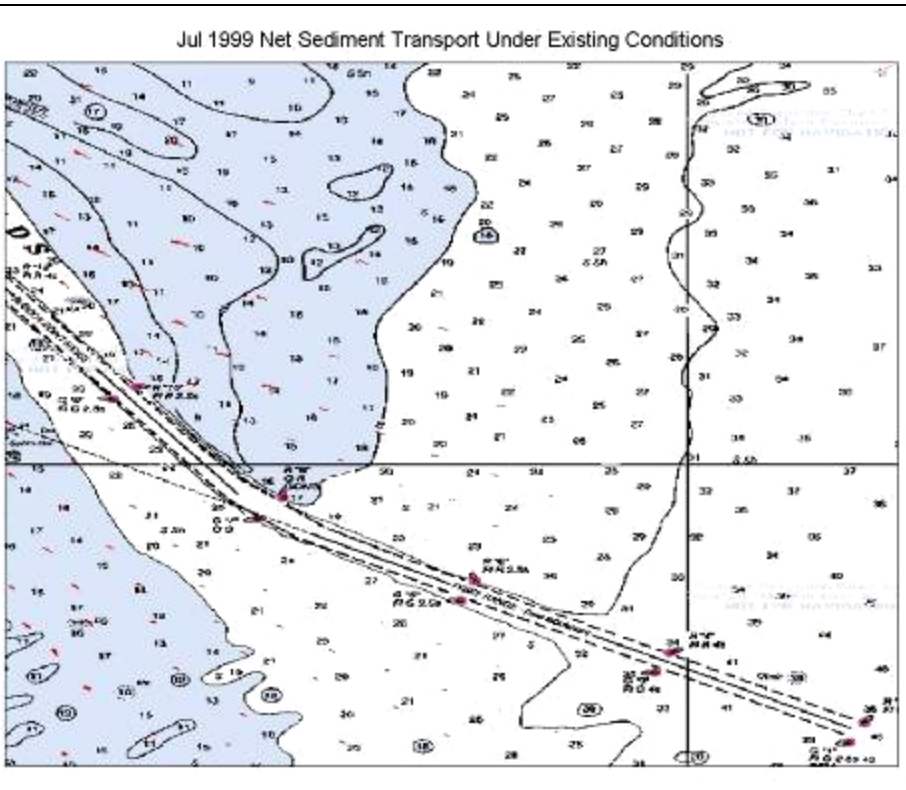

Figure B-23. Sediment transport rose plots for July 1999 existing conditions GTRAN simulation (southeastern domain).

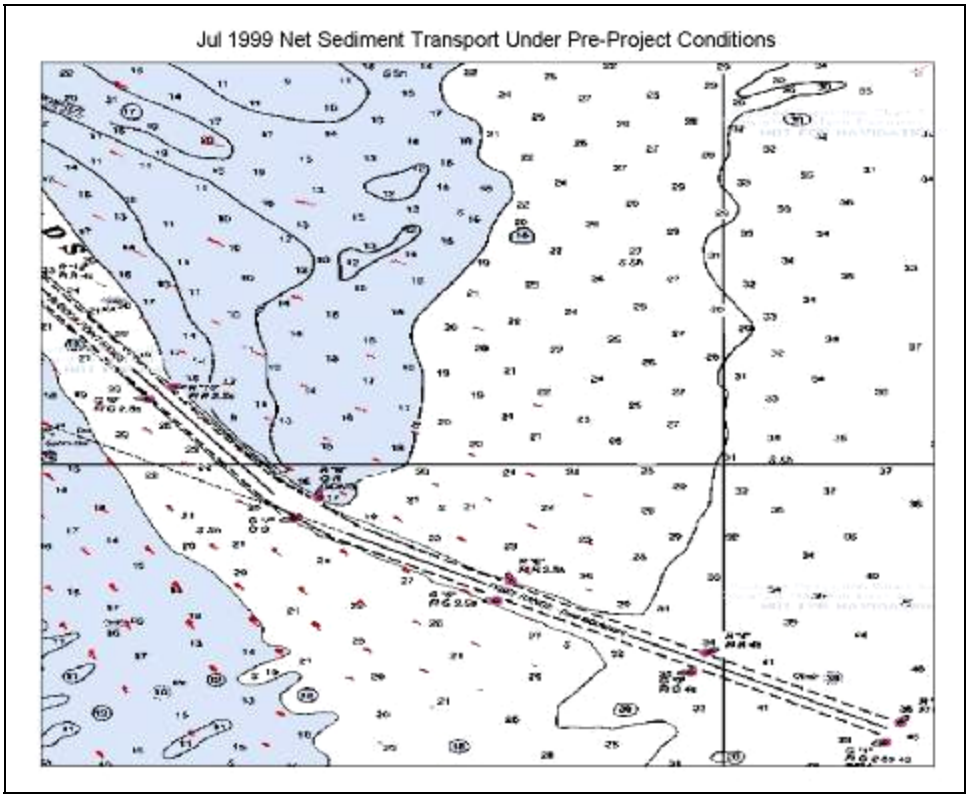

Figure B-24. Sediment transport rose plots for July 1999 pre-project GTRAN simulation (southeastern domain).

REPORT DOCUMENTATION PAGE

Form Approved
OMB No. 0704-0188

1. REPORT DATE *(DD-MM-YYYY)*	2. REPORT TYPE	3. DATES COVERED *(From - To)*
April 2008	Final report	

4. TITLE AND SUBTITLE

Impact of Savannah Harbor Deep Draft Navigation Project on Tybee Island Shelf and Shoreline

5a. CONTRACT NUMBER

5b. GRANT NUMBER

5c. PROGRAM ELEMENT NUMBER

6. AUTHOR(S)

Jane McKee Smith, Donald K. Stauble, Brian P. Williams, and Michael J. Wutkowski

5d. PROJECT NUMBER

5e. TASK NUMBER

5f. WORK UNIT NUMBER

7. PERFORMING ORGANIZATION NAME(S) AND ADDRESS(ES)

See reverse.

8. PERFORMING ORGANIZATION REPORT NUMBER

ERDC/CHL TR-08-5

9. SPONSORING / MONITORING AGENCY NAME(S) AND ADDRESS(ES)

U.S. Army Engineer District, Savannah
P.O. Box 889, Savannah, GA 31402-0889;
Headquarters, U.S. Army Corps of Engineers
Washington, DC 20314-1000

10. SPONSOR/MONITOR'S ACRONYM(S)

11. SPONSOR/MONITOR'S REPORT NUMBER(S)

12. DISTRIBUTION / AVAILABILITY STATEMENT

Approved for public release; distribution is unlimited.

13. SUPPLEMENTARY NOTES

14. ABSTRACT

The purpose of this study is to determine if the Savannah Harbor Deep Draft Navigation Project is adversely impacting the shores of Tybee Island (including sand lost from the beach and the Tybee shelf). The study methodology includes numerical modeling of waves, currents, water levels, and sediment transport rates and sediment budgets analysis for pre-project and post-project conditions. Sediment budgets were developed for the period 1854 to 1897 (pre-project) and 1897 to 2005/06/07 (post-project). The post-project bathymetry change shows a pattern of ebb shoal deflation on the Tybee shelf, which is a typical consequence of jetty construction and channel deepening. The ebb shoal deflation resulted from sediment pathways across the channel being disrupted. The major impact of the project is the loss of sand from the Tybee shelf. The ebb shoal deflation also resulted in shoreline change on Tybee Island, including erosion on the northern end of the island and accretion on the southern end of the island.

(Continued)

15. SUBJECT TERMS

ADCIRC
Channel impacts
GTRAN
Sediment budget
STWAVE
Tybee Island
Water levels
Waves

16. SECURITY CLASSIFICATION OF:			17. LIMITATION OF ABSTRACT	18. NUMBER OF PAGES	19a. NAME OF RESPONSIBLE PERSON
a. REPORT	b. ABSTRACT	c. THIS PAGE			19b. TELEPHONE NUMBER *(include area code)*
UNCLASSIFIED	UNCLASSIFIED	UNCLASSIFIED		204	

7. PERFORMING ORGANIZATION NAME(S) AND ADDRESS(ES) (Concluded)

U.S. Army Engineer Research and Development Center
Coastal and Hydraulics Laboratory
3909 Halls Ferry Road
Vicksburg, MS 39180-6199
U.S. Army Engineer District, Wilmington
Regional Engineering Center
69A Hagood Avenue
Charleston, SC 29403-5107;
U.S. Army Engineer District, Wilmington
69 Darlington Avenue
Wilmington, NC 28402-1890

14. ABSTRACT (Concluded)

The impact of the project is evaluated as the difference in volume loss rates (post-project minus pre-project) for the Tybee Island shelf cell of the sediment budget plus the estimated shoreline change rate (converted to a volume). The estimated combined shelf and shoreline impact at Tybee Island is 73.6 percent (including beach fill placement) or 78.5 percent (excluding beach fill placement) (±20 percent). This means that an estimated 73.6 percent (or 78.6 percent) of the reduction in sand volume on the Tybee shelf and shoreline is due to the project, with the remainder of the erosion attributed to the natural processes.